Programa de Doctorado en Matemática Aplicada

UNIVERSIDAD DEL BÍO-BÍO

Conforming and Nonconforming Virtual Element Methods for Problems in Fluid Mechanics

Thesis submitted to Universidad del Bío-Bío in fulfillment of the requirements for the degree of Doctor en Matemática Aplicada

by Alberth Antonio Silgado Ballesta

Director: David Mora Herrera
Co-director: Lourenco Beirão da Veiga

Conforming and Nonconforming Virtual Element Methods for Problems in Fluid Mechanics

por

ALBERTH ANTONIO SILGADO BALLESTA

Tesis presentada al Programa de Doctorado en Matemática Aplicada, de la Universidad del Bío-Bío, como requisito parcial para la obtención del Grado de Doctor en Matemática Aplicada.

Aprobada por:

Dr. David Mora Herrera
Director
Departamento de Matemática, Universidad del Bío-Bío, Chile.

Dr. Lourenco Beirão da Veiga
Co-Director
Dipartimento di Matematica e Applicazioni, Universitá degli studi di Milano-Bicocca, Italia.

Dr. Pablo Venegas Tapia (interno)
Profesor Informante
Departamento de Matemática, Universidad del Bío-Bío, Chile.

Dra. Jessika Camaño Valenzuela (externo)
Profesor Informante
Departamento de Matemática y Física Aplicadas, Universidad Católica de la Santísima Concepción, Chile.

Dr. Stefano Berrone (externo)
Profesor Informante
Dipartimento di Scienze Matematiche, Politecnico di Torino, Italia.

Universidad del Bío-Bío
Facultad de Ciencias
Departamento de Matemática

A mi madre:
Lady,
y a mis Abuelos:
José y Benilda.

AGRADECIMIENTOS

En primer lugar agradezco a mi madre, Lady Ballesta, por su dulce e incomparable amor, por sus sabios consejos y por su apoyo incondicional en momentos cruciales, que sin estos no estuviese cumpliendo este sueño. Agradezco a mis queridos hermanos: Eberto, "Beni" y "Abrahamcho" por la confianza y el cariño que me tienen, de igual forma a mi padre Eberto por sus buenos consejos. De manera muy especial a mis queridos abuelos José y Benilda por su amor y por siempre inspirarme a ser buena persona. También a mis tí@s y prim@s por su gran cariño y por estar siempre atentos a mi.

A mi novia, Alicia Meneses, quien ha sido mi soporte durante todo este tiempo. ¡Gracias por tu amor, paciencia, comprensión y ayuda en cada paso de este proceso!

Agradezco a mi director, el Profesor David Mora, por aceptar dirigir esta tesis doctoral, por su gran apoyo, tanto en el ámbito académico como en el "no-académico", paciencia y disponibilidad para guiar mis ideas y responder mis dudas. Por su amistad, las "tallas", "chelas", pizzas, y por las productivas y no-productivas conversaciones... ¡Gracias profe por ser chévere conmigo!

A mi co-director, el Profesor Lourenco Beirão da Veiga, por su invaluable y activo aporte a esta tesis, que sin duda ha marcado una gran diferencia. Gracias por su amabilidad, hospitalidad, tiempo y buena disposición para trabajar durante las dos estadías que realicé en la Universidad de Milano-Biccoca, Italia y también desde la distancia. Además, por las conversaciones, los cafés y las bromas... ¡Grazie mille "Lord Beirão"!

A los Profesores del Programa de Doctorado. En especial, a la Profesora Verónica Anaya por toda su ayuda y apoyo, los cuales han sido muy importante para mi. También a los Profesores: Juan Bobenrieth, Dante Carrasco, Felipe Lepe, Ricardo Oyarzúa, Pablo Venegas y Luis Villada, por sus enseñanzas y su buena vibra.

Agradezco en Colombia al Profesor Carlos Reales por su amistad, motivaciones y recomendación para continuar mis estudios de postgrado. También por las "frías" y asados en su casa cuando he viajado a Colombia. Agradezco también al Profesor Hugo Aduén, por infundir el amor por las Matemáticas y por la motivación a seguir los estudios de maestría y doctorado.

A mi hermano de la vida, Daniel Torres, por su amistad y apoyo desde la distancia en todo este proceso. ¡Gracias manín, por la fraternidad, las bromas y las "frías" cuando voy a Colombia!

Agradezco a Iván Velásquez, "Ivancho", por su gran amistad y carisma. También por su tiempo y buena disposición para compartir conmigo sus conocimientos "virtuales", y su invaluable ayuda en los aspectos teóricos y computacionales del VEM.

A mi amigo y compadre José Alfredo Angulo (Q.E.P.D), aunque ya no esté con nosotros siempre lo recodaré por su buena amistad y gran carisma. ¡Compadre, este logro también va dedicado a tu memoria!

A los compañeros del Doctorado, por los buenos momentos vividos durante estos años. En especial, a mis amigos del cubículo Colombo-Numérico: Eider Aldana, Juan Barajas y Rubén

Caraballo, que gracias a su compañerismo y carisma hicieron que no me sintiera tan lejos de mi hogar. También a la "colonia" Colombiana en Conce. En particular a Andy, Dalia, Harold y Luis Fernando, Rafa, por su gran carisma y por los "momentos colombianos" compartidos durante este tiempo.

En Italia al "Biccoca Team": a "Lord" Franco Dassi por su fraternidad y las charlas sobre Star Wars. A "Lord" Lorenzo Mascotto por su amistad y carisma durante mis dos estadías en Italia, por las salidas a la Certosa di Pavia, birras, pizzas y las jocosas conversaciones. Al Profesor Alessandro Russo, por su tiempo e invaluable ayuda en los aspectos computacionales del VEM con lados curvos. A Giuseppe Vacca, por su amistad y la invitación al Workshop en Bari... ¡Grazie mille per tutto ragazzi!

Agradezco a ANID-Chile, Programa de Becas, Doctorado Becas Chile 2020, 21201910, por financiar mis estudios de doctorado, por los gastos operacionales, la realización de pasantías y participación en Congresos. También, al Programa de Doctorado en Matemática Aplicada de la Universidad del Bío-Bío, el cual me facilitó sus instalaciones y recursos para trabajar adecuadamente durante mis estudios de Doctorado y también por apoyar mi participación en las pasantías y Congresos. Al personal del DMAT-UBB, por la hospitalidad y el trato cordial y afectuoso. En particular, a Ginette Rivas, por su fraternidad, disposición y gran ayuda en los trámites.

Alberth Silgado Ballesta

ABSTRACT

The main objective of this doctoral thesis is to design, analyze and implement novel conforming and nonconforming virtual element methods for solving problems that arise in fluid mechanics and large scale wind-driven ocean circulation, formulated in terms of the stream-function of the velocity field. The present study includes mathematical analysis for the continuous and discrete problems, a new and rigorous convergence analysis in several important norms. Moreover, it includes numerical implementation to validate the theoretical results and illustrate the behaviour of the discrete schemes.

Firstly, we propose and analyze a C^1-conforming virtual element scheme of low order for solving the stationary quasi-geostrophic equations of the ocean, formulated in terms of the stream-function variable. Under the assumption of small data and by using a fixed-point strategy, we establish the well-posedness of the discrete problem. Moreover, under standard assumptions on the computational domain, we provide error estimates in H^2-norm for the stream-function.

Subsequently, we write a weak formulation for the linear Oseen problem in terms of the stream-function on simply connected polygonal domains. Then, we propose and analyze C^1-conforming virtual discretization of arbitrary order $k \geq 2$. We establish that the resulting schemes converge with an optimal order in H^2-norm. Besides, we compute further variables of interest, such as the velocity, the vorticity and the pressure.

Additionally, we propose C^1 virtual element approximations of high order $k \geq 2$ for the Navier–Stokes equations in stream-function form. A novel analysis is developed to prove optimal error estimates in H^2-, H^1- and L^2-norms, under *minimal regularity* condition on the weak stream-function solution. Furthermore, we extend these schemes to the system with nonstandard boundary conditions on the pressure. Algorithms to compute the velocity, pressure and vorticity fields as a postprocess of the discrete stream-function are proposed and optimal error bounds are provided for these postprocessed variables.

Furthermore, we develop a fully-discrete virtual element scheme for the time dependent Boussinesq system formulated in terms of the stream-function and temperature unknowns. We employ the C^1- and C^0-conforming virtual element approaches to discretize the spatial variables and for time derivatives we use a classical Euler implicit method. We provide the well-posedness and unconditional stability of the fully-discrete scheme. Furthermore, we derive error estimates in $\mathrm{L}^2(\mathrm{H}^2) \cap \mathrm{L}^\infty(\mathrm{H}^1)$ and $\mathrm{L}^2(\mathrm{H}^1) \cap \mathrm{L}^\infty(\mathrm{L}^2)$-norms for the stream-function and temperature variables, respectively.

Finally, we design a Morley-type virtual element method for solving the Navier–Stokes problem in stream-function formulation. A rigorous stability and error analysis by employing a new enriching operator is developed. More precisely, by using such operator, we provide novel discrete Sobolev embeddings, which allows to establish the well-posedness of the discrete formulation and obtain optimal error bounds in broken H^2-, H^1- and L^2-seminorms, under minimal regularity condition on the weak solution. Some important variables such as the velocity, pressure and vorticity are obtained through postprocessing algorithms from the discrete stream-function.

For all the situations described above, several numerical experiments are reported on different families of polygonal meshes, illustrating the behavior of the virtual schemes and supporting our theoretical findings.

Key Words: Conforming and nonconforming virtual element methods, Quasi-geostrophic

equations, Navier–Stokes model, Oseen problem, nonstationary Boussinesq system, stream-function formulation, discrete Sobolev embeddings, optimal error estimates, minimal regularity, primitive variable recovery, polygonal meshes.

RESUMEN

El objetivo principal de esta tesis doctoral es diseñar, analizar e implementar nuevos métodos de elementos virtuales conformes y no conformes para resolver problemas que surgen en la mecánica de fluidos y la circulación oceánica impulsada por el viento a gran escala, formulados en términos de la función de corriente del campo de velocidades. El presente estudio incluye análisis matemático para los problemas continuos y discretos, un nuevo y riguroso análisis de convergencia en varias normas importantes. Además, se incluye implementación numérica para validar los resultados téricos e ilustrar el comportamiento de los esquemas discretos.

En primer lugar, proponemos y analizamos un esquema C^1-conforme de elementos virtuales de bajo orden, para resolver las ecuaciones cuasi-geostróficas estacionarias del océano, formuladas en términos de la variable de función de corriente. Bajo el supuesto de datos pequeños y mediante el uso de una estrategia de punto fijo, establecemos el bien planteamiento del problema discreto. Además, bajo suposiciones estándar sobre el dominio computacional proporcionamos estimaciones de error en norma H^2 para la función de corriente.

Posteriormente, escribimos una formulación débil para el problema lineal de Oseen en términos de la función de corriente en dominios poligonales simplemente conexos. Luego, proponemos y analizamos una discretización C^1 conforme de orden arbitrario $k \geq 2$. Establecemos que los esquemas resultantes convergen con un orden óptimo en norma H^2. Además, calculamos otras variables de interés, como la velocidad, la vorticidad y la presión.

Adicionalmente, proponemos aproximaciones C^1 de elementos virtuales de orden superior $k \geq 2$ para las ecuaciones de Navier–Stokes formuladas en términos de la función de corriente. Se desarrolla un novedoso análisis para probar estimaciones de error óptimas en las normas H^2, H^1 y L^2, bajo condiciones de *regularidad mínima* de la función de corriente débil. Además, extendemos estos esquemas al sistema con condiciones de contorno no estándar sobre la presión. Se proponen algoritmos para calcular los campos de velocidad, presión y vorticidad como un postproceso de la función de corriente discreta y se han proporcionado cotas de error óptimos para estas variables postprocesadas.

Además, desarrollamos un esquema de elementos virtual complemente discreto para el sistema Boussinesq dependiente del tiempo formulado en términos de las incógnitas función de corriente y temperatura. Empleamos los enfoques C^1 y C^0 de elementos virtuales conformes para discretizar las variables espaciales y para las derivadas temporales utilizamos un método implícito clásico de Euler. Proporcionamos la buena postura y la estabilidad incondicional del esquema totalmente discreto. Además, derivamos estimaciones de error en las normas $\mathrm{L}^2(\mathrm{H}^2) \cap \mathrm{L}^\infty(\mathrm{H}^1)$ y $\mathrm{L}^2(\mathrm{H}^1) \cap \mathrm{L}^\infty(\mathrm{L}^2)$ para las variables función de corriente y temperatura, respectivamente.

Finalmente, diseñamos un método de elementos virtuales tipo Morley para resolver el problema de Navier–Stokes en la formulación de la función de corriente. Se desarrolla un riguroso análisis de estabilidad y de error empleando un nuevo operador enriquecido. Más precisamente, utilizando dicho operador, proporcionamos novedosas inclusiones de Sobolev discretas, que permiten establecer el buen planteamiento de la formulación discreta y obtener cotas de error óptimas en las seminormas H^2, H^1 y L^2, bajo condiciones de regularidad mínima sobre la solución débil. Algunas variables importantes como la velocidad, la presión y la vorticidad se obtienen mediante novedosos algoritmos de posprocesamiento de la función de corriente discreta.

Para todas las situaciones descritas anteriormente, se reportan varios experimentos numéricos en diferentes familias de mallas poligonales, que ilustran el comportamiento de los esquemas virtuales y respaldan nuestros hallazgos teóricos.

Palabras Claves: Métodos de Elementos Virtuales conformes y no conformes, ecuaciones quasi-geostróficas del océano, modelo de Navier–Stokes, problema Oseen, sistema no estacionario de Boussinesq, formulación de la función de corriente, inclusiones discretas de Sobolev, estimaciones óptimas de error, mínima regularidad, recuperación de variables primitivas, mallas poligonales.

Contents

Agradecimientos **iv**

Abstract **vii**

Resumen **ix**

Contents **x**

List of Figures **xiii**

List of Tables **xvi**

1 Introduction **1**
- 1.1 Motivation and general background . . . 1
- 1.2 The Virtual Element Method . . . 2
- 1.3 Preliminary notations . . . 8

2 A C^1 virtual element method for the stationary quasi-geostrophic equations of the ocean **10**
- 2.1 Introduction . . . 10
- 2.2 The model problem . . . 11
- 2.3 The virtual element scheme . . . 15
  - 2.3.1 Virtual spaces and polynomial projections . . . 15
  - 2.3.2 Construction of the discrete forms . . . 18
  - 2.3.3 Discrete problem and fixed-point strategy . . . 20
- 2.4 Convergence analysis . . . 23
- 2.5 Numerical results . . . 27
  - 2.5.1 Test 1: Smooth solution . . . 28
  - 2.5.2 Test 2: Solution with western boundary layer . . . 30
  - 2.5.3 Test 3: Solution with vortex in the top-right corner of the domain . . . 30
  - 2.5.4 Test 4: L-shaped domain . . . 32

3 Virtual element methods for a stream-function formulation of the Oseen equations **34**
- 3.1 Introduction . . . 34
- 3.2 Model problem . . . 35
- 3.3 Virtual element method . . . 37
  - 3.3.1 Virtual spaces and polynomial projections operator . . . 37

3.3.2 Construction of the local and global discrete forms . . . 40
3.3.3 Discrete formulation . . . 42
3.4 Error analysis . . . 43
3.4.1 Preliminary results . . . 44
3.4.2 A priori error estimates . . . 45
3.5 Recovering the velocity, vorticity and pressure fields . . . 48
3.5.1 Computing the velocity field . . . 48
3.5.2 Computing the fluid vorticity . . . 49
3.5.3 Computing the fluid pressure . . . 50
3.6 Numerical results . . . 57
3.6.1 Test 1. Smooth solution . . . 58
3.6.2 Test 2. Solution with boundary layer . . . 58
3.6.3 Test 3. Solution with non homogeneous Dirichlet boundary conditions. . 61

4 Virtual elements for the Navier–Stokes system: stream function form and primitive variables recovery algorithms 63
4.1 Introduction . . . 63
4.2 Weak stream-function form and its well-posedness . . . 65
4.3 The C^1-virtual element approximation . . . 66
4.3.1 Virtual spaces and degrees of freedom . . . 67
4.3.2 Polynomial projections and the discrete formulation . . . 68
4.4 Theoretical analysis . . . 69
4.4.1 Fixed-point strategy . . . 70
4.4.2 Error estimates . . . 70
4.4.2.1 A priori estimate . . . 73
4.4.2.2 Error estimates in H^1 and L^2 . . . 74
4.5 Computing further variables of interest . . . 77
4.5.1 The fluid velocity and vorticity recovery algorithm . . . 77
4.5.2 The fluid pressure recovery algorithm . . . 78
4.5.2.1 Continuous variational formulation . . . 78
4.5.2.2 C^0-VE approximation . . . 78
4.5.2.3 Theoretical analysis . . . 79
4.6 Extension to the boundary conditions on the pressure case . . . 83
4.7 Numerical experiments . . . 84
4.7.1 Some aspects of the numerical implementation . . . 84
4.7.2 Test 1. The exact solution of Kovasznay flow . . . 85
4.7.3 Test 2. No flow problem for the Navier–Stokes equations . . . 85
4.7.4 Test 3. The lid-driven cavity problem . . . 87
4.7.5 Test 4. Solution with less regularity . . . 89
4.7.6 Test 5. The Navier–Stokes system with BCs on the pressure . . . 89

5 A fully-discrete virtual element method for the nonstationary Boussinesq equations in stream-function form 91
5.1 Introduction . . . 91
5.2 The continuous problem . . . 93
5.2.1 The time dependent Boussinesq system . . . 93
5.2.2 The time dependent stream-function–temperature formulation . . . 94

5.2.3 Well-posedness of the weak formulation . . . 95
5.3 Virtual elements discretization . . . 96
5.3.1 Polygonal decompositions and notations . . . 97
5.3.2 Virtual element space for the stream-function . . . 97
5.3.3 Virtual element space for the temperature . . . 99
5.3.4 L^2-projections and the discrete forms . . . 100
5.4 Fully-discrete formulation and its well posedness . . . 104
5.5 Convergence analysis . . . 109
5.5.1 Preliminary results . . . 109
5.5.2 Error estimates for the fully-discrete scheme . . . 113
5.6 Numerical results . . . 120
5.6.1 Accuracy assessment . . . 121
5.6.2 Performance of the VEM for small viscosity . . . 124
5.6.3 Natural convection in a cavity with the left wall heating . . . 125

6 The Morley-type virtual element method for the Navier–Stokes equations in stream-function form 128
6.1 Introduction . . . 128
6.2 Preliminaries and continuous weak form . . . 131
6.2.1 The stream-function weak form . . . 131
6.3 Morley-type virtual element approximation . . . 132
6.3.1 Some auxiliary spaces . . . 134
6.3.2 The Morley-type nonconforming virtual element space . . . 135
6.3.3 Polynomial projection operators and discrete forms . . . 136
6.4 Discrete formulation and its well-posedness . . . 138
6.4.1 A new enriching operator . . . 138
6.4.2 Discrete Sobolev embeddings and properties of the discrete forms . . . 141
6.4.3 A fixed-point strategy . . . 142
6.5 Error analysis . . . 143
6.5.1 An abstract convergence result . . . 144
6.5.2 Approximation results and a priori error estimate . . . 146
6.5.3 Error estimates in broken H^1 and L^2 . . . 148
6.6 Postprocessing of further fields of interest . . . 153
6.6.1 Postprocessing the velocity field . . . 153
6.6.2 Postprocessing the vorticity field . . . 154
6.6.3 Postprocessing the pressure field . . . 154
6.7 Numerical results . . . 159
6.7.1 Test 1. Kovasznay flow . . . 160
6.7.2 Test 2. L-shaped domain . . . 160
6.7.3 Test 3. The lid-driven cavity problem . . . 163
6.7.4 Test 4. Performance of the scheme for small viscosity . . . 164

7 Conclusions and future work 166
7.1 Concluding remarks . . . 166
7.2 Future work . . . 169

References 181

List of Figures

2.1 Sample meshes. $\mathcal{T}_h^1$, $\mathcal{T}_h^2$, $\mathcal{T}_h^3$ and $\mathcal{T}_h^4$ (from left to right). 28
2.2 Test 1. Exact and approximate solutions ψ and ψ_h, the streamlines of ψ_h and the velocity field $\mathbf{u}_h := \mathbf{curl}\,\psi_h$ (top left, top right, bottom left, bottom right, respectively), using the VEM method (2.3.26) with $\mathcal{T}_h^1$, $h = 1/32$. 29
2.3 Test 2. Exact and approximate solutions ψ, ψ_h, the streamlines of ψ_h and the velocity field $\mathbf{u}_h := \mathbf{curl}\,\psi_h$ and (top left, top right, bottom left, bottom right, respectively) using the VEM method (2.3.26) with $\mathcal{T}_h^2$, $h = 1/64$. 31
2.4 Test 3. Exact and approximate solutions ψ, ψ_h (top) and the velocity field $\mathbf{u}_h := \mathbf{curl}\,\psi_h$ (bottom) using the VEM method (2.3.26) with $\mathcal{T}_h^3$, $h = 1/32$. . . 32
2.5 Test 4. Exact and approximate solutions ψ, ψ_h (left and right, respectively) using the VEM method (2.3.26) with $\mathcal{T}_h^4$, $h = 1/16$. 33

3.1 Sample meshes. $\mathcal{T}_h^1$, $\mathcal{T}_h^2$ and $\mathcal{T}_h^3$. 57
3.2 Test 1. Exact (top panels) and computed (bottom panels) stream-function, pressure and vorticity, using the VEM methods (3.2.2) and (3.5.17) with $\mathcal{T}_h^1$, $h = 1/32$, $k = 3$ and $\nu = 1$. 59
3.3 Test 1. Velocity field obtained from the discrete stream-function with $\mathcal{T}_h^1$, $h = 1/32$, $k = 3$ and $\nu = 1$. 60
3.4 Test 2. Exact (top panels) and computed (bottom panels) stream-function, pressure and vorticity, using the VEM methods (3.2.2) and (3.5.17) with $\mathcal{T}_h^2$, $h = 1/64$, $k = 3$, $\nu = 10^{-3}$ and $\gamma = 50$. 61
3.5 Test 2. Velocity field and streamlines obtained from the discrete stream-function with $\mathcal{T}_h^2$, $k = 3$, $\nu = 10^{-3}$ and $\gamma = 50$. 62

4.1 Sample meshes. Ω_h^1, Ω_h^2, Ω_h^3 and Ω_h^4. 85
4.2 Test 1. Exact (top panels) and approximate (bottom panels) solutions stream-function, pressure and vorticity using the VEMs (4.3.7), (4.5.5) and postprocess (4.5.2), employing the mesh Ω_h^1, with $h^{-1} = 64$, $k = 3$ and $\mathrm{Re} = 40$. 87
4.3 Test 2. Velocity (a) and pressure (b) errors using the VEMs (4.3.7) and (4.5.5), with the meshes Ω_h^3 and Ω_h^4, $k = 3$, $\ell = 1$, $\nu = 1$ and taking different values for the parameter Ra. 88
4.4 Test 3. Profiles of the velocity, pressure and vorticity (from left to right): $\widehat{u}_{1h}$-velocity component, using the mesh Ω_h^1, with $h^{-1} = 48$ and taking different values for Reynolds number Re; pressure and vorticity profiles along horizontal, with the mesh Ω_h^1, with $h^{-1} = 128$ and $\mathrm{Re} = 1000$. 88

5.1 Domain discretized with different meshes. 121

5.2 Accuracy assessment. Errors (5.6.1) for simultaneous space and time refinements, using the VEM (5.4.1) with polynomial degrees $(k,\ell) = (2,1)$, physical parameters $\nu = \kappa = 1$ and the mesh families $\mathcal{T}_h^i$, $i = 1,\dots,4$. 123
5.3 Accuracy assessment. Errors (5.6.2), using the VEM (5.4.1) with polynomial degrees $(k,\ell) = (2,1)$, the physical parameters $\nu = \kappa = 1$ and the mesh families $\mathcal{T}_h^i$, $i = 1,\dots,4$. 124
5.4 Small viscosity test. Errors (5.6.1) of the VEM (5.4.1), for different values of ν and $\kappa = 1$, using the meshes $\mathcal{T}_h^2$, polynomial degrees $(k,\ell) = (2,1)$. 125
5.5 Natural convection cavity. Boundary conditions and domain discretized with mesh $\mathcal{T}_h^5$. 126
5.6 Natural convection cavity: streamlines (top panels) and isotherms (bottom panels), for Ra $= 10^3, 10^4, 10^5$ and 10^6, respectively (from left to right), using the mesh $\mathcal{T}_h^5$ $(h = 1/64)$. 126
5.7 Natural convection cavity. Nusselt number along the hot wall (left) and the cold wall (right) for varying Rayleigh numbers, using the VEM (5.4.1) and mesh $\mathcal{T}_h^5$, with $h = 1/64$. 127

6.1 Sample meshes. $\mathcal{T}_h^1$, $\mathcal{T}_h^2$, $\mathcal{T}_h^3$ and $\mathcal{T}_h^4$ (from left to right). 159
6.2 Test 1: Convergence of the stream-function ψ in broken H^2-, H^1- and L^2-norms with mesh refinement for different types of meshes, using $\nu = 1$. 160
6.3 Test 1: Convergence of the velocity field $\mathbf{u}$ in broken H^1- and L^2-norms, and vorticity field ω in L^2-norm (from left to right) with mesh refinement for different types of meshes, using $\nu = 1$. 161
6.4 Test 1: Convergence of the stream-function in broken H^2, H^1- L^2-norms with mesh refinement for different types of meshes, using $\nu = 0.01$. 161
6.5 Test 1: Convergence of the velocity field $\mathbf{u}$ in broken H^1- and L^2-norms, and vorticity field ω in L^2-norm (from left to right) with mesh refinement for different types of meshes, using $\nu = 0.01$. 162
6.6 Test 1: Convergence of the pressure (p) in L^2-norm with mesh refinement for different types of meshes, using $\nu = 1$ and $\nu = 0.01$. Left panel shows the errors curve of p for $\nu = 1$, and right panel shows the errors curve of p for $\nu = 0.01$. . 162
6.7 Test 1: "Snapshots" of the approximate stream-function and pressure, using $\nu = 1$ and the mesh $\mathcal{T}_h^1$, $h = 1/32$. 163
6.8 Test 3: "Snapshots" of the approximate stream-function and pressure for $\nu = 0.01$, using the mesh $\mathcal{T}_h^3$, with $h = 1/64$. 164
6.9 Test 4. Errors of the stream-function $\mathcal{E}_2(\psi)$, using the VE scheme (6.4.1) with the alternative load term (6.5.25), for different values of ν and the mesh $\mathcal{T}_h^1$. . . 165

List of Tables

1.1 The numbers of local and global DoFs for the conforming C^1-VEM of lowest order and for some typical C^1-FEMs, the polynomial spaces involved and regularity conditions on the weak solution to obtain error estimates. 4

2.1 Test 1. Errors and experimental rates for the stream-function ψ_h, using the meshes $\mathcal{T}_h^1$. 29
2.2 Test 2. Errors and experimental rates for the stream-function ψ_h, using the meshes $\mathcal{T}_h^2$. 30
2.3 Test 3. Errors and experimental rates for the stream-function ψ_h, using the meshes $\mathcal{T}_h^3$. 31
2.4 Test 4. Errors and experimental rates for the stream-function ψ_h, using the meshes $\mathcal{T}_h^4$. 33

3.1 Test 1. Errors and experimental rates for the stream-function ψ_h and vorticity ω_h, using the meshes $\mathcal{T}_h^1$, $k=2$, $\nu=1$ and $\gamma=100$. 59
3.2 Test 1. Errors and experimental rates for the stream-function ψ_h, pressure p_h and vorticity ω_h using the meshes $\mathcal{T}_h^1$, $k=3$, $\nu=1$ and $\gamma=100$. 59
3.3 Test 2. Errors and experimental rates for the stream-function ψ_h and vorticity ω_h, using the meshes $\mathcal{T}_h^2$, $k=2$, $\nu=10^{-3}$ and $\gamma=50$. 60
3.4 Test 2. Errors and experimental rates for the stream-function ψ_h, pressure p_h and vorticity ω_h using the meshes $\mathcal{T}_h^2$, $k=3$, $\nu=10^{-3}$ and $\gamma=50$. 61
3.5 Test 3. Errors and experimental rates for the stream-function ψ_h and vorticity ω_h, using the meshes $\mathcal{T}_h^3$, $k=2$, $\nu=10^{-7}$ and $\gamma=100$. 62

4.1 Test 1. Errors and experimental rates of convergence for the stream-function, velocity, vorticity and pressure, using the meshes Ω_h^1, $\mathrm{Re}=1,40,10^2,10^3$ and $k=3$. 86
4.2 Test 1. Mesh sizes, degrees of freedom and number of iterations of the Newton method with respect to parameter Re. 86
4.3 Test 4. Errors for the stream-function variable in H^2-norm on the L-shaped using with square elements Ω_h^1 and $k=2,3$. 89
4.4 Test 5. Errors in norm H^2- H^1- and L^2-norms for stream-function, velocity and vorticity fields, respectively, obtained with the VE scheme (4.6.4), the family mesh Ω_h^4 and $k=2$. 90

5.1 Accuracy assessment. Errors (5.6.1) using the VEM (5.4.1), with polynomial degrees $(k,\ell)=(2,1)$, physical parameters $\nu=\kappa=1$ and the mesh family mesh $\mathcal{T}_h^1$. 122

5.2 Accuracy assessment. Errors (5.6.2) using the VEM (5.4.1), with polynomial degrees $(k,\ell)=(2,1)$, the physical parameters $\nu=\kappa=1$ and the mesh family $\mathcal{T}_h^1$. 123
5.3 Natural convection cavity. Comparison of maximum vertical velocity $u_{1h}:=\Pi_h^1\partial_y\psi$ at $y=0.5$ with the VEM (5.4.1) and mesh $\mathcal{T}_h^5$ $(h=1/64)$. 127
5.4 Natural convection cavity. Comparison of maximum horizontal velocity $u_{2h}:=-\Pi_h^1\partial_x\psi$ at $x=0.5$ with the VEM (5.4.1) and mesh $\mathcal{T}_h^5$ $(h=1/64)$. 127

6.1 Test 2. Errors for the stream-function, and the post-processed velocity, vorticity fields in broken H^2-, H^1- and L^2-norms for $\nu=1$, using the mesh $\mathcal{T}_h^2$. 163
6.2 Test 2. Errors for the pressure variable in L^2-norm for $\nu=1$, using the mesh $\mathcal{T}_h^2$. 163

Chapter 1

Introduction

1.1 Motivation and general background

The numerical approximation of viscous incompressible fluid problems have acquired great interest due to the variety of applications in different research areas, such as: engineering, environmental and industrial processes, oceanography, climatology, biomedicine, among others. Depending on the type of phenomenon and the medium in which the fluid is located, different mathematical models, such as, Brinkman, Oseen, Navier-Stokes, and Boussinesq models can be used to obtain adequate results to study the dynamics of the fluid in terms of the specific variables of interest. Some examples are given by the velocity, pressure, temperature, pseudostress, vorticity, and more importantly for the present thesis, the stream-function. In general, the analytical solution of these problems is difficult to obtain. Therefore, it is necessary to develop efficient numerical schemes to approximate their solutions.

In this thesis we are interested in solving linear and nonlinear problems with applications to fluid mechanics and large scale wind-driven ocean circulation, namely: the one-layer Quasi-Geostrophic equations of the ocean, the Oseen problem, the Navier-Stokes equations and the Boussinesq system. In particular, for these models we are interested in formulations where the stream-function is the principal unknown.

The stream-function formulation

Typically, the velocity-pressure formulation is the most commonly used to discretize the Navier-Stokes equations (or other fluid flow problems). However, the stream-function formulation has shown to be a competitive alternative to discretize these systems. In fact, if $\Omega \subset \mathbb{R}^2$ is a bounded simply connected domain, then we can associate to a divergence-free velocity field $\mathbf{u}$ a scalar function ψ, such that

$$\mathbf{u} = \mathbf{curl}\,\psi, \tag{1.1.1}$$

which is called *stream-function*. By using the above identity, we have that the incompressible Navier-Stokes problem can be formulated in terms of this scalar variable. Such formulation is given by a single fourth-order problem (cf. (4.1.1)), which is characterized for the presence of the biharmonic operator. For further details, we refer to [103, Chapter IV, Section 2.1].

In the two dimensional case, we can highlight the following features of the stream-function form: the system is reduced in a single scalar weak formulation, with automatic satisfaction of the incompressibility constraint (by definition, see (1.1.1)), the possibility to recover further variables of physical interest, such as; the velocity, pressure and vorticity fields through post-processing algorithms from the stream-function. Additionally, it represents one of the most useful tools in flow visualization and for linear models (Stokes or Brinkman problems) the matrix associated turns out to be positive definite, allowing for more efficient methods such as Cholesky factorization or conjugate gradient. Moreover, for nonlinear problems (such as the Navier-Stokes and Boussinesq equations), the resulting trilinear form in the momentum is naturally skew-symmetric (without adding additional terms), allowing more direct stability and convergence arguments. Furthermore, the stream-function approach avoids the difficulties related to the implementation of the boundary vorticity values, which are presented in stream-function–vorticity form.

Due to the attractive characteristics discussed above, the stream-function formulation has received significant attention from many researchers. In particular, a notable number of works have been devoted to the design and analysis of numerical methods to approximate the Navier-Stokes problem. For instance, conforming and nonconforming Finite Element Methods (FEMs) in [71, 72, 90, 91, 68], Bivariate Spline methods [115], *hp*-version discontinuous FE [143], NURBS-based Isogeometric Analysis in [151]. Moreover, in [95, 111] C^1-conforming and nonconforming Morley FEMs has been studied for solving the steady quasi-geostrophic equations in stream-function formulation (compare below the systems (2.2.1) and (4.1.1)).

On the other hand, we recall that to discretize fourth-order problems in primal form, using the classical conforming FE spaces yields notable disadvantages: firstly, the construction of these spaces involve high-order polynomials and a large number of degrees of freedom (at least 18 for triangular polynomial elements), which commonly is considered a demanding task from the computational viewpoint. A possible alternative to avoid such high order polynomials is to resort to very complicated FE construction (for instance, the Hsieh-Clough-Tocher or the singular Zienkiewicz triangles). Moreover, the regularity requirements of the weak solution are high, which are not realistic and inappropriate in practice. The main reason of these difficulties is the required continuity of the first order partial derivatives across adjacent elements. For further details, we refer to [79, Chap. 6, sect. 6.1]).

In order to overcome these drawbacks, in this thesis we consider the approach presented in [58, 77, 18] to introduce C^1-virtual element methods to approximate linear and nonlinear fluid flow problems in stream-function formulation. On the other hand, we contribute to the development and analysis of novel nonconforming Morley-type virtual schemes to discretize the Navier-Stokes equations.

1.2 The Virtual Element Method

The *Virtual Element Method* (VEM) was presented to the scientific community for first time about 10 years ago in the pioneering paper [27] as an evolution of mimetic finite differences and a generalization of FEM. The VEM belongs to the group of polytopal Galerkin schemes for solving PDEs, which have received significant interest in recent years due to their versatility in dealing with complex geometries (see for instance [149, 86, 32, 108, 70, 88]).

According to [27] the general features of VEM can be summarized as follows:

- The discrete local spaces are built in such a way that they contain the polynomial spaces of degree up to k (this fact determines the accuracy of the method), and other non-polynomials functions that are solution of a PDE problem inside the element, which is never resolved. Therefore, the exact values in the interior of the polygon/polyhedron of these shape functions are unknown (hence the terminology “virtual”).

- Only the evaluation of the degrees of freedom is required in the design of the forms appearing in the discrete formulation. The degrees of freedom are chosen carefully so that the projections onto polynomial spaces can be computed using only their information.

- The bilinear forms appearing in the discrete formulation are built based on two main ingredients: projections from local virtual element spaces onto polynomial spaces and bilinear forms that stabilize the scheme.

From the first and second items, we observe that the approach of VEM allows to avoid an explicit construction of the discrete basis functions and this fact implies a high flexibility of the method, for instance, VEM has the ability to design numerical schemes of high-order on general polygonal meshes (including the desired nonconvex shapes and “hanging vertexes”) in a straightforward way. Moreover, the method has capability to build discrete spaces with high-regularity (C^{α}-regularity, with $\alpha \geq 1$) and construct divergence-free schemes in the context of fluid flow problems. Due to these characteristics, the VEM has achieved significant success in computational modeling and practical engineering uses, both in its *conforming* and *nonconforming* frameworks (see for instance [7, 65, 29, 39, 22, 126, 127, 153, 159, 116]). In particular, many works have been devoted to approximate the solutions of problems in fluid mechanics by using the VEM technology. Below are two list of representative works in the conforming and nonconforming cases; [17, 59, 34, 98, 35, 157, 41, 97, 21, 131] and [64, 118, 164, 119, 162], respectively.

Conforming and fully nonconforming VEMs for fourth-order problems

Due to its importance, applicability and challenging nature, the construction of Galerkin schemes to solve fourth-order problems has been a very active area of research. Indeed, a wide variety of numerical approaches have been presented for solving these systems, see for instance [79, 68, 142, 101, 53] and references therein, where classical conforming and nonconforming FE schemes, C^0-IP methods, among others have been developed and analyzed.

Recently, in [58] was introduced a family of C^1-VEM of high order $k \geq 2$, to solve the Kirchhoff-Love plate problem, which in the lowest order case employed only 3 degrees of freedom per mesh vertex (the function and its gradient values vertex). This fact makes C^1-VEM a very attractive and competitive approach compared to the typical C^1-FEMs.

Subsequently, in [18] was introduced a variant of this family. More precisely, by employing the enhancement technique [7], a C^1-VEM of lowest order was developed and analyzed for the two dimensional Cahn-Hillard equation. In the same year, the authors in [77] also designed a variant of the high-order VEMs presented in [58]. By using also the ideas developed in [7] the authors design an enhancement C^1-VEMs for solving fourth-order problems, obtaining now optimal error estimates in the weak L^2- and H^1-norms.

Additionally, in [36, 19], the authors investigated the application of VEM to construct finite dimensional spaces of arbitrarily regular C^{α}-functions, with $\alpha \geq 1$, where promising results have been observed to solve equations involving high order PDEs.

It is important to point out that in [30] the authors designed a C^1-VEM for the challenging case of three-dimensional fourth-order problems.

Since then, several schemes and analyses based on the C^1-conforming VEM have been designed for solving linear and nonlinear problems; below is a non-exhaustive list of works [38, 135, 116, 159, 139, 122, 3, 56, 1].

In Table 1.1, we illustrate a comparison between the C^1-VEM of lowest order and classical C^1-FEMs used to approximate fourth-order problems, namely; the Argyris and Bell triangles, the Hsieh–Clough–Tocher (HCT) element and the Bogner-Fox-Schmit rectangle. In particular, we show the numbers of local (N_K^{dof}) and global (N_h^{dof}) degrees of freedom (DoFs) for the numerical schemes, the polynomial spaces ($\mathbb{P}_k$) involved and the regularity conditions on the weak solution to obtain error estimates. We observe that the C^1-VEM in the lowest order case employ only 3 DoFs per vertex of the mesh, i.e, $3N_{\mathbf{v}}$, where $N_{\mathbf{v}}$ denotes the number of vertices in the polygonal mesh (9 on a triangle and 12 for rectangle), which is much smaller than that of the traditional conforming FEMs. Moreover, from the analysis developed in Section 4.4.2 (see also Theorem 4.4.3), we observe that the C^1-VEM of lowest order needs the slightest regularity requirement for the weak stream-function to establish error estimates, even for the nonlinear Navier-Stokes problem in stream-function form.

type of elements	N_K^{dof}	$\mathbb{P}_k$	N_h^{dof}	assumed regularity
C^1-VEMs of lowest order	9	$\mathbb{P}_2$	$3N_{\mathbf{v}}$	$\mathrm{H}^{2+s}(\Omega)$, $s \in (0,1]$
Argyris triangle	21	$\mathbb{P}_5$	$9N_{\mathbf{v}}$	$\mathrm{H}^6(\Omega)$
Bell triangle	18	$\mathbb{P}_4$	$6N_{\mathbf{v}}$	$\mathrm{H}^5(\Omega)$
HCT element	12	$\mathbb{P}_3$	$6N_{\mathbf{v}}$	$\mathrm{H}^4(\Omega)$
Bogner-Fox-Schmit rectangle	16	$\mathbb{P}_3$	$4N_{\mathbf{v}}$	$\mathrm{H}^4(\Omega)$

Table 1.1: The numbers of local and global DoFs for the conforming C^1-VEM of lowest order and for some typical C^1-FEMs, the polynomial spaces involved and regularity conditions on the weak solution to obtain error estimates.

On the other hand, in [20, 163] the authors introduced independently a few families of VEMs to solve fourth-order problems in an alternative way. The schemes are based on fully-nonconforming VEMs of high-order $k \geq 2$. In particular, the lowest order configuration (i.e., $k = 2$) of these VEMs can be consider as the extension of the popular Morley FE [141] to general polygonal meshes. Since then, several schemes and analysis based on these VEMs have been developed for linear problems; see for instance [116, 159, 81, 107, 67, 4].

According to the above discussion, in this thesis we are interested in further exploring the ability of the conforming and fully nonconforming VEM to approximate fourth-order problems that arise in fluid mechanics, considering the stream-function approach.

We summarize below the contributions of our study.

The stationary quasi-geostrophic equations of the ocean

The quasi-geostrophic equations (QGE) is a fundamental mathematical model used to describe the large scale wind-driven motions of the ocean. It is a simplified model that is particularly useful for understanding the dynamics of geophysical fluid flows in the Earths oceans (see for instance [124, 145, 156]) and due to their important role and applicability in the climate dynamics, in recent years there has been an increasing focus on the development of efficient numerical schemes to solve such equations. For instance, in the last decades several work developed discretization for this model formulated in terms of the vorticity–stream-function variables [69, 93, 130]. However, more recently the authors in [95] have been presented and analyzed for first time a FEM for these equations in pure stream-function formulation, which corresponds to a nonlinear Partial Differential Equation (PDE) of fourth-order (cf. (2.2.1)). This FE scheme is based on the conforming Argyris element. Moreover, in [113, 110, 10, 112, 111] other conforming and nonconforming FEMs have been designed to solve the stationary QGE.

In **Chapter** 2, we propose and analyze a C^1-conforming VEM to solve the stationary quasi-geostrophic equations with applications in the large scale wind-driven ocean circulation, formulated in terms of the stream-function. The C^1 virtual space and the discrete scheme are built in a straightforward way due to the flexibility of the virtual approach. Under the assumption of small data, we prove the well-posedness of the discrete problem using a fixed-point strategy and under standard assumptions on the computational domain, we establish error estimates in H^2-norm for the stream-function. Finally, we report four numerical experiments that illustrate the behaviour of the proposed scheme and confirm our theoretical results on different families of polygonal meshes.

The results contained in this chapter gave rise to the following article:

➤ D. Mora and A. Silgado, *A C^1 virtual element method for the stationary quasi-geostrophic equations of the ocean*, Comput. Math. Appl., **116** (2022), pp. 212–228.

The stream-function formulation of the Oseen equations

The Oseen equations results from a linearization of the steady (or alternatively from the implicit Euler time-discretization of the unsteady) Navier–Stokes problem. This equation provides a simplified yet accurate representation of fluid flow under certain conditions and has been instrumental in various engineering and scientific applications.

In the last year, several work have been devoted to the development and analysis of Galerkin schemes for the numerical solution of the Oseen equations employing different formulations. In particular, we mention [8, 13, 23, 24, 25, 52, 61, 78, 73, 94], where HHO, classical and stabilized FEMs, Least-squares methods, among others have been proposed.

In **Chapter** 3, we analyze VEMs to solve the Oseen equations in terms of the stream-function on simply connected polygonal domains. The methods are based on a C^1-conforming virtual discretization of arbitrary order $k \geq 2$. Under standard assumptions on the computational domain, we establish that the resulting schemes converge with an optimal order in H^2-norm. The proposed methods have the advantages of using general polygonal meshes and the possibility to compute further variables of interest, such as the velocity, the vorticity and the pressure. Finally, we report some numerical tests illustrating the behavior of the virtual schemes and supporting our theoretical results on different families of polygonal meshes.

The results contained in this work are in the following book chapter:

➤ D. Mora and A. Silgado, *Virtual element methods for a stream-function formulation of the Oseen equations.* In: Antonietti, P.F., Beirão da Veiga, L., Manzini, G. (eds), The Virtual Element Method and its Applications. SEMA SIMAI Springer Series, vol 31, pp. 321-361, (2022). Springer, Cham.

The stationary Navier-Stokes equations in stream-function formulation

The Navier-Stokes is one of most important and challenging problems in fluid mechanics. This system describes the motion of a viscous incompressible fluid in a medium. Mathematically, the standard model corresponds to a combination of the conservation of mass and a nonlinear PDEs, where the velocity and pressure are the unknowns, which is called the momentum equation (see (6.1.1)). The analytic solution of this system continues to be a paradigm in fluid flow problems. Thus, due to its importance and applicability, several numerical methods have been developed to approximate its solution. Among these schemes, we mention classical Galerkin methods in mixed form used to discretize its standard formulation in terms of the primitive variables velocity and pressure. In this framework, the discrete spaces must be constructed appropriately to satisfy the inf-sup condition, ensuring the well-posedness of the mixed discrete formulation (see [103]).

Another desirable yet restrictive condition for these schemes is the one associated with the incompressibility requirement, a scenario in which the error components are partly decouple (but indirectly in the load term approximation) and for which different approaches have been devoted to the construction of schemes satisfying this property (see for instance the review [109]).

As we discussed previously, by introducing the stream-function variable ψ (cf. (1.1.1)), the typical velocity-pressure form is reduced in a single nonlinear fourth-order PDEs (cf. (4.1.1)). For this formulation the discretization does not need the construction of discrete stable spaces satisfying the inf-sup condition, in addition the incompressibility constraint is automatically satisfied. Below we mention some works discretizing this formulation by using conforming and nonconforming FEMs [71, 72, 90, 91, 92, 68].

Motivated in the above discussion (and in the facts mentioned in the initial sections), we are interesting in keeping on exploring the flexibility and ability of VEM to solve the Navier-Stokes equation in stream-function formulation. In particular, we propose novel C^1-VEMs and a new Morley-type VEM to discretize this problem.

In **Chapter** 4, C^1-VEMs of arbitrary order $k \geq 2$ for the two-dimensional Navier-Stokes equations in stream-function form are proposed and analyzed. A novel analysis is developed to prove optimal error estimates in H^2-, H^1- and L^2-norms, under *minimal regularity* condition on the weak stream-function solution. Moreover, we extend these schemes to the system with boundary conditions on the pressure. Strategies to compute the velocity, pressure and vorticity fields as a postprocess of the discrete stream-function are proposed and optimal error estimates have been established for these variables. The theoretical findings are further confirmed via illustrative numerical experiments on different families of polygonal meshes.

The results of this conforming approach are in the following submitted article:

- D. Mora and A. Silgado, *Virtual elements for the Navier-Stokes system: stream-function form and primitive variables recovery algorithms*, submitted for publication (2023).

On the other hand, in **Chapter** 6, we propose an alternative to discretize the Navier-Stokes equations in stream-function form. Indeed, we design a nonconforming Morley-type virtual element method for solving such system on simply connected polygonal domains (not necessarily convex). A rigorous analysis by using a new *enriching operator* is developed. More precisely, by employing such operator, we provide novel discrete Sobolev embeddings, which allow to establish the well-posedness of the discrete scheme and obtain optimal error estimates in broken H^2-, H^1- and L^2-norms under *minimal regularity* condition on the weak solution. The velocity and vorticity fields are recovered via postprocessing formulas. Furthermore, a new algorithm for pressure recovery based on a Stokes complex sequence is presented. Optimal error estimates are obtained for all the postprocessed variables. Finally, the theoretical error bounds and the good performance of the method are validated through several benchmark tests.

The results with this nonconforming approach are in the following article:

➤ D. Adak, D. Mora and A. Silgado, *The Morley-type virtual element method for the Navier-Stokes equations in stream-function form*, Comput. Methods Appl. Mech. Engrg., 419 (2024), Paper No. 116573.

The nonstationary Boussinesq system in stream-function form

The Boussinesq system describes the behavior of fluid flow in the presence of buoyancy effects. This system are particularly useful for studying natural convection phenomena, where fluids experience motion due to differences in temperature. The primary focus of these equations is to capture the interplay between the pressure, velocity, and temperature fields in the fluid domain. This model is a valuable tool in understanding and predicting the complex behavior of fluids under the influence of buoyancy forces and have numerous applications in areas such as meteorology, environmental, industrial and engineering process, among others.

Due to its relevance and presence in the different applications mentioned above, many works have been devoted to studying these equations (and some variants). For instance, regarding the analysis of stability and regularity, we refer to [140, 121]. Besides, over the last decades several numerical schemes have been developed to approximate this problem in its steady and/or unsteady regimens, considering temperature-dependent parameters, and using the classical velocity–pressure–temperature and pseudostress–velocity–temperature formulations, see for instance [47, 50, 150, 161, 144, 9, 82, 85, 11] and the references therein. In addition, some numerical work have been devoted to approximate these equation by using the stream-function–vorticity approaches, see for instance [148, 152, 120, 160].

In **Chapter** 5, we propose and analyze fully-coupled virtual element approximations of high order for solving the two dimensional nonstationary Boussinesq system in terms only of the stream-function and temperature fields. The discretization for the spatial variables is based on the coupling C^1- and C^0-conforming virtual element approaches, while a backward Euler scheme is employed for the temporal variable. Well-posedness and unconditional stability of the fully-discrete problem are provided. Moreover, error estimates in $\mathrm{L}^2(\mathrm{H}^2) \cap \mathrm{L}^\infty(\mathrm{H}^1)$ and $\mathrm{L}^2(\mathrm{H}^1) \cap \mathrm{L}^\infty(\mathrm{L}^2)$-norms are derived for the stream-function and temperature, respectively. Finally, a set of benchmark tests are reported to confirm the theoretical error bounds and illustrate the behavior of the fully-discrete scheme.

The results contained in this chapter are in the following article:

➤ L. Beirão da Veiga, D. Mora and A. Silgado, *A fully-discrete virtual element method for the nonstationary Boussinesq equations in stream-function form*, Comput.

Methods Appl. Mech. Engrg., 408 (2023), Paper No. 115947.

1.3 Preliminary notations

In this section we will introduce some preliminary notations that will be used throughout this thesis, including those already employed above. Thenceforth, Ω will denote a simply connected, open and bounded domain of $\mathbb{R}^2$, with polygonal Lipschitz-continuous boundary $\Gamma := \partial\Omega$. The vector $\mathbf{n} = (n_i)_{1\le i\le 2}$ will denote the outward unit normal vector to the boundary Γ, while $\mathbf{t} = (t_i)_{i=1,2} := (-n_2, n_1)$ denote the unit tangent vector to Γ. Moreover, we denote by $\partial_{\mathbf{n}}$ and $\partial_{\mathbf{t}}$ the normal and tangential derivatives, respectively.

According to [6], for any open measurable bounded domain $\mathcal{D} \subseteq \Omega$, with Lipschitz-continuous boundary we will employ the usual notation for the Banach spaces $\mathrm{L}^p(\mathcal{D})$ and the Sobolev spaces $\mathrm{W}^s_p(\mathcal{D})$, with $s \ge 0$ and $p \in [1, +\infty]$, with the corresponding seminorms and norms are denoted by $|\cdot|_{\mathrm{W}^s_p(\mathcal{D})}$ and $\|\cdot\|_{\mathrm{W}^s_p(\mathcal{D})}$, respectively. We adopt the convention $\mathrm{W}^0_p(\mathcal{D}) := \mathrm{L}^p(\mathcal{D})$ and in particular when $p = 2$, we write $\mathrm{H}^s(\mathcal{D})$ instead to $\mathrm{W}^s_2(\mathcal{D})$, the corresponding seminorm and norm of these space will be denoted by $|\cdot|_{s,\mathcal{D}}$ and $\|\cdot\|_{s,\mathcal{D}}$, respectively. Furthermore, for any integer $\ell \ge 0$ denote by $\mathbb{P}_\ell(\mathcal{D})$ the space of polynomials of degree up to ℓ defined on an open bounded subdomain $\mathcal{D} \subset \mathbb{R}^2$.

In addition, we denote by $\mathbf{S}$ the corresponding vectorial version of a generic scalar S space, examples of this are: $\mathbf{W}^s_p(\mathcal{D}) := [\mathrm{W}^s_p(\mathcal{D})]^2$ and $\mathbf{P}_\ell(\mathcal{D}) = [\mathbb{P}_\ell(\mathcal{D})]^2$.

For any tensor fields $\boldsymbol{\tau} = (\tau_{ij})_{i,j=1,2}$ and $\boldsymbol{\sigma} = (\sigma_{ij})_{i,j=1,2}$, we consider the standard scalar product of 2×2-matrices: $\boldsymbol{\tau} : \boldsymbol{\sigma} = \sum_{i=1}^2 \tau_{ij}\sigma_{ij}$. Moreover, for any scalar field φ and vector fields $\mathbf{v} = (v_i)_{i=1,2}, \mathbf{w} = (w_i)_{i=1,2}$, the scalar, vectorial and tensorial L^2-inner products will be denoted by

$$(\varphi, \phi)_{0,\mathcal{D}} = \int_{\mathcal{D}} \varphi\, \phi \,\mathrm{d}\mathcal{D}, \qquad (\mathbf{v}, \mathbf{w})_{0,\mathcal{D}} = \int_{\mathcal{D}} \mathbf{v}\cdot\mathbf{w}\,\mathrm{d}\mathcal{D}, \qquad (\boldsymbol{\tau}, \boldsymbol{\sigma})_{0,\mathcal{D}} = \int_{\mathcal{D}} \boldsymbol{\tau} : \boldsymbol{\sigma}\,\mathrm{d}\mathcal{D}.$$

We recall the following differential operators (gradients, curl, matrix Hessian, divergence and rotational):

$$\nabla\varphi := \begin{pmatrix} \partial_1\varphi \\ \partial_2\varphi \end{pmatrix}, \qquad \mathbf{curl}\,\varphi := \begin{pmatrix} \partial_2\varphi \\ -\partial_1\varphi \end{pmatrix}, \qquad \mathrm{D}^2\varphi := (\partial_{ij}\varphi)_{i,j=1,2}$$
$$\boldsymbol{\nabla}\mathbf{v} := (\partial_i v_j)_{i,j=1,2}, \quad \operatorname{div}\mathbf{v} := \partial_1 v_1 + \partial_2 v_2, \quad \operatorname{rot}\mathbf{v} := \partial_1 v_2 - \partial_2 v_1.$$

Besides, the Laplacian and Bilaplacian operators are defined by $\Delta\varphi := \operatorname{div}(\nabla\varphi)$ and $\Delta^2\varphi := \Delta(\Delta\varphi)$, respectively. The bold symbols $\boldsymbol{\nabla}$ and $\boldsymbol{\Delta}$ denote the gradient and Laplacian operators for vector fields, respectively.

On the other hand. From the Green Theorem, for all $q \in \mathrm{H}^1(\mathcal{D})$, $u \in \mathrm{H}^2(\mathcal{D})$ and for any $\mathbf{v} \in \mathbf{H}^1(\mathcal{D})$, we have the following integration by parts.

$$\int_{\mathcal{D}} \nabla q\cdot\mathbf{v} = -\int_{\mathcal{D}} q \operatorname{div}\mathbf{v} + \int_{\partial\mathcal{D}} q\,(\mathbf{v}\cdot\mathbf{n}_{\mathcal{D}}),$$
$$\int_{\mathcal{D}} q\,\Delta u = -\int_{\mathcal{D}} \nabla u\cdot\nabla q + \int_{\partial\mathcal{D}} q\partial_{\mathbf{n}_{\mathcal{D}}} u,$$
$$\int_{\mathcal{D}} \mathbf{curl}\, q\cdot\mathbf{v} = \int_{\mathcal{D}} q \operatorname{rot}\mathbf{v} + \int_{\partial\mathcal{D}} q\,(\mathbf{v}\cdot\mathbf{t}_{\mathcal{D}}).$$

For the evolution problem studied in **Chapter 5**, we will denote by t the temporal variable with values in the interval $I := (0, T]$, where $T > 0$ is a given final time. Moreover, given a Banach space V endowed with the norm $\|\cdot\|_V$, we define the space $\mathrm{L}^p(0, T; V)$ as the space of classes of functions $\phi : (0, T) \to V$ that are Bochner measurable and such that $\|\phi\|_{\mathrm{L}^p(0,T;V)} < \infty$, with

$$\|\phi\|_{\mathrm{L}^p(0,T;V)} := \left(\int_0^T \|\phi(t)\|_V^p \mathrm{d}t \right)^{1/p} \quad \text{and} \quad \|\phi\|_{\mathrm{L}^\infty(0,T;V)} := \operatorname*{ess\,sup}_{t \in [0,T]} \|\phi(t)\|_V .$$

In what follows, c and C, with or without subscripts, tildes, or hats, will represent a generic constant independent of the mesh parameter h, that might have distinct values in different occurrences.

Chapter 2

A C^1 virtual element method for the stationary quasi-geostrophic equations of the ocean

2.1 Introduction

The quasi-geostrophic equations (QGE) is one of the popular mathematical models employed for understanding the behavior of the large scale wind-driven ocean circulation [124, 145, 156]. Due to their important role in the climate system, there has been a growing interest in recent years towards developing efficient numerical schemes to solve such equations. We are going to consider the so-called one-layer QGE (also called as the barotropic vorticity equation), where the flow is assumed to be homogeneous in the vertical direction. Thus, stratification effects are ignored in this model and a bi-dimensional nonlinear fourth order partial differential equation, in terms of the stream-function variable, can be written. Despite the simplifications, the model preserves many of the essential features of the underlying large scale ocean flows. Further details related to the derivation of these equations can be found in [123, 129]. On the other hand, we note that the QGE equations can be seen as an extension of the stream-function formulation of the Navier–Stokes equations (NSE).

Different finite element discretizations have been developed recently for these equations. For instance, in [95] is presented a conforming finite element based on the Argyris element, optimal error estimates are obtained and several numerical experiment are reported. In [113] the authors present a B-spline based conforming finite element method to approximate the stream-function, also several numerical simulations are performed. Error estimates for this method are presented in [110] and a posteriori error analysis has been recently analyzed in [10]. In [112], is presented a non-conforming C^0-discontinuous Galerkin method, the authors introduced the new variational form of the method and they established consistency and error estimates. In addition, the quasi-geostrophic equations have been solved by using different finite element methods in terms of the stream-function and vorticity variables in the following references [69, 93, 130, 132]. Moreover, finite element methods for the Navier–Stokes equations in stream-function formulation have been presented in [71, 72, 90, 92].

It is well known that conforming finite element spaces of H^2 are of complex implementation and contain high order polynomials (see [79]). In order to overcome this drawback, in this work, we extend the virtual element approach proposed in [18] for the numerical solution of the QGE equations in stream-function formulation, which can be applied to general polygonal meshes and is simple in terms of degrees of freedom and coding aspects. In fact, it has been shown that the VEM permits to easily implement highly regular discrete spaces on general polygonal meshes. For instance, global discrete virtual spaces of H^2 to solve fourth order PDEs have been presented in [18, 58, 77] (see also [38, 135]). Moreover, it has been recently presented in [30] a C^1 virtual element method on polyhedral meshes. The numerical solution by virtual elements of incompressible flow problems (Stokes, Brinkman, Stokes–Darcy and Navier–Stokes equations) have been recently developed in the following references [17, 34, 35, 41, 59, 64, 76, 84, 98, 117, 118, 154, 164].

According to the above discussion, in the present contribution, we are interested in keeping on exploring the flexibility of the VEM to solve the QGE equations with applications in oceanic circulation. More precisely, we propose and analyze a conforming C^1 virtual element discretization of lowest order, which is based on the virtual space introduced in [18], to solve the quasi-geostrophic equations in stream-function formulation. We observe that the functions, in the virtual space, have continuous trace and the trace of the gradient is also continuous; thus, the method delivers a conforming solution. We write a discrete formulation by using projector operators to construct discrete version of the local bilinear forms and trilinear form along with a discrete load term.

We prove well-posedness of the discrete virtual formulation by using the Banach fixed-point Theorem and assuming that the data is in a certain sense small enough. We write error estimates in H^2-norm for the stream-function under rather mild assumptions on the polygonal meshes. Finally, we point out that, the present analysis for the stationary QGE equations constitutes a stepping-stone towards others related problems. For instance, two-layer quasi-geostrophic model [130] or time dependent QGE equations [96].

This chapter is organized as follows: In Section 2.2, we recall the quasi-geostrophic equations in terms of the stream-function and introduce the corresponding variational formulation for the system. In Section 2.3, we present the C^1-virtual element discretization of the variational formulation. Under the assumption of small data, we prove the existence and uniqueness of the discrete problem by using the Banach fixed-point Theorem. In Section 2.4, we establish error estimates for the stream-function. Four numerical tests that allow us to assess the convergence properties of the method and to check whether the experimental rates of convergence agree with the theoretical ones are reported in Section 2.5.

2.2 The model problem

We consider the steady one-layer quasi-geostrophic equations in stream-function formulation (for further details, see for instance [95]):

$$\begin{aligned} \mathrm{Re}^{-1}\Delta^2\psi - \mathbf{curl}\,\psi\cdot\nabla(\Delta\psi) - \mathrm{Ro}^{-1}\partial_x\psi &= \mathrm{Ro}^{-1}f \qquad \text{in } \Omega,\\ \psi = \partial_{\mathbf{n}}\psi &= 0 \qquad\quad\;\; \text{on } \Gamma, \end{aligned} \tag{2.2.1}$$

where ψ is the stream-function of the velocity field $\mathbf{u}$, i.e., $\mathbf{u} = \mathbf{curl}\,\psi$, and f is the source term. The constants Re and Ro denote the Reynolds and Rossby numbers, respectively. These parameters are defined by (see [95, 104, 106]):

$$\mathrm{Re} := \frac{U\,L}{A_H} \qquad \text{and} \qquad \mathrm{Ro} := \frac{U}{\beta\,L^2},$$

where the coefficient β is the coefficient multiplying the y-coordinate in the β-plane (see [156]), L is the characteristic length scale, U is the characteristic velocity scale and A_H is the eddy viscosity parametrization.

In order to write a weak formulation of problem (2.2.1), we consider the following space:

$$X := \left\{\phi \in \mathrm{H}^2(\Omega) : \phi = \partial_{\mathbf{n}}\phi = 0 \quad \text{on} \quad \Gamma\right\}.$$

We endow the space X with the following norm

$$\|\phi\|_X := |\phi|_{2,\Omega} \qquad \forall \phi \in X.$$

Now, we multiply the corresponding equation by a test function $\phi \in X$, integrate twice by parts in Ω and using the boundary conditions, we obtain the following variational problem: find $\psi \in X$ such that:

$$\mathrm{Re}^{-1}A(\psi,\phi) + B(\psi;\psi,\phi) - \mathrm{Ro}^{-1}C(\psi,\phi) = \mathrm{Ro}^{-1}F(\phi) \qquad \forall \phi \in X, \tag{2.2.2}$$

where $A, C : X \times X \to \mathbb{R}$ are bilinear forms, $B : X \times X \times X \to \mathbb{R}$ is a trilinear form and $F : X \to \mathbb{R}$ is a linear functional, defined as follows:

$$A(\psi,\phi) := \int_\Omega \mathrm{D}^2\psi : \mathrm{D}^2\phi \qquad \forall \psi,\phi \in X, \tag{2.2.3}$$

$$B(\zeta;\psi,\phi) := \int_\Omega \Delta\zeta\, \mathbf{curl}\,\psi \cdot \nabla\phi \qquad \forall \zeta,\psi,\phi \in X, \tag{2.2.4}$$

$$C(\psi,\phi) := \int_\Omega \partial_x\psi\,\phi \qquad \forall \psi,\phi \in X, \tag{2.2.5}$$

$$F(\phi) := \int_\Omega f\,\phi \qquad \forall \phi \in X. \tag{2.2.6}$$

Using integration by part and the boundary conditions, it is easy to see that the bilinear form $C(\cdot,\cdot)$ defined in (2.2.5) satisfies,

$$C(\psi,\phi) = -\,C(\phi,\psi) \qquad \forall \psi,\phi \in X.$$

Now, we introduce the following bilinear form $C_{\mathrm{skew}} : X \times X \to \mathbb{R}$:

$$C_{\mathrm{skew}}(\psi,\phi) := \frac{1}{2}C(\psi,\phi) - \frac{1}{2}C(\phi,\psi) = \frac{1}{2}\int_\Omega \partial_x\psi\,\phi - \frac{1}{2}\int_\Omega \partial_x\phi\,\psi \qquad \forall \psi,\phi \in X. \tag{2.2.7}$$

Clearly

$$C_{\mathrm{skew}}(\psi,\phi) = C(\psi,\phi) \qquad \forall \psi,\phi \in X.$$

Thus, according to the above equality, we rewrite the variational problem (2.2.2) in the following equivalent weak form: find $\psi \in X$ such that:

$$\mathrm{Re}^{-1}A(\psi,\phi) + B(\psi;\psi,\phi) - \mathrm{Ro}^{-1}C_{\mathrm{skew}}(\psi,\phi) = \mathrm{Ro}^{-1}F(\phi) \qquad \forall \phi \in X. \tag{2.2.8}$$

Remark 2.2.1. *We observe that our VEM discretization will be based on the above weak form. In particular, to discretize the skew-symmetric bilinear form $C_{\mathrm{skew}}(\cdot,\cdot)$ (cf. (2.2.7)), we construct a simple discrete form that preserves the skew-symmetry property at discrete level, which makes the analysis of the method simpler. For instance, we observe that the analysis of existence and uniqueness of the discrete problem and the convergence analysis of the method (see Sections 2.3.3 and 2.4, respectively) are facilitated using the skew-symmetric bilinear form.*

The following lemma establishes some properties for the forms defined in (2.2.3), (2.2.4), (2.2.6) and (2.2.7), these properties will play an important role in the forthcoming sections.

Lemma 2.2.1. *There exist positive constants $\widehat{C}_B, \widehat{C}_1$ such that*

$$
\begin{aligned}
|A(\psi,\phi)| &\leq \|\psi\|_X\|\phi\|_X && \forall \psi,\phi\in X, && (2.2.9)\\
A(\phi,\phi) &\geq \|\phi\|_X^2 && \forall \phi\in X, && (2.2.10)\\
|B(\zeta;\psi,\phi)| &\leq \widehat{C}_B\,\|\zeta\|_X\|\psi\|_X\|\phi\|_X && \forall \zeta,\psi,\phi\in X, && (2.2.11)\\
B(\zeta;\psi,\phi) &= -B(\zeta;\phi,\psi) && \forall \zeta,\psi,\phi\in X, && (2.2.12)\\
B(\zeta;\phi,\phi) &= 0 && \forall \zeta,\phi\in X, && (2.2.13)\\
|C_{\text{skew}}(\psi,\phi)| &\leq \widehat{C}_1\,\|\psi\|_X\|\phi\|_X && \forall \psi,\phi\in X, && (2.2.14)\\
C_{\text{skew}}(\phi,\phi) &= 0 && \forall \phi\in X, && (2.2.15)\\
|F(\phi)| &\leq \|f\|_{-2,\Omega}\|\phi\|_X && \forall \phi\in X. && (2.2.16)
\end{aligned}
$$

Proof. The proof follows standard arguments. □

In order to prove the well-posedness of problem (2.2.8), we will employ a fixed-point strategy. Indeed, given $\zeta\in X$, we define the following operator

$$
\begin{aligned}
T : X &\longrightarrow X\\
\zeta &\longmapsto T(\zeta)=\varphi,
\end{aligned}
$$

where φ is the solution of the following linear problem: find $\varphi\in X$ such that

$$\mathcal{Q}_\zeta(\varphi,\phi)=\mathrm{Ro}^{-1}F(\phi)\qquad \forall\phi\in X, \tag{2.2.17}$$

where the bilinear form $\mathcal{Q}_\zeta(\cdot,\cdot)$ is given by

$$\mathcal{Q}_\zeta(\varphi,\phi):=\mathrm{Re}^{-1}A(\varphi,\phi)+B(\zeta;\varphi,\phi)-\mathrm{Ro}^{-1}C_{\text{skew}}(\varphi,\phi).$$

We note that $\psi\in X$ is a solution of problem (2.2.8) if and only if $T(\psi)=\psi$. Thus, to prove the well-posedness of (2.2.8), we will prove that T has a unique fixed point by means of the classical Banach fixed-point Theorem.

The following lemma establishes that the bilinear form $\mathcal{Q}_\zeta(\cdot,\cdot)$ is bounded and elliptic. Thus, operator T is well-defined.

Lemma 2.2.2. *There exists a positive constant $C_{\mathcal{Q}}$ such that*

$$\mathcal{Q}_\zeta(\varphi,\phi)\leq C_{\mathcal{Q}}\|\varphi\|_X\|\phi\|_X\qquad \forall\varphi,\phi\in X,$$

and

$$\mathcal{Q}_\zeta(\phi,\phi)\geq \mathrm{Re}^{-1}\|\phi\|_X^2\qquad \forall\phi\in X.$$

Proof. The result follows from Lemma 2.2.1. □

By a direct application of Lax-Milgram Theorem we conclude that problem (2.2.17) has a unique solution. In addition, from the definition of the continuous problem (cf. (2.2.17)), (2.2.13), (2.2.15) and (2.2.16), the following continuous dependence holds

$$\|\varphi\|_X\leq \mathrm{Ro}^{-1}\mathrm{Re}\,\|f\|_{-2,\Omega}.$$

Thus, operator T is well-defined.

In what follows, we will prove that T is a contraction mapping. Let $\delta := \mathrm{Ro}^{-1}\mathrm{Re}\|f\|_{-2,\Omega}$, then we consider the following bounded set

$$\mathcal{N} := \{\phi \in X : \|\phi\|_X \leq \delta\},$$

and using the previous lemma, we have that $T(\mathcal{N}) \subseteq \mathcal{N}$.

The following lemma establishes that T is a contraction mapping and hence, according to the Banach fixed-point Theorem, it has a unique fixed point in $\mathcal{N}$.

Lemma 2.2.3. *Assume that*

$$\widehat{C}_B \mathrm{Ro}^{-1}\mathrm{Re}^2\|f\|_{-2,\Omega} < 1. \tag{2.2.18}$$

Then, T is a contraction mapping in $\mathcal{N}$.

Proof. Let $\zeta_1, \psi_1, \zeta_2, \psi_2 \in \mathcal{N}$, such that

$$T(\zeta_1) = \psi_1 \qquad \text{and} \qquad T(\zeta_2) = \psi_2,$$

then from the definition of the operator $T(\cdot)$, we have

$$\mathrm{Re}^{-1}A(\psi_1,\phi) + B(\zeta_1;\psi_1,\phi) - \mathrm{Ro}^{-1}C_{\text{skew}}(\psi_1,\phi) = \mathrm{Ro}^{-1}F(\phi) \qquad \forall\phi \in X, \tag{2.2.19}$$

$$\mathrm{Re}^{-1}A(\psi_2,\phi) + B(\zeta_2;\psi_2,\phi) - \mathrm{Ro}^{-1}C_{\text{skew}}(\psi_2,\phi) = \mathrm{Ro}^{-1}F(\phi) \qquad \forall\phi \in X. \tag{2.2.20}$$

Subtracting (2.2.20) from (2.2.19), we get

$$\mathrm{Re}^{-1}A(\psi_1-\psi_2,\phi) + [B(\zeta_1;\psi_1,\phi) - B(\zeta_2;\psi_2,\phi)] - \mathrm{Ro}^{-1}C_{\text{skew}}(\psi_1-\psi_2,\phi) = 0 \quad \forall\phi \in X.$$

Now, taking $\phi := \psi_1 - \psi_2$ in the above equation, we have that $C_{\text{skew}}(\cdot,\cdot)$ vanishes (cf. (2.2.15)). Thus, we obtain

$$\mathrm{Re}^{-1}A(\psi_1-\psi_2,\psi_1-\psi_2) + B(\zeta_1;\psi_1,\psi_1-\psi_2) - B(\zeta_2;\psi_2,\psi_1-\psi_2) = 0.$$

Then, by adding and subtracting ψ_2 in the second term, we have

$$\begin{aligned}
0 =& \mathrm{Re}^{-1}A(\psi_1-\psi_2,\psi_1-\psi_2) + B(\zeta_1;\psi_1-\psi_2,\psi_1-\psi_2) + B(\zeta_1;\psi_2,\psi_1-\psi_2) \\
&- B(\zeta_2;\psi_2,\psi_1-\psi_2) \\
=& \mathrm{Re}^{-1}A(\psi_1-\psi_2,\psi_1-\psi_2) + B(\zeta_1;\psi_2,\psi_1-\psi_2) - B(\zeta_2;\psi_2,\psi_1-\psi_2) \\
=& \mathrm{Re}^{-1}A(\psi_1-\psi_2,\psi_1-\psi_2) + B(\zeta_1-\zeta_2;\psi_2,\psi_1-\psi_2),
\end{aligned}$$

where we have used (2.2.13). Therefore

$$\mathrm{Re}^{-1}A(\psi_1-\psi_2,\psi_1-\psi_2) = -B(\zeta_1-\zeta_2;\psi_2,\psi_1-\psi_2),$$

by using (2.2.10), (2.2.11) and the Cauchy-Schwarz inequality, we obtain

$$\mathrm{Re}^{-1}\|\psi_1-\psi_2\|_X^2 \leq \widehat{C}_B\|\psi_2\|_X\|\zeta_1-\zeta_2\|_X\|\psi_1-\psi_2\|_X,$$

then, using the fact that $\psi_2 \in \mathcal{N}$, we get

$$\|\psi_1-\psi_2\|_X \leq \widehat{C}_B\mathrm{Re}\left(\mathrm{Ro}^{-1}\mathrm{Re}\|f\|_{-2,\Omega}\right)\|\zeta_1-\zeta_2\|_X = \widehat{C}_B\mathrm{Ro}^{-1}\mathrm{Re}^2\|f\|_{-2,\Omega}\|\zeta_1-\zeta_2\|_X.$$

Therefore, according to assumption (2.2.18), we obtain that T is a contraction mapping, which concludes the proof. □

The following result follows from Lemma 2.2.3 and the Banach fixed-point Theorem.

Theorem 2.2.1. *If*

$$\lambda := \widehat{C}_B \,\mathrm{Re}^2\mathrm{Ro}^{-1}\|f\|_{-2,\Omega} < 1,$$

there exists a unique $\psi \in \mathcal{N}$ solution to problem (2.2.8), which satisfies the following continuous dependence

$$\|\psi\|_X \leq \mathrm{Re}\,\mathrm{Ro}^{-1}\|f\|_{-2,\Omega}.$$

In what follows, we will assume that the source term satisfies $f \in \mathrm{L}^2(\Omega)$. Now, we state an additional regularity result for the solution of problem (2.2.8). The proof of this result can be found in [111, Lemma 2.3] (see also [49]).

Theorem 2.2.2. *Let $\psi \in \mathcal{N}$ be the unique solution of problem (2.2.8). Then, there exist $s \in (1/2, 1]$ and $\widetilde{C} > 0$, such that $\psi \in \mathrm{H}^{2+s}(\Omega)$ and*

$$\|\psi\|_{2+s,\Omega} \leq \widetilde{C}\|f\|_{0,\Omega}.$$

2.3 The virtual element scheme

In the present section, we will introduce a C^1-virtual element discretization for the numerical approximation of (2.2.8). The discrete method will be based on the virtual space introduced in [18] for the Cahn–Hilliard equation.

We begin with some notations and assumptions to construct the projectors on polynomial spaces, which are going to be used to build a conforming virtual space of X and to construct the respective discrete bilinear forms, the discrete trilinear form and the discrete functional. Finally, we prove existence and uniqueness of the discrete formulation by using the Banach fixed-point Theorem.

Now, we have the standard mesh assumptions. Let $\{\mathcal{T}_h\}_{h>0}$ be a sequence of decompositions of Ω into general polygonal elements K. We will denote by h_K the diameter of the element K and by h the maximum of the diameters of all the elements of the mesh, i.e.,

$$h := \max_{K\in\mathcal{T}_h} h_K.$$

We denote by N_K the number of vertices of K, by e a generic edge of $\mathcal{T}_h$ and for all $e \in \partial K$, we define a unit normal vector $\mathbf{n}_K^e$ that points outside of K and a unit tangent vector $\mathbf{t}_K^e$.

2.3.1 Virtual spaces and polynomial projections

Now, for every polygon $K \in \mathcal{T}_h$, we introduce the following preliminary augmented local virtual space (see [18]):

$$\begin{aligned}\widetilde{X}_h(K) := \big\{\phi_h \in \mathrm{H}^2(K) : \Delta^2\phi_h \in \mathbb{P}_2(K), \phi_h|_{\partial K} \in C^0(\partial K), \phi_h|_e \in \mathbb{P}_3(e)\ \forall e \in \partial K,\\ \nabla\phi_h|_{\partial K} \in \boldsymbol{C}^0(\partial K), \partial_{\mathbf{n}_K^e}\phi_h|_e \in \mathbb{P}_1(e)\ \forall e \in \partial K\big\},\end{aligned}$$

Next, for a given $\phi_h \in \widetilde{X}_h(K)$, we introduce two sets $\mathbf{O_1}$ and $\mathbf{O_2}$ of linear operators from the local virtual space $\widetilde{X}_h(K)$ into $\mathbb{R}$:

- $\mathbf{O_1}$: contains linear operators evaluating ϕ_h at the N_K vertices of K;
- $\mathbf{O_2}$: contains linear operators evaluating $\nabla\phi_h$ at the N_K vertices of K.

Now, we decompose the bilinear form $A(\cdot,\cdot)$ as follows:

$$A(\varphi,\phi) = \sum_{K\in\mathcal{T}_h} A^K(\varphi,\phi) \qquad \forall\varphi,\phi\in X, \tag{2.3.1}$$

where

$$A^K(\varphi,\phi) = \int_K \mathrm{D}^2\varphi : \mathrm{D}^2\phi \qquad \forall\varphi,\phi\in \mathrm{H}^2(K). \tag{2.3.2}$$

In a similar way, we can decompose the forms $B(\cdot;\cdot,\cdot)$ and $C_{\text{skew}}(\cdot,\cdot)$, with the following local forms:

$$B^K(\zeta;\psi,\phi) := \int_K \Delta\zeta\,\mathbf{curl}\,\psi\cdot\nabla\phi \qquad \forall\zeta,\psi,\phi\in\mathrm{H}^2(K). \tag{2.3.3}$$

$$C^K_{\text{skew}}(\psi,\phi) = \frac{1}{2}\int_K \partial_x\psi\,\phi - \frac{1}{2}\int_K \partial_x\phi\,\psi \qquad \forall\psi,\phi\in\mathrm{H}^2(K). \tag{2.3.4}$$

Projection operators. The next step is to build some projector operators from the local virtual space onto $\mathbb{P}_2(K)$ to construct the discrete version of the local bilinear forms and trilinear form along with the discrete load term. The first projector will be constructed by using the local bilinear form (2.3.2). Indeed, for each polygon K, we define the projector $\Pi^{\mathrm{D}}_K : \widetilde{X}_h(K) \to \mathbb{P}_2(K) \subseteq \widetilde{X}_h(K)$ as follows: for each $\phi_h \in \widetilde{X}_h(K)$, $\Pi^{\mathrm{D}}_K\phi_h \in \mathbb{P}_2(K)$ is the solution of the following local problem (on each polygon K):

$$\begin{aligned} A^K(\Pi^{\mathrm{D}}_K\phi_h,q) &= A^K(\phi_h,q) \quad \forall q\in\mathbb{P}_2(K),\\ ((\Pi^{\mathrm{D}}_K\phi_h,q))_K &= ((\phi_h,q))_K \quad \forall q\in\mathbb{P}_1(K), \end{aligned}$$

where $((\varphi_h,\phi_h))_K$ is defined as follows:

$$((\varphi_h,\phi_h))_K := \sum_{i=1}^{N_K}\varphi_h(\mathbf{v}_i)\phi_h(\mathbf{v}_i) \qquad \forall\varphi_h,\phi_h\in C^0(\partial K),$$

with $\mathbf{v}_i$, $1\le i\le N_K$, being the vertices of K.

The following result establishes that the projector Π^{D}_K is computable using of the sets $\mathbf{O_1}$ and $\mathbf{O_2}$ (see [18]).

Lemma 2.3.1. *The operator $\Pi^{\mathrm{D}}_K : \widetilde{X}_h(K) \to \mathbb{P}_2(K)$ is explicitly computable for every $\phi_h \in \widetilde{X}_h(K)$, using only the information of the linear operators $\mathbf{O_1}$ and $\mathbf{O_2}$.*

Next, we introduce, for each $K\in\mathcal{T}_h$, our local enhanced virtual space as follows:

$$X_h(K) := \left\{\phi_h\in\widetilde{X}_h(K) : (\phi_h - \Pi^{\mathrm{D}}_K\phi_h, q)_{0,K} = 0, \quad \forall q\in\mathbb{P}_2(K)\right\}.$$

In the space $X_h(K)$, we have the following properties (for further details, see [18]):

- the sets of linear operators $\mathbf{O_1}$ and $\mathbf{O_2}$ constitutes a set of degrees of freedom;

- $\Pi^{\mathrm{D}}_K : X_h(K) \to \mathbb{P}_2(K)$ is well-defined and it is computable using the information the of degrees of freedom $\mathbf{O_1}$ and $\mathbf{O_2}$.

Now, for each $K \in \Omega_h$, we consider the L^2-projection onto $\mathbb{P}_2(K)$, defined as follows: for each $\phi \in \mathrm{L}^2(K), \Pi^2_K\phi \in \mathbb{P}_2(K)$ is the unique function such that

$$\int_K q\Pi^2_K\phi = \int_K q\phi \qquad \forall q \in \mathbb{P}_2(K). \tag{2.3.5}$$

We observe that, using the definition of the local space $X_h(K)$, for each $\phi \in X_h(K)$, the polynomial function $\Pi^2_K\phi \in \mathbb{P}_2(K)$ is fully computable. In fact, due to the particular property appearing in the definition of space $X_h(K)$, the right hand side in (2.3.5) is computable using $\Pi^{\mathrm{D}}_K\phi$. Actually, it is easy to check that on the space $X_h(K)$ the projectors $\Pi^2_K\phi$ and $\Pi^{\mathrm{D}}_K\phi$ are the same operator. In fact:

$$\int_K q\Pi^2_K\phi = \int_K q\,\Pi^{\mathrm{D}}_K\phi \qquad \forall q \in \mathbb{P}_2(K). \tag{2.3.6}$$

Now, we will consider the following projection onto the polynomial space $\mathbf{P}_1(K)$: we define $\boldsymbol{\Pi}^1_K : \mathbf{L}^2(K) \to \mathbf{P}_1(K)$, for each $\mathbf{v} \in \mathbf{L}^2(K)$ by

$$\int_K \boldsymbol{\Pi}^1_K\mathbf{v}\cdot\mathbf{q} = \int_K \mathbf{v}\cdot\mathbf{q} \qquad \forall \mathbf{q} \in \mathbf{P}_1(K). \tag{2.3.7}$$

Using integration by parts, it is easy to see that for any $\phi_h \in X_h(K)$, the vector functions $\boldsymbol{\Pi}^1_K\mathbf{curl}\,\phi_h \in \mathbf{P}_1(K)$ and $\boldsymbol{\Pi}^1_K\nabla\phi_h \in \mathbf{P}_1(K)$ can be explicitly computed from the degrees of freedom $\mathbf{O_1}$ and $\mathbf{O_2}$. In fact, for all $K \in \mathcal{T}_h$ and for all $\phi_h \in X_h(K)$, using integration by parts on the right hand side of (2.3.7) (with $\mathbf{curl}\,\phi_h$ instead of $\mathbf{v}$), we have

$$\begin{aligned}\int_K \mathbf{curl}\,\phi_h\cdot\mathbf{q} &= \int_K \phi_h\,\mathrm{rot}\,\mathbf{q} - \int_{\partial K}\phi_h(\mathbf{q}\cdot\mathbf{t}^e_K) \qquad \forall \mathbf{q} \in \mathbf{P}_1(K)\\ &= \mathrm{rot}\,\mathbf{q}\int_K(\Pi^{\mathrm{D}}_K\phi_h) - \int_{\partial K}\phi_h(\mathbf{q}\cdot\mathbf{t}^e_K) \qquad \forall \mathbf{q} \in \mathbf{P}_1(K),\end{aligned}$$

where we have used the definition of $\Pi^2_K\phi_h$ and (2.3.6). The first term on the right hand side above depends only on $\Pi^{\mathrm{D}}_K\phi_h$ and this depends only on the values of the degrees of freedom (see Lemma 2.3.1). The second term is an integral on the boundary of the element K, which is fully computable. Similarly, we have that $\boldsymbol{\Pi}^1_K\nabla\phi_h$ is fully computable from the degrees of freedom.

Also, we note that for each $\phi_h \in X_h(K)$ the projection function $\Pi^0_K\Delta\phi_h \in \mathbb{P}_0(K)$ is computable using the degrees of freedom $\mathbf{O_1}$ and $\mathbf{O_2}$. Indeed, for each $\phi_h \in X_h(K)$ and for all $q_0 \in \mathbb{P}_0(K)$ we have

$$\int_K q_0\,\Pi^0_K\Delta\phi_h = \int_K q_0\,\Delta\phi_h = \int_{\partial K} q_0\,\partial_{\mathbf{n}}\phi_h,$$

from the equality above with have that

$$\Pi^0_K\Delta\phi_h = \frac{1}{|K|}\int_{\partial K}\partial_{\mathbf{n}}\phi_h,$$

where $|K|$ denotes the area of polygon K.

Now, by combining the local spaces $X_h(K)$ and incorporating the homogeneous Dirichlet boundary conditions, we define the global virtual space for the numerical approximation of (2.2.8): for every decomposition $\mathcal{T}_h$ of Ω into polygons K, we define

$$X_h := \{\phi_h \in X : \ \phi_h|_K \in X_h(K)\}.$$

The degrees of freedom for X_h are:

- $\mathbf{OG_1}$: pointwise values of ϕ_h on all vertices of $\mathcal{T}_h$ excluding the vertices on Γ;
- $\mathbf{OG_2}$: pointwise values of $\nabla\phi_h$ on all vertices of $\mathcal{T}_h$ excluding the vertices on Γ.

2.3.2 Construction of the discrete forms

In this section, we will construct the discrete version of the continuous bilinear forms, the trilinear form and the right hand side, using the projection operators introduced in Section 2.3.1.

First, let $\mathcal{S}_{\mathrm{D}}^K(\cdot,\cdot)$ be any symmetric positive definite bilinear form to be chosen as to satisfy:

$$c_0 A^K(\phi_h,\phi_h) \leq \mathcal{S}_{\mathrm{D}}^K(\phi_h,\phi_h) \leq c_1 A^K(\phi_h,\phi_h) \qquad \forall \phi_h \in X_h(K), \text{ with } \Pi_K^{\mathrm{D}}\phi_h = 0, \tag{2.3.8}$$

with c_0 and c_1 positive constants independent of h and K.

Now, using the projector operator Π_K^{D} and the bilinear form $\mathcal{S}_{\mathrm{D}}^K(\cdot,\cdot)$, we introduce the following computable discrete local bilinear form:

$$A^{h,K}(\psi_h,\phi_h) := A^K\left(\Pi_K^{\mathrm{D}}\psi_h, \Pi_K^{\mathrm{D}}\phi_h\right) + \mathcal{S}_{\mathrm{D}}^K\left(\psi_h - \Pi_K^{\mathrm{D}}\psi_h, \phi_h - \Pi_K^{\mathrm{D}}\phi_h\right), \tag{2.3.9}$$

as an approximation of the continuous bilinear form $A^K(\cdot,\cdot)$ (cf. (2.3.1)).

We choose the following representation for the bilinear form $\mathcal{S}_{\mathrm{D}}^K(\cdot,\cdot)$ satisfying (2.3.8) (see [18, 135]):

$$\mathcal{S}_{\mathrm{D}}^K(\psi_h,\phi_h) := \sigma_{\mathrm{D}}^K \sum_{i=1}^{N_K} \left[\psi_h(\mathbf{v}_i)\phi_h(\mathbf{v}_i) + h_{\mathbf{v}_i}^2 \nabla\psi_h(\mathbf{v}_i)\cdot\nabla\phi_h(\mathbf{v}_i)\right] \quad \forall \psi_h,\phi_h \in X_h(K),$$

where $\mathbf{v}_1,\ldots,\mathbf{v}_{N_K}$ are the vertices of the element K, $h_{\mathbf{v}_i}$ corresponds to the maximum diameter of the elements with $\mathbf{v}_i$ as a vertex. The parameter σ_{D}^K is a multiplicative factor to take into account the h-scaling, for instance, in the numerical test we have taken σ_{D}^K as the trace of the matrix $A^K(\Pi_K^{\mathrm{D}}\psi_h, \Pi_K^{\mathrm{D}}\phi_h)$ (cf. (2.3.9)).

For the approximation of the local trilinear form $B^K(\cdot;\cdot,\cdot)$ (cf. (2.3.3)), we consider the following computable form:

$$B^{h,K}(\zeta_h;\psi_h,\phi_h) := \int_K \left[\left(\Pi_K^0\Delta\zeta_h\right)\left(\boldsymbol{\Pi}_K^1 \mathbf{curl}\,\psi_h\right)\right]\cdot \boldsymbol{\Pi}_K^1\nabla\phi_h \qquad \forall \zeta_h,\psi_h,\phi_h \in X_h(K). \tag{2.3.10}$$

For the approximation of the bilinear form $C_{\text{skew}}^K(\cdot,\cdot)$ (cf. (2.3.4)), we consider the skew-symmetric discrete local form:

$$C_{\text{skew}}^{h,K}(\psi_h,\phi_h) := \frac{1}{2}\int_K \Pi_K^2(\partial_x\psi_h)\,\Pi_K^2\phi_h - \frac{1}{2}\int_K \Pi_K^2\psi_h\,\Pi_K^2(\partial_x\phi_h). \tag{2.3.11}$$

We recall that all the above forms are computable using only the degrees of freedom $\mathbf{O_1}$ and $\mathbf{O_2}$.

Then, we define the global bilinear forms and trilinear form as follows:

$$A^h : X_h \times X_h \to \mathbb{R}, \quad A^h(\psi_h, \phi_h) := \sum_{K \in \mathcal{T}_h} A^{h,K}(\psi_h, \phi_h), \tag{2.3.12}$$

$$B^h : X_h \times X_h \times X_h \to \mathbb{R}, \quad B^h(\zeta_h; \psi_h, \phi_h) := \sum_{K \in \mathcal{T}_h} B^{h,K}(\zeta_h; \psi_h, \phi_h), \tag{2.3.13}$$

$$C^h_{\text{skew}} : X_h \times X_h \to \mathbb{R}, \quad C^h_{\text{skew}}(\psi_h, \phi_h) := \sum_{K \in \mathcal{T}_h} C^{h,K}_{\text{skew}}(\psi_h, \phi_h), \tag{2.3.14}$$

for all $\zeta_h, \psi_h, \phi_h \in X_h$. Moreover, we observe that the forms $B^h(\cdot;\cdot,\cdot)$ and $C^h_{\text{skew}}(\cdot,\cdot)$ can be extended to the whole X.

The next step consists in constructing a computable approximation of the right hand side (2.2.6), using the sets of degrees of freedom $\mathbf{O_1}$ and $\mathbf{O_2}$. With this aim, for each element K we define the following term:

$$F^{h,K}(\phi_h) := \int_K \Pi^2_K f \phi_h \equiv \int_K f\, \Pi^2_K \phi_h \qquad \forall \phi_h \in X_h(K),$$

where we have used the L^2-projection operator (2.3.5). Thus, we introduce the following approximation for the functional defined in (2.2.6):

$$F^h(\phi_h) := \sum_{K \in \mathcal{T}_h} F^{h,K}(\phi_h) \qquad \forall \phi_h \in X_h. \tag{2.3.15}$$

The following result establishes the classical consistency and stability properties for the discrete local bilinear forms.

Proposition 2.3.1. *The local bilinear forms $A^K(\cdot,\cdot)$, $A^{h,K}(\cdot,\cdot)$, $C^K_{\text{skew}}(\cdot,\cdot)$ and $C^{h,K}_{\text{skew}}(\cdot,\cdot)$, defined in (2.3.2), (2.3.9), (2.3.4) and (2.3.11), respectively, on each element K satisfies the following properties:*

- *Consistency: for all $h > 0$ and for all $K \in \mathcal{T}_h$, we have that*

$$A^{h,K}(q, \phi_h) = A^K(q, \phi_h) \qquad \forall q \in \mathbb{P}_2(K), \qquad \forall \phi_h \in X_h(K), \tag{2.3.16}$$

$$C^{h,K}_{\text{skew}}(q, \phi_h) = C^K_{\text{skew}}(q, \phi_h) \qquad \forall q \in \mathbb{P}_2(K), \qquad \forall \phi_h \in X_h(K), \tag{2.3.17}$$

- *Stability and boundedness: There exist positive constants α_1 and α_2, independent of h and K, such that:*

$$\alpha_1 A^K(\phi_h, \phi_h) \leq A^{h,K}(\phi_h, \phi_h) \leq \alpha_2 A^K(\phi_h, \phi_h) \qquad \forall \phi_h \in X_h(K). \tag{2.3.18}$$

Proof. The proof follows basically from the definition of the bilinear forms. We omit further details and we refer to [18, 27]. □

The following lemma, which can be seen as the discrete version of Lemma 2.2.1, establishes additional properties for the discrete forms.

Lemma 2.3.2. *There exist positive constants $\widehat{C_{B^h}}$, $\widehat{C}_2$ and C_1, independent of h, such that the forms defined in (2.3.12)-(2.3.15) satisfies the following properties:*

$$|A^h(\psi_h,\phi_h)| \leq \alpha_2 \,\|\psi_h\|_X\|\phi_h\|_X \qquad \forall \psi_h,\phi_h \in X_h, \tag{2.3.19}$$

$$A^h(\phi_h,\phi_h) \geq \alpha_1 \,\|\phi_h\|_X^2 \qquad \forall \phi_h \in X_h, \tag{2.3.20}$$

$$B^h(\zeta_h;\psi_h,\phi_h) \leq \widehat{C_{B^h}}\|\zeta_h\|_X\|\psi_h\|_X\|\phi_h\|_X \qquad \forall \zeta_h,\psi_h,\phi_h \in X_h, \tag{2.3.21}$$

$$B^h(\zeta_h;\phi_h,\phi_h) = 0, \qquad \forall \zeta_h,\phi_h \in X_h, \tag{2.3.22}$$

$$|C^h_{\text{skew}}(\psi_h,\phi_h)| \leq \widehat{C}_2 \,\|\psi_h\|_X\|\phi_h\|_X \qquad \forall \psi_h,\phi_h \in X_h, \tag{2.3.23}$$

$$C^h_{\text{skew}}(\phi_h,\phi_h) = 0, \qquad \forall \phi_h \in X_h, \tag{2.3.24}$$

$$|F^h(\phi_h)| \leq C_1\|f\|_{0,\Omega}\|\phi_h\|_X \qquad \forall \phi_h \in X_h. \tag{2.3.25}$$

Proof. Properties (2.3.19) and (2.3.20) follows from (2.3.18) and the ellipticity of the bilinear form $A^K(\cdot,\cdot)$. To prove property (2.3.21), we use the definition of the trilinear form $B^h(\cdot;\cdot,\cdot)$ (cf. (2.3.13)) and Hölder inequality, we have

$$\begin{aligned} B^h(\zeta_h;\psi_h,\phi_h) &= \sum_{K\in\mathcal{T}_h}\int_K \left[\left(\Pi^0_K\Delta\zeta_h\right)\left(\mathbf{\Pi}^1_K\mathbf{curl}\,\psi_h\right)\right]\cdot\mathbf{\Pi}^1_K\nabla\phi_h \\ &\leq \sum_{K\in\mathcal{T}_h}\|\Pi^0_K\Delta\zeta_h\|_{0,K}\|\mathbf{\Pi}^1_K\mathbf{curl}\,\psi_h\|_{\mathrm{L}^4(K)}\|\mathbf{\Pi}^1_K\nabla\phi_h\|_{\mathrm{L}^4(K)}. \end{aligned}$$

Using the continuity of the operator Π^0_K with respect to the L^2-norm and the continuity of the operator $\mathbf{\Pi}^1_K$ with respect to the L^4-norm (see [35]), we have

$$B^h(\zeta_h;\psi_h,\phi_h) \leq C\sum_{K\in\mathcal{T}_h}\|\Delta\zeta_h\|_{0,K}\|\mathbf{curl}\,\psi_h\|_{\mathrm{L}^4(K)}\|\nabla\phi_h\|_{\mathrm{L}^4(K)}.$$

Now, applying the Hölder inequality (for sequences), we obtain

$$\begin{aligned} B^h(\zeta_h;\psi_h,\phi_h) &\leq C\Big(\sum_{K\in\mathcal{T}_h}\|\Delta\zeta_h\|^2_{0,K}\Big)^{\frac{1}{2}}\Big(\sum_{K\in\mathcal{T}_h}\|\mathbf{curl}\,\psi_h\|^4_{\mathrm{L}^4(K)}\Big)^{\frac{1}{4}}\Big(\sum_{K\in\mathcal{T}_h}\|\nabla\phi_h\|^4_{\mathrm{L}^4(K)}\Big)^{\frac{1}{4}} \\ &\leq C\|\Delta\zeta_h\|_{0,\Omega}\|\mathbf{curl}\,\psi_h\|_{\mathrm{L}^4(\Omega)}\|\nabla\phi_h\|_{\mathrm{L}^4(\Omega)}. \end{aligned}$$

Then, by Sobolev embedding theorem, it holds that

$$B^h(\zeta_h;\psi_h,\phi_h) \leq \widehat{C_{B^h}}\|\zeta_h\|_X\|\psi_h\|_X\|\phi_h\|_X,$$

where $\widehat{C_{B^h}}$ is a constant independent of h.

Finally, (2.3.22)-(2.3.25) follows from the definition of the corresponding forms. We conclude the proof. □

2.3.3 Discrete problem and fixed-point strategy

In this section, we will write the discrete VEM formulation to solve the quasi-geostrophic equations presented in (2.2.8). Our scheme will be based on the discrete forms and the results introduced in the previous section. Then, we will analyze a point-fixed strategy to establish the existence and uniqueness of the discrete virtual scheme.

The discrete problem reads as follows: find $\psi_h \in X_h$, such that

$$\mathrm{Re}^{-1}A^h(\psi_h,\phi_h) + B^h(\psi_h;\psi_h,\phi_h) - \mathrm{Ro}^{-1}C^h_{\text{skew}}(\psi_h,\phi_h) = \mathrm{Ro}^{-1}F^h(\phi_h) \qquad \forall \phi_h \in X_h, \quad (2.3.26)$$

where $A^h(\cdot,\cdot)$ and $C^h_{\text{skew}}(\cdot,\cdot)$ are the discrete bilinear forms defined in (2.3.12) and (2.3.14), respectively, $B^h(\cdot;\cdot,\cdot)$ is the discrete trilinear form defined in (2.3.13), and $F^h(\cdot)$ is the functional introduced in (2.3.15).

In order to prove well-posedness of problem (2.3.26), we are going to use, as in the continuous case, a fixed-point strategy. Indeed, given $\zeta_h \in X_h$, we define the following operator

$$\begin{aligned} T^h : X_h &\longrightarrow X_h \\ \zeta_h &\longmapsto T^h(\zeta_h) = \psi_h, \end{aligned}$$

where ψ_h is the solution of the following linear problem: find $\psi_h \in X_h$ such that

$$\mathcal{Q}_{\zeta_h}(\psi_h,\phi_h) = \mathrm{Ro}^{-1}F^h(\phi_h) \qquad \forall \phi_h \in X_h, \quad (2.3.27)$$

where the bilinear form $\mathcal{Q}_{\zeta_h}(\cdot,\cdot)$ is given by

$$\mathcal{Q}_{\zeta_h}(\psi_h,\phi_h) := \mathrm{Re}^{-1}A^h(\psi_h,\phi_h) + B^h(\zeta_h;\psi_h,\phi_h) - \mathrm{Ro}^{-1}C^h_{\text{skew}}(\psi_h,\phi_h).$$

The following lemma establishes that the operator T^h is well-defined.

Lemma 2.3.3. *Given $\zeta_h \in X_h$, there exists a unique $\psi_h \in X_h$ such that $T^h(\zeta_h) = \psi_h$.*

Proof. We are going to use the Lax-Milgram Theorem to prove that problem (2.3.27) is well-posed. Indeed, using the properties (2.3.19), (2.3.21) and (2.3.23), we have that $\mathcal{Q}_{\zeta_h}(\cdot,\cdot)$ is bounded with a positive constant independent of h. On the other hand, for each $\phi_h \in X_h$, using (2.3.22) and (2.3.24), we have

$$\begin{aligned} \mathcal{Q}_{\zeta_h}(\phi_h,\phi_h) &= \mathrm{Re}^{-1}A^h(\phi_h,\phi_h) + B^h(\zeta_h;\phi_h,\phi_h) - \mathrm{Ro}^{-1}C^h_{\text{skew}}(\phi_h,\phi_h) \\ &= \mathrm{Re}^{-1}A^h(\phi_h,\phi_h) \\ &\geq \mathrm{Re}^{-1}\alpha_1\|\phi_h\|^2_X, \end{aligned}$$

where (2.3.20) has been used in the last inequality. Thus, by a direct application of the Lax-Milgram Theorem, we conclude that problem (2.3.27) has a unique solution $\psi_h \in X_h$. Moreover, from the definition of the discrete problem (cf. (2.3.27)), properties (2.3.22), (2.3.24) and (2.3.25), the following estimate holds

$$\|\psi_h\|_X \leq C_1\alpha_1^{-1}\,\mathrm{Ro}^{-1}\mathrm{Re}\,\|f\|_{0,\Omega}.$$

Therefore, operator T^h is well-defined. □

Now, we introduce the following set

$$\mathcal{N}_h := \{\phi_h \in X_h : \|\phi_h\|_X \leq R\},$$

where $R := C_1\alpha_1^{-1}\,\mathrm{Ro}^{-1}\mathrm{Re}\,\|f\|_{0,\Omega}$. As an immediate consequence of the previous lemma, we have that $T^h(\mathcal{N}_h) \subseteq \mathcal{N}_h$. Note that our discrete virtual scheme (2.3.26) is well-posed if only if operator T^h has a unique fixed point in $\mathcal{N}_h$.

The following lemma establishes that under some assumption on the data, the operator T^h is a contraction mapping in $\mathcal{N}_h$.

Lemma 2.3.4. *Assume that*

$$\frac{\widehat{C_{B^h}}C_1\mathrm{Ro}^{-1}\mathrm{Re}^2\|f\|_{0,\Omega}}{\alpha_1^2} < 1. \tag{2.3.28}$$

Then, T^h is a contraction mapping in $\mathcal{N}_h$.

Proof. Let $\zeta_h^1, \psi_h^1, \zeta_h^2, \psi_h^2 \in \mathcal{N}_h$, such that $T^h(\zeta_h^1) = \psi_h^1$ and $T^h(\zeta_h^2) = \psi_h^2$, then from the definition of the operator $T^h(\cdot)$, we have

$$\mathrm{Re}^{-1}A^h(\psi_h^1,\phi_h) + B^h(\zeta_h^1;\psi_h^1,\phi_h) - \mathrm{Ro}^{-1}C^h_{\mathrm{skew}}(\psi_h^1,\phi_h) = \mathrm{Ro}^{-1}F^h(\phi_h) \qquad \forall \phi_h \in \mathcal{N}_h, \tag{2.3.29}$$
$$\mathrm{Re}^{-1}A^h(\psi_h^2,\phi_h) + B^h(\zeta_h^2;\psi_h^2,\phi_h) - \mathrm{Ro}^{-1}C^h_{\mathrm{skew}}(\psi_h^2,\phi_h) = \mathrm{Ro}^{-1}F^h(\phi_h) \qquad \forall \phi_h \in \mathcal{N}_h. \tag{2.3.30}$$

Subtracting (2.3.30) from (2.3.29), due to the properties of the bilinear forms $A^h(\cdot,\cdot)$ and $C^h_{\mathrm{skew}}(\cdot,\cdot)$, we have that

$$\mathrm{Re}^{-1}A^h(\psi_h^1-\psi_h^2,\phi_h) + [B^h(\zeta_h^1;\psi_h^1,\phi_h) - B^h(\zeta_h^2;\psi_h^2,\phi_h)] - \mathrm{Ro}^{-1}C^h_{\mathrm{skew}}(\psi_h^1-\psi_h^2,\phi_h) = 0,$$

for all $\phi_h \in \mathcal{N}_h$. Now, taking $\phi_h := \psi_h^1 - \psi_h^2$ in the above equality, we have that $C^h_{\mathrm{skew}}(\cdot,\cdot)$ vanishes (cf. (2.3.24)). Thus, we obtain

$$\mathrm{Re}^{-1}A^h(\psi_h^1-\psi_h^2,\psi_h^1-\psi_h^2) + B^h(\zeta_h^1;\psi_h^1,\psi_h^1-\psi_h^2) - B^h(\zeta_h^2;\psi_h^2,\psi_h^1-\psi_h^2) = 0.$$

Then, adding and subtracting ψ_h^2 in the second term of the left hand above, we get

$$\begin{aligned}
0 =& \mathrm{Re}^{-1}A^h(\psi_h^1-\psi_h^2,\psi_h^1-\psi_h^2) + B^h(\zeta_h^1;\psi_h^1-\psi_h^2,\psi_h^1-\psi_h^2) + B^h(\zeta_h^1;\psi_h^2,\psi_h^1-\psi_h^2)\\
&- B^h(\zeta_h^2;\psi_h^2,\psi_h^1-\psi_h^2)\\
=& \mathrm{Re}^{-1}A^h(\psi_h^1-\psi_h^2,\psi_h^1-\psi_h^2) + B^h(\zeta_h^1;\psi_h^2,\psi_h^1-\psi_h^2) - B^h(\zeta_h^2;\psi_h^2,\psi_h^1-\psi_h^2)\\
=& \mathrm{Re}^{-1}A^h(\psi_h^1-\psi_h^2,\psi_h^1-\psi_h^2) + B^h(\zeta_h^1-\zeta_h^2;\psi_h^2,\psi_h^1-\psi_h^2),
\end{aligned}$$

where we have used (2.3.22). Then, we have

$$\mathrm{Re}^{-1}A^h(\psi_h^1-\psi_h^2,\psi_h^1-\psi_h^2) = -B^h(\zeta_h^1-\zeta_h^2;\psi_h^2,\psi_h^1-\psi_h^2),$$

then applying the Cauchy-Schwarz inequality, (2.3.20) and (2.3.21), we obtain

$$\mathrm{Re}^{-1}\alpha_1\|\psi_h^1-\psi_h^2\|_X^2 \le \widehat{C_{B^h}}\|\psi_h^2\|_X\|\zeta_h^1-\zeta_h^2\|_X\|\psi_h^1-\psi_h^2\|_X,$$

using the fact that $\psi_h^2 \in \mathcal{N}_h$, we obtain

$$\|\psi_h^1-\psi_h^2\|_X \le \frac{\widehat{C_{B^h}}C_1\mathrm{Ro}^{-1}\mathrm{Re}^2\|f\|_{0,\Omega}}{\alpha_1^2}\|\zeta_h^1-\zeta_h^2\|_X.$$

Thus, according to assumption (2.3.28), we have that T^h is a contraction mapping. The proof is complete. □

The following result is a direct consequence of Lemma 2.3.4 and the Banach fixed-point Theorem.

Theorem 2.3.1. *If*

$$\lambda_h := \frac{\widehat{C_{B^h}}C_1\mathrm{Ro}^{-1}\mathrm{Re}^2\|f\|_{0,\Omega}}{\alpha_1^2} < 1, \tag{2.3.31}$$

there exists a unique $\psi_h \in \mathcal{N}_h$ solution to problem (2.3.26), which satisfies the following continuous dependence

$$\|\psi_h\|_X \le \frac{C_1\mathrm{Ro}^{-1}\mathrm{Re}\,\|f\|_{0,\Omega}}{\alpha_1}.$$

2.4 Convergence analysis

In this section, we will analyze the convergence properties of the discrete virtual element scheme presented in Section 2.3.3. In the forthcoming analysis, we will make the following assumptions for the polygonal mesh $\mathcal{T}_h$: there exists a real number $C_{\mathcal{T}_h} > 0$ such that, for every h and every $K \in \mathcal{T}_h$ we have

A1 : $K \in \mathcal{T}_h$ is star-shaped with respect to every point of a ball of radius $C_{\mathcal{T}_h} h_K$;

A2 : the ratio between the shortest edge and the diameter h_K of K is larger than $C_{\mathcal{T}_h}$.

We introduce the following broken H^ℓ-seminorm, for each integer $\ell \geq 0$:

$$|\phi|_{\ell,h} := \Big(\sum_{K\in\mathcal{T}_h} |\phi|^2_{\ell,K} \Big)^{1/2},$$

which is well-defined for every $\phi \in \mathrm{L}^2(\Omega)$ such that $\phi|_K \in \mathrm{H}^\ell(K)$ for all polygon $K \in \mathcal{T}_h$.

The following approximation results will play a relevant role in our error analysis (see [18, 38, 54]).

Proposition 2.4.1. *Assume* **A2** *is satisfied, then there exists a constant $C > 0$, such that for every $\phi \in \mathrm{H}^\delta(K)$, there exists $\phi_\pi \in \mathbb{P}_2(K)$, such that*

$$|\phi - \phi_\pi|_{\ell,K} \leq C h_K^{\delta-\ell} |\phi|_{\delta,K}, \quad 0 \leq \delta \leq 3,\ \ell = 0, 1, \dots, [\delta],$$

where $[\delta]$ denotes the largest integer equal to or smaller than $\delta \in \mathbb{R}$.

Proposition 2.4.2. *Assume that* **A1** – **A2** *are satisfied. Then, for each $\phi \in \mathrm{H}^{2+s}(\Omega)$, with $s \in (1/2, 1]$ there exist $\phi_I \in X_h$ and $C > 0$, independent of h, such that*

$$\|\phi - \phi_I\|_X \leq C h^s |\phi|_{2+s,\Omega}.$$

Proof. The proof follows repeating the arguments from [38, Proposition 4.2] (see also [18, Proposition 3.1]). □

We will also use the following approximation property (see [35]):

Lemma 2.4.1. *Let $K \in \mathcal{T}_h$, and δ, p two real numbers such that $0 \leq \delta \leq 1$ and $1 < p \leq \infty$. Then, there exists a constant $C > 0$, independent of h_K, such that for every $\mathbf{v} \in \mathbf{W}^\delta_p(K)$*

$$|\mathbf{v} - \boldsymbol{\Pi}^1_K \mathbf{v}|_{\mathrm{L}^p(K)} \leq C h_K^\delta |\mathbf{v}|_{\mathrm{W}^\delta_p(K)}.$$

Now, we start with the following bound.

Proposition 2.4.3. *Let $f \in \mathrm{L}^2(\Omega)$ and let $F(\cdot)$ and $F^h(\cdot)$ be the functionals defined in (2.2.6) and (2.3.15), respectively. Then, we have the following estimate:*

$$\|F - F^h\|_{X_h'} := \sup_{\substack{\phi_h \in X_h \\ \phi_h \neq 0}} \frac{|F(\phi_h) - F^h(\phi_h)|}{\|\phi_h\|_X} \leq C h^2 \|f\|_{0,\Omega}.$$

Proof. The proof follows from the definition of the functionals $F(\cdot)$ and $F^h(\cdot)$, together with approximation properties of the projector Π_K^2. $\square$

The next step is to establish two technical results for the trilinear forms $B(\cdot;\cdot,\cdot)$ and $B^h(\cdot;\cdot,\cdot)$. We begin with the following lemma.

Lemma 2.4.2. *Let $v \in \mathrm{H}^{2+s}(\Omega) \cap X$, with $s \in (1/2, 1]$. Then for all $w \in X$, we have that*

$$|B(v;v,w) - B^h(v;v,w)| \leq Ch^s(\|v\|_{1+s,\Omega} + \|v\|_X)\|v\|_{2+s,\Omega}\|w\|_X.$$

Proof. Let $v \in \mathrm{H}^{2+s}(\Omega) \cap X$ and $w \in X$, then adding and subtracting suitable terms and using orthogonality properties of the projectors Π_K^0 and $\boldsymbol{\Pi}_K^1$, we have that

$$\begin{aligned}
B(v;v,w) - B^h(v;v,w) &= \sum_{K\in\mathcal{T}_h} \int_K \left[\Delta v\, \mathbf{curl}\, v \cdot \nabla w - \left(\Pi_K^0 \Delta v\, \boldsymbol{\Pi}_K^1 \mathbf{curl}\, v\right) \cdot \boldsymbol{\Pi}_K^1 \nabla w\right] \\
&= \sum_{K\in\mathcal{T}_h} \int_K \Delta v\, \mathbf{curl}\, v \cdot (\nabla w - \boldsymbol{\Pi}_K^1 \nabla w) \\
&\quad + \sum_{K\in\mathcal{T}_h} \int_K \left(\Delta v \left(\mathbf{curl}\, v - \boldsymbol{\Pi}_K^1 \mathbf{curl}\, v\right)\right) \cdot \boldsymbol{\Pi}_K^1 \nabla w \\
&\quad + \sum_{K\in\mathcal{T}_h} \int_K \left(\left(\Delta v - \Pi_K^0 \Delta v\right) \boldsymbol{\Pi}_K^1 \mathbf{curl}\, v\right) \cdot \boldsymbol{\Pi}_K^1 \nabla w \\
&=: T_1 + T_2 + T_3.
\end{aligned} \tag{2.4.1}$$

We will bound the terms in the last equality. Applying Hölder inequality and approximation properties of projector $\boldsymbol{\Pi}_K^1$ (see Lemma 2.4.1), we bound the term T_1 as follows

$$\begin{aligned}
T_1 &\leq \sum_{K\in\mathcal{T}_h} C\|\Delta v\|_{\mathrm{L}^4(K)} \|\mathbf{curl}\, v\|_{\mathrm{L}^4(K)} \|\nabla w - \boldsymbol{\Pi}_K^1 \nabla w\|_{0,K} \\
&\leq \sum_{K\in\mathcal{T}_h} C\|\Delta v\|_{\mathrm{L}^4(K)} \|\mathbf{curl}\, v\|_{\mathrm{L}^4(K)} Ch|\nabla w|_{1,K},
\end{aligned}$$

then using Hölder inequality (for sequences) and the fact that $\mathrm{H}^s(\Omega) \hookrightarrow \mathrm{L}^4(\Omega)$, we obtain that

$$\begin{aligned}
T_1 &\leq Ch\Big(\sum_{K\in\mathcal{T}_h} \|\Delta v\|_{\mathrm{L}^4(K)}^4\Big)^{\frac{1}{4}} \Big(\sum_{K\in\mathcal{T}_h} \|\mathbf{curl}\, v\|_{\mathrm{L}^4(K)}^4\Big)^{\frac{1}{4}} \Big(\sum_{K\in\mathcal{T}_h} |w|_{2,K}^2\Big)^{\frac{1}{2}} \\
&\leq Ch\|\Delta v\|_{\mathrm{L}^4(\Omega)} \|\mathbf{curl}\, v\|_{\mathrm{L}^4(\Omega)} \|w\|_X \\
&\leq Ch\|\Delta v\|_{s,\Omega} \|\mathbf{curl}\, v\|_{s,\Omega} \|w\|_X \\
&\leq Ch\|v\|_{2+s,\Omega} \|v\|_{1+s,\Omega} \|w\|_X.
\end{aligned} \tag{2.4.2}$$

Now, for the term T_2, we use again Hölder inequality, approximation properties of projector $\boldsymbol{\Pi}_K^1$ in Sobolev spaces (see Lemma 2.4.1), and continuity of $\boldsymbol{\Pi}_K^1$ with respect L^4-norm (see [35]), to get

$$\begin{aligned}
T_2 &\leq \sum_{K\in\mathcal{T}_h} C\|\Delta v\|_{0,K} \|\mathbf{curl}\, v - \boldsymbol{\Pi}_K^1 \mathbf{curl}\, v\|_{\mathrm{L}^4(K)} \|\boldsymbol{\Pi}_K^1 \nabla w\|_{\mathrm{L}^4(K)} \\
&\leq \sum_{K\in\mathcal{T}_h} C\|\Delta v\|_{0,K} h^s \|\mathbf{curl}\, v\|_{\mathrm{W}_4^s(K)} \|\nabla w\|_{\mathrm{L}^4(K)}.
\end{aligned}$$

Now, using again Hölder inequality (for sequences) and Sobolev embeddings $\mathrm{H}^s(\Omega) \hookrightarrow \mathrm{L}^4(\Omega)$ and $\mathrm{H}^{1+s}(\Omega) \hookrightarrow \mathrm{W}_4^s(\Omega)$, we obtain that

$$
\begin{aligned}
T_2 &\leq Ch^s\Big(\sum_{K\in\mathcal{T}_h}\|\Delta v\|_{0,K}^2\Big)^{\frac{1}{2}}\Big(\sum_{K\in\mathcal{T}_h}\|\mathbf{curl}\,v\|_{\mathrm{W}_4^s(K)}^4\Big)^{\frac{1}{4}}\Big(\sum_{K\in\mathcal{T}_h}\|\nabla w\|_{\mathrm{L}^4(K)}^4\Big)^{\frac{1}{4}} \\
&\leq Ch^s\|\Delta v\|_{0,\Omega}|\mathbf{curl}\,v|_{\mathrm{W}_4^s(\Omega)}\|\nabla w\|_{\mathrm{L}^4(\Omega)} \\
&\leq Ch^s\|v\|_X|\mathbf{curl}\,v|_{1+s,\Omega}\|w\|_X \\
&\leq Ch^s\|v\|_X\|v\|_{2+s,\Omega}\|w\|_X.
\end{aligned} \tag{2.4.3}
$$

We continue with the term T_3. We use Hölder inequality and the continuity of the projector $\mathbf{\Pi}_K^1$ with respect L^4-norm and the approximation property for projector Π_K^0, it holds that

$$
\begin{aligned}
T_3 &\leq \sum_{K\in\mathcal{T}_h} C\|\Delta v-\Pi_K^0\Delta v\|_{0,K}\|\mathbf{\Pi}_K^1\mathbf{curl}\,v\|_{\mathrm{L}^4(K)}\|\mathbf{\Pi}_K^1\nabla w\|_{\mathrm{L}^4(K)} \\
&\leq \sum_{K\in\mathcal{T}_h} Ch^s\|\Delta v\|_{s,K}\|\mathbf{curl}\,v\|_{\mathrm{L}^4(K)}\|\nabla w\|_{\mathrm{L}^4(K)}.
\end{aligned}
$$

By employing the Hölder inequality (for sequences) and Sobolev embedding theorem, we have that

$$
T_3 \leq Ch^s\|v\|_{2+s,\Omega}|v|_{1+s,\Omega}\|w\|_X. \tag{2.4.4}
$$

Finally, the proof follows from the estimates (2.4.2), (2.4.3), (2.4.4) and (2.4.1). □

Now, we state the second technical result.

Lemma 2.4.3. *For all $\zeta,\varphi,\phi\in X$ we have that*

$$
|B^h(\varphi;\varphi,\phi)-B^h(\zeta;\zeta,\phi)| \leq \widehat{C_{B^h}}\left(\|\zeta\|_X\|\phi\|_X+\|\varphi-\zeta+\phi\|_X(\|\varphi\|_X+\|\zeta\|_X)\right)\|\phi\|_X.
$$

Proof. Let $\zeta,\varphi,\phi\in X$. Then, adding and subtracting suitable terms, using the trilineality of the form $B^h(\cdot;\cdot,\cdot)$ and the property (2.3.22), we have

$$
\begin{aligned}
B^h(\varphi;\varphi,\phi)-B^h(\zeta;\zeta,\phi) &= B^h(\varphi;\varphi-\zeta,\phi)+B^h(\varphi-\zeta;\zeta,\phi) \\
&= B^h(\varphi;\varphi-\zeta+\phi,\phi)-B^h(\varphi;\phi,\phi)+B^h(\varphi-\zeta+\phi;\zeta,\phi)-B^h(\phi;\zeta,\phi) \\
&= B^h(\varphi;\varphi-\zeta+\phi,\phi)+B^h(\varphi-\zeta+\phi;\zeta,\phi)-B^h(\phi;\zeta,\phi).
\end{aligned}
$$

Thus, the proof follows from (2.3.21). □

The following theorem provides the rate of convergence of our virtual element scheme.

Theorem 2.4.1. *Let ψ and ψ_h be the unique solutions of problem (2.2.8) and problem (2.3.26), respectively. Then, there exists a positive constant C, independent of h, such that*

$$
\|\psi-\psi_h\|_X \leq C\,h^s\mathcal{G}(f;\mathrm{Re},\mathrm{Ro},\lambda,\lambda_h),
$$

where $s\in(1/2,1]$ is such that $\psi\in\mathrm{H}^{2+s}(\Omega)\cap X$ (cf. Theorem 2.2.2) and $\mathcal{G}$ is a suitable function independent of h.

Proof. Let $\psi_I \in X_h$ be the interpolant of ψ, such that Proposition 2.4.2 holds true. We set $w_h := \psi_h - \psi_I$. Thus,

$$\|\psi - \psi_h\|_X \le \|\psi - \psi_I\|_X + \|w_h\|_X. \tag{2.4.5}$$

The bound of first term on the right hand side above follows from Proposition 2.4.2. Thus, we bound the second term. In virtue to the properties (2.3.20), (2.3.21) and (2.3.22), we have that

$$\begin{aligned}
&\mathrm{Re}^{-1}\alpha_1\|w_h\|_X^2 \le \mathrm{Re}^{-1}A^h(w_h,w_h) = \mathrm{Re}^{-1}A^h(\psi_h,w_h) - \mathrm{Re}^{-1}A^h(\psi_I,w_h)\\
&= \mathrm{Re}^{-1}A^h(\psi_h,w_h) + B^h(\psi_h;w_h,w_h) - \mathrm{Ro}^{-1}C^h_{\text{skew}}(w_h,w_h) - \mathrm{Re}^{-1}A^h(\psi_I,w_h)\\
&= \left[\mathrm{Re}^{-1}A^h(\psi_h,w_h) + B^h(\psi_h;\psi_h,w_h) - \mathrm{Ro}^{-1}C^h_{\text{skew}}(\psi_h,w_h)\right]\\
&\quad - B^h(\psi_h;\psi_I,w_h) + \mathrm{Ro}^{-1}C^h_{\text{skew}}(\psi_I,w_h) - \mathrm{Re}^{-1}A^h(\psi_I,w_h)\\
&= \mathrm{Ro}^{-1}F^h(w_h) - \mathrm{Re}^{-1}A^h(\psi_I,w_h) - B^h(\psi_h;\psi_I,w_h) + \mathrm{Ro}^{-1}C^h_{\text{skew}}(\psi_I,w_h),
\end{aligned}$$

where we have used the definition of the discrete scheme (2.3.26). Now, adding and subtracting the term $\mathrm{Ro}^{-1}F(w_h)$ on the right hand side above, and using the definition of the continuous problem (cf. (2.2.8)), we get

$$\begin{aligned}
\mathrm{Re}^{-1}\alpha_1\|w_h\|_X^2 &\le \mathrm{Ro}^{-1}\left[F^h(w_h) - F(w_h)\right] + \mathrm{Re}^{-1}\left[A(\psi,w_h) - A^h(\psi_I,w_h)\right]\\
&\quad + \left[B(\psi;\psi,w_h) - B^h(\psi_h;\psi_I,w_h)\right] + \mathrm{Ro}^{-1}\left[C_{\text{skew}}(\psi,w_h) - C^h_{\text{skew}}(\psi_I,w_h)\right]\\
&\le C\,\mathrm{Ro}^{-1}\|F - F^h\|_{X_h'}\|w_h\|_X + \mathrm{Re}^{-1}\left[A(\psi,w_h) - A^h(\psi_I,w_h)\right]\\
&\quad + \left[B(\psi;\psi,w_h) - B^h(\psi_h;\psi_I,w_h)\right] + \mathrm{Ro}^{-1}\left[C_{\text{skew}}(\psi,w_h) - C^h_{\text{skew}}(\psi_I,w_h)\right]\\
&=: T_F + T_A + T_B + T_C.
\end{aligned} \tag{2.4.6}$$

Now, we bound each term on the right hand side above. First, the term T_F can be easily bounded by using Proposition 2.4.3. Then, we estimate the term T_A as follows. Adding and subtracting $\psi_\pi \in \mathbb{P}_2(K)$ such that Proposition 2.4.1 holds true, and using the consistency of the bilinear form $A^{h,K}(\cdot,\cdot)$ (cf. (2.3.16)), we have that

$$\begin{aligned}
T_A &= \mathrm{Re}^{-1}\sum_{K\in\mathcal{T}_h}\left[A^K(\psi-\psi_\pi,w_h) - A^{h,K}(\psi_I-\psi_\pi,w_h)\right]\\
&\le C\mathrm{Re}^{-1}h^s\|\psi\|_{2+s,\Omega}\|w_h\|_X,
\end{aligned} \tag{2.4.7}$$

where we have used the continuity of the bilinear form $A^{h,K}(\cdot,\cdot)$, Propositions 2.4.1 and 2.4.2 and Cauchy-Schwarz inequality. Analogously, the term T_C can be estimated by using (2.3.17), as follows

$$\begin{aligned}
T_C &= \mathrm{Ro}^{-1}\sum_{K\in\mathcal{T}_h}\left[C^K_{\text{skew}}(\psi-\psi_\pi,w_h) - C^{h,K}_{\text{skew}}(\psi_I-\psi_\pi,w_h)\right]\\
&\le C\mathrm{Ro}^{-1}h^s\|\psi\|_{2+s,\Omega}\|w_h\|_X.
\end{aligned} \tag{2.4.8}$$

The next step is to bound the term T_B. We proceed as follows

$$\begin{aligned}
T_B &= \left[B(\psi;\psi,w_h) - B^h(\psi_h;\psi_h,w_h)\right] + \left[B^h(\psi_h;\psi_h,w_h) - B^h(\psi_h;\psi_I,w_h)\right]\\
&= \left[B(\psi;\psi,w_h) - B^h(\psi_h;\psi_h,w_h)\right] + \left[B^h(\psi_h;w_h,w_h)\right]\\
&= B(\psi;\psi,w_h) - B^h(\psi_h;\psi_h,w_h),
\end{aligned} \tag{2.4.9}$$

where we have used (2.3.22) to obtain the last equality. Now, we add and subtract the term $B^h(\psi;\psi,w_h)$, then we use Lemmas 2.4.2 and 2.4.3 to obtain that

$$\begin{aligned} T_B &= \left[B(\psi;\psi,w_h) - B^h(\psi;\psi,w_h)\right] + \left[B^h(\psi;\psi,w_h) - B^h(\psi_h;\psi_h,w_h)\right] \\ &\leq C\,h^s(\|\psi\|_X + \|\psi\|_{1+s,\Omega})\|\psi\|_{2+s,\Omega}\|w_h\|_X \\ &\quad + \widehat{C_{B^h}}\left(\|\psi_h\|_X\|w_h\|_X + Ch^s\|\psi\|_{2+s,\Omega}(\|\psi\|_X + \|\psi_h\|_X)\right)\|w_h\|_X, \end{aligned} \tag{2.4.10}$$

where we have used that $w_h = \psi_h - \psi_I$ and then Proposition 2.4.2.

Therefore, from (2.4.6), using (2.4.7)-(2.4.10), we obtain

$$\begin{aligned} \mathrm{Re}^{-1}\alpha_1\|w_h\|_X \leq C\,\mathrm{Ro}^{-1}\,h^2\|f\|_{0,\Omega} &+ C(\mathrm{Re}^{-1} + \mathrm{Ro}^{-1})h^s\|\psi\|_{2+s,\Omega} \\ &+ C\,h^s(\|\psi\|_X + \|\psi\|_{1+s,\Omega})\|\psi\|_{2+s,\Omega} \\ &+ \widehat{C_{B^h}}\|\psi_h\|_X\|w_h\|_X + \widehat{C_{B^h}}\,Ch^s(\|\psi\|_X + \|\psi_h\|_X)\|\psi\|_{2+s,\Omega}. \end{aligned}$$

From the inequality above, we get

$$\begin{aligned} &\mathrm{Re}^{-1}\alpha_1(1 - \widehat{C_{B^h}}\mathrm{Re}\alpha_1^{-1}\|\psi_h\|_X)\|w_h\|_X \leq C\,\mathrm{Ro}^{-1}h^2\|f\|_{0,\Omega} \\ &\quad + C(\mathrm{Re}^{-1} + \mathrm{Ro}^{-1})h^s\|\psi\|_{2+s,\Omega} + C\,h^s(\|\psi\|_X + \|\psi\|_{1+s,\Omega})\|\psi\|_{2+s,\Omega} \\ &\quad + \widehat{C_{B^h}}\,Ch^s(\|\psi\|_X + \|\psi_h\|_X)\|\psi\|_{2+s,\Omega}. \end{aligned} \tag{2.4.11}$$

Next, from (2.3.31) and the fact that $\psi_h \in \mathcal{N}_h$, it holds that

$$1 - \frac{\widehat{C_{B^h}}\|\psi_h\|_X}{\mathrm{Re}^{-1}\alpha_1} \geq 1 - \frac{\widehat{C_{B^h}}\,C_1\,\mathrm{Re}^2\,\mathrm{Ro}^{-1}\|f\|_{0,\Omega}}{\alpha_1^2} = 1 - \lambda_h > 0. \tag{2.4.12}$$

Therefore, from (2.4.11), (2.4.12) and Theorem 2.3.1, we get

$$\begin{aligned} \|w_h\|_X &\leq \frac{C\,\mathrm{Re}\,\mathrm{Ro}^{-1}\,h^2\,\|f\|_{0,\Omega}}{\alpha_1\,(1-\lambda_h)} + \frac{C\,\mathrm{Re}\,(\mathrm{Re}^{-1} + \mathrm{Ro}^{-1})h^s}{\alpha_1\,(1-\lambda_h)}\|\psi\|_{2+s,\Omega} \\ &\quad + \frac{C\,\mathrm{Re}\,h^s}{\alpha_1\,(1-\lambda_h)}(\|\psi\|_X + \|\psi\|_{1+s,\Omega})\|\psi\|_{2+s,\Omega} \\ &\quad + \frac{\widehat{C_{B^h}}\,C\,\mathrm{Re}\,h^s}{\alpha_1\,(1-\lambda_h)}(\|\psi\|_X + \|\psi_h\|_X)\|\psi\|_{2+s,\Omega} \\ &\leq C\,h^s\mathcal{G}(f;\mathrm{Re},\mathrm{Ro},\lambda,\lambda_h), \end{aligned} \tag{2.4.13}$$

where we have also used Theorem 2.2.2. Finally, the proof follows from (2.4.5), (2.4.13) and Proposition 2.4.2. □

2.5 Numerical results

In this section, we present four numerical experiments, to test the behavior of the proposed VEM discretization (2.3.26) and in order to verify the theoretical results established in Section 2.4.

We have tested the virtual scheme by using different families of polygonal meshes (cf. Figure 2.1). For reasons of brevity, we do not report the results obtained with all meshes for all test problems. The non reported results are in accordance with the ones shown.

- $\mathcal{T}_h^1$: Sequence of CVT (Centroidal Voronoi Tessellation);
- $\mathcal{T}_h^2$: Trapezoidal meshes;
- $\mathcal{T}_h^3$: Distorted concave rhombic quadrilaterals;
- $\mathcal{T}_h^4$: Uniform triangular meshes.

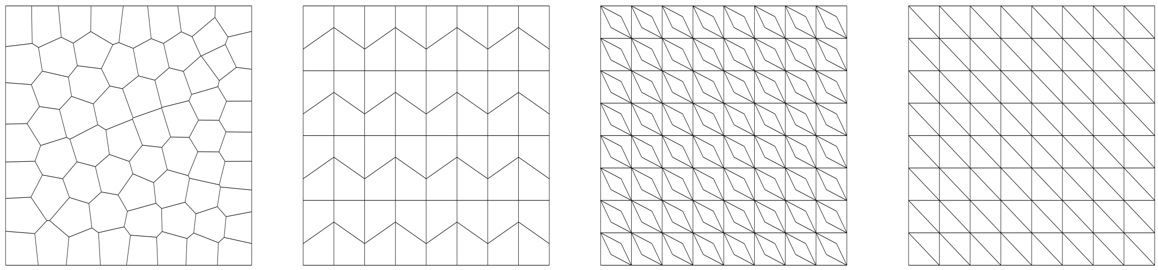

Figure 2.1: Sample meshes. $\mathcal{T}_h^1$, $\mathcal{T}_h^2$, $\mathcal{T}_h^3$ and $\mathcal{T}_h^4$ (from left to right).

In order to test the convergence of the proposed scheme, we introduce the following computable quantities:

$$\mathtt{e}_i(\psi) := |\psi - \Pi_K^{\mathrm{D}}\psi_h|_{i,h}, \quad i = 0, 1, 2.$$

We will compute experimental rates of convergence for each individual error as follows:

$$\mathtt{r}_i(\psi) := \frac{\log(\mathtt{e}_i(\psi)/\mathtt{e}_i'(\psi))}{\log(h/h')}, \quad i = 0, 1, 2.$$

where h, h' denote two consecutive mesh sizes with their respective errors $\mathtt{e}_i$ and $\mathtt{e}_i'$.

For each test to solve the resulting nonlinear system, we used the Newton method with maximum 10 iterations, a tolerance Tol= $1\mathtt{e}-8$ and we take $\psi_h^0 = 0$ as an initial guess; moreover, we have taken the Reynolds number as $\mathrm{Re} = 1.667$ and the Rossby number as $\mathrm{Ro} = 1\mathtt{e}-4$ (see [95]). Finally, we consider $\Omega := (0,1)^2$ as computational domain in the first three examples and an L-shaped domain in the last example.

2.5.1 Test 1: Smooth solution

In this numerical test, we take the load term in such a way that the analytical solution of the quasi-geostrophic equations (2.2.1) is given by:

$$\psi(x,y) := \frac{1}{\pi^2}\sin^2(\pi x)\sin^2(\pi y)e^{x^2+y^2}.$$

We report in Table 2.1 the convergence history of our virtual scheme on the meshes $\mathcal{T}_h^1$. The table includes the number of degrees of freedom (dofs), the discrete errors $\mathtt{e}_i(\psi)$, the convergence rates $\mathtt{r}_i(\psi)$ for $i = 0, 1, 2$, and the number of iterations (iter) used by the method of Newton to achieve tolerance at each level of refinement.

dofs	h	$\mathtt{e}_0(\psi)$	$\mathtt{r}_0(\psi)$	$\mathtt{e}_1(\psi)$	$\mathtt{r}_1(\psi)$	$\mathtt{e}_2(\psi)$	$\mathtt{r}_2(\psi)$	iter
294	1/8	4.214341e-2	—	1.338770e-1	—	3.676844e-1	—	3
1371	1/16	1.100219e-2	1.937	4.993576e-2	1.422	1.924777e-1	0.933	3
5796	1/32	2.329921e-3	2.239	1.229111e-2	2.022	9.401329e-2	1.033	3
23874	1/64	5.576055e-4	2.062	3.109190e-3	1.983	4.633333e-2	1.020	3
96855	1/128	1.089853e-4	2.355	7.895256e-4	1.977	2.308295e-2	1.005	3

Table 2.1: Test 1. Errors and experimental rates for the stream-function ψ_h, using the meshes $\mathcal{T}_h^1$.

We observe that the asymptotic $\mathcal{O}(h)$ decay of the discrete error $\mathtt{e}_2(\psi)$ observed for the stream-function confirms the optimal convergence predicted by Theorem 2.4.1. It can be also seen that the errors $\mathtt{e}_0(\psi)$ and $\mathtt{e}_1(\psi)$ decay much faster. However, we have not proved the higher order in these cases. The table also shows that a maximum of four iterations are required for the Newton method.

Sample approximate solutions generated with the virtual method on a coarse mesh are portrayed in Figure 2.2.

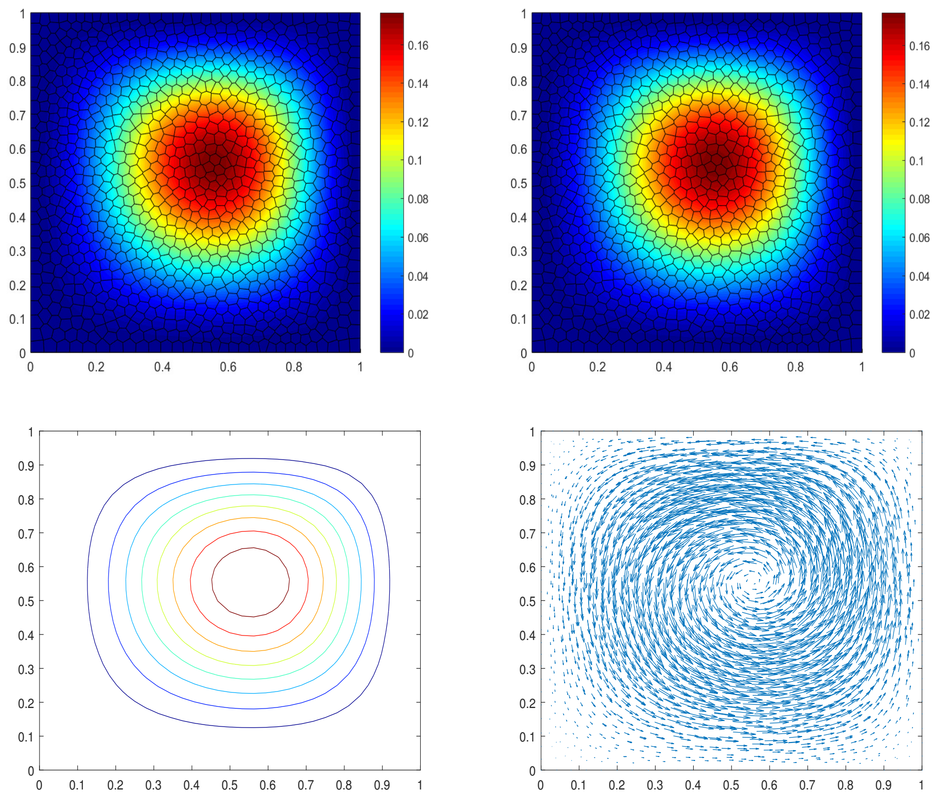

Figure 2.2: Test 1. Exact and approximate solutions ψ and ψ_h, the streamlines of ψ_h and the velocity field $\mathbf{u}_h := \mathbf{curl}\,\psi_h$ (top left, top right, bottom left, bottom right, respectively), using the VEM method (2.3.26) with $\mathcal{T}_h^1$, $h = 1/32$.

2.5.2 Test 2: Solution with western boundary layer

In this numerical example, we solve the quasi-geostrophic equations (2.2.1) by taking the load term in such a way that the analytical solution is given by:

$$\psi(x,y) = \frac{1}{(20\pi)^2}\left((1-x)\left(1-e^{-20x}\right)\sin(\pi y)\right)^2.$$

We observe that in this case the solution has a boundary layer on the left hand side.

In Table 2.2 we report the convergence history of our virtual scheme on the meshes $\mathcal{T}_h^2$. The table includes the number of degrees of freedom (dofs), the discrete errors $\mathtt{e}_i(\psi)$, and the convergence rates $\mathtt{r}_i(\psi)$ for $i = 0,1,2$. Once again, the expected order of convergence for the discrete errors $\mathtt{e}_2(\psi)$ is reached.

dofs	h	$\mathtt{e}_0(\psi)$	$\mathtt{r}_0(\psi)$	$\mathtt{e}_1(\psi)$	$\mathtt{r}_1(\psi)$	$\mathtt{e}_2(\psi)$	$\mathtt{r}_2(\psi)$	iter
147	1/8	7.600646e-5	—	1.549666e-3	—	2.834095e-2	—	3
675	1/16	1.616079e-5	2.233	4.688010e-4	1.724	1.390167e-2	1.027	2
2883	1/32	2.976015e-6	2.441	1.110449e-4	2.077	7.254667e-3	0.938	2
11907	1/64	6.202604e-7	2.262	2.706962e-5	2.036	3.804474e-3	0.931	2
48387	1/128	1.451048e-7	2.095	6.730940e-6	2.007	1.938996e-3	0.972	3

Table 2.2: Test 2. Errors and experimental rates for the stream-function ψ_h, using the meshes $\mathcal{T}_h^2$.

In addition, in Figure 2.3 we display the stream-function (exact and numerical solution), the streamlines of ψ_h and the approximate velocity field.

2.5.3 Test 3: Solution with vortex in the top-right corner of the domain

In this numerical example, we solve the quasi-geostrophic equations (2.2.1) by taking the load term in such a way that the analytical solution is given by:

$$\psi(x,y) = \frac{1}{4\pi^2}\left(1-\cos\left(\frac{2\pi(e^{R_1x}-1)}{e^{R_1}-1}\right)\right)\left(1-\cos\left(\frac{2\pi(e^{R_2y}-1)}{e^{R_2}-1}\right)\right).$$

In this experiment it is expected to observe a counter-clockwise rotating vortex with center (x_c, y_c) which depends on the values of R_1 and R_2. The coordinates of the center of the vortex are given by:

$$x_c = \frac{1}{R_1}\log\left(\frac{e^{R_1}+1}{2}\right) \qquad y_c = \frac{1}{R_2}\log\left(\frac{e^{R_2}+1}{2}\right).$$

In particular, we have chosen $R_1 = R_2 = 4$, then the center of the vortex is located at the top-right corner of the domain. More precisely, $(x_c, y_c) \approx (0.83125, 0.83125)$.

We proceed to study the accuracy of our VEM scheme by solving the discrete problem on a sequence of polygonal meshes $\mathcal{T}_h^3$. Once again, we compute the discrete errors $\mathtt{e}_i(\psi)$ for $i = 0,1,2$. The error history is collected in Table 2.3, which indicates that the scheme, as

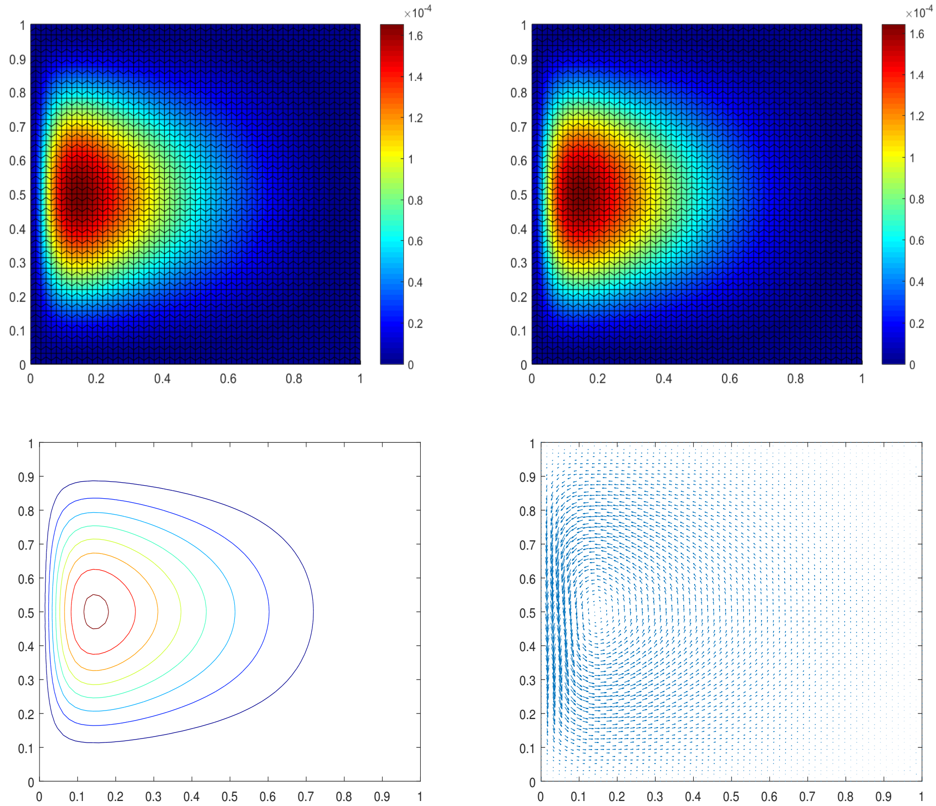

Figure 2.3: Test 2. Exact and approximate solutions ψ, ψ_h, the streamlines of ψ_h and the velocity field $\mathbf{u}_h := \mathbf{curl}\,\psi_h$ and (top left, top right, bottom left, bottom right, respectively) using the VEM method (2.3.26) with $\mathcal{T}_h^2$, $h = 1/64$.

dofs	h	$\mathtt{e}_0(\psi)$	$\mathtt{r}_0(\psi)$	$\mathtt{e}_1(\psi)$	$\mathtt{r}_1(\psi)$	$\mathtt{e}_2(\psi)$	$\mathtt{r}_2(\psi)$	iter
123	1/4	1.153577e-2	—	2.116982e-1	—	4.17475e+0	—	4
531	1/8	9.705065e-3	0.249	1.328881e-1	0.671	3.21654e+0	0.376	3
2211	1/16	2.444361e-3	1.989	4.017754e-2	1.725	1.72708e+0	0.897	3
9027	1/32	4.937103e-4	2.307	9.985092e-3	2.008	8.549397e-1	1.014	4
36483	1/64	1.118995e-4	2.141	2.479913e-3	2.009	4.275213e-1	0.999	4

Table 2.3: Test 3. Errors and experimental rates for the stream-function ψ_h, using the meshes $\mathcal{T}_h^3$.

predicted by the theory, converges with an $\mathcal{O}(h)$ in the discrete error $\mathtt{e}_2(\psi)$. The table also shows that a maximum of four iterations are required for the Newton method.

In Figure 2.4 we display the stream-function (exact and numerical solution) and the approximate velocity field.

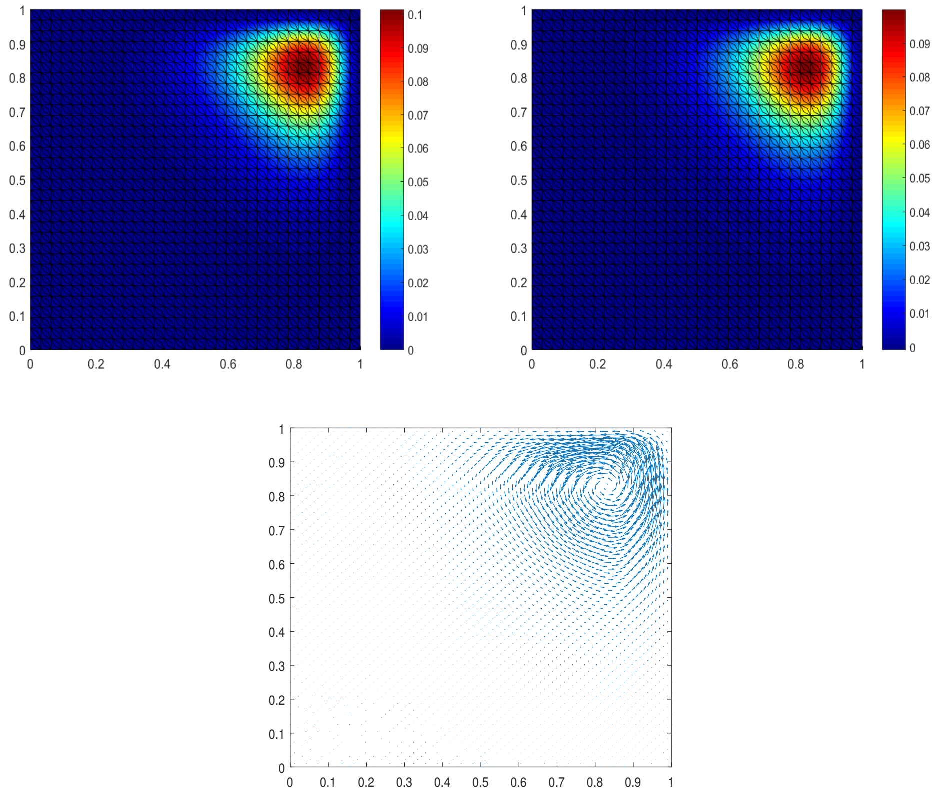

Figure 2.4: Test 3. Exact and approximate solutions ψ, ψ_h (top) and the velocity field $\mathbf{u}_h := \mathbf{curl}\,\psi_h$ (bottom) using the VEM method (2.3.26) with $\mathcal{T}_h^3$, $h = 1/32$.

2.5.4 Test 4: L-shaped domain

Finally, we solve the quasi-geostrophic equations (2.2.1) on an L-shape domain: $\Omega := (-1,1)^2 \setminus ([0,1) \times (-1,0])$. We take the right hand side term and non-homogeneous Dirichlet boundary conditions in such a way that the exact solution in polar coordinates is given by

$$\psi(r,\theta) = r^{5/3} \sin\left(\frac{5}{3}\theta\right).$$

The analytical solution contains a singularity at the re-entrant corner of Ω; here, we have $\psi \in \mathrm{H}^{8/3-\varepsilon}(\Omega)$ for all $\varepsilon > 0$.

Table 2.4 shows the errors and experimental convergence rates of our virtual scheme on the meshes $\mathcal{T}_h^4$. Since the analytical solution is singular, we are not going to obtain linear (in H^2) and quadratic (in H^1 and L^2) order of convergences as in the previous examples. More precisely, according to the regularity of ψ, we expect an order of convergence in H^2 as $\mathcal{O}(h^{2/3})$.

It can be seen from Table 2.4 that the expected order of convergence for the discrete errors $\mathsf{e}_2(\psi)$ is obtained. We also observe that the errors $\mathsf{e}_0(\psi)$ and $\mathsf{e}_1(\psi)$ decay much faster.

Finally, Figure 2.5 shows the stream-function (exact and numerical solution).

dofs	h	$\mathtt{e}_0(\psi)$	$\mathtt{r}_0(\psi)$	$\mathtt{e}_1(\psi)$	$\mathtt{r}_1(\psi)$	$\mathtt{e}_2(\psi)$	$\mathtt{r}_2(\psi)$	iter
483	1/8	2.985997e-4	—	6.677776e-3	—	2.614276e-1	—	4
2115	1/16	1.448822e-4	1.043	2.446762e-3	1.448	1.643765e-1	0.669	4
8835	1/32	6.100395e-5	1.247	9.069247e-4	1.431	1.040009e-1	0.660	4
36099	1/64	2.538614e-5	1.264	3.411994e-4	1.410	6.577727e-2	0.660	4
145923	1/128	1.063002e-5	1.255	1.316359e-4	1.374	4.155790e-2	0.662	4

Table 2.4: Test 4. Errors and experimental rates for the stream-function ψ_h, using the meshes $\mathcal{T}_h^4$.

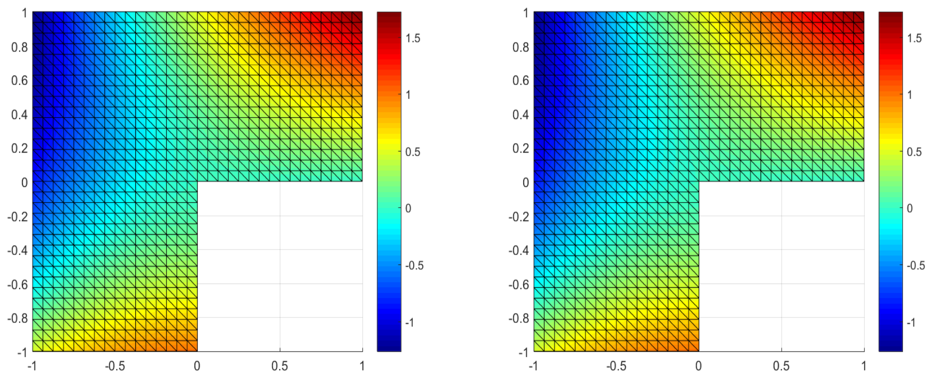

Figure 2.5: Test 4. Exact and approximate solutions ψ, ψ_h (left and right, respectively) using the VEM method (2.3.26) with $\mathcal{T}_h^4$, $h = 1/16$.

Chapter 3

Virtual element methods for a stream-function formulation of the Oseen equations

3.1 Introduction

The numerical solution of the time-dependent Navier–Stokes equations is still a great challenge of computational fluid dynamics. Using time discretization and linearization, the generalized Oseen problem arises as an important subproblem. Different formulation and discretizations have been proposed and analyzed in the last years for the Oseen equations; see for instance [8, 13, 23, 24, 25, 52, 61, 78, 73, 94] and the references therein.

The aim of the present chapter is to introduce and analyze conforming virtual element methods (VEM) to solve the Oseen equations on polygonal simply connected domains, formulated in terms of the stream-function of the velocity field. We observe that it corresponds to a fourth-order PDE. Thus, a conforming discretization requires globally C^1 continuity. Among the important advantages of VEM, in this work, we will exploit the possibility of easily implement global discrete spaces of $\mathrm{H}^2(\Omega)$ (see [58, 77]) to solve the Oseen problem.

The VEM introduced in [27] is a recent generalization of the finite element method that allows to use general polygonal/polyhedral meshes. The method has been applied successfully in a large range of problems in fluid mechanics; see for instance [17, 34, 35, 41, 59, 60, 64, 84, 98, 117, 118, 154, 164], where Stokes, Brinkman, Stokes–Darcy, Navier–Stokes and Boussinesq equations have been developed.

Recently in [133], it has been presented a C^1 VEM method for the Brinkman problem written in term of the stream-function. In this contribution, we will extend these results to the generalized Oseen problem, where an additional term is presented in the momentum equation. There are several advantages of utilizing the stream-function formulation for fluid flow problems: there is only one scalar variable, the incompressible condition is satisfied automatically, the stream-function is one of the most useful tools in flow visualization. Moreover, further variables of interest, such as the velocity, the fluid vorticity and the pressure, can be easily obtained from the VEM discrete stream-function. In fact, we will show that we compute the velocity by a simple postprocess, and we recover the fluid pressure by solving a primal formulation of a second order elliptic problem with right hand side coming from the discrete stream-function (see [133, 115]). We note that there are other procedures to recover fluid pressure. For instance, in [71] has been presented an algorithm for pressure recovery which is based on a mixed finite element discretization with inf-sup stable pairs. In addition, we will propose a novel strategy to recover the fluid vorticity, which is key in several applications [89, 46, 12], from the virtual element stream-function solution with the help of a proper polynomial projector.

This chapter is concerned with a non-symmetric VEM discretization of arbitrary order $k \geq 2$ for the Oseen equations formulated in terms of the stream-function, which will be analyzed using the Lax-Milgram Theorem and we will show well-posedness provided a CFL-type condition is satisfied (cf. (3.3.22)). Under standard assumptions on the polygonal meshes, we establish optimal order error estimates in H^2. Moreover, we show that velocity, vorticity and pressure can be recovered (cf. Section 3.5). We also derive error estimates for these fields. In particular, under the assumptions that the family of polygonal meshes is quasi-uniform and that the continuous solutions are sufficiently smooth (pressure and stream-function), we write an error estimate in H^1 for the fluid pressure. In summary, the advantages of the proposed VEM methods are: the use of general polygonal meshes and the possibility to recover further variables of interest for fluid flow problems.

The rest of the chapter is organized as follows: In Section 3.2, we introduce the variational formulation of the Oseen problem in terms of the stream-function. We prove existence and uniqueness of this formulation by using the Lax-Milgram Theorem. In Section 3.3, we present the virtual element discretization of arbitrary order $k \geq 2$. We also prove the existence and uniqueness of the discrete formulation. In Section 3.4, we obtain error estimates for the stream-function in H^2. In Section 3.5, we recover other important variables for fluid flow problems from the discrete stream-function, such as the velocity $\mathbf{u}$, the fluid vorticity ω and the fluid pressure p. In Section 3.6, we report a set of numerical examples which allows us to assess the performance of the proposed method.

3.2 Model problem

The incompressible Oseen equations are given by the following set of equations and boundary conditions:

$$\begin{aligned} -\nu\boldsymbol{\Delta}\mathbf{u} + (\boldsymbol{\nabla}\mathbf{u})\boldsymbol{\beta} + \gamma\mathbf{u} + \nabla p &= \mathbf{f} && \text{in} \quad \Omega, \\ \operatorname{div}\mathbf{u} &= 0 && \text{in} \quad \Omega, \\ \mathbf{u} &= \mathbf{0} && \text{on} \quad \Gamma, \\ (p,1)_{0,\Omega} &= 0, \end{aligned} \tag{3.2.1}$$

where $\mathbf{u} : \Omega \to \mathbb{R}^2$ is the velocity field, $p : \Omega \to \mathbb{R}$ is the pressure field, $\mathbf{f} : \Omega \to \mathbb{R}^2$ is the external body force, $\nu > 0$ the kinematic viscosity, $\boldsymbol{\beta} \in \mathbf{W}^1_\infty(\Omega)$ with $\operatorname{div}\boldsymbol{\beta} = 0$ a given convective velocity field, and $\gamma \in \mathrm{L}^\infty(\Omega)$ a given scalar function, respectively. We assume that there exists γ_0 such that $\gamma(\mathbf{x}) \geq \gamma_0 > 0$ for almost all $\mathbf{x} \in \Omega$.

The standard velocity-pressure variational formulation of the Oseen problem reads as follows: find $(\mathbf{u}, p) \in \mathbf{H}^1_0(\Omega) \times \mathrm{L}^2_0(\Omega)$, such that

$$\begin{aligned} \nu\int_\Omega \boldsymbol{\nabla}\mathbf{u} : \boldsymbol{\nabla}\mathbf{v} + \int_\Omega (\boldsymbol{\nabla}\mathbf{u})\boldsymbol{\beta}\cdot\mathbf{v} + \int_\Omega \gamma\mathbf{u}\cdot\mathbf{v} - \int_\Omega p\operatorname{div}\mathbf{v} &= \int_\Omega \mathbf{f}\cdot\mathbf{v} && \forall \mathbf{v} \in \mathbf{H}^1_0(\Omega), \\ \int_\Omega q\operatorname{div}\mathbf{u} &= 0 && \forall q \in \mathrm{L}^2_0(\Omega), \end{aligned}$$

where $\mathrm{L}_0^2(\Omega) := \{q \in \mathrm{L}^2(\Omega) : (q,1)_{0,\Omega} = 0\}$.

Let us introduce the space of divergence-free functions

$$\mathbf{V} := \left\{\mathbf{v} \in \mathbf{H}_0^1(\Omega) : \operatorname{div} \mathbf{v} = 0 \quad \text{in} \quad \Omega\right\}.$$

Since Ω is a simply connected domain, a well known result states that a vector function $\mathbf{v} \in \mathbf{V}$ if and only if there exists a scalar function $\varphi \in \mathrm{H}^2(\Omega)$, which is called *stream-function*, such that

$$\mathbf{v} = \mathbf{curl}\,\varphi \in \mathbf{H}_0^1(\Omega).$$

The function φ is defined up to a constant (see [103]). Thus, we consider the following space

$$X := \left\{\varphi \in \mathrm{H}^2(\Omega) : \varphi = \partial_{\mathbf{n}}\varphi = 0 \quad \text{on} \quad \Gamma\right\},$$

where $\partial_{\mathbf{n}}$ denotes the normal derivative. We endow X with the norm

$$\|\varphi\|_X := |\varphi|_{2,\Omega} \qquad \forall \varphi \in X.$$

Then, choosing $\psi \in X$ the *stream-function* of the velocity field $\mathbf{u} \in \mathbf{V}$ (i.e. $\mathbf{u} = \mathbf{curl}\,\psi$), we write the following equivalent weak formulation of the Oseen problem: find $\psi \in X$ such that

$$\nu \int_\Omega \mathrm{D}^2\psi : \mathrm{D}^2\phi + \int_\Omega (\boldsymbol{\nabla}\mathbf{curl}\,\psi)\boldsymbol{\beta}\cdot\mathbf{curl}\,\phi + \int_\Omega \gamma\,\mathbf{curl}\,\psi\cdot\mathbf{curl}\,\phi = \int_\Omega \mathbf{f}\cdot\mathbf{curl}\,\phi \quad \forall \phi \in X,$$

We rewrite this variational problem as follows: find $\psi \in X$ such that

$$\mathcal{O}(\psi,\phi) := \nu A(\psi,\phi) + B(\psi,\phi) + C(\psi,\phi) = F(\phi) \qquad \forall \phi \in X, \tag{3.2.2}$$

where $A : X \times X \to \mathbb{R}$, $B : X \times X \to \mathbb{R}$ and $C : X \times X \to \mathbb{R}$ are the bilinear forms and $F : X \to \mathbb{R}$ is a linear functional, defined as follows:

$$A(\psi,\phi) := \int_\Omega \mathrm{D}^2\psi : \mathrm{D}^2\phi, \quad \forall \psi,\phi \in X, \tag{3.2.3}$$

$$B(\psi,\phi) := \int_\Omega (\boldsymbol{\nabla}\mathbf{curl}\,\psi)\boldsymbol{\beta}\cdot\mathbf{curl}\,\phi \quad \forall \psi,\phi \in X, \tag{3.2.4}$$

$$C(\psi,\phi) := \int_\Omega \gamma\,\mathbf{curl}\,\psi\cdot\mathbf{curl}\,\phi \quad \forall \psi,\phi \in X, \tag{3.2.5}$$

$$F(\phi) := \int_\Omega \mathbf{f}\cdot\mathbf{curl}\,\phi \quad \forall \phi \in X. \tag{3.2.6}$$

The following lemma establishes some properties for the bilinear forms and the linear functional previously defined.

Lemma 3.2.1. *There exist positive constants $C_{\boldsymbol{\beta}}$ and C_γ such that the forms defined in (3.2.3)-(3.2.6) satisfies the following properties:*

$$\begin{aligned}
|A(\varphi,\phi)| &\le \|\varphi\|_X\|\phi\|_X && \forall \varphi,\phi \in X,\\
A(\phi,\phi) &\ge \|\phi\|_X^2 && \forall \phi \in X,\\
|B(\varphi,\phi)| &\le C_{\boldsymbol{\beta}}\|\varphi\|_X\|\phi\|_X && \forall \varphi,\phi \in X,\\
|C(\varphi,\phi)| &\le C_\gamma\|\varphi\|_X\|\phi\|_X && \forall \varphi,\phi \in X,\\
C(\phi,\phi) &\ge \gamma_0|\phi|_{1,\Omega}^2 && \forall \phi \in X,\\
|F(\phi)| &\le \|F\|_{-2,\Omega}\|\phi\|_X && \forall \phi \in X.
\end{aligned}$$

As a consequence of Lemma 3.2.1, the fact that div $\boldsymbol{\beta} = 0$, and the Lax-Milgram Theorem, we state the solvability of the continuous problem (3.2.2).

Theorem 3.2.1. *There exists a unique $\psi \in X$ solution to problem (3.2.2), which satisfies the following continuous dependence on the data*

$$\|\psi\|_X \leq C\|F\|_{-2,\Omega},$$

where C is a positive constant.

Remark 3.2.1. *In this chapter, we will require an additional regularity for the unique solution of problem (3.2.2). More precisely, in what follows we assume that there exists $s > 1/2$ such that $\psi \in \mathrm{H}^{2+s}(\Omega)$. This additional regularity will play an important role in the error analysis (cf. Sections 3.4 and 3.5).*

The goal of this chapter is to propose a conforming C^1-VEM of arbitrary order to solve problem (3.2.2) and to prove that the method is optimally convergent. In addition, we will propose simple post-processes from the discrete stream-function to recover the velocity, pressure and vorticity fields.

3.3 Virtual element method

In this section, we will write a C^1-virtual element discretization for the numerical approximation of problem (3.2.2). We start by introducing some notations and assumptions to construct a discrete virtual subspace X_h^k, for arbitrary order $k \geq 2$ and to write the discrete bilinear forms and the discrete linear functional to propose the discrete scheme.

Let $\{\mathcal{T}_h\}_{h>0}$ be a sequence of decompositions of Ω into general polygonal elements K. Let h_K denote the diameter of the element K and h the maximum of the diameters of all the elements of the mesh, i.e., $h := \max_{K\in\mathcal{T}_h} h_K$. In what follows, we denote by N_K the number of vertices of K, by $\mathbf{v}_i$ a generic vertex of K, with $i \in \{1, \ldots, N_K\}$ and by e a generic edge of $\mathcal{T}_h$. In addition for all e, we denote by h_e the length of edge and we define a unit normal vector $\mathbf{n}_K^e$ that points outside of K. Also, we denote by x_e and $\mathbf{x}_K$ the midpoint of e and the baricenter of K, respectively.

For the theoretical analysis, we will consider the following assumptions: there exists a real number $C_{\mathcal{T}_h} > 0$ such that, for every h and every $K \in \mathcal{T}_h$,

A1 : the ratio between the shortest edge and the diameter h_K of K is larger than $C_{\mathcal{T}_h}$;

A2 : K is star-shaped with respect to every point of a ball of radius $C_{\mathcal{T}_h} h_K$.

3.3.1 Virtual spaces and polynomial projections operator

We will denote by $\mathbb{M}_\ell^*(K)$ the set of scaled monomials defined on each polygon K:

$$\mathbb{M}_\ell^*(K) := \left\{ \left(\frac{\mathbf{x}-\mathbf{x}_K}{h_K}\right)^{\boldsymbol{a}} : |\boldsymbol{a}| = \ell \right\}, \tag{3.3.1}$$

where for a non-negative multi-index $\boldsymbol{a} = (a_1, a_2)$, we set $|\boldsymbol{a}| := a_1 + a_2$ and $\mathbf{x}^{\boldsymbol{a}} = x_1^{a_1} x_2^{a_2}$, with $\mathbf{x} = (x_1, x_2)$. Now, we define $\mathbb{M}_k(K) := \bigcup_{\ell \leq k} \mathbb{M}^*_\ell(K) =: \{m_j\}_{j=1}^{d_k}$ as a basis of $\mathbb{P}_k(K)$, where $d_k = \dim(\mathbb{P}_k(K))$. Also we consider the set of the scaled monomials defined on each edge e:

$$\mathbb{M}_\ell(e) := \left\{ 1, \frac{x - x_e}{h_e}, \left(\frac{x - x_e}{h_e}\right)^2, \ldots, \left(\frac{x - x_e}{h_e}\right)^\ell \right\}.$$

Now, for any integer $k \geq 2$ and for every polygon $K \in \mathcal{T}_h$, we introduce the following preliminary local virtual space [77]:

$$\begin{aligned} \widetilde{X}_h^k(K) := \big\{ \phi_h \in \mathrm{H}^2(K) : \Delta^2 \phi_h \in \mathbb{P}_{k-2}(K), \phi_h|_{\partial K} \in C^0(\partial K), \phi_h|_e \in \mathbb{P}_r(e) \; \forall e \in \partial K, \\ \nabla \phi_h|_{\partial K} \in \mathbf{C}^0(\partial K), \partial_{\mathbf{n}_K^e} \phi_h|_e \in \mathbb{P}_\alpha(e) \; \forall e \in \partial K \big\}, \end{aligned}$$

where $r := \max\{3, k\}$ and $\alpha := k - 1$.

Next, for a given $\phi_h \in \widetilde{X}_h^k(K)$, we introduce the following sets of linear operators from the local virtual space $\widetilde{X}_h^k(K)$ into $\mathbb{R}$:

- $\mathbf{D_1}$: contains linear operators evaluating ϕ_h at the N_K vertices of K;
- $\mathbf{D_2}$: contains linear operators evaluating $h_{\mathbf{v}_i} \nabla \phi_h$ at the N_K vertices of K;
- $\mathbf{D_3}$: for $r > 3$, the moments $\displaystyle\frac{1}{h_e} \int_e q(\zeta) \phi_h(\zeta) \, d\zeta \quad \forall q \in \mathbb{M}_{r-4}(e), \quad \forall \text{edge } e;$
- $\mathbf{D_4}$: for $\alpha > 1$, the moments $\displaystyle\int_e q(\zeta) \partial_{\mathbf{n}_K^e} \phi_h(\zeta) \, d\zeta \quad \forall q \in \mathbb{M}_{\alpha-2}(e), \quad \forall \text{edge } e;$
- $\mathbf{D_5}$: for $k \geq 4$, the moments $\displaystyle\frac{1}{h_K^2} \int_K q(\mathbf{x}) \phi_h(\mathbf{x}) \, d\mathbf{x} \quad \forall q \in \mathbb{M}_{k-4}(K), \quad \forall \text{polygon } K,$

where $h_{\mathbf{v}_i}$ corresponds to the average of the diameters corresponding to the elements with $\mathbf{v}_i$ as a vertex.

Now, we decompose into local contributions the bilinear forms $A(\cdot,\cdot)$, $B(\cdot,\cdot)$ and $C(\cdot,\cdot)$:

$$A(\varphi, \phi) = \sum_{K \in \mathcal{T}_h} A^K(\varphi, \phi) := \sum_{K \in \mathcal{T}_h} \int_K \mathrm{D}^2 \varphi : \mathrm{D}^2 \phi \qquad \forall \varphi, \phi \in X,$$

$$B(\varphi, \phi) = \sum_{K \in \mathcal{T}_h} B^K(\varphi, \phi) := \sum_{K \in \mathcal{T}_h} \int_K (\boldsymbol{\nabla} \mathbf{curl}\, \varphi) \boldsymbol{\beta} \cdot \mathbf{curl}\, \phi \qquad \forall \varphi, \phi \in X,$$

$$C(\varphi, \phi) = \sum_{K \in \mathcal{T}_h} C^K(\varphi, \phi) = \sum_{K \in \mathcal{T}_h} \int_K \gamma \, \mathbf{curl}\, \varphi \cdot \mathbf{curl}\, \phi, \qquad \forall \varphi, \phi \in X.$$

In what follows, we are going to build discrete version of the local bilinear forms. With this aim, for each polygon K, we define the following projector:

$$\begin{aligned} \Pi_K^{k,\mathrm{D}} : \widetilde{X}_h^k(K) &\longrightarrow \mathbb{P}_k(K) \subseteq \widetilde{X}_h^k(K), \\ \phi_h &\longmapsto \Pi_K^{k,\mathrm{D}} \phi_h, \end{aligned}$$

where $\Pi_K^{k,\mathrm{D}}\phi_h$ is the solution of the local problems:

$$A^K(\Pi_K^{k,\mathrm{D}}\phi_h, q) = A^K(\phi_h, q) \quad \forall q \in \mathbb{P}_k(K),$$
$$\widehat{\Pi_K^{k,\mathrm{D}}\phi_h} = \widehat{\phi_h}, \quad \widehat{\nabla\Pi_K^{k,\mathrm{D}}\phi_h} = \widehat{\nabla\phi_h},$$

with $\widehat{(\cdot)}$ is defined as follows:

$$\widehat{\varphi_h} := \frac{1}{N_K}\sum_{i=1}^{N_K}\varphi_h(\mathbf{v}_i) \qquad \forall \varphi_h \in C^0(\partial K), \tag{3.3.2}$$

and $\mathbf{v}_i, 1 \leq i \leq N_K$, are the vertices of K.

The following result establishes that the projector $\Pi_K^{k,\mathrm{D}}$ is fully computable using the sets $\mathbf{D_1} - \mathbf{D_5}$ (see [77]).

Lemma 3.3.1. *The operator $\Pi_K^{k,\mathrm{D}} : \widetilde{X}_h^k(K) \to \mathbb{P}_k(K)$ is explicitly computable for every $\phi_h \in \widetilde{X}_h^k(K)$, using only the information of the linear operators $\mathbf{D_1} - \mathbf{D_5}$.*

For each $K \in \mathcal{T}_h$ our local virtual space is given by:

$$X_h^k(K) := \left\{\phi_h \in \widetilde{X}_h^k(K) : \int_K q_\ell^*\,\Pi_K^{k,\mathrm{D}}\phi_h = \int_K q_\ell^*\,\phi_h, \quad \forall q^* \in \mathbb{M}_{k-3}^*(K) \cup \mathbb{M}_{k-2}^*(K)\right\}, \tag{3.3.3}$$

where $\mathbb{M}_{k-3}^*(K)$ and $\mathbb{M}_{k-2}^*(K)$ are scaled monomials of degree $k-3$ and $k-2$, respectively (see (3.3.1)), with the convention that $\mathbb{M}_{-1}^*(K) = \emptyset$ (for further details, see [77]).

It is easy to observe that $\mathbb{P}_k(K) \subseteq X_h^k(K) \subseteq \widetilde{X}_h^k(K)$. Moreover, the sets of linear operators $\mathbf{D_1} - \mathbf{D_5}$ constitutes a set of degrees of freedom for $X_h^k(K)$ (see [77]). Additionally, we note that the condition appearing in the definition of the local space $X_h^k(K)$ will be useful to construct an L^2-projection which will be employed to build the discrete bilinear forms. In fact, we consider the $\mathrm{L}^2(K)$-projection onto $\mathbb{P}_{k-2}(K)$. For each $\phi \in \mathrm{L}^2(K)$, $\Pi_K^{k-2}\phi \in \mathbb{P}_{k-2}(K)$ satisfies

$$\int_K q\phi = \int_K q(\Pi_K^{k-2}\phi) \qquad \forall q \in \mathbb{P}_{k-2}(K).$$

The following lemma establishes that Π_K^{k-2} is computable on $X_h^k(K)$. The proof follows from the definition of the local virtual space and the set of degrees of freedom.

Lemma 3.3.2. *The operator $\Pi_K^{k-2} : X_h^k(K) \to \mathbb{P}_{k-2}(K)$ is explicitly computable for each $\phi_h \in X_h^k(K)$, using only the information of the degrees freedom $\mathbf{D_1} - \mathbf{D_5}$.*

Now, for $k \geq 2$, we will consider the following projection onto the polynomial space $\mathbf{P}_{k-1}(K)$: we define $\boldsymbol{\Pi}_K^{k-1} : \mathbf{L}^2(K) \to \mathbf{P}_{k-1}(K)$, for each $\mathbf{v} \in \mathbf{L}^2(K)$ by

$$\int_K \mathbf{q}\cdot\mathbf{v} = \int_K \mathbf{q}\cdot\boldsymbol{\Pi}_K^{k-1}\mathbf{v} \quad \forall \mathbf{q} \in \mathbf{P}_{k-1}(K). \tag{3.3.4}$$

Using integration by parts, it is easy to see that for any $\phi_h \in X_h^k(K)$, the vector function $\boldsymbol{\Pi}_K^{k-1}\mathbf{curl}\,\phi_h \in \mathbf{P}_{k-1}(K)$ can be explicitly computed from the degrees of freedom $\mathbf{D_1} - \mathbf{D_5}$ (see [133]).

Now, we will establish a stability property of the projector defined above. To achieve this, we recall the following inverse inequality for polynomials on polygons, which hold true under assumption **A2** (see [33, Remark 6.1]).

Lemma 3.3.3. *If the assumption* **A2** *is satisfied, then there exists $\widetilde{C} > 0$, independent of h, such that*

$$|q|_{1,K} \le \widetilde{C} h_K^{-1} \|q\|_{0,K} \quad \forall q \in \mathbb{P}_\ell(K), \quad \ell \ge 0.$$

Thus, using Lemma 3.3.3 the projector $\boldsymbol{\Pi}_K^{k-1}$ satisfies the following stability property: let $K \in \mathcal{T}_h$, then for each $\phi_h \in X_h^k(K)$, there exists $C_N > 0$, independent to K and h, such that

$$|\boldsymbol{\Pi}_K^{k-1} \mathbf{curl}\, \phi_h|_{1,K} \le C_N |\phi_h|_{2,K}. \tag{3.3.5}$$

Now, for $k \ge 2$, we introduce an additional projector which will be used to write the virtual scheme; we define $\Pi_K^{k,\nabla^\perp} : X_h^k(K) \longrightarrow \mathbb{P}_k(K) \subseteq X_h^k(K)$ for each $\phi_h \in X_h^k(K)$ as the solution of the following local problem:

$$\int_K \mathbf{curl}\, \Pi_K^{k,\nabla^\perp} \phi_h \cdot \mathbf{curl}\, q = \int_K \mathbf{curl}\, \phi_h \cdot \mathbf{curl}\, q \qquad \forall q \in \mathbb{P}_k(K),$$
$$\widehat{\Pi_K^{k,\nabla^\perp} \phi_h} = \widehat{\phi_h},$$

where $\widehat{(\cdot)}$ has been defined in (3.3.2). The following result states that this operator is fully computable using the sets $\mathbf{D_1} - \mathbf{D_5}$ (see [133, Lemma 3.3]).

Lemma 3.3.4. *The operator $\Pi_K^{k,\nabla^\perp} : X_h^k(K) \to \mathbb{P}_k(K) \subseteq X_h^k(K)$ is explicitly computable for each $\phi_h \in X_h^k(K)$, using only the information of the set of degrees freedom $\mathbf{D_1} - \mathbf{D_5}$.*

Now, we introduce the global virtual space to approximate the solution of the problem (3.2.2). For every decomposition $\mathcal{T}_h$ of Ω into polygons K, we define

$$X_h^k := \left\{ \phi_h \in X : \ \phi_h|_K \in X_h^k(K) \right\}.$$

3.3.2 Construction of the local and global discrete forms

In this section, we will construct the discrete version of the continuous local bilinear forms and the right hand side, using the projection operators introduced in Section 3.3.1.

First, let $\mathcal{S}_{\mathrm{D}}^K(\cdot,\cdot)$ and $\mathcal{S}_{\mathbf{curl}}^K(\cdot,\cdot)$ be any symmetric positive definite bilinear forms to be chosen as to satisfy:

$$\begin{aligned}
&c_0 A^K(\phi_h,\phi_h) \le \mathcal{S}_{\mathrm{D}}^K(\phi_h,\phi_h) \le c_1 A^K(\phi_h,\phi_h) && \forall \phi_h \in X_h^k(K), \quad \text{with} \quad \Pi_K^{k,\mathrm{D}} \phi_h = 0,\\
&c_2 C^K(\phi_h,\phi_h) \le \mathcal{S}_{\mathbf{curl}}^K(\phi_h,\phi_h) \le c_3 C^K(\phi_h,\phi_h) && \forall \phi_h \in X_h^k(K), \quad \text{with} \quad \Pi_K^{k,\nabla^\perp} \phi_h = 0,
\end{aligned} \tag{3.3.6}$$

with c_0, c_1, c_2 and c_3 positive constants independent of h and K. We will introduce bilinear forms $\mathcal{S}_{\mathrm{D}}^K(\cdot,\cdot)$ and $\mathcal{S}_{\mathbf{curl}}^K(\cdot,\cdot)$ satisfying (3.3.6) in Section 3.6.

For all $\psi_h, \phi_h \in X_h^k(K)$ we now define the local discrete bilinear forms

$$A^{h,K}(\psi_h,\phi_h) := A^K\left(\Pi_K^{k,\mathrm{D}}\psi_h, \Pi_K^{k,\mathrm{D}}\phi_h\right) + \mathcal{S}_{\mathrm{D}}^K\left(\psi_h - \Pi_K^{k,\mathrm{D}}\psi_h, \phi_h - \Pi_K^{k,\mathrm{D}}\phi_h\right), \tag{3.3.7}$$

$$B^{h,K}(\psi_h,\phi_h) := \int_K \left(\boldsymbol{\nabla}\boldsymbol{\Pi}_K^{k-1}\mathbf{curl}\,\psi_h\right)\boldsymbol{\beta} \cdot \boldsymbol{\Pi}_K^{k-1}\mathbf{curl}\,\phi_h, \tag{3.3.8}$$

$$\begin{aligned}
C^{h,K}(\psi_h,\phi_h) := &\int_K \gamma\, \boldsymbol{\Pi}_K^{k-1}\mathbf{curl}\,\psi_h \cdot \boldsymbol{\Pi}_K^{k-1}\mathbf{curl}\,\phi_h \\
&+ \mathcal{S}_{\mathbf{curl}}^K\left(\psi_h - \Pi_K^{k,\nabla^\perp}\psi_h, \phi_h - \Pi_K^{k,\nabla^\perp}\phi_h\right).
\end{aligned} \tag{3.3.9}$$

Next, for all $\psi_h, \phi_h \in X_h^k$, we define the global discrete bilinear form as follows:

$$A^h : X_h^k \times X_h^k \to \mathbb{R}, \quad A^h(\psi_h, \phi_h) := \sum_{K \in \mathcal{T}_h} A^{h,K}(\psi_h, \phi_h), \tag{3.3.10}$$

$$B^h : X_h^k \times X_h^k \to \mathbb{R}, \quad B^h(\psi_h, \phi_h) := \sum_{K \in \mathcal{T}_h} B^{h,K}(\psi_h, \phi_h), \tag{3.3.11}$$

$$C^h : X_h^k \times X_h^k \to \mathbb{R}, \quad C^h(\psi_h, \phi_h) := \sum_{K \in \mathcal{T}_h} C^{h,K}(\psi_h, \phi_h). \tag{3.3.12}$$

We note that the bilinear form $B^h(\cdot,\cdot)$ is immediately extendable to the continuous space X.

The following result establishes the usual consistency and stability properties for the discrete local forms $A^{h,K}(\cdot,\cdot)$ and $C^{h,K}(\cdot,\cdot)$. The proof follows standard arguments in the VEM literature (see [18, 27, 28]). We omit further details.

Proposition 3.3.1. *The local bilinear form $A^{h,K}(\cdot,\cdot)$, $C^{h,K}(\cdot,\cdot)$ defined in (3.3.7) and (3.3.9) respectively, on each element K satisfies*

- *Consistency: for all $h > 0$ and for all $K \in \mathcal{T}_h$, we have that*

$$A^{h,K}(q, \phi_h) = A^K(q, \phi_h) \qquad \forall q \in \mathbb{P}_k(K), \qquad \forall \phi_h \in X_h^k(K).$$

- *Stability and boundedness: There exist positive constants $\alpha_i, i = 0, 1, 2, 3$ independent of K, such that:*

$$\alpha_0 A^K(\phi_h, \phi_h) \le A^{h,K}(\phi_h, \phi_h) \le \alpha_1 A^K(\phi_h, \phi_h) \qquad \forall \phi_h \in X_h^k(K),$$
$$\alpha_2 C^K(\phi_h, \phi_h) \le C^{h,K}(\phi_h, \phi_h) \le \alpha_3 C^K(\phi_h, \phi_h) \qquad \forall \phi_h \in X_h^k(K).$$

The next step consists in constructing a computable approximation of the linear functional defined in (3.2.6). With this aim, we define, for each element K, the following computable term:

$$F^{h,K}(\phi_h) := \int_K \boldsymbol{\Pi}_K^{k-1}\mathbf{f} \cdot \mathbf{curl}\, \phi_h \equiv \int_K \mathbf{f} \cdot \boldsymbol{\Pi}_K^{k-1}\mathbf{curl}\, \phi_h \qquad \forall \phi_h \in X_h^k(K).$$

Thus, we consider the following approximation of the functional defined in (3.2.6):

$$F^h(\phi_h) := \sum_{K \in \mathcal{T}_h} F^{h,K}(\phi_h) \qquad \forall \phi_h \in X_h^k. \tag{3.3.13}$$

The following lemma establishes some properties for the discrete forms defined in (3.3.10), (3.3.11), (3.3.12) and (3.3.13).

Lemma 3.3.5. *There exist positive constants C_{A^h}, C_{B^h}, C_2 and C_{F^h}, independent of h, such that the forms defined in (3.3.10)-(3.3.13) satisfies the following properties:*

$$|A^h(\psi_h, \phi_h)| \le C_{A^h} \|\psi_h\|_X \|\phi_h\|_X \qquad \forall \psi_h, \phi_h \in X_h^k, \tag{3.3.14}$$

$$A^h(\phi_h, \phi_h) \ge \alpha_0 \|\phi_h\|_X^2 \qquad \forall \phi_h \in X_h^k, \tag{3.3.15}$$

$$|B^h(\psi_h, \phi_h)| \le C_{B^h} \|\psi_h\|_X \|\phi_h\|_X \qquad \forall \psi_h, \phi_h \in X_h^k, \tag{3.3.16}$$

$$|C^h(\psi_h, \phi_h)| \le C_2 \|\psi_h\|_X \|\phi_h\|_X \qquad \forall \psi_h, \phi_h \in X_h^k, \tag{3.3.17}$$

$$C^h(\phi_h, \phi_h) \ge \alpha_2 \gamma_0 |\phi_h|_{1,\Omega}^2 \qquad \forall \psi_h, \phi_h \in X_h^k, \tag{3.3.18}$$

$$|F^h(\phi_h)| \le C_{F^h} \|\mathbf{f}\|_{0,\Omega} \|\phi_h\|_X \qquad \forall \phi_h \in X_h^k. \tag{3.3.19}$$

Proof. The proof of these properties follow standard arguments in the VEM literature (see [18, 27, 28]). Nevertheless, we will prove the property (3.3.16). Indeed, let $\psi_h, \phi_h \in X_h^k$, then using the definition of the bilinear form $B^h(\cdot,\cdot)$ and the Cauchy-Schwarz inequality, we have that

$$
\begin{aligned}
|B^h(\psi_h,\phi_h)| &\le \sum_{K\in\mathcal{T}_h} \left| \int_K \left(\boldsymbol{\nabla}\boldsymbol{\Pi}_K^{k-1}\mathbf{curl}\,\psi_h\right)\boldsymbol{\beta}\cdot\boldsymbol{\Pi}_K^{k-1}\mathbf{curl}\,\phi_h \right| \\
&\le \sum_{K\in\mathcal{T}_h} \|\boldsymbol{\beta}\|_{\mathrm{L}^\infty(K)} \|\boldsymbol{\nabla}\boldsymbol{\Pi}_K^{k-1}\mathbf{curl}\,\psi_h\|_{0,K} \|\boldsymbol{\Pi}_K^{k-1}\mathbf{curl}\,\phi_h\|_{0,K} \\
&\le \|\boldsymbol{\beta}\|_{\mathrm{L}^\infty(\Omega)} \sum_{K\in\mathcal{T}_h} |\boldsymbol{\Pi}_K^{k-1}\mathbf{curl}\,\psi_h|_{1,K} \|\mathbf{curl}\,\phi_h\|_{0,K} \\
&\le C_N \|\boldsymbol{\beta}\|_{\mathrm{L}^\infty(\Omega)} \sum_{K\in\mathcal{T}_h} |\psi_h|_{2,K} |\phi_h|_{1,K} \\
&\le C_N \|\boldsymbol{\beta}\|_{\mathrm{L}^\infty(\Omega)} \|\psi_h\|_X |\phi_h|_{1,\Omega} \\
&\le C_N C_p \|\boldsymbol{\beta}\|_{\mathrm{L}^\infty(\Omega)} \|\psi_h\|_X \|\phi_h\|_X,
\end{aligned}
\tag{3.3.20}
$$

where we have used the inequality (3.3.5) and $C_p > 0$ is the constant such that

$$|\phi_h|_{1,\Omega} \le C_p \|\phi_h\|_X,$$

which is independent of h and K, for all $K \in \mathcal{T}_h$. Then, taking $C_{B^h} := C_N C_p \|\boldsymbol{\beta}\|_{\mathrm{L}^\infty(\Omega)} > 0$, we conclude the proof. □

Remark 3.3.1. *We observe that using the projector $\Pi_K^{k,\nabla^\perp}$ it is possible to construct alternative discrete bilinear forms in* (3.3.8) *and* (3.3.9) *More precisely, we can consider the following computable discrete forms:*

$$
\begin{aligned}
\widetilde{B}^{h,K}(\psi_h,\phi_h) &:= \int_K \left(\boldsymbol{\nabla}\mathbf{curl}\,\Pi_K^{k,\nabla^\perp}\psi_h\right)\boldsymbol{\beta}\cdot\mathbf{curl}\,\Pi_K^{k,\nabla^\perp}\phi_h, \\
\widetilde{C}^{h,K}(\psi_h,\phi_h) &:= \int_K \gamma\,\mathbf{curl}\,\Pi_K^{k,\nabla^\perp}\psi_h\cdot\mathbf{curl}\,\Pi_K^{k,\nabla^\perp}\psi_h + \mathcal{S}_{\mathbf{curl}}^K\left(\psi_h - \Pi_K^{k,\nabla^\perp}\psi_h, \phi_h - \Pi_K^{k,\nabla^\perp}\phi_h\right).
\end{aligned}
$$

With these new forms, it is possible to write a different discrete formulation to solve the Oseen problem. We will test the discrete method derived with these forms in the numerical result section (see Section 3.6.3).

3.3.3 Discrete formulation

Now we write the discrete formulation by using the discrete forms and employing the results of the previous sections we establish existence and uniqueness for our discrete scheme.

The virtual element discretization reads as follows: find $\psi_h \in X_h^k$ such that

$$\mathcal{O}^h(\psi_h,\phi_h) := \nu A^h(\psi_h,\phi_h) + B^h(\psi_h,\phi_h) + C^h(\psi_h,\phi_h) = F^h(\phi_h) \quad \forall \phi_h \in X_h^k. \tag{3.3.21}$$

The following result establishes that the bilinear form $\mathcal{O}^h(\cdot,\cdot)$ is elliptic.

Lemma 3.3.6. *Let C_N be the constant such that (3.3.5) hold true. Suppose that*

$$\frac{C_N^2 \|\boldsymbol{\beta}\|^2_{\mathrm{L}^\infty(\Omega)}}{2\nu\gamma_0\alpha_0\alpha_2} < 1, \tag{3.3.22}$$

then there exists $\widehat{\alpha} > 0$, independent of h, such that

$$\mathcal{O}^h(\phi_h, \phi_h) \geq \widehat{\alpha}\|\phi_h\|_X^2 \qquad \forall \phi_h \in X_h^k.$$

Proof. Let $\phi_h \in X_h^k$. Then, using (3.3.15), (3.3.18) and (3.3.20) we get

$$\begin{aligned}
\mathcal{O}^h(\phi_h, \phi_h) &= \nu A^h(\phi_h, \phi_h) + B^h(\phi_h, \phi_h) + C^h(\phi_h, \phi_h) \\
&\geq \nu\alpha_0\|\phi_h\|_X^2 - C_N\|\boldsymbol{\beta}\|_{\mathrm{L}^\infty(\Omega)}\|\phi_h\|_X|\phi_h|_{1,\Omega} + \alpha_2\gamma_0|\phi_h|^2_{1,\Omega} \\
&\geq \nu\alpha_0\|\phi_h\|_X^2 - \frac{C_N^2\|\boldsymbol{\beta}\|^2_{\mathrm{L}^\infty(\Omega)}}{2\alpha_2\gamma_0}\|\phi_h\|_X^2 - \frac{\alpha_2\gamma_0}{2}|\phi_h|^2_{1,\Omega} + \alpha_2\gamma_0|\phi_h|^2_{1,\Omega} \\
&= \left(\nu\alpha_0 - \frac{C_N^2\|\boldsymbol{\beta}\|^2_{\mathrm{L}^\infty(\Omega)}}{2\alpha_2\gamma_0}\right)\|\phi_h\|_X^2 + \frac{\alpha_2\gamma_0}{2}|\phi_h|^2_{1,\Omega} \\
&\geq \left(\nu\alpha_0 - \frac{C_N^2\|\boldsymbol{\beta}\|^2_{\mathrm{L}^\infty(\Omega)}}{2\alpha_2\gamma_0}\right)\|\phi_h\|_X^2,
\end{aligned}$$

where we have used the Young inequality. Then, taking $\widehat{\alpha} := \nu\alpha_0 - \dfrac{C_N^2\|\boldsymbol{\beta}\|^2_{\mathrm{L}^\infty(\Omega)}}{2\alpha_2\gamma_0} > 0$, the proof is complete. □

As a consequence of the previous lemma, we have the following result.

Theorem 3.3.1. *Suppose that (3.3.22) holds true. Then, there exists a unique $\psi_h \in X_h^k$ solution to problem (3.3.21) satisfying the following estimate*

$$\|\psi_h\|_X \leq C\|\mathbf{f}\|_{0,\Omega},$$

where C is a positive constant independent to h.

Remark 3.3.2. *Assumption (3.3.22) holds provided one selects γ appropriately. For instance, when the Oseen system is derived as a time discretisation of Navier–Stokes equations, this parameter represents the inverse of the timestep. Thus, the aforementioned relation can be regarded as a CFL-type condition at a discrete level.*

3.4 Error analysis

In the present section, we develop an error analysis for the discrete virtual element scheme presented in Section 3.3. We start with some preliminary results.

3.4.1 Preliminary results

First, we recall the estimate for the interpolant $\phi_I \in X_h^k$ of ϕ (see [18, 38]).

Proposition 3.4.1. *Assume that* **A1** *and* **A2** *are satisfied. Then, for each* $\phi \in \mathrm{H}^\delta(\Omega)$*, there exist* $\phi_I \in X_h^k$ *and* $C > 0$*, independent of* h*, such that*

$$\|\phi - \phi_I\|_{m,\Omega} \leq Ch^{\delta-m}|\phi|_{\delta,\Omega}, \quad m = 0,1,2, \quad 2 \leq \delta \leq k+1, \quad k \geq 2.$$

Now, invoking the Scott-Dupont Theory (see [54]) for the polynomial approximation, we have

Proposition 3.4.2. *If the assumption* **A2** *is satisfied, then there exists a constant* $C > 0$*, such that for every* $\phi \in \mathrm{H}^\delta(K)$*, there exists* $\phi_\pi \in \mathbb{P}_k(K)$*,* $k \geq 0$*, such that*

$$|\phi - \phi_\pi|_{m,K} \leq Ch_K^{\delta-m}|\phi|_{\delta,K}, \quad 0 \leq m \leq \delta \leq k+1,\ \ell = 0,1,\ldots,[\delta],$$

where $[\delta]$ *denoting largest integer equal or smaller than* $\delta \in \mathbb{R}$*.*

We are going to use the following standard approximation property (see [54, 59]):

Lemma 3.4.1. *There exists a constant* $C > 0$*, independent of* h_K*, such that for all* $\mathbf{v} \in \mathbf{H}^\delta(K)$

$$\|\mathbf{v} - \boldsymbol{\Pi}_K^{k-1}\mathbf{v}\|_{m,K} \leq Ch_K^{\delta-m}|\mathbf{v}|_{\delta,K} \quad 0 \leq m \leq \delta \leq k, \quad k \geq 1.$$

Now, we start with the following bound for the continuous and discrete linear functionals.

Proposition 3.4.3. *Let* $k \geq 2$*. Assume that* $\mathbf{f} \in \mathbf{L}^2(\Omega)$ *such that* $\mathbf{f}|_K \in \mathbf{H}^{k-2}(K)$ *for each* $K \in \mathcal{T}_h$*. Let* $F(\cdot)$ *and* $F^h(\cdot)$ *be the functionals defined in* (3.2.6) *and* (3.3.13)*, respectively. Then, we have the following estimate:*

$$\|F - F^h\| := \sup_{\substack{\phi_h \in X_h^k \\ \phi_h \neq 0}} \frac{|F(\phi_h) - F^h(\phi_h)|}{\|\phi_h\|_X} \leq Ch^{k-1}|\mathbf{f}|_{k-2,h}.$$

Since γ is a scalar function, the bilinear form $C^{h,K}(\cdot,\cdot)$ does not satisfy the consistency property. Nevertheless, we have the following auxiliary results which will be useful to prove the error estimates.

Lemma 3.4.2. *Let* $K \in \mathcal{T}_h$ *and let* γ *be a smooth scalar field defined on* K*. For any* $\mathbf{p}, \mathbf{q}$ *smooth enough vector fields defined on* K*, we have*

$$\begin{aligned}(\gamma\,\mathbf{p}, \mathbf{q})_{0,K} - (\gamma\,\boldsymbol{\Pi}_K^{k-1}\mathbf{p}, \boldsymbol{\Pi}_K^{k-1}\mathbf{q})_{0,K} \leq & \|\gamma\,\mathbf{p} - \boldsymbol{\Pi}_K^{k-1}(\gamma\,\mathbf{p})\|_{0,K}\|\mathbf{q} - \boldsymbol{\Pi}_K^{k-1}\mathbf{q}\|_{0,K} \\ & + \|\mathbf{p} - \boldsymbol{\Pi}_K^{k-1}\mathbf{p}\|_{0,K}\|\gamma\,\mathbf{q} - \boldsymbol{\Pi}_K^{k-1}(\gamma\,\mathbf{q})\|_{0,K} \\ & + \|\gamma\|_{\mathrm{L}^\infty(K)}\|\mathbf{p} - \boldsymbol{\Pi}_K^{k-1}\mathbf{p}\|_{0,K}\|\mathbf{q} - \boldsymbol{\Pi}_K^{k-1}\mathbf{q}\|_{0,K}.\end{aligned}$$

Proof. The proof follows adding and subtracting suitable terms and using the properties of the projection $\boldsymbol{\Pi}_K^{k-1}$ (Lemma 3.4.1). We omit further details. □

As an immediate consequence of Lemma 3.4.2, we have the following result.

Lemma 3.4.3. *For all $K \in \mathcal{T}_h$ and for all $\varphi_h, \phi_h \in X_h^k(K)$, we have that*

$$\begin{aligned} C^K(\varphi_h,\phi_h) - C^{h,K}(\varphi_h,\phi_h) \\ &\leq \|\gamma\,\mathbf{curl}\,\varphi_h - \boldsymbol{\Pi}_K^{k-1}(\gamma\mathbf{curl}\,\varphi_h)\|_{0,K}\|\mathbf{curl}\,\phi_h - \boldsymbol{\Pi}_K^{k-1}\mathbf{curl}\,\phi_h\|_{0,K} \\ &\quad + \|\gamma\,\mathbf{curl}\,\phi_h - \boldsymbol{\Pi}_K^{k-1}(\gamma\mathbf{curl}\,\phi_h)\|_{0,K}\|\mathbf{curl}\,\varphi_h - \boldsymbol{\Pi}_K^{k-1}\mathbf{curl}\,\varphi_h\|_{0,K} \\ &\quad + C_\gamma\|\mathbf{curl}\,\phi_h - \boldsymbol{\Pi}_K^{k-1}\mathbf{curl}\,\phi_h\|_{0,K}\|\mathbf{curl}\,\varphi_h - \boldsymbol{\Pi}_K^{k-1}\mathbf{curl}\,\varphi_h\|_{0,K} \\ &\quad + \mathcal{S}^K_{\mathbf{curl}}(\varphi_h - \Pi_K^{k,\nabla^\perp}\varphi_h, \phi_h - \Pi_K^{k,\nabla^\perp}\phi_h), \end{aligned}$$

where $C_\gamma > 0$ is a constant depending on the function γ.

For the bilinear forms $B^K(\cdot,\cdot)$ and $B^{h,K}(\cdot,\cdot)$, we have the following analogous result.

Lemma 3.4.4. *For all $K \in \mathcal{T}_h$ and for all $\varphi_h, \phi_h \in X_h^k(K)$, we have that*

$$\begin{aligned} B^K(\varphi_h,\phi_h) - B^{h,K}(\varphi_h,\phi_h) \\ &\leq \|(\boldsymbol{\nabla}\mathbf{curl}\,\varphi_h)\boldsymbol{\beta} - \boldsymbol{\Pi}_K^{k-1}[(\boldsymbol{\nabla}\mathbf{curl}\,\varphi_h)\boldsymbol{\beta}]\|_{0,K}\|\mathbf{curl}\,\phi_h - \boldsymbol{\Pi}_K^{k-1}\mathbf{curl}\,\phi_h\|_{0,K} \\ &\quad + \|\boldsymbol{\beta}\|_{\mathrm{L}^\infty(K)}|\mathbf{curl}\,\varphi_h - \boldsymbol{\Pi}_K^{k-1}\mathbf{curl}\,\varphi_h|_{1,K}\|\boldsymbol{\Pi}_K^{k-1}\mathbf{curl}\,\phi_h\|_{0,K}. \end{aligned}$$

Proof. Let $\varphi_h, \phi_h \in X_h^k(K)$. Then, by using the definition of the bilinear forms $B^K(\cdot,\cdot)$ and $B^{h,K}(\cdot,\cdot)$, adding and subtracting suitable terms and using the properties of the projection $\boldsymbol{\Pi}_K^{k-1}$, we have

$$\begin{aligned} B^K(\varphi_h,\phi_h) - B^{h,K}(\varphi_h,\phi_h) &= \int_K (\boldsymbol{\nabla}\mathbf{curl}\,\varphi_h)\boldsymbol{\beta}\cdot(\mathbf{curl}\,\phi_h - \boldsymbol{\Pi}_K^{k-1}\mathbf{curl}\,\phi_h) \\ &\quad + \int_K (\boldsymbol{\nabla}\mathbf{curl}\,\varphi_h - \boldsymbol{\nabla}\boldsymbol{\Pi}_K^{k-1}\mathbf{curl}\,\varphi_h)\boldsymbol{\beta}\cdot\boldsymbol{\Pi}_K^{k-1}\mathbf{curl}\,\phi_h \\ &= \int_K \big((\boldsymbol{\nabla}\mathbf{curl}\,\varphi_h)\boldsymbol{\beta} - \boldsymbol{\Pi}_K^{k-1}[(\boldsymbol{\nabla}\mathbf{curl}\,\varphi_h)\boldsymbol{\beta}]\big)\cdot(\mathbf{curl}\,\phi_h - \boldsymbol{\Pi}_K^{k-1}\mathbf{curl}\,\phi_h) \\ &\quad + \int_K (\boldsymbol{\nabla}\mathbf{curl}\,\varphi_h - \boldsymbol{\nabla}\boldsymbol{\Pi}_K^{k-1}\mathbf{curl}\,\varphi_h)\boldsymbol{\beta}\cdot\boldsymbol{\Pi}_K^{k-1}\mathbf{curl}\,\phi_h \\ &\leq \|(\boldsymbol{\nabla}\mathbf{curl}\,\varphi_h)\boldsymbol{\beta} - \boldsymbol{\Pi}_K^{k-1}[(\boldsymbol{\nabla}\mathbf{curl}\,\varphi_h)\boldsymbol{\beta}]\|_{0,K}\|\mathbf{curl}\,\phi_h - \boldsymbol{\Pi}_K^{k-1}\mathbf{curl}\,\phi_h\|_{0,K} \\ &\quad + \|\boldsymbol{\beta}\|_{\mathrm{L}^\infty(K)}|\mathbf{curl}\,\varphi_h - \boldsymbol{\Pi}_K^{k-1}\mathbf{curl}\,\varphi_h|_{1,K}\|\boldsymbol{\Pi}_K^{k-1}\mathbf{curl}\,\phi_h\|_{0,K}, \end{aligned}$$

where in the last step we have used the Cauchy-Schwarz inequality. $\square$

3.4.2 A priori error estimates

We start with the following result.

Lemma 3.4.5. *Suppose that (3.3.22) holds true. Let ψ and ψ_h be the unique solutions of problem (3.2.2) and problem (3.3.21), respectively. Moreover, suppose that $\psi \in \mathrm{H}^{2+s}(\Omega)$, $\boldsymbol{\beta} \in \mathbf{W}_\infty^{s-1}(\Omega)$ and $\gamma \in \mathrm{W}_\infty^{1+s}(\Omega)$, for $1/2 < s \leq k-1$, then there exists a constant $C > 0$, independent of h, such that*

$$\|\psi - \psi_h\|_X \leq C\left(\|F - F^h\| + \|\psi - \psi_I\|_X + |\psi - \psi_\pi|_{1,h} + |\psi - \psi_\pi|_{2,h} + h^s\|\psi\|_{2+s,\Omega}\right),$$

for all $\psi_I \in X_h^k$ and for all $\psi_\pi \in \mathrm{L}^2(\Omega)$ such that $\psi_\pi|_K \in \mathbb{P}_k(K)$ for all polygon $K \in \mathcal{T}_h$.

Proof. Let $\psi_I \in X_h^k$. We set $\delta_h := \psi_h - \psi_I$, then

$$\|\psi - \psi_h\|_X \leq \|\psi - \psi_I\|_X + \|\delta_h\|_X. \tag{3.4.1}$$

We will bound the second term above, we begin by using Lemma 3.3.6, adding and subtracting the term $\mathcal{O}(\psi, \delta_h)$ and using the definition of the continuous and discrete problems (3.2.2) and (3.3.21), respectively, we have

$$\begin{aligned}
\widehat{\alpha}\|\delta_h\|_X^2 \leq\ & \mathcal{O}^h(\delta_h, \delta_h) = \mathcal{O}^h(\psi_h, \delta_h) - \mathcal{O}^h(\psi_I, \delta_h) \\
=\ & F^h(\delta_h) - \mathcal{O}^h(\psi_I, \delta_h) \\
=\ & F^h(\delta_h) - F(\delta_h) + \mathcal{O}(\psi, \delta_h) - \mathcal{O}^h(\psi_I, \delta_h) \\
=\ & (F^h(\delta_h) - F(\delta_h)) + \sum_{K\in\mathcal{T}_h} \Big\{\nu A^K(\psi, \delta_h) + B^K(\psi, \delta_h) + C^K(\psi, \delta_h)\Big\} \\
& - \sum_{K\in\mathcal{T}_h} \Big\{\nu A^{h,K}(\psi_I, \delta_h) + B^{h,K}(\psi_I, \delta_h) + C^{h,K}(\psi_I, \delta_h)\Big\} \\
=\ & (F^h(\delta_h) - F(\delta_h)) + \sum_{K\in\mathcal{T}_h} \Big\{\nu A^K(\psi - \psi_\pi, \delta_h) - \nu A^{h,K}(\psi_I - \psi_\pi, \delta_h)\Big\} \\
& + \sum_{K\in\mathcal{T}_h} \Big\{B^K(\psi, \delta_h) - B^{h,K}(\psi_I, \delta_h)\Big\} \\
& + \sum_{K\in\mathcal{T}_h} \Big\{C^K(\psi, \delta_h) - C^{h,K}(\psi_I, \delta_h)\Big\} \\
=:\ & T_F + \sum_{K\in\mathcal{T}_h} \{T_A\} + \sum_{K\in\mathcal{T}_h} \{T_B\} + \sum_{K\in\mathcal{T}_h} \{T_C\},
\end{aligned} \tag{3.4.2}$$

where we have added and subtracted $\psi_\pi \in \mathbb{P}_k(K)$ for all $K \in \mathcal{T}_h$ (recall $k \geq 2$) and we have used the consistency property of bilinear form $A^h(\cdot, \cdot)$. Next, we bound each term on the right hand side above.

For the term T_F, we have

$$T_F \leq \|F - F^h\| \|\delta_h\|_X. \tag{3.4.3}$$

Now, for the term T_A, we use the continuity of the bilinear forms $A^K(\cdot, \cdot)$ and $A^{h,K}(\cdot, \cdot)$, together with the triangular inequality to obtain that

$$\begin{aligned}
T_A &= \nu\Big\{A^K(\psi - \psi_\pi, \delta_h) + A^{h,K}(\psi_I - \psi_\pi, \delta_h)\Big\} \\
&\leq C(|\psi - \psi_\pi|_{2,K}|\delta_h|_{2,K} + |\psi_I - \psi_\pi|_{2,K}|\delta_h|_{2,K}) \\
&\leq C\left(|\psi - \psi_\pi|_{2,K} + |\psi - \psi_I|_{2,K}\right)|\delta_h|_{2,K}.
\end{aligned} \tag{3.4.4}$$

For term T_B, we add and subtract $B^K(\psi_I, \delta_h)$,

$$\begin{aligned}
T_B &= B^K(\psi, \delta_h) - B^{h,K}(\psi_I, \delta_h) \\
&= B^K(\psi, \delta_h) - B^K(\psi_I, \delta_h) + B^K(\psi_I, \delta_h) - B^{h,K}(\psi_I, \delta_h) \\
&= B^K(\psi - \psi_I, \delta_h) + \big(B^K(\psi_I, \delta_h) - B^{h,K}(\psi_I, \delta_h)\big) \\
&\leq C|\psi - \psi_I|_{2,K}|\delta_h|_{2,K} + \big(B^K(\psi_I, \delta_h) - B^{h,K}(\psi_I, \delta_h)\big),
\end{aligned} \tag{3.4.5}$$

where we have used the continuity of $B^K(\cdot,\cdot)$. To bound the second term on the right hand side above, we use Lemma 3.4.4 along with the stability and approximation properties of projector $\boldsymbol{\Pi}_K^{k-1}$. We have that

$$
\begin{aligned}
&B^K(\psi_I,\delta_h) - B^{h,K}(\psi_I,\delta_h)\\
&\qquad \le \|(\boldsymbol{\nabla}\mathbf{curl}\,\psi_I)\boldsymbol{\beta} - \boldsymbol{\Pi}_K^{k-1}[(\boldsymbol{\nabla}\mathbf{curl}\,\psi_I)\boldsymbol{\beta}]\|_{0,K}\|\mathbf{curl}\,\delta_h - \boldsymbol{\Pi}_K^{k-1}\mathbf{curl}\,\delta_h\|_{0,K}\\
&\qquad\quad + \|\boldsymbol{\beta}\|_{\mathrm{L}^\infty(K)}|\mathbf{curl}\,\psi_I - \boldsymbol{\Pi}_K^{k-1}\mathbf{curl}\,\psi_I|_{1,K}\|\boldsymbol{\Pi}_K^{k-1}\mathbf{curl}\,\delta_h\|_{0,K}\\
&\qquad \le C\|(\boldsymbol{\nabla}\mathbf{curl}\,\psi_I)\boldsymbol{\beta} - \boldsymbol{\Pi}_K^{k-1}[(\boldsymbol{\nabla}\mathbf{curl}\,\psi_I)\boldsymbol{\beta}]\|_{0,K}\, h_K|\delta_h|_{2,K}\\
&\qquad\quad + C\|\boldsymbol{\beta}\|_{\mathrm{L}^\infty(K)}|\mathbf{curl}\,\psi_I - \boldsymbol{\Pi}_K^{k-1}\mathbf{curl}\,\psi_I|_{1,K}|\delta_h|_{2,K}\\
&\qquad = Ch_K|\delta_h|_{2,K}E_1 + C|\delta_h|_{2,K}E_2.
\end{aligned}
\tag{3.4.6}
$$

In what follows, we bound the terms E_1 and E_2. For the term E_1, we have

$$
\begin{aligned}
E_1 &:= \|(\boldsymbol{\nabla}\mathbf{curl}\,\psi_I)\boldsymbol{\beta} - \boldsymbol{\Pi}_K^{k-1}[(\boldsymbol{\nabla}(\mathbf{curl}\,\psi_I)\boldsymbol{\beta}]\|_{0,K}\\
&\le \|(\boldsymbol{\nabla}\mathbf{curl}\,\psi_I)\boldsymbol{\beta} - (\boldsymbol{\nabla}\mathbf{curl}\,\psi)\boldsymbol{\beta}\|_{0,K} + \|(\boldsymbol{\nabla}\mathbf{curl}\,\psi)\boldsymbol{\beta} - \boldsymbol{\Pi}_K^{k-1}[(\boldsymbol{\nabla}\mathbf{curl}\,\psi)\boldsymbol{\beta}]\|_{0,K}\\
&\quad + \|\boldsymbol{\Pi}_K^{k-1}[(\boldsymbol{\nabla}\mathbf{curl}\,\psi)\boldsymbol{\beta}] - \boldsymbol{\Pi}_K^{k-1}[(\boldsymbol{\nabla}\mathbf{curl}\,\psi_I)\boldsymbol{\beta}]\|_{0,K}\\
&\le \|(\nabla\mathbf{curl}\,(\psi_I-\psi))\boldsymbol{\beta}\|_{0,K} + \|(\boldsymbol{\nabla}\mathbf{curl}\,\psi)\boldsymbol{\beta} - \boldsymbol{\Pi}_K^{k-1}[(\boldsymbol{\nabla}\mathbf{curl}\,\psi)\boldsymbol{\beta}]\|_{0,K}\\
&\quad + \|(\boldsymbol{\nabla}\mathbf{curl}\,(\psi-\psi_I))\boldsymbol{\beta}\|_{0,K}\\
&\le 2\|\boldsymbol{\beta}\|_{\mathrm{L}^\infty(K)}|\psi-\psi_I|_{2,K} + h_K^{s-1}|\boldsymbol{\nabla}(\mathbf{curl}\,\psi)\boldsymbol{\beta}|_{s-1,K}\\
&\le 2\|\boldsymbol{\beta}\|_{\mathrm{L}^\infty(K)}|\psi-\psi_I|_{2,K} + h_K^{s-1}\|\boldsymbol{\beta}\|_{\mathrm{W}_\infty^{s-1}(K)}\|\boldsymbol{\nabla}(\mathbf{curl}\,\psi)\|_{s-1,K}\\
&\le 2\|\boldsymbol{\beta}\|_{\mathrm{L}^\infty(K)}|\psi-\psi_I|_{2,K} + h_K^{s-1}\|\boldsymbol{\beta}\|_{\mathrm{W}_\infty^{s-1}(K)}\|\psi\|_{2+s,K},
\end{aligned}
\tag{3.4.7}
$$

where we have used the approximation and stability properties of projector $\boldsymbol{\Pi}_K^{k-1}$. Now, for the term E_2, we proceed as follows,

$$
\begin{aligned}
E_2 &:= |\mathbf{curl}\,\psi_I - \boldsymbol{\Pi}_K^{k-1}\mathbf{curl}\,\psi_I|_{1,K}\\
&\le |\mathbf{curl}\,\psi_I - \mathbf{curl}\,\psi|_{1,K} + |\mathbf{curl}\,\psi - \boldsymbol{\Pi}_K^{k-1}\mathbf{curl}\,\psi|_{1,K}\\
&\qquad + |\boldsymbol{\Pi}_K^{k-1}\mathbf{curl}\,\psi - \boldsymbol{\Pi}_K^{k-1}\mathbf{curl}\,\psi_I|_{1,K}\\
&\le C\left(|\psi-\psi_I|_{2,K} + h^s|\mathbf{curl}\,\psi|_{1+s,K} + |\boldsymbol{\Pi}_K^{k-1}\mathbf{curl}\,(\psi-\psi_I)|_{1,K}\right)\\
&\le C(|\psi-\psi_I|_{2,K} + h^s|\mathbf{curl}\,\psi|_{1+s,K} + |\psi-\psi_I|_{2,K})\\
&\le C(|\psi-\psi_I|_{2,K} + h^s|\psi|_{2+s,K}),
\end{aligned}
\tag{3.4.8}
$$

where, once again, we have used the approximation and stability properties of $\boldsymbol{\Pi}_K^{k-1}$.

Inserting (3.4.7) and (3.4.8) into (3.4.6), we obtain

$$
\begin{aligned}
&B^K(\psi_I,\delta_h) - B^{h,K}(\psi_I,\delta_h)\\
&\qquad \le C(\|\boldsymbol{\beta}\|_{\mathrm{L}^\infty(\Omega)}h_K|\psi-\psi_I|_{2,K} + h_K^s\|\boldsymbol{\beta}\|_{\mathrm{W}_\infty^{s-1}(\Omega)}\|\psi\|_{2+s,K})|\delta_h|_{2,K}\\
&\qquad\quad + C\|\boldsymbol{\beta}\|_{\mathrm{L}^\infty(\Omega)}(|\psi-\psi_I|_{2,K} + h^s\|\psi\|_{2+s,K})|\delta_h|_{2,K}\\
&\qquad \le C(|\psi-\psi_I|_{2,K} + h_K^s\|\psi\|_{2+s,K})|\delta_h|_{2,K}.
\end{aligned}
\tag{3.4.9}
$$

Now, using estimate (3.4.9), from (3.4.5), we obtain

$$
T_B \le C(|\psi-\psi_I|_{2,K} + h_K^s\|\psi\|_{2+s,K})|\delta_h|_{2,K}. \tag{3.4.10}
$$

By using Lemma 3.4.3 and repeating analogous arguments as above, we can prove that

$$T_C \leq C \left(|\psi - \psi_I|_{2,K} + |\psi - \psi_\pi|_{1,K} + h_K^{s+1} \|\psi\|_{2+s,K} \right) |\delta_h|_{2,K}. \tag{3.4.11}$$

Then, inserting (3.4.3), (3.4.4), (3.4.10) and (3.4.11) into (3.4.2) and employing the Hölder inequality (for sequences), we obtain

$$\widehat{\alpha} \|\delta_h\|_X \leq C \left(\|F - F^h\| + \|\psi - \psi_I\|_X + |\psi - \psi_\pi|_{1,h} + |\psi - \psi_\pi|_{2,h} + h^s \|\psi\|_{2+s,\Omega} \right). \tag{3.4.12}$$

Therefore, the proof follows from (3.4.1) and (3.4.12). □

Theorem 3.4.1. *Let $k \geq 2$ and $\mathbf{f} \in \mathbf{L}^2(\Omega)$ such that $\mathbf{f}|_K \in \mathbf{H}^{k-2}(K)$ for each $K \in \mathcal{T}_h$. Suppose that (3.3.22) holds true. Let ψ and ψ_h be the unique solutions of problem (3.2.2) and problem (3.3.21), respectively. We suppose that $\psi \in \mathrm{H}^{2+s}(\Omega)$, $\boldsymbol{\beta} \in \mathbf{W}_\infty^{s-1}(\Omega)$ and $\gamma \in \mathrm{W}_\infty^{1+s}(\Omega)$, for $1/2 < s \leq k-1$, then there exists a constant $C > 0$, independent of h, such that*

$$\|\psi - \psi_h\|_X \leq C h^s \left(|\mathbf{f}|_{k-2,h} + \|\psi\|_{2+s,\Omega} \right).$$

Proof. The result follows from Lemma 3.4.5 and Propositions 3.4.1, 3.4.2 and 3.4.3. □

3.5 Recovering the velocity, vorticity and pressure fields

The solution of the proposed virtual element method (3.3.21) delivers an approximation of the stream-function field. We remark that one of the advantages of solving fluid flow problems through a stream-function formulation is the possibility of computing further variables of interest, such as the velocity $\mathbf{u}$, the fluid pressure p and the fluid vorticity ω. In this section, we will present strategies to recover these three fields. We compute a discrete velocity and discrete vorticity as a simple postprocess of the computed stream-function using suitable projections, while to recover the pressure we will write a generalized Poisson problem with data coming from the computed stream-function and the load term $\mathbf{f}$, then we propose a discrete virtual scheme, based on the C^0 enhanced virtual element space from [7] to approximate the pressure. Also in this section, we will establish error estimates in a broken H^1-norm for the velocity and in the L^2-norm for the vorticity. Moreover, under the assumptions that Ω is a convex domain and that the family of polygonal meshes $\mathcal{T}_h$ is quasi-uniform also we will establish an error estimate for the pressure in the H^1-norm.

3.5.1 Computing the velocity field

We start by noticing that if the stream-function $\psi \in X$ is the unique solution of (3.2.2), then we have that the velocity $\mathbf{u}$ satisfies:

$$\mathbf{u} = \mathbf{curl}\, \psi. \tag{3.5.1}$$

At the discrete level, we compute a discrete velocity as a post-processing of the computed stream-function $\psi_h \in X_h^k$ as follows: if ψ_h is the unique solution of problem (3.3.21), then the function

$$\mathbf{u}_h := \boldsymbol{\Pi}_h^{k-1} \mathbf{curl}\, \psi_h, \tag{3.5.2}$$

is an approximation of the velocity, where $\mathbf{\Pi}_h^{k-1}$ is defined in $\mathbf{L}^2(\Omega)$ by

$$(\mathbf{\Pi}_h^{k-1}\mathbf{v})|_K = \mathbf{\Pi}_K^{k-1}(\mathbf{v}|_K) \qquad \forall K \in \mathcal{T}_h.$$

The following result establishes the accuracy of the discrete velocity:

Theorem 3.5.1. *Assume that the hypotheses of Theorem 3.4.1 hold true, then there exists a positive constant C, independent of h, such that*

$$|\mathbf{u} - \mathbf{u}_h|_{1,h} \le Ch^s \left(|\mathbf{f}|_{k-2,h} + \|\psi\|_{2+s,\Omega}\right).$$

Proof. From (3.5.1) and (3.5.2), triangular inequality and property (3.3.5), we have

$$\begin{aligned}
|\mathbf{u} - \mathbf{u}_h|_{1,h}^2 &= |\mathbf{curl}\,\psi - \mathbf{\Pi}_h^{k-1}\mathbf{curl}\,\psi_h|_{1,h}^2 \\
&= \sum_{K\in\mathcal{T}_h} |\mathbf{curl}\,\psi - \mathbf{\Pi}_K^{k-1}\mathbf{curl}\,\psi_h|_{1,K}^2 \\
&\le C \sum_{K\in\mathcal{T}_h} \left(|\mathbf{curl}\,\psi - \mathbf{\Pi}_K^{k-1}\mathbf{curl}\,\psi|_{1,K}^2 + |\mathbf{\Pi}_K^{k-1}(\mathbf{curl}\,\psi - \mathbf{curl}\,\psi_h)|_{1,K}^2\right) \\
&\le C\Big(\sum_{K\in\mathcal{T}_h} h_K^{2s}\|\mathbf{curl}\,\psi\|_{1+s,K}^2 + \sum_{K\in\mathcal{T}_h} |\mathbf{\Pi}_K^{k-1}\mathbf{curl}\,(\psi - \psi_h)|_{1,K}^2\Big) \\
&\le Ch^{2s}\Big(\sum_{K\in\mathcal{T}_h} \|\psi\|_{2+s,K}^2 + C_N \sum_{K\in\mathcal{T}_h} |\psi - \psi_h|_{2,K}^2\Big) \\
&\le C(h^{2s}\|\psi\|_{2+s,\Omega}^2 + \|\psi - \psi_h\|_X^2) \\
&\le Ch^{2s}\left(|\mathbf{f}|_{k-2,h}^2 + \|\psi\|_{2+s,\Omega}^2\right),
\end{aligned}$$

where we have used the approximation properties of projector $\mathbf{\Pi}_K^{k-1}$ and Theorem 3.4.1. The proof is complete □

3.5.2 Computing the fluid vorticity

Now, we will present an strategy to recover the fluid vorticity ω, which is key in several important applications in fluid mechanics (see [46, 89, 14, 15]). First, we remark that $\omega = \operatorname{rot}\mathbf{u}$, then using the identity $\mathbf{u} = \mathbf{curl}\,\psi$, we have that

$$\omega = \operatorname{rot}\mathbf{u} = \operatorname{rot}(\mathbf{curl}\,\psi) = -\Delta\psi. \tag{3.5.3}$$

We introduce an L^2-orthogonal projection which will be used to construct the discrete vorticity. For $k \ge 2$ and for each $K \in \mathcal{T}_h$, we consider the L^2-projection onto $\mathbb{P}_{k-2}(K)$: for $v \in \mathrm{L}^2(K)$, $\Pi_K^{k-2}v \in \mathbb{P}_{k-2}(K)$ is the unique function such that

$$(v - \Pi_K^{k-2}v, q)_{0,K} = 0 \quad \forall q \in \mathbb{P}_{k-2}(K). \tag{3.5.4}$$

We have the following approximation result (see [54, 28]).

Proposition 3.5.1. *Let Π_K^{k-2} be the projection defined in (3.5.4). Then, the following approximation property hold true: there exists a constant $\hat{C}$, independent of h_K, such that*

$$\|v - \Pi_K^{k-2}v\|_{m,K} \le \hat{C}h_K^{\delta-m}|v|_{\delta,K} \quad \forall v \in \mathrm{H}^\delta(K), \qquad 0 \le m \le \delta \le k-1, \quad k \ge 2.$$

Now, we compute a discrete vorticity as follows: if $\psi_h \in X_h^k$ is the unique solution of (3.3.21), then the function

$$\omega_h := -\Pi_h^{k-2}(\Delta\psi_h), \tag{3.5.5}$$

is an approximation of the vorticity, where we have used the notation

$$(\Pi_h^{k-2}v)|_K = \Pi_K^{k-2}(v|_K) \qquad \forall v \in \mathrm{L}^2(\Omega) \quad \text{and} \quad \forall K \in \mathcal{T}_h.$$

Remark 3.5.1. *We observe that for each $\phi_h \in X_h^k(K)$ the polynomial function $\Pi_K^{k-2}(\Delta\phi_h) \in \mathbb{P}_{k-2}(K)$, $k \geq 2$, is computable using the degrees of freedom $\mathbf{D_1} - \mathbf{D_5}$, where $X_h^k(K)$ is the local virtual space defined in (3.3.3). Indeed, for each $\phi_h \in X_h^k(K)$ and for all $q \in \mathbb{P}_{k-2}(K)$, we have*

$$\int_K q\,\Pi_K^{k-2}(\Delta\phi_h) = \int_K q\,\Delta\phi_h = \int_K \phi_h \Delta q - \int_{\partial K} \phi_h\,\partial_{\mathbf{n}_K} q + \int_{\partial K} q\,\partial_{\mathbf{n}_K}\phi_h,$$

since $\Delta q \in \mathbb{P}_{k-4}(K)$, the first integral on the right hand side above is computable using the output values of the set $\mathbf{D_5}$. Moreover, the boundary terms are fully computable using the information of $\mathbf{D_1} - \mathbf{D_4}$.

Now, we can prove the following convergence result for the discrete vorticity.

Theorem 3.5.2. *Assume that the hypotheses of Theorem 3.4.1 hold true, then there exists a positive constant C, independent of h, such that*

$$\|\omega - \omega_h\|_{0,\Omega} \leq Ch^s\left(|\mathbf{f}|_{k-2,h} + \|\psi\|_{2+s,\Omega}\right).$$

Proof. From (3.5.3) and (3.5.5), triangular inequality, we have

$$\begin{aligned}
\|\omega - \omega_h\|_{0,\Omega}^2 = \|\Delta\psi - \Pi_h^{k-2}(\Delta\psi_h)\|_{0,\Omega}^2 &= \sum_{K\in\mathcal{T}_h} \|\Delta\psi - \Pi_K^{k-2}(\Delta\psi_h)\|_{0,K}^2 \\
&\leq C \sum_{K\in\mathcal{T}_h} \left(\|\Delta\psi - \Pi_K^{k-2}(\Delta\psi)\|_{0,K}^2 + \|\Pi_K^{k-2}(\Delta\psi - \Delta\psi_h)\|_{0,K}^2\right) \\
&\leq C\left(\sum_{K\in\mathcal{T}_h} h_K^{2s}\|\Delta\psi\|_{s,K}^2 + \sum_{K\in\mathcal{T}_h} \|\Pi_K^{k-2}\Delta(\psi-\psi_h)\|_{0,K}^2\right) \\
&\leq C(h^{2s}\|\psi\|_{2+s,\Omega}^2 + \|\psi - \psi_h\|_X^2) \\
&\leq Ch^{2s}\left(|\mathbf{f}|_{k-2,h}^2 + \|\psi\|_{2+s,\Omega}^2\right),
\end{aligned}$$

where we have used Proposition 3.5.1 and Theorem 3.4.1. The proof is complete. □

3.5.3 Computing the fluid pressure

Next, we will present an strategy to recover the fluid pressure. We will follow recent results presented in [133] for the Brinkman equations.

We start by considering the following Hilbert space:

$$\widetilde{\mathrm{H}}^1(\Omega) := \left\{q \in \mathrm{H}^1(\Omega) : (q,1)_{0,\Omega} = 0\right\}.$$

By using the identity $-\Delta\mathbf{u} = \mathbf{curl}\,(\mathrm{rot}\,\mathbf{u}) - \nabla(\mathrm{div}\,\mathbf{u})$ in the momentum equation of problem (3.2.1) and the fact that $\mathbf{u} = \mathbf{curl}\,\psi$, we have that

$$\begin{aligned}\mathbf{f} &= -\nu\,\Delta\mathbf{u} + (\boldsymbol{\nabla}\mathbf{u})\boldsymbol{\beta} + \gamma\,\mathbf{u} + \nabla p\\ &= \nu\,(\mathbf{curl}\,(\mathrm{rot}\,\mathbf{u}) - \nabla(\mathrm{div}\,\mathbf{u})) + (\boldsymbol{\nabla}\mathbf{u})\boldsymbol{\beta} + \gamma\,\mathbf{u} + \nabla p\\ &= \nu\,\mathbf{curl}\,(\mathrm{rot}(\mathbf{curl}\,\psi)) + (\boldsymbol{\nabla}\mathbf{curl}\,\psi)\boldsymbol{\beta} + \gamma\,\mathbf{curl}\,\psi + \nabla p,\end{aligned}$$

where we have used that $\mathrm{div}\mathbf{u} = 0$ in Ω (cf. (3.2.1)). Now using the identity $\mathrm{rot}(\mathbf{curl}\psi) = -\Delta\psi$, the above equality can be rewritten as follows:

$$\nabla p = \mathbf{f} - \gamma\,\mathbf{curl}\,\psi - (\boldsymbol{\nabla}\mathbf{curl}\,\psi)\boldsymbol{\beta} + \nu\,\mathbf{curl}\,(\Delta\psi). \tag{3.5.6}$$

Then, by testing (3.5.6) with ∇q for $q \in \widetilde{\mathrm{H}}^1(\Omega)$, we get the following variational problem to calculate the fluid pressure: find $p \in \widetilde{\mathrm{H}}^1(\Omega)$ such that

$$D_\nabla(p,q) = G^\psi(q) \quad \forall q \in \widetilde{\mathrm{H}}^1(\Omega), \tag{3.5.7}$$

where $D_\nabla : \widetilde{\mathrm{H}}^1(\Omega) \times \widetilde{\mathrm{H}}^1(\Omega) \to \mathbb{R}$ is defined by

$$D_\nabla(p,q) := \int_\Omega \nabla p \cdot \nabla q \qquad \forall p,q \in \widetilde{\mathrm{H}}^1(\Omega) \tag{3.5.8}$$

and $G^\psi : \widetilde{\mathrm{H}}^1(\Omega) \to \mathbb{R}$ is the functional defined by:

$$G^\psi(q) := \int_\Omega \mathbf{f}\cdot\nabla q - \gamma\,\mathbf{curl}\,\psi\cdot\nabla q - (\boldsymbol{\nabla}\mathbf{curl}\,\psi)\boldsymbol{\beta}\cdot\nabla q + \nu\,\mathbf{curl}\,(\Delta\psi)\cdot\nabla q \quad \forall q \in \widetilde{\mathrm{H}}^1(\Omega). \tag{3.5.9}$$

From now on, we assume that Ω is a convex domain. As a consequence, we have an additional regularity for the unique solution of problem (3.2.2). More precisely, we have that $\psi \in \mathrm{H}^3(\Omega)$ and that there exists a positive constant C such that

$$\|\psi\|_{3,\Omega} \le C\|\mathbf{f}\|_{0,\Omega}.$$

As an immediate consequence of the above regularity result, the generalized Poincaré inequality and the Lax-Milgram Theorem, we have the following result.

Theorem 3.5.3. *There exists a unique $p \in \widetilde{\mathrm{H}}^1(\Omega)$ solution of problem (3.5.7). In addition, there exists $C > 0$ such that*

$$\|p\|_{1,\Omega} \le C\|\mathbf{f}\|_{0,\Omega}.$$

In what follows, we will propose a lowest order discrete virtual element scheme to approximate the fluid pressure over the same polygonal mesh $\mathcal{T}_h$ used to solve the stream-function discrete formulation (3.3.21). With this aim, we split the bilinear form $D_\nabla(\cdot,\cdot)$, as a contribution element by element as follows:

$$D_\nabla(p,q) := \sum_{K\in\mathcal{T}_h} D_\nabla^K(p,q) = \sum_{K\in\mathcal{T}_h}\int_K \nabla p\cdot\nabla q, \qquad \forall p,q \in \widetilde{\mathrm{H}}^1(\Omega). \tag{3.5.10}$$

Now, for each polygon $K \in \mathcal{T}_h$, we consider the finite-dimensional space $\widetilde{W}_h(K)$, defined as

$$\widetilde{W}_h(K) := \left\{q_h \in \mathrm{H}^1(K)\cap C^0(\partial K) : q_h|_e \in \mathbb{P}_1(e) \quad \forall e \subset \partial K,\ \Delta q_h \in \mathbb{P}_0(K)\right\}.$$

The following set of linear operator is defined for all $q_h \in \widetilde{W}_h(K)$:

$\mathbf{P_1}$: the values of q_h at the vertices of K.

We define the projector $\Pi_K^{\nabla} : \widetilde{W}_h(K) \to \mathbb{P}_1(K) \subseteq \widetilde{W}_h(K)$ for each $q_h \in \widetilde{W}_h(K)$ as the solution of

$$D_{\nabla}^K(\Pi_K^{\nabla} q_h, p_1) = D_{\nabla}^K(q_h, p_1) \qquad \forall p_1 \in \mathbb{P}_1(K),$$
$$\widehat{\Pi_K^{\nabla} q_h} = \widehat{q}_h,$$

where $\widehat{(\cdot)}$ is defined in (3.3.2). We note that the operator Π_K^{∇} is explicitly computable using the set $\mathbf{P_1}$ (see [28]). In addition, using this projection and the definition of $\widetilde{W}_h(K)$, we introduce our local virtual space:

$$W_h(K) := \left\{ q_h \in \widetilde{W}_h(K) : (q_h - \Pi_K^{\nabla} q_h, 1)_{0,K} = 0 \right\}.$$

It is easy to observe that $\mathbb{P}_1(K) \subseteq W_h(K) \subseteq \widetilde{W}_h(K)$. Moreover, we have that the set $\mathbf{P_1}$ constitutes a set of degrees of freedom for $W_h(K)$ and operator Π_K^{∇} is also computable using only the set $\mathbf{P_1}$ (see [28]).

Now, we define the following global virtual space to approximate the pressure

$$W_h := \left\{ q_h \in \widetilde{\mathrm{H}}^1(\Omega) : q_h|_K \in W_h(K) \quad \forall K \in \mathcal{T}_h \right\}.$$

Next, we will continue with the construction of the discrete version of the bilinear form and the linear functional introduced in (3.5.8) and (3.5.9), respectively. To do that, we consider an L^2-orthogonal projection. For each $K \in \mathcal{T}_h$, we define $\mathbf{\Pi}_K^0 : \mathbf{L}^2(K) \to \mathbf{P}_0(K)$ as the unique function such that

$$\int_K (\mathbf{v} - \mathbf{\Pi}_K^0 \mathbf{v}) \cdot \mathbf{q} = 0 \qquad \forall \mathbf{q} \in \mathbf{P}_0(K).$$

It is easy to check that $\mathbf{\Pi}_K^0 \nabla q_h$ is fully computable, using the degrees of freedom $\mathbf{P_1}$, for each $q_h \in W_h(K)$.

Let $\mathcal{S}_{\nabla}^K(\cdot,\cdot)$ be any symmetric positive definite bilinear form such that

$$c_4 D_{\nabla}^K(q_h, q_h) \le \mathcal{S}_{\nabla}^K(q_h, q_h) \le c_5 D_{\nabla}^K(q_h, q_h) \quad \forall q_h \in W_h(K), \text{ with } \Pi_K^{\nabla} q_h = 0, \tag{3.5.11}$$

for some positive constants c_4 and c_5 independent of K. We will make a choose for $\mathcal{S}_{\nabla}^K(\cdot,\cdot)$ satisfying (3.5.11) in Section 3.6.

Then, we set

$$D_{\nabla}^h(p_h, q_h) := \sum_{K \in \mathcal{T}_h} D_{\nabla}^{h,K}(p_h, q_h) \qquad \forall p_h, q_h \in W_h, \tag{3.5.12}$$

where

$$D_{\nabla}^{h,K}(p_h, q_h) := \int_K \mathbf{\Pi}_K^0 \nabla p_h \cdot \mathbf{\Pi}_K^0 \nabla q_h + \mathcal{S}_{\nabla}^K\left(p_h - \Pi_K^{\nabla} p_h, q_h - \Pi_K^{\nabla} q_h\right) \qquad \forall p_h, q_h \in W_h(K). \tag{3.5.13}$$

The following result gives us consistency and stability properties of the local discrete bilinear form $D_{\nabla}^{h,K}(\cdot,\cdot)$.

Proposition 3.5.2. *The local bilinear forms $D_{\nabla}^K(\cdot,\cdot)$ and $D_{\nabla}^{h,K}(\cdot,\cdot)$ defined in (3.5.10) and (3.5.13), respectively, satisfies the following properties:*

- *Consistency: for each $h > 0$ and any $K \in \mathcal{T}_h$, we have*

$$D_{\nabla}^{h,K}(q_h, p_1) = D_{\nabla}^{K}(q_h, p_1) \quad \forall p_1 \in \mathbb{P}_1(K), \quad \forall q_h \in W_h(K). \tag{3.5.14}$$

- *Stability: there exist positive constants α_4, α_5, independent of h_K and K, such that*

$$\alpha_4 D_{\nabla}^{K}(q_h, q_h) \leq D_{\nabla}^{h,K}(q_h, q_h) \leq \alpha_5 D_{\nabla}^{K}(q_h, q_h) \quad \forall q_h \in W_h(K). \tag{3.5.15}$$

The next step consists in constructing an approximation of the right hand side (3.5.9), which depends on the stream-function ψ and the source term $\mathbf{f}$. With this aim, from now on, we assume that the discrete problem (3.3.21) has been solved with $k = 3$. So, $\psi_h \in X_h^3$ is available and satisfy the error bound presented in Theorem 3.4.1.

Now, for each $K \in \mathcal{T}_h$ and each $q_h \in W_h(K)$, we define the following discrete linear functional:

$$G^{\psi_h,K}(q_h) := \int_K \mathbf{f} \cdot \mathbf{\Pi}_K^0 \nabla q_h - \int_K \left(\boldsymbol{\nabla}\mathbf{\Pi}_K^2 \mathbf{curl}\, \psi_h\right) \boldsymbol{\beta} \cdot \mathbf{\Pi}_K^0 \nabla q_h$$
$$- \int_K \gamma \mathbf{\Pi}_K^2 \mathbf{curl}\, \psi_h \cdot \mathbf{\Pi}_K^0 \nabla q_h + \nu \int_K \mathbf{curl}\, (\Pi_K^1(\Delta\psi_h)) \cdot \mathbf{\Pi}_K^0 \nabla q_h,$$

where $\mathbf{\Pi}_K^2$ and Π_K^1 are the projections defined in (3.3.4) and (3.5.4), for $k = 3$, respectively. We have that $G^{\psi_h,K}(\cdot)$ is fully computable for each $K \in \mathcal{T}_h$ using the degrees of freedom $\mathbf{P_1}$.

We define the following global (computable) linear functional:

$$G^{\psi_h}(q_h) := \sum_{K \in \mathcal{T}_h} G^{\psi_h,K}(q_h) \qquad \forall q_h \in W_h. \tag{3.5.16}$$

Therefore, we propose the following virtual element discretization of lowest order to recover the fluid pressure: Given $\psi_h \in X_h^3$, find $p_h \in W_h$ such that

$$D_{\nabla}^{h}(p_h, q_h) = G^{\psi_h}(q_h) \qquad \forall q_h \in W_h. \tag{3.5.17}$$

We observe that by virtue of (3.5.15) the bilinear form $D_{\nabla}^h(\cdot,\cdot)$ is bounded. Moreover, the following result states that it is also elliptic.

Lemma 3.5.1. *There exists a constant $\alpha_p > 0$, independent of h, such that*

$$D_{\nabla}^{h}(q_h, q_h) \geq \alpha_p \|q_h\|_{1,\Omega}^2 \qquad \forall q_h \in W_h.$$

Next, we will prove that the linear functional defined in (3.5.16) is bounded. To do that, we consider the following approximation result (see [54]).

Proposition 3.5.3. *If the assumption* **A2** *is satisfied, then there exists a constant $C > 0$, such that for every $v \in \mathrm{H}^2(K)$, there exists $v_\pi \in \mathbb{P}_1(K)$ such that*

$$\|v - v_\pi\|_{0,K} + h_K |v - v_\pi|_{1,K} \leq C h_K^2 |v|_{2,K}.$$

Now, we present an interpolation result in the virtual space W_h (see [63, 134]).

Proposition 3.5.4. *If the assumptions* **A1** *and* **A2** *are satisfied, then there exists a constant* $C > 0$*, independent of* h*, such that for each* $v \in \mathrm{H}^2(\Omega)$ *there exists* $v_I \in W_h$ *such that*

$$\|v - v_I\|_{0,\Omega} + h|v - v_I|_{1,\Omega} \leq Ch^2|v|_{2,\Omega}.$$

To prove that the functional $G^{\psi_h}(\cdot)$ defined in (3.5.16) is bounded we will assume that the family of polygonal meshes $\mathcal{T}_h$ is quasi-uniform. More precisely, from now on, we will assume the following:

A3: For each $h > 0$ and for each $K \in \mathcal{T}_h$, there exists a constant $\widehat{c} > 0$, independent of h, such that $h_K \geq \widehat{c}\,h$.

The following result establishes that the linear functional $G^{\psi_h}(\cdot)$ defined in (3.5.16) is bounded under assumptions **A1**, **A2** and **A3**.

Lemma 3.5.2. *Let* $\psi \in \mathrm{H}^3(\Omega)$ *be the unique solution of problem* (3.2.2) *and let* $\psi_h \in X_h^3$ *be the unique solution of problem* (3.3.21)*. We assume that* **A1** $-$ **A3** *are satisfied, then the functional* $G^{\psi_h} : W_h \to \mathbb{R}$ *defined in* (3.5.16) *is bounded.*

Proof. The result follows repeating the arguments used in the proof of Proposition 4.20 in [133]. □

As a consequence of Lemmas 3.5.1, 3.5.2 and the Lax-Milgram Theorem, we have the following result.

Theorem 3.5.4. *The discrete virtual element scheme* (3.5.17) *admits a unique solution* $p_h \in W_h$ *and there exists* $C > 0$*, independent to* h*, such that*

$$\|p_h\|_{1,\Omega} \leq C\left(\|\mathbf{f}\|_{0,\Omega} + |\mathbf{f}|_{1,h}\right).$$

In what follows, we will establish the order of convergence of the discrete scheme (3.5.17) under the assumptions **A1** $-$ **A3** and the additional regularity results $p \in \mathrm{H}^2(\Omega)$ and $\psi \in \mathrm{H}^4(\Omega)$. This additional regularity for the stream-function can be attained, for instance, if $\mathbf{f} \in \mathbf{L}^2(\Omega)$ and Ω is a rectangular domain (see [57]). We begin with the following result which proof follows standard arguments in the VEM literature (see [27, 65]).

Proposition 3.5.5. *Let* p *and* p_h *be the unique solutions of problems* (3.5.7) *and* (3.5.17)*, respectively. If the assumptions* **A1** $-$ **A3** *are satisfied, then there exists* $C > 0$*, independent of* h*, such that*

$$\|p - p_h\|_{1,\Omega} \leq C\left(\|G^{\psi} - G^{\psi_h}\| + \|p - p_I\|_{1,\Omega} + |p - p_\pi|_{1,h}\right),$$

for all $p_I \in H_h$ *and for each* $p_\pi \in \mathrm{L}^2(\Omega)$ *such that* $p_\pi|_K \in \mathbb{P}_1(K)$ *for all* $K \in \mathcal{T}_h$*, where*

$$\|G^{\psi} - G^{\psi_h}\| := \sup_{\substack{q_h \in W_h \\ q_h \neq 0}} \frac{|G^{\psi}(q_h) - G^{\psi_h}(q_h)|}{\|q_h\|_{1,\Omega}}.$$

Now, we will bound the term $\|G^{\psi} - G^{\psi_h}\|$.

Proposition 3.5.6. *Let $\mathbf{f} \in \mathbf{L}^2(\Omega)$ such that $\mathbf{f}|_K \in \mathbf{H}^1(K)$ for all $K \in \mathcal{T}_h$. Let $\psi \in \mathrm{H}^4(\Omega)$ and $\psi_h \in X_h^3$ be the unique solutions of the problems (3.2.2) and (3.3.21), respectively. Let $G^{\psi}(\cdot)$ and $G^{\psi_h}(\cdot)$ be the linear functionals defined in (3.5.9) and (3.5.16), respectively. Then, there exists $C > 0$, independent of h, such that*

$$\left\|G^{\psi} - G^{\psi_h}\right\| \leq Ch\left(\|\psi\|_{4,\Omega} + |\mathbf{f}|_{1,h}\right).$$

Proof. Let $q_h \in W_h$, then using the definition of $G^{\psi}(\cdot)$ and $G^{\psi_h}(\cdot)$, and the Cauchy-Schwarz inequality, we have

$$\begin{aligned}
|G^{\psi}(q_h) - G^{\psi_h}(q_h)| \leq & \sum_{K\in\mathcal{T}_h} \left| \int_K \mathbf{f} \cdot \left(\nabla q_h - \mathbf{\Pi}_K^0 \nabla q_h\right) \right| \\
& + \sum_{K\in\mathcal{T}_h} \left| \int_K (\boldsymbol{\nabla} \mathbf{curl}\, \psi)\boldsymbol{\beta} \cdot \nabla q_h - (\boldsymbol{\nabla} \mathbf{\Pi}_K^2 \mathbf{curl}\, \psi_h)\boldsymbol{\beta} \cdot \mathbf{\Pi}_K^0 \nabla q_h \right| \\
& + \sum_{K\in\mathcal{T}_h} \left| \int_K \gamma \mathbf{curl}\, \psi \cdot \nabla q_h - \gamma \mathbf{\Pi}_K^2 \mathbf{curl}\, \psi_h \cdot \mathbf{\Pi}_K^0 \nabla q_h \right| \\
& + \sum_{K\in\mathcal{T}_h} \nu \left| \int_K \mathbf{curl}\, (\Delta\psi) \cdot \nabla q_h - \mathbf{curl}\, \left(\Pi_K^1(\Delta\psi_h)\right) \cdot \mathbf{\Pi}_K^0 \nabla q_h \right| \\
:= & \, T_1 + T_2 + T_3 + T_4.
\end{aligned}$$

Now, repeating the arguments used in the proof of Proposition 4.23 of [133], we have that

$$T_1 \leq Ch|\mathbf{f}|_{1,h}\|q_h\|_{1,\Omega}, \tag{3.5.18}$$

$$T_3 \leq Ch(\|\psi_h\|_X + |\mathbf{f}|_{1,h} + \|\psi\|_{4,\Omega})\|q_h\|_{1,\Omega}, \tag{3.5.19}$$

and

$$T_4 \leq Ch\left(\|\psi\|_{4,\Omega} + |\mathbf{f}|_{1,h}\right)\|q_h\|_{1,\Omega}. \tag{3.5.20}$$

Thus, in what follows, we are going to estimate the term T_2. We start by adding and subtracting suitable terms, and employing the triangular inequality, we have that

$$\begin{aligned}
T_2 \leq & \sum_{K\in\mathcal{T}_h} \left| \int_K (\boldsymbol{\nabla} \mathbf{curl}\, \psi)\boldsymbol{\beta} \cdot (\nabla q_h - \mathbf{\Pi}_K^0 \nabla q_h) \right| \\
& + \sum_{K\in\mathcal{T}_h} \left| \int_K \left[\boldsymbol{\nabla}(\mathbf{curl}\, \psi - \mathbf{\Pi}_K^2 \mathbf{curl}\, \psi_h)\right] \boldsymbol{\beta} \cdot \mathbf{\Pi}_K^0 \nabla q_h \right| \\
=: & \, I + II.
\end{aligned} \tag{3.5.21}$$

We will bound the terms I and II. Indeed, we begin with the term I. By using the properties of the operator $\mathbf{\Pi}_K^0$, we get

$$
\begin{aligned}
I :&= \sum_{K\in\mathcal{T}_h} \left| \int_K \left[(\boldsymbol{\nabla}\mathbf{curl}\,\psi)\boldsymbol{\beta} - \mathbf{\Pi}_K^0\big((\boldsymbol{\nabla}\mathbf{curl}\,\psi)\boldsymbol{\beta}\big) \right] \cdot (\nabla q_h - \mathbf{\Pi}_K^0 \nabla q_h) \right| \\
&\le \sum_{K\in\mathcal{T}_h} \|(\boldsymbol{\nabla}\mathbf{curl}\,\psi)\boldsymbol{\beta} - \mathbf{\Pi}_K^0\big((\boldsymbol{\nabla}\mathbf{curl}\,\psi)\boldsymbol{\beta}\big)\|_{0,K} \|\nabla q_h - \mathbf{\Pi}_K^0 \nabla q_h\|_{0,K} \\
&\le C \sum_{K\in\mathcal{T}_h} h_K |(\boldsymbol{\nabla}\mathbf{curl}\,\psi)\boldsymbol{\beta}|_{1,K} \|\nabla q_h\|_{0,K} \\
&\le Ch \left(\sum_{K\in\mathcal{T}_h} |(\boldsymbol{\nabla}\mathbf{curl}\,\psi)\boldsymbol{\beta}|_{1,K}^2 \right)^{1/2} \left(\sum_{K\in\mathcal{T}_h} \|\nabla q_h\|_{0,K}^2 \right)^{1/2} \\
&\le Ch \|(\boldsymbol{\nabla}\mathbf{curl}\,\psi)\boldsymbol{\beta}\|_{1,\Omega} |q_h|_{1,\Omega} \\
&\le Ch \|\boldsymbol{\beta}\|_{\mathrm{W}^1_\infty(\Omega)} \|\boldsymbol{\nabla}(\mathbf{curl}\,\psi)\|_{1,\Omega} \|q_h\|_{1,\Omega} \\
&\le Ch \|\psi\|_{3,\Omega} \|q_h\|_{1,\Omega}.
\end{aligned}
\tag{3.5.22}
$$

Now, we continue by estimating II (cf. (3.5.21)). By using the approximation properties of operator $\mathbf{\Pi}_K^2$, we obtain that

$$
\begin{aligned}
II :&= \sum_{K\in\mathcal{T}_h} \left| \int_K \left[\nabla(\mathbf{curl}\,\psi - \mathbf{\Pi}_K^2 \mathbf{curl}\,\psi_h) \right] \boldsymbol{\beta} \cdot \mathbf{\Pi}_K^0 \nabla q_h \right| \\
&\le \sum_{K\in\mathcal{T}_h} \|\boldsymbol{\beta}\|_{L^\infty(K)} \|\nabla(\mathbf{curl}\,\psi - \mathbf{\Pi}_K^2\mathbf{curl}\,\psi_h)\|_{0,K} \|\mathbf{\Pi}_K^0 \nabla q_h\|_{0,K} \\
&\le C \|\boldsymbol{\beta}\|_{L^\infty(\Omega)} \sum_{K\in\mathcal{T}_h} |\mathbf{curl}\,\psi - \mathbf{\Pi}_K^2 \mathbf{curl}\,\psi_h|_{1,K} \|\nabla q_h\|_{0,K} \\
&\le C \sum_{K\in\mathcal{T}_h} \big(|\mathbf{curl}\,\psi - \mathbf{\Pi}_K^2\mathbf{curl}\,\psi|_{1,K} + |\mathbf{\Pi}_K^2 \mathbf{curl}\,(\psi - \psi_h)|_{1,K} \big) \|\nabla q_h\|_{0,K} \\
&\le C \sum_{K\in\mathcal{T}_h} (h_K \|\mathbf{curl}\,\psi\|_{1,K} + C_N |\psi - \psi_h|_{2,K}) \|\nabla q_h\|_{0,K} \\
&\le Ch(|\mathbf{f}|_{1,h} + \|\psi\|_{4,\Omega}) \|q_h\|_{1,\Omega},
\end{aligned}
\tag{3.5.23}
$$

where we have added and subtracted the term $\mathbf{\Pi}_K^2\mathbf{curl}\,\psi$, we used Lemma 3.3.3, Hölder inequality and (3.3.5). Then, inserting (3.5.22) and (3.5.23) into (3.5.21), we obtain

$$
T_2 \le Ch\left(\|\psi\|_{4,\Omega} + |\mathbf{f}|_{1,h}\right) \|q_h\|_{1,\Omega}. \tag{3.5.24}
$$

Finally, the proof follows from the estimates (3.5.18)-(3.5.20) and (3.5.24). □

The following theorem provides the rate of convergence of our virtual element scheme (3.5.17) to recover the fluid pressure. The proof follows from Propositions 3.5.5, 3.5.6, 3.5.3 and 3.5.4.

Theorem 3.5.5. *Let $\mathbf{f} \in \mathrm{L}^2(\Omega)^2$ such that $\mathbf{f}|_K \in \mathbf{H}^1(K)$ for all $K \in \mathcal{T}_h$. Let ψ, ψ_h, p and p_h be the unique solutions of problems (3.2.2), (3.3.21), (3.5.7) and (3.5.17), respectively. Suppose that* **A1** − **A3** *are satisfied, $p \in \mathrm{H}^2(\Omega)$ and $\psi \in \mathrm{H}^4(\Omega)$. Then, there exists $C > 0$, independent of h, such that*

$$
\|p - p_h\|_{1,\Omega} \le Ch\left(\|\psi\|_{4,\Omega} + |\mathbf{f}|_{1,h}\right).
$$

3.6 Numerical results

In this section, we present three numerical experiments in order to illustrate the practical performance of the proposed virtual element methods (3.3.21) and (3.5.17) and to confirm the theoretical results established in previous sections. We will test the method for the cases $k = 2$ and $k = 3$ on different polygonal meshes.

Now, we introduce the bilinear forms $\mathcal{S}_{\mathrm{D}}^K(\cdot,\cdot)$ and $\mathcal{S}_{\mathbf{curl}}^K(\cdot,\cdot)$ (cf. (2.3.8)) to complete the virtual element discretization (3.3.21). We take (see [18, 58, 133]):

$$\mathcal{S}_{\mathrm{D}}^K(\psi_h,\phi_h) := \sigma^K \sum_{i=1}^{N_K^{\mathrm{dof}}} \mathrm{dof}_i(\psi_h)\mathrm{dof}_i(\phi_h) \qquad \forall \psi_h,\phi_h \in X_h^k(K),$$
$$\mathcal{S}_{\mathbf{curl}}^K(\psi_h,\phi_h) := \sigma_\gamma^K \sum_{i=1}^{N_K^{\mathrm{dof}}} \mathrm{dof}_i(\psi_h)\mathrm{dof}_i(\phi_h) \qquad \forall \psi_h,\phi_h \in X_h^k(K).$$

where for each polygon $K \in \mathcal{T}_h$, N_K^{dof} denotes the number of degrees freedom of $X_h^k(K)$ and dof_i, with $1 \leq i \leq \dim(X_h^k(K))$, denotes the operator that to each smooth enough function ϕ associates the ith local degree of freedom $\mathrm{dof}_i(\phi)$ and the parameter $\sigma^K, \sigma_\gamma^K > 0$ are a multiplicative factors to take into account the physical magnitudes and the h-scaling. On the other hand, the bilinear form $\mathcal{S}_{\nabla}^K(\cdot,\cdot)$ (cf. (3.5.11)), is given by (see [27, 134]):

$$\mathcal{S}_{\nabla}^K(p_h,q_h) := \sum_{i=1}^{N_K} p_h(\mathbf{v}_i)q_h(\mathbf{v}_i) \quad \forall p_h,q_h \in W_h(K).$$

We have tested the method by using the following families of meshes:

- $\mathcal{T}_h^1$: Distorted concave rhombic quadrilaterals;
- $\mathcal{T}_h^2$: Trapezoidal meshes;
- $\mathcal{T}_h^3$: Sequence of CVT (Centroidal Voronoi Tessellation).

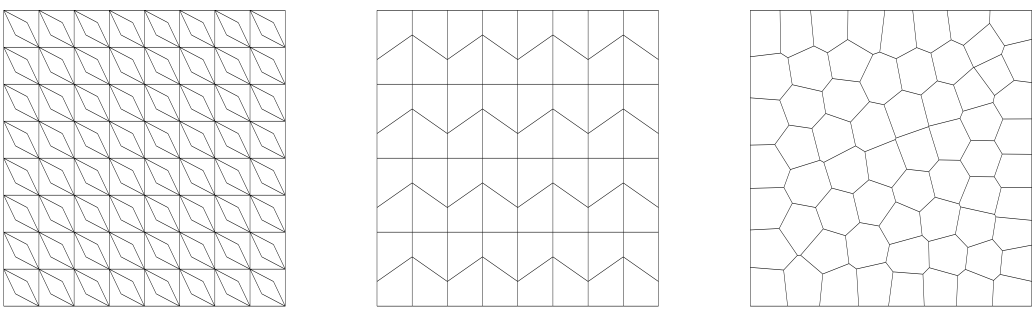

Figure 3.1: Sample meshes. $\mathcal{T}_h^1$, $\mathcal{T}_h^2$ and $\mathcal{T}_h^3$.

In order to compute the VEM errors, we consider the following computable error quantities.

$$\mathtt{e}_i(\psi) = \mathtt{error}(\psi, \mathrm{H}^i) := \Big(\sum_{K\in\mathcal{T}_h} |\psi - \Pi_K^{k,\mathrm{D}}\psi_h|^2_{i,K} \Big)^{1/2}, \quad i = 0,1,2.$$

$$\mathtt{e}_1(p) = \mathtt{error}(p, \mathrm{H}^1) := \Big(\sum_{K\in\mathcal{T}_h} \big|p - \Pi_K^{\nabla}p_h\big|^2_{1,K} \Big)^{1/2},$$

$$\mathtt{e}_0(\omega) = \mathtt{error}(\omega, \mathrm{L}^2) := \Big(\sum_{K\in\mathcal{T}_h} \big\|\omega - \Pi_K^{0}(\Delta\psi_h)\big\|^2_{0,K} \Big)^{1/2}.$$

Also, if h, h' denote two consecutive mesh sizes with their respective errors $\mathtt{e}_i$ and $\mathtt{e}'_i$, then we will compute experimental rates of convergence for each variable as follows:

$$\mathtt{r}_i(\cdot) := \frac{\log(\mathtt{e}_i(\cdot)/\mathtt{e}'_i(\cdot))}{\log(h/h')}, \quad i = 0,1,2.$$

3.6.1 Test 1. Smooth solution

In this test we solve the Oseen equations (3.2.1) on the square domain $\Omega := (0,1)^2$. We take $\nu = 1$, $\gamma = 100$, and the load term $\mathbf{f}$ and boundary conditions in such a way that the analytical solution is given by:

$$\mathbf{u}(x,y) = \begin{pmatrix} 2x^2(1-x)^2y(y-1)(2y-1) \\ -2y^2(1-y)^2x(x-1)(2x-1) \end{pmatrix}, \qquad \omega(x,y) = \operatorname{rot}\mathbf{u} = -\Delta\psi,$$

$$p(x,y) = x^3 + y^3 - \frac{1}{2} \qquad \text{and} \qquad \psi(x,y) = x^2(1-x)^2y^2(1-y)^2.$$

Moreover, we consider the following convective velocity:

$$\boldsymbol{\beta}(x,y) = \begin{pmatrix} \sin(x)\sin(y) \\ \cos(x)\cos(y) \end{pmatrix}.$$

Table 3.1 shows the convergence history of the virtual element scheme (3.3.21) applied to our test problem for $k = 2$. In addition, Table 3.2 shows the convergence history of the virtual element schemes (3.3.21) and (3.5.17) for $k = 3$. In both cases, we have considered meshes $\mathcal{T}_h^1$.

It can be seen from Tables 3.1 and 3.2 that the methods converge with an optimal order for all the variables.

Figure 3.2 shows plots of the exact (top) and computed (bottom) stream-function, pressure and vorticity, obtained with the virtual element methods analyzed in this chapter, using the meshes $\mathcal{T}_h^1$, with $h = 1/32$, $k = 3$ and $\nu = 1$.

In Figure 3.3 we depict approximate velocity field obtained from the discrete stream-function using the meshes $\mathcal{T}_h^1$, with $h = 1/32$, $k = 3$, $\nu = 1$ and $\gamma = 100$.

3.6.2 Test 2. Solution with boundary layer

In this numerical experiment, we solve the Oseen equations (3.2.1) on the square domain $\Omega := (0,1)^2$. We take $\nu = 10^{-3}$, $\gamma = 50$ and the load term $\mathbf{f}$ and boundary conditions in such a way that the analytical solution is given by:

$$\mathbf{u}(x,y) = \frac{2}{\lambda^2}\begin{pmatrix} x^2y(e^{\lambda(x-1)}-1)^2(e^{\lambda(y-1)}-1)(e^{\lambda(y-1)}+\lambda ye^{\lambda(y-1)}-1) \\ -xy^2(e^{\lambda(y-1)}-1)^2e^{\lambda(x-1)}-1)(e^{\lambda(x-1)}+\lambda xe^{\lambda(x-1)}-1) \end{pmatrix},$$

h	$\mathtt{e}_0(\psi)$	$\mathtt{r}_0(\psi)$	$\mathtt{e}_1(\psi)$	$\mathtt{r}_1(\psi)$	$\mathtt{e}_2(\psi)$	$\mathtt{r}_2(\psi)$	$\mathtt{e}_0(\omega)$	$\mathtt{r}_0(\omega)$
1/4	7.473458e-4	—	3.931137e-3	—	3.515403e-2	—	2.579728e-2	—
1/8	1.219438e-4	2.61	8.002679e-4	2.29	1.606165e-2	1.13	8.728651e-3	1.56
1/16	1.750743e-5	2.80	1.633574e-4	2.29	7.852990e-3	1.03	3.750317e-3	1.21
1/32	3.151107e-6	2.47	3.947501e-5	2.04	3.894174e-3	1.01	1.738230e-3	1.10
1/64	6.698881e-7	2.23	9.958959e-6	1.98	1.942167e-3	1.00	8.414948e-4	1.04

Table 3.1: Test 1. Errors and experimental rates for the stream-function ψ_h and vorticity ω_h, using the meshes $\mathcal{T}_h^1$, $k = 2$, $\nu = 1$ and $\gamma = 100$.

h	$\mathtt{e}_0(\psi)$	$\mathtt{r}_0(\psi)$	$\mathtt{e}_1(\psi)$	$\mathtt{r}_1(\psi)$	$\mathtt{e}_2(\psi)$	$\mathtt{r}_2(\psi)$	$\mathtt{e}_1(p)$	$\mathtt{r}_1(p)$	$\mathtt{e}_0(\omega)$	$\mathtt{r}_0(\omega)$
1/4	1.852106e-4	—	1.106299e-3	—	1.949383e-2	—	3.158359e-1	—	1.970323e-2	—
1/8	1.405414e-5	3.72	1.110736e-4	3.31	5.057026e-3	1.94	1.622020e-1	0.96	5.128756e-3	1.94
1/16	1.027443e-6	3.77	1.160837e-5	3.25	1.285563e-3	1.97	8.253523e-2	0.97	1.303501e-3	1.97
1/32	7.173524e-8	3.84	1.230588e-6	3.23	3.062095e-4	2.06	4.055215e-2	1.02	3.103413e-4	2.07
1/64	4.450005e-9	4.01	1.352796e-7	3.18	7.017355e-5	2.12	1.986404e-2	1.02	7.098042e-5	2.12

Table 3.2: Test 1. Errors and experimental rates for the stream-function ψ_h, pressure p_h and vorticity ω_h using the meshes $\mathcal{T}_h^1$, $k = 3$, $\nu = 1$ and $\gamma = 100$.

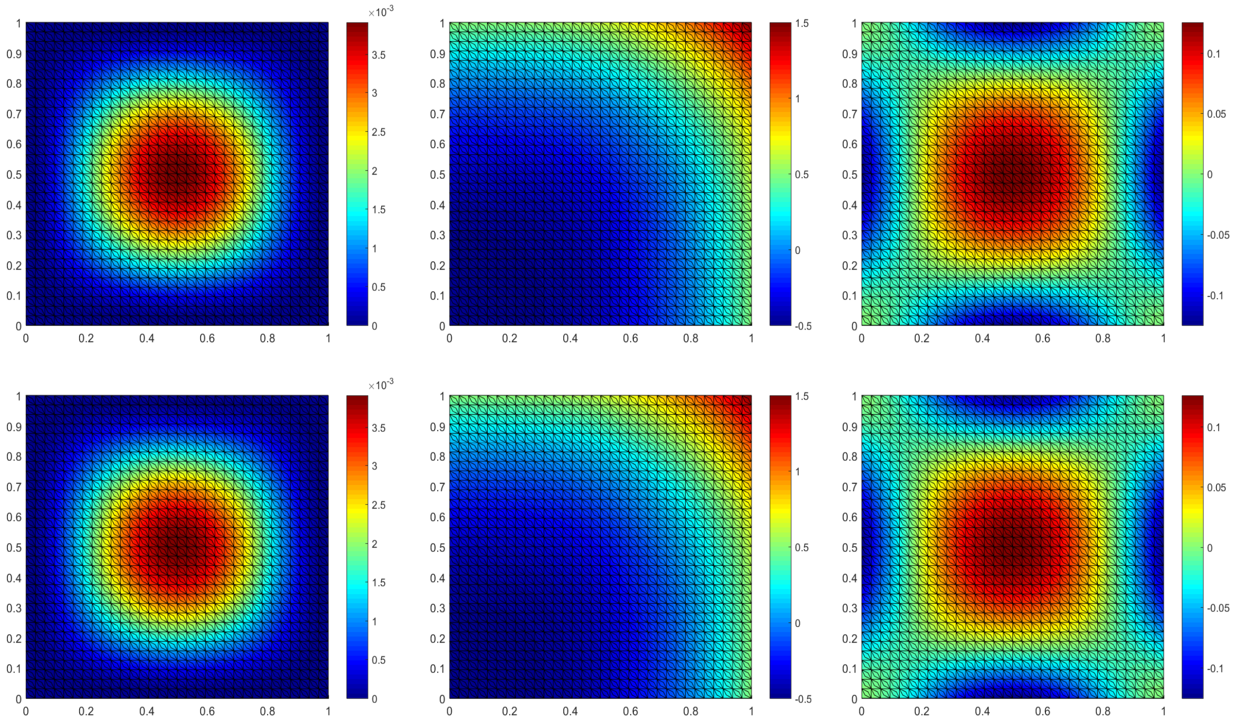

Figure 3.2: Test 1. Exact (top panels) and computed (bottom panels) stream-function, pressure and vorticity, using the VEM methods (3.2.2) and (3.5.17) with $\mathcal{T}_h^1$, $h = 1/32$, $k = 3$ and $\nu = 1$.

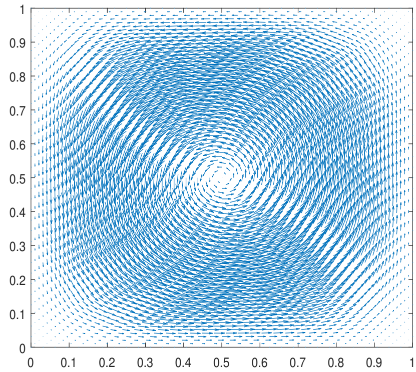

Figure 3.3: Test 1. Velocity field obtained from the discrete stream-function with $\mathcal{T}_h^1$, $h = 1/32$, $k = 3$ and $\nu = 1$.

h	$\mathtt{e}_0(\psi)$	$\mathtt{r}_0(\psi)$	$\mathtt{e}_1(\psi)$	$\mathtt{r}_1(\psi)$	$\mathtt{e}_2(\psi)$	$\mathtt{r}_2(\psi)$	$\mathtt{e}_0(\omega)$	$\mathtt{r}_0(\omega)$
1/8	2.784694e-4	—	2.973866e-3	—	9.076308e-2	—	5.838607e-2	—
1/16	1.030198e-4	1.43	1.690738e-3	0.81	7.965350e-2	0.18	4.042055e-2	0.53
1/32	1.926182e-5	2.14	6.324576e-4	1.41	5.785738e-2	0.46	3.638668e-2	0.15
1/64	1.992073e-6	3.27	1.607822e-4	1.97	3.321376e-2	0.88	2.211350e-2	0.71
1/128	3.418173e-7	2.54	3.208248e-5	2.32	1.593417e-2	1.05	9.492817e-3	1.22

Table 3.3: Test 2. Errors and experimental rates for the stream-function ψ_h and vorticity ω_h, using the meshes $\mathcal{T}_h^2$, $k = 2$, $\nu = 10^{-3}$ and $\gamma = 50$.

$$\omega(x, y) = \operatorname{rot}\mathbf{u} = -\Delta\psi, \qquad p(x, y) = e^{x+y} - (e-1)^2,$$

and

$$\psi(x, y) = \frac{1}{\lambda^2} x^2 y^2 (1 - e^{\lambda(x-1)})^2 (1 - e^{\lambda(y-1)})^2,$$

where $\lambda = 0.5/\sqrt{\nu}$, while the convective velocity is $\boldsymbol{\beta} = (1, 1)$. We observe that ψ has a boundary layer on the top-right corner of the domain for small values of ν.

Table 3.3 shows the convergence history of our virtual element scheme (3.3.21) applied to the present test for $k = 2$, while Table 3.4 shows the convergence history of the virtual element schemes (3.3.21) and (3.5.17) for $k = 3$. In both cases, the set of decompositions utilized is $\mathcal{T}_h^2$.

In this numerical example, we notice that the rate of convergence predicted by Theorems 3.4.1, 3.5.2 and 3.5.5 is attained by all the variables, in the corresponding norms. However, in Table 3.4 we observe a degeneracy of the optimal convergence rate for the stream-function in the L^2-norm, we attribute this to the existence of the boundary layer on the top-right corner of the domain.

Figure 3.4 shows plots of the exact (top) and computed (bottom) stream-function, pressure and vorticity, obtained with the virtual element methods analyzed in this work, using the meshes $\mathcal{T}_h^2$, with $h = 1/64$, $k = 3$, $\nu = 10^{-3}$ and $\gamma = 50$.

Figure 3.5 shows the approximate velocity field obtained from the discrete stream-function and the streamlines using the meshes $\mathcal{T}_h^2$, with $h = 1/64$, $k = 3$, $\nu = 10^{-3}$ and $\gamma = 50$.

h	$\mathtt{e}_0(\psi)$	$\mathtt{r}_0(\psi)$	$\mathtt{e}_1(\psi)$	$\mathtt{r}_1(\psi)$	$\mathtt{e}_2(\psi)$	$\mathtt{r}_2(\psi)$	$\mathtt{e}_1(p)$	$\mathtt{r}_1(p)$	$\mathtt{e}_0(\omega)$	$\mathtt{r}_0(\omega)$
1/8	2.197659e-4	—	2.548761e-3	—	8.465258e-2	—	2.466608e-1	—	8.483406e-2	—
1/16	4.584130e-5	2.26	1.000595e-3	1.34	5.882760e-2	0.52	1.244517e-1	0.98	5.890052e-2	0.52
1/32	3.579805e-6	3.67	2.019404e-4	2.30	2.659083e-2	1.14	6.250501e-2	0.99	2.659606e-2	1.14
1/64	2.381437e-7	3.90	3.314490e-5	2.60	8.793503e-3	1.59	3.130231e-2	0.99	8.787307e-3	1.59
1/128	3.084086e-8	2.94	4.223090e-6	2.97	2.148259e-3	2.03	1.565467e-2	0.99	2.144776e-3	2.03

Table 3.4: Test 2. Errors and experimental rates for the stream-function ψ_h, pressure p_h and vorticity ω_h using the meshes $\mathcal{T}_h^2$, $k=3$, $\nu=10^{-3}$ and $\gamma=50$.

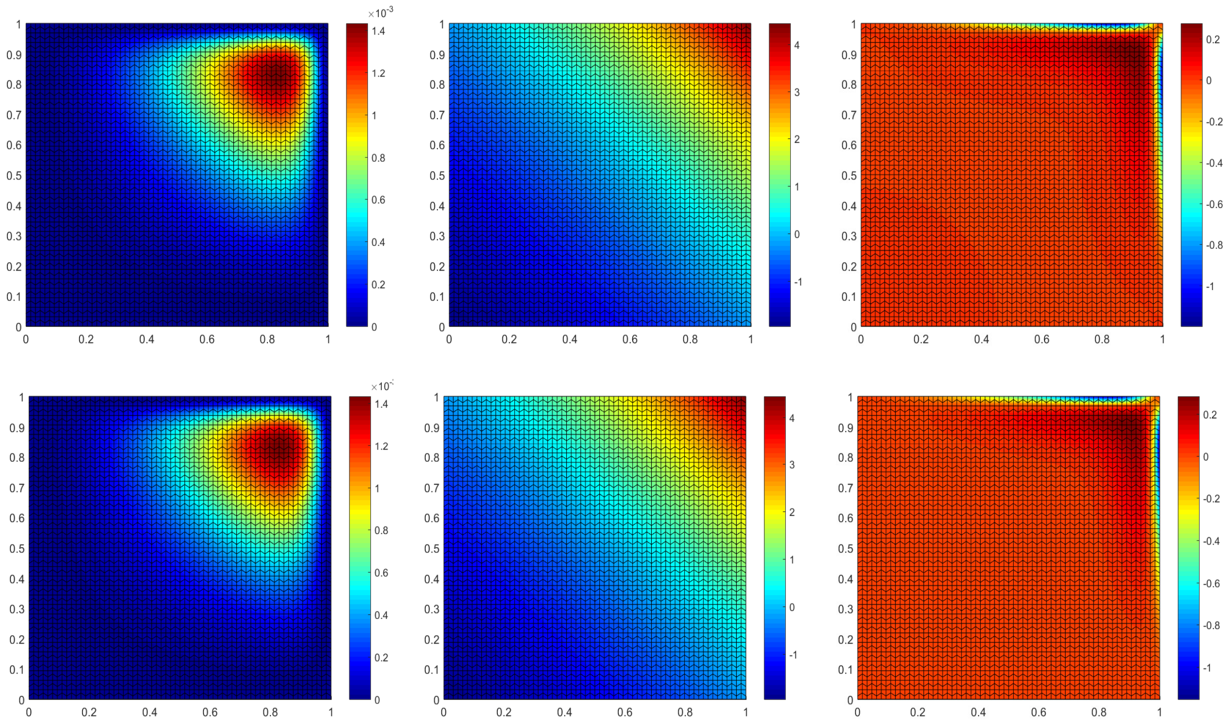

Figure 3.4: Test 2. Exact (top panels) and computed (bottom panels) stream-function, pressure and vorticity, using the VEM methods (3.2.2) and (3.5.17) with $\mathcal{T}_h^2$, $h=1/64$, $k=3$, $\nu=10^{-3}$ and $\gamma=50$.

3.6.3 Test 3. Solution with non homogeneous Dirichlet boundary conditions.

The aim of this numerical test is twofold: consider small values of viscosity and solve the Oseen equations (3.2.1) with non homogeneous boundary conditions on the square domain $\Omega := (0,1)^2$ with the proposed scheme (3.3.21) and with the scheme obtained by using the projection $\Pi_K^{k,\nabla^\perp}$ to discretize (3.3.11)-(3.3.12) (cf. Remark 3.3.1).

We take $\nu=10^{-7}$, $\gamma=100$, $\boldsymbol{\beta}=(1,1)$ and the load term $\mathbf{f}$ and boundary conditions in

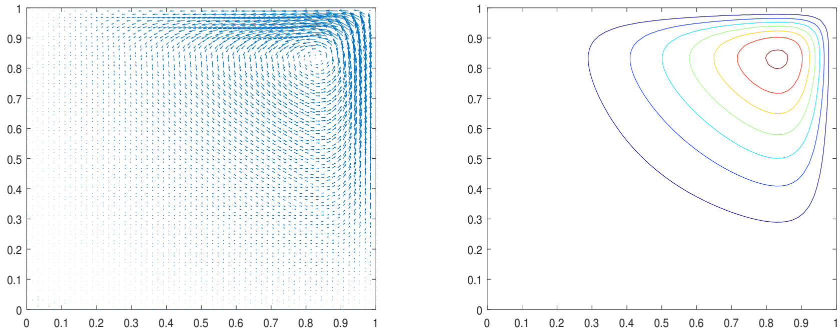

Figure 3.5: Test 2. Velocity field and streamlines obtained from the discrete stream-function with $\mathcal{T}_h^2$, $k=3$, $\nu=10^{-3}$ and $\gamma=50$.

such a way that the analytical solution is given by:

$$\mathbf{u}(x,y)=\frac{1}{4\pi^2}\begin{pmatrix} e^{x^2+y^2}\sin(2\pi x)(y\cos(2\pi y)-\pi\sin(2\pi y)) \\ -e^{x^2+y^2}\cos(2\pi y)(x\sin(2\pi x)+\pi\cos(2\pi x))\end{pmatrix}, \quad \omega(x,y)=\operatorname{rot}\mathbf{u},$$

$$p(x,y)=\sin(x)-\sin(y) \qquad \text{and} \qquad \psi(x,y)=\frac{1}{8\pi^2}\sin(2\pi x)\cos(2\pi y)e^{x^2+y^2}.$$

Table 3.5 shows the convergence history of the scheme (3.3.21) and the scheme obtained by using the projection $\Pi_K^{k,\nabla^\perp}$ to discretize (3.3.11)-(3.3.12) for $k=2$ with meshes $\mathcal{T}_h^3$.

In this numerical example, we notice that the rate of convergence predicted by Theorems 3.4.1 and 3.5.2 is attained by all the variables for both methods. However, we have not proved any order of convergence for the second method (denoted by $\Pi_K^{k,\nabla^\perp}$).

h	$\mathtt{e}_2(\psi)$	$\mathtt{r}_2(\psi)$	$\mathtt{e}_0(\omega)$	$\mathtt{r}_0(\omega)$	$\mathtt{e}_2(\psi)$	$\mathtt{r}_2(\psi)$	$\mathtt{e}_0(\omega)$	$\mathtt{r}_0(\omega)$
	$\boldsymbol{\Pi}_K^{k-1}\mathbf{curl}$				$\Pi_K^{k,\nabla^\perp}$			
1/4	7.3531e-1	—	4.1926e-1	—	7.0801e-1	—	3.4725e-1	—
1/8	3.8849e-1	0.92	1.4227e-1	1.55	3.7940e-1	0.90	1.0708e-1	1.69
1/16	2.1101e-1	0.88	7.3202e-2	0.95	2.0710e-1	0.87	6.0683e-2	0.81
1/32	1.0322e-1	1.03	3.0794e-2	1.24	1.0136e-1	1.03	2.3762e-2	1.35
1/64	5.0594e-2	1.02	1.4993e-2	1.03	4.9576e-2	1.03	1.1003e-2	1.11
1/128	2.5125e-2	1.00	6.8078e-3	1.13	2.4766e-2	1.00	5.3181e-3	1.04

Table 3.5: Test 3. Errors and experimental rates for the stream-function ψ_h and vorticity ω_h, using the meshes $\mathcal{T}_h^3$, $k=2$, $\nu=10^{-7}$ and $\gamma=100$.

Chapter 4

Virtual elements for the Navier–Stokes system: stream function form and primitive variables recovery algorithms

4.1 Introduction

Let $\Omega \subset \mathbb{R}^2$ be a bounded simply connected domain, then we can associate to a divergence-free velocity field $\mathbf{u}$ a scalar function ψ, such that $\mathbf{u} = \mathbf{curl}\,\psi$, which is called *stream-function*. Employing this relation, we have that the incompressible Navier–Stokes equations formulated in terms of the stream-function are given by the following nonlinear fourth-order problem (for more details, see for instance [103, Chap. IV, sect. 2.1]: given a sufficiently smooth force density $\mathbf{f} : \Omega \to \mathbb{R}^2$, seek $\psi : \Omega \to \mathbb{R}$, such that

$$\begin{aligned} \nu\Delta^2\psi - \mathbf{curl}\,\psi \cdot \nabla(\Delta\psi) &= \operatorname{rot}\mathbf{f} \qquad \text{in } \Omega, \\ \psi = g_0, \quad \partial_{\mathbf{n}}\psi &= g_1 \qquad \text{on } \partial\Omega, \end{aligned} \tag{4.1.1}$$

where $\nu > 0$ represent the fluid viscosity and $\partial_{\mathbf{n}}$ denotes the normal derivative, g_0 and g_1 are prescribed boundary data. This system describes the motion of an incompressible viscous fluid in the domain Ω, whose applications are found in different areas and sciences, such as: engineering, oceanography, biomedicine and environmental processes, among others. Due to the importance of its applications, during the past decades a great variety of numerical methods have been developed to approximate the solution of the Navier–Stokes equations. Among these methods, we mention those based on the mixed Galerkin schemes to discretize the standard velocity-pressure formulation, for which the discrete spaces must be adequately constructed in such a way that they satisfy the inf-sup condition to ensure the well-posedness of the mixed discrete problem (see [103]). Another restrictive but desirable condition for these schemes is the one associated with the incompressibility condition, where the error components are partly decouple and for which different approaches have been devoted to the construction of schemes satisfying this property (see for instance [109, 35, 41]).

For the two dimensional case, by introducing the stream-function variable ψ, the classical velocity-pressure formulation is reduced in the single nonlinear fourth-order PDEs (cf. (4.1.1)), whose discretization does not need the construction of discrete inf-sup stable spaces and the incompressibility constraint is automatically satisfied by construction. Furthermore, the formulation (4.1.1) in addition to having a single unknown, has the advantage of avoiding the difficulties associated with the definition of boundary values for the vorticity field, present in stream-function–vorticity formulation. Salient features related to the naturally skew-symmetry property of the resulting trilinear form, allows the development of more direct stability and convergence arguments (see below Remark 4.3.1). We observe that both the velocity and pressure are not present in the system (4.1.1). However, if these fields are required them can be recovered through stream-function postprocessing (see for instance [71, 115, 133]). In the present work, we propose *high-order* approximations for the primitive variables. Furthermore, we provide a suitable approximations for the vorticity field, via simple postprocessing formula. The above facts turn the stream-function form into a very attractive formulation and for this reason different works have been devoted to the development and analysis of efficient schemes to approximate the Navier–Stokes equations formulated in terms of the stream-function. For instance, in [71, 115, 91, 143] conforming Finite Element Methods (FEMs), bivariate spline and *hp*-version discontinuous Galerkin FEMs have been proposed and analyzed. In Reference [95] a C^1-conforming FEM has been developed for the stationary Quasi-Geostrophic equations, which is strongly related with the formulation (4.1.1).

In addition to modeling fluid flow problems in stream-function form, the fourth-order PDEs are present in the modeling of different physical phenomenon, for instance, these kinds of equations also arise naturally in plate bending problems and the Cahn–Hilliard phase-field model. Due to its importance and challenging nature, this topic has been a very active area of research, and a wide variety of numerical approaches have been presented for solving these systems. For instance, conforming and nonconforming FE schemes [79, 68]), C^0-IP methods [142, 101, 53], among others. In particular, to discretize fourth-order problems in primal form, using the classical conforming FE spaces, it is well know that a notable disadvantage arises: the construction of these spaces involve high-order polynomials and a large number of degrees of freedom, which is often regarded as a challenging endeavor, particularly from the computational viewpoint, even when dealing with the classical triangular elements (see [79, Chap. 6, sect. 6.1]). In order to overcome this inconvenience, we consider the approach presented in [58, 77, 18] to introduce C^1-virtual schemes of arbitrary order $k \geq 2$ to solve numerically the nonlinear fourth-order Navier–Stokes problem (cf. (4.1.1)). The Virtual Element Method (in short, VEM) has been originally introduced in [27] and it belongs to the group of polytopal Galerkin schemes for solving PDEs, which have received substantial attention in recent decades due to their inherent versatility in dealing with complex geometries [87, 62, 88]. Since its introduction the VEM has been employed to discretize a wide variety of problems, for instance in [65, 58, 77, 18, 56, 139, 116, 1], where second- and fourth-order problems have been developed and analyzed. In these works can be observed the ability of VEMs to develop high-order numerical schemes to discretize PDEs on general polytopal meshes. Moreover, it can observed another important feature of the VEM; its capability to construct discrete schemes with high-regularity, by using few degrees of freedom and low polynomial degrees. For instance, the lowest order polynomial degree is $k = 2$ and it used only 3 degrees of freedom per mesh vertex (the function and its gradient values vertex). On the other hand, in the context of fluid mechanic, among the models studied by using the VEM, we list [17, 35, 41, 100, 133, 3].

The main objectives of the present contribution are the following: i) *the design of high-order stream VEMs on polygonal meshes and the development of novel error analysis for these methods:* we design C^1-VEMs of high-order for solving the Navier–Stokes equations in stream-function form on polygonal meshes. By using the important advantage of natural skew-symmetry property of the resulting trilinear form and others standard arguments of the VEM, we write directly an abstract convergence result for our nonlinear schemes, which allows the derivation of an optimal error estimate in H^2-norm, under *minimal regularity* of the weak stream-function solution (namely, $\psi \in \mathrm{H}^{2+s}(\Omega)$, with $s > 0$, see below Theorem 4.4.3). Moreover, we write new optimal error estimates in the H^1- and L^2-norms by using duality arguments. In addition, we extend these schemes to the system with boundary conditions on the pressure [45]; ii) *the development of algorithms to recover additional variables of physical interest:* we present procedures to compute further important fields in fluid mechanics, such as: the velocity, pressure and vorticity. More precisely, we propose high-order approximations for the velocity and vorticity fields via postprocessing formulas from the discrete stream-function and employing adequate polynomial projections. Such formulas are directly computable from the degrees of freedom and allow to obtain optimal error estimates for these postprocessed variables. For pressure recovery technique we consider an additional second-order elliptic problem with right hand side coming from the source term and the discrete virtual stream-function. In order to discretize this linear second-order problem, we propose a scheme of *high-order* based on the enhanced C^0-conforming VE approach from [7, 65]; iii) *the assessment of the numerical performance by using the stream-function approach:* we provide a set of benchmark tests that highlight interesting features of the present stream VE schemes, including the approximation of the Kovasznay and lid-driven cavity solutions on general polygonal meshes and using small values of ν. In addition, we investigate the behaviour of our VEM considering a hydrostatic fluid problem. We observed that the results obtained are in accordance with another exactly divergence-free Galerkin schemes, where the partial decoupling of the velocity and pressure errors leads a positive effect on the velocity computation (see [35] in the VEM approach). Finally, we present two numerical examples, which validates our new theoretical findings of item i) and the extension for mixed boundary conditions.

A brief outline of the chapter follows. In Section 4.2 we introduce a variational formulation of problem (4.1.1) and we establish its well-posedness. In Section 4.3 we present the C^1-VE discretization. In Section 4.4 we prove the existence and uniqueness of the discrete problem. Furthermore, in the same section we derive optimal error estimates in H^2, H^1- and L^2-norms for the stream-function. In Section 4.5 we present strategies to compute the velocity, pressure and vorticity fields, while in Section 4.6, we discuss the extension to the Navier–Stokes system with boundary conditions on the pressure. Finally, in Section 4.7 five numerical test are presented.

4.2 Weak stream-function form and its well-posedness

For simplicity, we will work with homogeneous boundary conditions in the system (4.1.1), i.e, $\psi = \partial_{\mathbf{n}}\psi = 0 \quad \text{on} \quad \Gamma$. Nevertheless, such restriction does not affect the generality of the forthcoming analysis.

A weak form of problem (4.1.1), is given by: seek $\psi \in \mathcal{W} := \mathrm{H}_0^2(\Omega)$, such that

$$\nu\mathcal{A}(\psi,\phi) + \mathcal{B}(\psi;\psi,\phi) = \mathcal{F}(\phi) \qquad \forall \phi \in \mathcal{W}, \tag{4.2.1}$$

where the bilinear form $\mathcal{A} : \mathcal{W} \times \mathcal{W} \to \mathbb{R}$, the trilinear form $\mathcal{B} : \mathcal{W} \times \mathcal{W} \times \mathcal{W} \to \mathbb{R}$ and the linear functional $\mathcal{F} : \mathcal{W} \to \mathbb{R}$, are given by the following expressions:

$$\mathcal{A}(\varphi,\phi) := (\mathrm{D}^2\varphi, \mathrm{D}^2\phi)_{0,\Omega}, \qquad \forall \varphi,\phi \in \mathcal{W}, \tag{4.2.2}$$

$$\mathcal{B}(\zeta;\varphi,\phi) := (\Delta\zeta\, \mathbf{curl}\,\varphi, \nabla\phi)_{0,\Omega} \qquad \forall \zeta,\varphi,\phi \in \mathcal{W}, \tag{4.2.3}$$

$$\mathcal{F}(\phi) := (\mathbf{f}, \mathbf{curl}\,\phi)_{0,\Omega} \qquad \forall \phi \in \mathcal{W}. \tag{4.2.4}$$

In what follows, we will assume that the force density satisfies $\mathbf{f} \in \mathbf{L}^2(\Omega)$ and we will endow it with the norm: $\|\varphi\|_{\mathcal{W}} := \mathcal{A}(\varphi,\varphi)^{1/2} \quad \forall \varphi \in \mathcal{W}$.

Using the Banach fixed-point Theorem, we prove that problem (4.2.1) is well-posed. More precisely, we have the following result.

Theorem 4.2.1. *If*

$$\lambda := \widehat{C_B} C_{\mathcal{F}} \nu^{-2} \|\mathbf{f}\|_{0,\Omega} < 1, \tag{4.2.5}$$

then there exists a unique $\psi \in \mathcal{W}$ solution to problem (4.2.1).

We finish this section with the following remark regarding the PDEs (4.1.1).

Remark 4.2.1. *We recall that the steady Navier–Stokes equations in its standard velocity-pressure formulation reads as: given the sufficiently smooth force density $\mathbf{f}$, seek $(\mathbf{u}, p)$ such that*

$$\begin{aligned} -\nu \boldsymbol{\Delta} \mathbf{u} + (\mathbf{u} \cdot \boldsymbol{\nabla})\mathbf{u} + \nabla p = \mathbf{f}, \qquad \operatorname{div} \mathbf{u} = 0 \qquad in \quad \Omega, \\ \mathbf{u} = \mathbf{g} \qquad on \quad \Gamma, \qquad (p,1)_{0,\Omega} = 0, \end{aligned} \tag{4.2.6}$$

where $\mathbf{u} : \Omega \to \mathbb{R}^2$ is the velocity field, $p : \Omega \to \mathbb{R}$ is the fluid pressure and $\mathbf{g}$ is a boundary data. We have that the above problem is equivalent to system (4.1.1). Moreover, the set of boundary conditions g_0 and g_1 for the stream-function can be deduced from the boundary condition $\mathbf{g}$ for the primitive variable $\mathbf{u}$ (for more details, see for instance [103, Chap. I, sect. 5.2 and Chap. IV, sect. 2.2]).

4.3 The C^1-virtual element approximation

In this section we will introduce the C^1-conforming VEMs of high-order $k \geq 2$, for the numerical approximation of problem (4.2.1). We start by introducing some basic tools and notations to construct the discrete scheme. Then, we introduce the local and global virtual spaces along with the degrees of freedom. Finally, we present the discrete stream-function formulation.

Notation and mesh assumptions

Henceforth, we will adopt the usually notation for the virtual element framework (see for instance [27, 65, 133]). In particular, we will denote by K a general polygon, Let Ω_h be a sequence of decompositions of Ω into general non-overlapping polygons K, where $h := \max_{K \in \Omega_h} h_K$. Furthermore, for any K and each integer $\ell \geq 0$ we denote by $\mathbb{P}_\ell(\Omega_h)$, the classical discontinuous piecewise ℓ-order polynomial space. Moreover, for $t > 0$, we consider the broken Hilbert space: $\mathrm{H}^t(\Omega_h) := \big\{\phi \in \mathrm{L}^2(\Omega) : \phi|_K \in \mathrm{H}^t(K) \quad \forall K \in \Omega_h\big\}$, endowed with the following broken seminorm $|\phi|_{t,h} := \big(\sum_{K \in \Omega_h} |\phi|^2_{t,K}\big)^{1/2}$.

For the theoretical analysis, we suppose that Ω_h satisfies the following assumptions: there exists a real number $\rho > 0$ such that, every $K \in \Omega_h$, we have

A1 : K is star-shaped with respect to every point of a ball of radius $\geq \rho h_K$;

A2 : the length h_e of every edge $e \subset \partial K$, satisfies $h_e \geq \rho h_K$.

4.3.1 Virtual spaces and degrees of freedom

With the notations presented in the above subsection we will introduce the VE spaces and the degrees of freedom. For every polygon $K \in \Omega_h$ and any integer $k \geq 2$, we consider the number $r := \max\{k, 3\}$ and the following finite dimensional space introduced in [77]:

$$\widetilde{\mathrm{W}}_k^h(K) := \left\{\phi_h \in \mathrm{H}^2(K) \cap C^1(\partial K) : \Delta^2\phi_h \in \mathbb{P}_{k-2}(K), \phi_h|_e \in \mathbb{P}_r(e),\ \partial_{\mathbf{n}_K^e}\phi_h \in \mathbb{P}_{k-1}(e)\ \forall e \in \partial K\right\},$$

Next, for $\phi_h \in \widetilde{\mathrm{W}}_k^h(K)$, we introduce the following set of linear operators:

- $\mathbf{D_W1}$: the values of $\phi_h(\mathbf{v}_i)$ for all vertex $\mathbf{v}_i$ of the polygon K;
- $\mathbf{D_W2}$: the values of $h_{\mathbf{v}_i}\nabla\phi_h(\mathbf{v}_i)$ for all vertex $\mathbf{v}_i$ of the polygon K;
- $\mathbf{D_W3}$: for $k \geq 3$, the moments: $(q, \partial_{\mathbf{n}_K^e}\phi_h)_{0,e} \quad \forall q \in \mathbb{M}_{k-3}(e), \quad \forall\,\text{edge } e$;
- $\mathbf{D_W4}$: for $r \geq 4$, the moments: $h_e^{-1}(q, \phi_h)_{0,e} \quad \forall q \in \mathbb{M}_{r-4}(e), \quad \forall\,\text{edge } e$;
- $\mathbf{D_W5}$: for $k \geq 4$, the moments: $h_K^{-2}(q, \phi_h)_{0,K} \quad \forall q \in \mathbb{M}_{k-4}(K), \quad \forall\,\text{polygon } K$,

where for each vertex $\mathbf{v}_i$ we set $h_{\mathbf{v}_i}$ as the average of the diameters of the elements having $\mathbf{v}_i$ as a vertex. In order to construct an approximation for the form $\mathcal{A}(\cdot,\cdot)$, we define the operator $\mathsf{P}_0 : C^0(\partial K) \to \mathbb{P}_0(K)$, as the following average:

$$\mathsf{P}_0\varphi = \frac{1}{N_K}\sum_{i=1}^{N_K}\varphi(\mathbf{v}_i), \tag{4.3.1}$$

where $\mathbf{v}_i, 1 \leq i \leq N_K$, are the vertices of K.

Next, for each polygon K, we define the projector $\Pi_K^{k,\mathrm{D}} : \widetilde{\mathrm{W}}_k^h(K) \to \mathbb{P}_k(K) \subseteq \widetilde{\mathrm{W}}_k^h(K)$, as the solution of the local problems:

$$\begin{aligned}
&\mathcal{A}_K(\phi_h - \Pi_K^{k,\mathrm{D}}\phi_h, q_k) = 0 \qquad \forall q_k \in \mathbb{P}_k(K),\\
&\mathsf{P}_0(\phi_h - \Pi_K^{k,\mathrm{D}}\phi_h) = 0, \quad \mathsf{P}_0(\nabla(\phi - \Pi_K^{k,\mathrm{D}}\phi_h)) = 0.
\end{aligned}$$

For each $K \in \Omega_h$ and any integer $k \geq 2$ the local enhanced virtual space is given by:

$$\mathrm{W}_k^h(K) := \left\{\phi_h \in \widetilde{\mathrm{W}}_k^h(K) : \left(q^*, \phi_h - \Pi_K^{k,\mathrm{D}}\phi_h\right)_{0,K} = 0 \quad \forall q^* \in \mathbb{M}_{k-3}^*(K) \cup \mathbb{M}_{k-2}^*(K)\right\},$$

where $\mathbb{M}_{k-3}^*(K)$ and $\mathbb{M}_{k-2}^*(K)$ are scaled monomials of degree $k-3$ and $k-2$, respectively, with the convention that $\mathbb{M}_{-1}^*(K) := \emptyset$. Besides, we have that the sets of linear operators $\mathbf{D_W1} - \mathbf{D_W5}$ constitutes a set of degrees of freedom for $\mathrm{W}_k^h(K)$ and the operator $\Pi_K^{k,\mathrm{D}}$: $\mathrm{W}_k^h(K) \to \mathbb{P}_k(K)$ is computable using the degrees of freedom $\mathbf{D_W1} - \mathbf{D_W5}$ For further details, see for instance [77, 133] (see also [58, 7]).

Now, for every decomposition Ω_h of Ω into polygons K and for any $k \geq 2$, we define the global virtual space to the numerical approximation of the solution of problem (4.2.1), as follows:

$$\mathrm{W}_k^h := \left\{\phi_h \in \mathcal{W} :\ \phi_h|_K \in \mathrm{W}_k^h(K) \quad \forall K \in \Omega_h\right\}.$$

4.3.2 Polynomial projections and the discrete formulation

In this subsection we introduce other polynomial projections, which will be useful to build an approximation of forms $\mathcal{B}(\cdot;\cdot,\cdot)$ and $\mathcal{F}(\cdot)$ (cf. (4.2.3) and (4.2.4), respectively). We start denoting by $\Pi_K^{k-2}:\mathrm{L}^2(K)\to\mathbb{P}_{k-2}(K)$ the usual $\mathrm{L}^2(K)$-projection onto the polynomial space $\mathbb{P}_{k-2}(K)$. Next, we will consider the projection onto the vectorial polynomial space $\mathbf{P}_{k-1}(K)$, i.e., $\mathbf{\Pi}_K^{k-1}:\mathbf{L}^2(K)\to\mathbf{P}_{k-1}(K)$.

The following lemma establishes that certain polynomial functions are computable on $\mathrm{W}_k^h(K)$, using only the information of the degrees of freedom $\mathbf{D_W1}-\mathbf{D_W5}$.

Lemma 4.3.1. *For each $\phi_h\in\mathrm{W}_k^h(K)$ the polynomial functions $\Pi_K^{k-2}\phi_h$, $\Pi_K^{k-2}\Delta\phi_h$, $\mathbf{\Pi}_K^{k-1}\nabla\phi_h$ and $\mathbf{\Pi}_K^{k-1}\mathbf{curl}\,\phi_h$ are computable using only the information of the degrees of freedom* $\mathbf{D_W1}-\mathbf{D_W5}$.

Proof. To prove that the polynomial function $\Pi_K^{k-2}\Delta\phi_h$ is computable, let $\phi_h\in\mathrm{W}_k^h(K)$ and $q\in\mathbb{P}_{k-2}(K)$, then using the definition of the projection Π_K^{k-2} and integration by parts, we have

$$(q,\Pi_K^{k-2}\Delta\phi_h)_{0,K}=(q,\Delta\phi_h)_{0,K}=(\phi_h,\Delta q)_{0,K}-(\phi_h,\partial_{\mathbf{n}_K}q)_{0,\partial K}+(q,\partial_{\mathbf{n}_K}\phi_h)_{0,\partial K}.$$

we observe that all term above are fully computable using the information of $\mathbf{D_W1}-\mathbf{D_W5}$. The remaining of the proof follow from the arguments presented in [65, 77, 133]. □

Now, using the operators previously defined, we will construct the discrete version of the forms defined in (4.2.2),(4.2.3) and (4.2.4). First, let $\mathcal{S}_K:\mathrm{W}_k^h(K)\times\mathrm{W}_k^h(K)\to\mathbb{R}$ be any symmetric positive definite bilinear forms to be chosen as to satisfy:

$$c_0\mathcal{A}_K(\phi_h,\phi_h)\le\mathcal{S}_K(\phi_h,\phi_h)\le c_1\mathcal{A}_K(\phi_h,\phi_h)\qquad\forall\phi_h\in\mathrm{Ker}(\Pi_K^{k,\mathrm{D}}),\tag{4.3.2}$$

with c_0 and c_1 positive constants independent of K. We will choose the following representation satisfying (4.3.2) (see [27, 58, 133]):

$$\mathcal{S}_K(\varphi_h,\phi_h):=h_K^{-2}\sum_{i=1}^{N_K^{\mathrm{dof}}}\mathrm{dof}_i(\varphi_h)\mathrm{dof}_i(\phi_h),$$

where $N_K^{\mathrm{dof}}:=\dim(\mathrm{W}_k^h(K))$.

Next, we consider the following discrete local bilinear form, $\mathcal{A}_K^h:\mathrm{W}_k^h(K)\times\mathrm{W}_k^h(K)\to\mathbb{R}$ approximating the continuous form $\mathcal{A}_K(\cdot,\cdot)$.

$$\mathcal{A}_K^h(\varphi_h,\phi_h):=\mathcal{A}_K\big(\Pi_K^{k,\mathrm{D}}\varphi_h,\Pi_K^{k,\mathrm{D}}\phi_h\big)+\mathcal{S}_K\big((\mathrm{I}-\Pi_K^{k,\mathrm{D}})\varphi_h,(\mathrm{I}-\Pi_K^{k,\mathrm{D}})\phi_h\big)\quad\forall\varphi_h,\phi_h\in\mathrm{W}_k^h(K).$$

For the approximation of the local trilinear form $\mathcal{B}_K(\cdot;\cdot,\cdot)$, we consider set

$$\mathcal{B}_K^h(\zeta_h;\varphi_h,\phi_h):=\big(\Pi_K^{k-2}\Delta\zeta_h\,\mathbf{\Pi}_K^{k-1}\mathbf{curl}\,\varphi_h,\,\mathbf{\Pi}_K^{k-1}\nabla\phi_h\big)_{0,K}\qquad\forall\zeta_h,\varphi_h,\phi_h\in\mathrm{W}_k^h(K).\tag{4.3.3}$$

Thus, for all $\zeta_h,\varphi_h,\phi_h\in\mathrm{W}_k^h$, we define the global bilinear form and trilinear form as follows:

$$\mathcal{A}^h:\mathrm{W}_k^h\times\mathrm{W}_k^h\to\mathbb{R},\qquad\mathcal{A}^h(\varphi_h,\phi_h):=\sum_{K\in\Omega_h}\mathcal{A}_K^h(\varphi_h,\phi_h),\tag{4.3.4}$$

$$\mathcal{B}^h:\mathrm{W}_k^h\times\mathrm{W}_k^h\times\mathrm{W}_k^h\to\mathbb{R},\qquad\mathcal{B}^h(\zeta_h;\varphi_h,\phi_h):=\sum_{K\in\Omega_h}\mathcal{B}_K^h(\zeta_h;\varphi_h,\phi_h).\tag{4.3.5}$$

We recall the forms defined above are computable using the degrees of freedom $\mathbf{D_W1} - \mathbf{D_W5}$. In addition, we have that the trilinear form $\mathcal{B}^h(\cdot;\cdot,\cdot)$ is immediately extendable to the whole $\mathcal{W}$, and the local discrete bilinear form $\mathcal{A}_K^h(\cdot,\cdot)$ satisfies the usual k-consistency and stability VEM properties (see for instance [3, Proposition 3.6]).

We consider the following computable approximation of the right hand side

$$\mathcal{F}^h(\phi_h) := \sum_{K\in\Omega_h} (\boldsymbol{\Pi}_K^{k-1}\mathbf{f}, \mathbf{curl}\,\phi_h)_{0,K} \equiv \sum_{K\in\Omega_h} (\mathbf{f}, \boldsymbol{\Pi}_K^{k-1}\mathbf{curl}\,\phi_h)_{0,K} \quad \forall \phi_h \in \mathrm{W}_k^h. \tag{4.3.6}$$

We finish this section by presenting the discrete problem for the numerical approximation of system (4.2.1).

The discrete stream-function formulation reads as: seek $\psi_h \in \mathrm{W}_k^h$, such that

$$\nu\mathcal{A}^h(\psi_h,\phi_h) + \mathcal{B}^h(\psi_h;\psi_h,\phi_h) = \mathcal{F}^h(\phi_h) \qquad \forall \phi_h \in \mathrm{W}_k^h, \tag{4.3.7}$$

where $\mathcal{A}^h(\cdot,\cdot)$ is the discrete bilinear form defined in (4.3.4), $\mathcal{B}^h(\cdot;\cdot,\cdot)$ is the discrete trilinear form defined in (4.3.5), and $\mathcal{F}^h(\cdot)$ is the functional introduced in (4.3.6).

Remark 4.3.1. *We note that the discrete form $\mathcal{B}^h$ built in (4.3.5), preserves the natural skew-symmetry property of the continuous version $\mathcal{B}$ (cf. (4.2.3)). Thus, at discrete level there is no requirement to add any extra term to ensure this property, unlike velocity-pressure VE discretizations, where a transpose term is necessary added (see for instance [35] in the conforming approach). This important fact, allows to establish stability and convergence of our schemes, by using more direct arguments (see below Section 4.4). Besides, advantages from the computational viewpoint can be observed.*

4.4 Theoretical analysis

In this section we develop a rigorous analysis for the method proposed in Section 4.3. In particular, we establish that the discrete problem (4.3.7) is well-posed by using the skew-symmetry property of the discrete trilinear form and the classical Banach fixed-point Theorem. Furthermore, we provide optimal *a priori* error estimates for the discrete stream-function in H^2-norm and using duality arguments we also provide an error estimate in H^1- and L^2-norms.

We begin this section recalling the boundedness of projections Π_K^{k-2} and $\boldsymbol{\Pi}_K^{k-1}$ with respect to general semi-norms, which will play an important role in the forthcoming sections. More precisely, given $p > 1$, there exists $C_{\texttt{bd}} \geq 1$, independent of K, such that (for more details, see for instance [100]):

$$|\Pi_K^{k-2} v|_{\mathrm{W}_p^t(K)} \leq C_{\texttt{bd}} |v|_{\mathrm{W}_p^t(K)} \qquad \forall v \in \mathrm{W}_p^t(K), \qquad 0 \leq t \leq k-1, \quad k \geq 2, \tag{4.4.1}$$

$$|\boldsymbol{\Pi}_K^{k-1}\mathbf{v}|_{\mathrm{W}_p^t(K)} \leq C_{\texttt{bd}} |\mathbf{v}|_{\mathrm{W}_p^t(K)} \qquad \forall \mathbf{v} \in \mathbf{W}_p^t(K), \qquad 0 \leq t \leq k, \qquad k \geq 1. \tag{4.4.2}$$

Also, we recall the following Sobolev embeddings: given a real $t > 0$, we have $\mathrm{H}^{1+t}(\Omega) \hookrightarrow \mathrm{W}_4^t(\Omega)$, i.e., there exists $C_{\texttt{sob}} > 0$ independent of h, such that

$$|v|_{\mathrm{W}_4^t(\Omega)} \leq C_{\texttt{sob}} \|v\|_{1+t,\Omega} \qquad \forall v \in \mathrm{H}^{1+t}(\Omega). \tag{4.4.3}$$

The following lemma summarize some properties of the discrete forms defined in Section 4.3.2. These properties will be used to establish the well-posedness of the discrete problem (4.3.7).

Lemma 4.4.1. *There exist positive constants α_1, α_2 and $\widehat{C_h}$, independent of h, such that for any virtual functions $\zeta_h, \varphi_h, \phi_h \in \mathrm{W}_k^h$ the forms defined in (4.3.4), (4.3.5) and (4.3.6) satisfies the following properties:*

$$|\mathcal{A}^h(\varphi_h, \phi_h)| \leq \alpha_1 \|\varphi_h\|_{\mathcal{W}} \|\phi_h\|_{\mathcal{W}}, \qquad \mathcal{A}^h(\phi_h, \phi_h) \geq \alpha_2 \|\phi_h\|_{\mathcal{W}}^2, \tag{4.4.4}$$

$$\mathcal{B}^h(\zeta_h; \varphi_h, \phi_h) \leq \widehat{C_h} \|\zeta_h\|_{\mathcal{W}} \|\varphi_h\|_{\mathcal{W}} \|\phi_h\|_{\mathcal{W}}, \quad \mathcal{B}^h(\zeta_h; \phi_h, \phi_h) = 0, \tag{4.4.5}$$

Proof. The proof follows from the definition of the corresponding forms and standard arguments. □

4.4.1 Fixed-point strategy

In order to prove the well-posedness of problem (4.3.7), we will establish a fixed-point strategy. Indeed, given $\xi_h \in \mathrm{W}_k^h$, we define the operator:

$$\begin{aligned} \mathscr{T}^h : \mathrm{W}_k^h &\longrightarrow \mathrm{W}_k^h \\ \xi_h &\longmapsto \mathscr{T}^h(\xi_h) = \varphi_h, \end{aligned}$$

where φ_h is the solution of the following linear problem: seek $\varphi_h \in \mathrm{W}_k^h$, such that

$$\mathcal{N}_{\xi_h}(\varphi_h, \phi_h) := \nu \mathcal{A}^h(\varphi_h, \phi_h) + \mathcal{B}^h(\xi_h; \varphi_h, \phi_h) = \mathcal{F}^h(\phi_h) \qquad \forall \phi_h \in \mathrm{W}_k^h.$$

By employing Lemma 4.4.1 and the Lax-Milgram Theorem we prove that the operator $\mathscr{T}^h$ is well-defined. More precisely, given $\xi_h \in \mathrm{W}_k^h$, there exists a unique $\varphi_h \in \mathrm{W}_k^h$ such that $\mathscr{T}^h(\xi_h) = \varphi_h$.

Now, we consider the ball $\mathcal{K}_h := \left\{\phi_h \in \mathrm{W}_k^h : \|\phi_h\|_{\mathcal{W}} \leq C_{\mathcal{F}^h} (\alpha_2 \nu)^{-1} \|\mathbf{f}\|_{0,\Omega}\right\}$, and using the previous lemma, we have that $\mathscr{T}^h(\mathcal{K}_h) \subseteq \mathcal{K}_h$. Observe that the problem (4.3.7) is well-posed if only if $\mathscr{T}^h$ has a unique point-fixed in $\mathcal{K}_h$.

In order to demonstrate the existence and uniqueness, from now on, we make the following assumption:

$$\lambda_h := \widehat{C_h} C_{\mathcal{F}^h} (\alpha_2 \nu)^{-2} \|\mathbf{f}\|_{0,\Omega} < 1. \tag{4.4.6}$$

The following result establishes the well-posedness of problem (4.3.7).

Theorem 4.4.1. *If the assumption (4.4.6) is satisfied, then $\mathscr{T}^h : \mathcal{K}_h \to \mathcal{K}_h$ is a contraction mapping. As a consequence, there exists a unique $\psi_h \in \mathrm{W}_k^h$ solution to problem (4.3.7) satisfying the following dependence of the data*

$$\|\psi_h\|_{\mathcal{W}} \leq C_{\mathcal{F}^h} (\alpha_2 \nu)^{-1} \|\mathbf{f}\|_{0,\Omega}. \tag{4.4.7}$$

Proof. The proof follows form standard arguments and the Banach point-fixed Theorem. □

4.4.2 Error estimates

In the present section we develop an error analysis for the VE scheme presented in Section 4.3. First, we will establish some preliminary error estimates, which will play an important role in the forthcoming sections.

Preliminary results

We start by recalling the following approximation result for polynomials on star-shaped domains (see, for instance [54]).

Proposition 4.4.1. *If the assumption* **A1** *is satisfied, then there exists a constant* $C > 0$*, such that for every* $\phi \in \mathrm{H}^m(K)$*, there exists* $\phi_\pi \in \mathbb{P}_k(K)$*,* $k \geq 0$*, such that*

$$\|\phi - \phi_\pi\|_{t,K} \leq C h_K^{m-t} |\phi|_{m,K}, \quad 0 \leq m \leq k+1,\, t = 0, 1, \ldots, [m],$$

where $[m]$ *denoting the largest integer equal to or smaller than* $m \in \mathbb{R}$*.*

We have the following approximation properties for the projectors Π_K^{k-2} and $\boldsymbol{\Pi}_K^{k-1}$ with respect to general Sobolev semi-norms (see, for instance [54] and [100]).

Proposition 4.4.2. *Assume that* **A1** *is satisfied. Then for each* $K \in \Omega_h$ *and* $p > 1$*, there exists* $C_{\mathtt{aprx}} > 0$*, independent of* K*, such that*

$$|v - \Pi_K^{k-2} v|_{\mathrm{W}_p^t(K)} \leq C_{\mathtt{aprx}} h_K^{m-t} |v|_{\mathrm{W}_p^m(K)} \quad \forall v \in \mathrm{W}_p^m(K),\ 0 \leq t \leq m \leq k-1,\ k \geq 2,$$
$$|\mathbf{v} - \boldsymbol{\Pi}_K^{k-1} \mathbf{v}|_{\mathrm{W}_p^t(K)} \leq C_{\mathtt{aprx}} h_K^{m-t} |\mathbf{v}|_{\mathrm{W}_p^m(K)} \quad \forall \mathbf{v} \in \mathbf{W}_p^m(K), \quad 0 \leq t \leq m \leq k, \quad k \geq 1.$$

Now, we present the estimate for the interpolant $\phi_I \in \mathrm{W}_k^h$ (see [58, 77]).

Proposition 4.4.3. *Assume that* **A1** *and* **A2** *are satisfied. Then, for each* $\phi \in \mathrm{H}^m(\Omega)$*, there exist* $\phi_I \in \mathrm{W}_k^h$ *and* $C_I > 0$*, independent of* h*, such that*

$$\|\phi - \phi_I\|_{t,\Omega} \leq C_I h^{m-t} |\phi|_{m,\Omega}, \quad t = 0, 1, 2, \quad 2 \leq m \leq k+1, \quad k \geq 2.$$

By using Propositions 4.4.1 and 4.4.2, we will establish bounds involving the forms $\mathcal{F}(\cdot)$, $\mathcal{B}(\cdot;\cdot,\cdot)$ and $\mathcal{B}^h(\cdot;\cdot,\cdot)$. We start with the following bound for a dual norm. In what follows, we will assume that the assumptions **A1** and **A2** of Section 4.3 are satisfied.

Proposition 4.4.4. *Let* $k \geq 2$ *and* $\mathbf{f} \in \mathbf{H}^{k-2}(\Omega_h)$*,* $\mathcal{F}(\cdot)$ *and* $\mathcal{F}^h(\cdot)$ *the functionals defined in* (4.2.4) *and* (4.3.6)*, respectively. Then, we have the following estimation:*

$$\|\mathcal{F} - \mathcal{F}^h\| := \sup_{\substack{\phi_h \in \mathrm{W}_k^h \\ \phi_h \neq 0}} \frac{|\mathcal{F}(\phi_h) - \mathcal{F}^h(\phi_h)|}{\|\phi_h\|_{\mathcal{W}}} \leq C h^{k-1} |\mathbf{f}|_{k-2,h}.$$

In order to obtain optimal a priori error estimate for our scheme, under *minimal regularity* condition on the weak solution, we start with the following result, which is a consequence of [26, Theorem 7.4].

Proposition 4.4.5. *Let* Ω *be a bounded domain in* $\mathbb{R}^n$ *with Lipschitz continuous boundary. For* $i = 1, 2$*, assume* s_i, s *are real numbers satisfying:* $s_i \geq s \geq 0$ *and* $s_1 + s_2 - s > \dfrac{n}{2}$*. If* $u \in \mathrm{H}^{s_1}(\Omega)$ *and* $v \in \mathrm{H}^{s_2}(\Omega)$*, then* $uv \in \mathrm{H}^s(\Omega)$*. Moreover, the pointwise multiplication of functions is a continuous bilinear map* $\mathrm{H}^{s_1}(\Omega) \times \mathrm{H}^{s_2}(\Omega) \to \mathrm{H}^s(\Omega)$*, i.e.,* $\|uv\|_{s,\Omega} \leq C_{n,\Omega} \|u\|_{s_1,\Omega} \|v\|_{s_2,\Omega}$*.*

Proof. The result follows from [26, Theorem 7.4], taking the particular case when $p_i = p = 2$. □

Next lemma is the main result of this subsection, which improve the error bound presented in [3, Lemma 5.4]. Notice that in this case we can consider $t > 0$.

Lemma 4.4.2. *Let $\varphi \in \mathrm{H}^{2+t}(\Omega) \cap \mathcal{W}$, with $0 < t \leq k-1$. Then, for all $\phi \in \mathcal{W}$, there exists $C > 0$, independent to h, such that*

$$B = |\mathcal{B}(\varphi;\varphi,\phi) - \mathcal{B}^h(\varphi;\varphi,\phi)| \leq Ch^t(\|\varphi\|_{2+t,\Omega} + \|\varphi\|_{\mathcal{W}})\|\varphi\|_{2+t,\Omega}\|\phi\|_{\mathcal{W}}.$$

Proof. By using the definition of the continuous and discrete nonlinear terms $\mathcal{B}(\cdot;\cdot,\cdot)$ and $\mathcal{B}^h(\cdot;\cdot,\cdot)$ (cf. (4.2.3) and (4.3.3), respectively), we have

$$\begin{aligned}
B &= \sum_{K\in\Omega_h} \big((\Delta\varphi\mathbf{curl}\,\varphi,\ \nabla\phi)_{0,K} - (\Pi_K^{k-2}\Delta\varphi\boldsymbol{\Pi}_K^{k-1}\mathbf{curl}\,\varphi,\ \boldsymbol{\Pi}_K^{k-1}\nabla\phi)_{0,K}\big),\\
&= \sum_{K\in\Omega_h} \big((\Delta\varphi\mathbf{curl}\,\varphi,\ (I-\boldsymbol{\Pi}_K^{k-1})\nabla\phi)_{0,K} + (\Delta\varphi\ (I-\boldsymbol{\Pi}_K^{k-1})\mathbf{curl}\,\varphi\cdot\boldsymbol{\Pi}_K^{k-1}\nabla\phi)_{0,K}\\
&\quad + ((\Delta\varphi - \Pi_K^{k-2}\Delta\varphi)\,\boldsymbol{\Pi}_K^{k-1}\mathbf{curl}\,\varphi,\ \boldsymbol{\Pi}_K^{k-1}\nabla\phi)_{0,K}\big) =: T_1 + T_2 + T_3.
\end{aligned}$$

In what follows we will bound each terms in the above identity. For the term T_1, we consider two case. First, we study the case $0 < t \leq 1$. Then, we apply the Cauchy-Schwarz inequality, and approximation properties of $\boldsymbol{\Pi}_K^{k-1}$ to obtain

$$\begin{aligned}
T_1 &= \sum_{K\in\Omega_h} \big(\Delta\varphi\mathbf{curl}\,\varphi,\ (I-\boldsymbol{\Pi}_K^{k-1})\nabla\phi\big)_{0,K} \leq Ch\|\Delta\varphi\mathbf{curl}\,\varphi\|_{0,\Omega}|\nabla\phi|_{1,\Omega}\\
&\leq Ch\|\Delta\varphi\|_{t,\Omega}\|\mathbf{curl}\,\varphi\|_{1+t,\Omega}\|\phi\|_{\mathcal{W}} \leq Ch^t\|\varphi\|_{2+t,\Omega}\|\varphi\|_{2+t,\Omega}\|\phi\|_{\mathcal{W}},
\end{aligned}$$

where we have applied Proposition 4.4.5, with $s_1 = t$, $s_2 = 1+t$ and $s = 0$. For the case $1 < t \leq k-1$, we use the orthogonality property of the projection operator $\boldsymbol{\Pi}_K^{k-1}$, the Cauchy-Schwarz inequality, to get

$$\begin{aligned}
T_1 &= \sum_{K\in\Omega_h} \big((I-\boldsymbol{\Pi}_K^{k-1})(\Delta\varphi\mathbf{curl}\,\varphi),(I-\boldsymbol{\Pi}_K^{k-1})\nabla\phi_h\big)_{0,K}\\
&\leq Ch^{t-1}\|\Delta\varphi\mathbf{curl}\,\varphi\|_{t-1,\Omega}h\|\phi\|_{\mathcal{W}} \leq Ch^t\|\varphi\|_{2+t,\Omega}\|\varphi\|_{1+t,\Omega}\|\phi\|_{\mathcal{W}},
\end{aligned}$$

where once again we have used the Proposition 4.4.5, but now with $s_1 = s_2 = t$ and $s = t-1$. The remaining terms are estimated by using the approximation and continuity properties of the involving operators together Sobolev embeddings, only requiring $0 < t \leq k-1$ as in [3, Lemma 5.4]. □

We finish this subsection with the following result.

Lemma 4.4.3. *For all $\zeta,\varphi,\phi \in \mathcal{W}$ we have that*

$$|\mathcal{B}^h(\varphi;\varphi,\phi) - \mathcal{B}^h(\zeta;\zeta,\phi)| \leq \widehat{C_h}\left(\|\zeta\|_{\mathcal{W}}\|\phi\|_{\mathcal{W}} + \|\varphi-\zeta+\phi\|_{\mathcal{W}}(\|\varphi\|_{\mathcal{W}} + \|\zeta\|_{\mathcal{W}})\right)\|\phi\|_{\mathcal{W}}.$$

Proof. The proof follows from adding and subtracting adequate terms, together with properties in (4.4.5). □

4.4.2.1 A priori estimate

In this section we will provide a new error estimate in H^2-norm for our nonlinear discrete scheme under *minimal regularity* conditions on the weak stream-function solution. First, we start establishing a Strang-type lemma. Indeed, given $\psi \in \mathcal{W}$ the solution of continuous problem (4.2.1), then we introduce the following consistence error as:

$$\mathcal{C}^h(\psi, \phi_h) := \mathcal{B}(\psi; \psi, \phi_h) - \mathcal{B}^h(\psi; \psi, \phi_h) \qquad \forall \phi_h \in \mathrm{W}_k^h. \tag{4.4.8}$$

which measure of the variational crime associated to the approximation of the trilinear form $\mathcal{B}(\cdot; \cdot, \cdot)$. Next, we present the following abstract convergence result.

Theorem 4.4.2. *Let ψ and ψ_h be the unique solutions to problems (4.2.1) and (4.3.7), respectively. Then, there exists $C > 0$, independent of h, such that*

$$\|\psi - \psi_h\|_{\mathcal{W}} \leq C\Big(\inf_{\phi_h \in \mathrm{W}_k^h} \|\psi - \phi_h\|_{\mathcal{W}} + \inf_{\varphi_k \in \mathbb{P}_k(\Omega_h)} |\psi - \varphi_k|_{2,h} + \|\mathcal{F} - \mathcal{F}^h\| + \sup_{\substack{\phi_h \in \mathrm{W}_k^h \\ \phi_h \neq 0}} \frac{|\mathcal{C}^h(\psi, \phi_h)|}{\|\phi_h\|_{\mathcal{W}}} \Big),$$

where $\mathcal{C}^h(\psi, \cdot)$ is the consistency errors defined in (4.4.8).

Proof. Let $\phi_h \in \mathrm{W}_k^h$ and set $\chi_h := \psi_h - \phi_h$. Thus, $\psi - \psi_h = (\psi - \phi_h) + \chi_h$. Now, by the coercivity and consistency properties of bilinear form $\mathcal{A}^h(\cdot, \cdot)$, adding and subtracting adequate terms we have that

$$\begin{aligned}
\nu\alpha_2 \|\chi_h\|_{\mathcal{W}}^2 &\leq \nu\mathcal{A}^h(\chi_h, \chi_h) = \nu\mathcal{A}^h(\psi_h, \chi_h) - \nu\mathcal{A}^h(\psi_I, \chi_h) \\
&= \nu\mathcal{A}^h(\psi_h, \chi_h) - \nu\mathcal{A}(\psi, \chi_h) + \nu \sum_{K \in \Omega_h} \left(\mathcal{A}_K^h(\varphi_k - \phi_h, \chi_h) + \mathcal{A}_K^h(\psi - \varphi_k, \chi_h) \right) \\
&= \left(\mathcal{F}^h(\chi_h) - \mathcal{F}(\chi_h) \right) + \left(\mathcal{B}(\psi; \psi, \chi_h) - \mathcal{B}^h(\psi_h; \psi_h, \chi_h) \right) \\
&\quad + \nu \sum_{K \in \Omega_h} \left(\mathcal{A}_K^h(\varphi_k - \phi_h, \chi_h) + \mathcal{A}_K^h(\psi - \varphi_k, \chi_h) \right),
\end{aligned}$$

where $\varphi_k \in \mathbb{P}_k(K)$ is arbitrary. Now, we employ the continuity of bilinear forms $\mathcal{A}_K(\cdot, \cdot)$, $\mathcal{A}_K^h(\cdot, \cdot)$, and the triangular inequality, to obtain

$$\sum_{K \in \Omega_h} \left(\mathcal{A}_K^h(\varphi_k - \phi_h, \chi_h) + \mathcal{A}_K^h(\psi - \varphi_k, \chi_h) \right) \leq C(\|\phi_h - \psi\|_{\mathcal{W}} + |\psi - \varphi_k|_{2,h}) \|\chi_h\|_{\mathcal{W}}.$$

On the another hand, by adding and subtracting the term $\mathcal{B}^h(\psi; \psi, \chi_h)$ and applying Lemma 4.4.3, we obtain

$$\begin{aligned}
|\mathcal{B}^h(\psi_h; \psi_h, \chi_h) - \mathcal{B}(\psi; \psi, \chi_h)| &\leq |\mathcal{B}^h(\psi_h; \psi_h, \chi_h) - \mathcal{B}^h(\psi; \psi, \chi_h)| + |\mathcal{B}^h(\psi; \psi, \chi_h) - \mathcal{B}(\psi; \psi, \chi_h)| \\
&\leq \widehat{C_h} \left(\|\psi_h\|_{\mathcal{W}} \|\chi_h\|_{\mathcal{W}} + \|\psi - \phi_h\|_{\mathcal{W}} (\|\psi\|_{\mathcal{W}} + \|\psi_h\|_{\mathcal{W}}) \right) \|\chi_h\|_{\mathcal{W}} + |\mathcal{C}^h(\psi, \chi_h)|.
\end{aligned}$$

By combining the three previous estimates we have that

$$\nu\alpha_2 \|\chi_h\|_{\mathcal{W}} \leq C(\|\psi - \phi_h\|_{\mathcal{W}} + |\psi - \varphi_k|_{2,h}) + \widehat{C_h} \|\psi_h\|_{\mathcal{W}} \|\chi_h\|_{\mathcal{W}} + \|\mathcal{F} - \mathcal{F}^h\| + \frac{|\mathcal{C}^h(\psi, \chi_h)|}{\|\chi_h\|_{\mathcal{W}}}.$$

Thus, by using (4.4.7) and (4.4.6) we obtain $(1 - \widehat{C_h}(\nu\alpha_2)^{-1} \|\psi_h\|_{\mathcal{W}}) \geq 1 - \lambda_h > 0$.

Therefore, from above inequality, we obtain

$$\|\chi_h\|_{\mathcal{W}} \leq C\Big(\|\psi - \phi_h\|_{\mathcal{W}} + |\psi - \varphi_k|_{2,h} + \|\mathcal{F} - \mathcal{F}^h\| + \frac{|\mathcal{C}^h(\psi, \chi_h)|}{\|\chi_h\|_{\mathcal{W}}} \Big).$$

Finally, the desired result follows from and triangle inequality the above bound. □

The following theorem is the main result of this section and it provides the accuracy of our VE schemes in H^2-norm under *minimal regularity* of the weak solution.

Theorem 4.4.3. *Under assumptions (4.2.5) and (4.4.6), let ψ and ψ_h be the unique solutions of problems (4.2.1) and (4.3.7), respectively. Assuming that $\mathbf{f} \in \mathbf{H}^{k-2}(\Omega_h)$ and $\psi \in \mathrm{H}^{2+s}(\Omega)$, with $s > 0$, then there exists $C_{\texttt{conv}} > 0$ such that*

$$\|\psi - \psi_h\|_{\mathcal{W}} \leq C_{\texttt{conv}}\, h^{\min\{s,k-1\}} \left(\|\psi\|_{2+s,\Omega} + |\mathbf{f}|_{k-2,h} \right),$$

where $C_{\texttt{conv}} := C(\mathbf{f}; \nu, \lambda, \lambda_h)$ is a suitable constant independent of h.

Proof. The proof follows by combining Theorem 4.4.2, Propositions 4.4.1, 4.4.3, 4.4.4, and Lemma 4.4.2. □

4.4.2.2 Error estimates in H^1 and L^2

In this subsection we will lead the main ingredients to derive optimal error estimates in H^1- and L^2-norms for the stream-function. First, we consider the following dual problem: given $\psi \in \mathcal{W}$ (the unique solution of problem (4.2.1)), seek $\phi \in \mathcal{W}$, such that

$$\nu\mathcal{A}(\varphi, \phi) + \mathcal{B}(\psi; \varphi, \phi) + \mathcal{B}(\varphi; \psi, \phi) = \mathcal{L}(\varphi) \qquad \forall \varphi \in \mathcal{W}, \tag{4.4.9}$$

where $\mathcal{A}(\cdot,\cdot)$ and $\mathcal{B}(\cdot;\cdot,\cdot)$ are the forms defined in (4.2.2) and (4.2.3), respectively and $\mathcal{L} \in \mathrm{H}^{-i}(\Omega)$, with $i = 1, 2$ is a functional, which will be specified later. Following the same arguments presented in [111] we have that problem (4.4.9) is well-posed.

In order to develop the error estimates in H^1- and L^2-norms, from now on, we make the following assumption for the solution of problem (4.2.1):

Assumption 4.4.1. *There exists $s > 1/2$ such that $\psi \in \mathrm{H}^{2+s}(\Omega)$. Moreover, for the particular case $1/2 < s \leq 1$, there exists $C_{\texttt{reg}} > 0$, independent of h, satisfying $\|\psi\|_{2+s,\Omega} \leq C_{\texttt{reg}}\|\mathbf{f}\|_{0,\Omega}$.*

We have the following previous result involving the trilinear forms $\mathcal{B}(\cdot;\cdot,\cdot)$ and $\mathcal{B}^h(\cdot;\cdot,\cdot)$ defined in (4.2.3) and (4.3.5), respectively.

Lemma 4.4.4. *Let $\psi \in \mathcal{W} \cap \mathrm{H}^{2+s}(\Omega)$ and $\psi_h \in \mathrm{W}_k^h$ be the unique solutions of problems (4.2.1) and (4.3.7), respectively. Assuming that $\mathbf{f} \in \mathbf{H}^{k-2}(\Omega_h)$ and let $\varphi \in \mathrm{H}^{2+t}(\Omega)$, with $t \in (1/2, 1]$. Then, it holds*

$$\begin{aligned} I := \mathcal{B}^h(\psi_h; \psi_h, \varphi) - \mathcal{B}(\psi_h; \psi_h, \varphi) &\leq 2\widehat{C_h} C_{\texttt{reg}} \|\mathbf{f}\|_{0,\Omega} |\psi - \psi_h|_{1,\Omega} \|\varphi\|_{2+t,\Omega} \\ &+ C(h^{t+\min\{s,k-1\}} + h^{2\min\{s,k-1\}}) \left(|\mathbf{f}|_{k-2,h} + \|\psi\|_{2+s,\Omega} \right) \|\varphi\|_{2+t,\Omega}, \end{aligned}$$

where $C > 0$ is a constant independent of h, $\widehat{C_h}$ and $C_{\texttt{reg}}$ are the constants in (4.4.5), respectively and Assumption 4.4.1.

Proof. By using the definition of trilinear forms $\mathcal{B}(\cdot;\cdot,\cdot)$ and $\mathcal{B}^h(\cdot;\cdot,\cdot)$, adding and subtracting suitable terms we have the following identity

$$\begin{aligned}
I = \sum_{K\in\Omega_h} & \big((I-\Pi_K^{k-2})\Delta\psi_h)(\mathbf{curl}\,\psi_h - \mathbf{curl}\,\psi),\ \nabla\varphi\big)_{0,K} \\
&+ \big(\Pi_K^{k-2}(\Delta(\psi_h-\psi))(I-\boldsymbol{\Pi}_K^{k-1})\mathbf{curl}\,\psi_h,\ \nabla\varphi\big)_{0,K} \\
&+ \big(\Pi_K^{k-2}(\Delta(\psi_h-\psi))\boldsymbol{\Pi}_K^{k-1}\mathbf{curl}\,\psi_h,\ (I-\boldsymbol{\Pi}_K^{k-1})\nabla\varphi\big)_{0,K} \\
&+ \big(\Pi_K^{k-2}\Delta\psi\boldsymbol{\Pi}_K^{k-1}(\mathbf{curl}\,(\psi_h-\psi)),\ (I-\boldsymbol{\Pi}_K^{k-1})\nabla\varphi\big)_{K} \\
&+ \big(\Pi_K^{k-2}\Delta\psi((I-\boldsymbol{\Pi}_K^{k-1})\mathbf{curl}\,\psi_h)\ \nabla\varphi\big)_{0,K} + \big((I-\Pi_K^{k-2})\Delta\psi_h)\mathbf{curl}\,\psi,\ \nabla\varphi\big)_{0,K} \\
&+ \big(\Pi_K^{k-2}\Delta\psi\ \boldsymbol{\Pi}_K^{k-1}\mathbf{curl}\,\psi,\ (I-\boldsymbol{\Pi}_K^{k-1})\nabla\varphi\big)_{0,K} =: I_1+I_2+I_3+I_4+I_5+I_6+I_7.
\end{aligned}$$

In what follows, we will bound each terms of the above expression. Indeed, for the term I_1 we use the Hölder and triangle inequalities, along with approximations properties of Π_K^{k-2}, to obtain

$$\begin{aligned}
I_1 &\leq \sum_{K\in\Omega_h} (2\|\Delta\psi_h-\Delta\psi\|_{0,K} + \|\Delta\psi-\Pi_K^{k-2}\Delta\psi\|_{0,K})\|\mathbf{curl}\,(\psi_h-\psi)\|_{\mathrm{L}^4(K)}\|\nabla\varphi\|_{\mathrm{L}^4(K)} \\
&\leq C(\|\psi-\psi_h\|_{\mathcal{W}} + h^{\min\{s,k-1\}}\|\psi\|_{2+s,\Omega})\|\mathbf{curl}\,(\psi-\psi_h)\|_{\mathrm{L}^4(\Omega)}\|\nabla\varphi\|_{\mathrm{L}^4(\Omega)} \\
&\leq Ch^{2\min\{s,k-1\}}(|\mathbf{f}|_{k-2,h} + \|\psi\|_{2+s,\Omega})\|\varphi\|_{2+t,\Omega},
\end{aligned}$$

where we have used the Hölder inequality (for sequences), the Sobolev inclusion (4.4.3) and Theorem 4.4.3. Following similar arguments (with some slight variations) we estimate the remaining terms. In particular, we prove

$$I_2+I_3+I_4+I_6+I_7 \leq C(h^{t+\min\{s,k-1\}} + h^{2\min\{s,k-1\}})\,(|\mathbf{f}|_{k-2,h} + \|\psi\|_{2+s,\Omega})\,\|\varphi\|_{2+t,\Omega}.$$

Moreover, by using the Sobolev inclusion $\mathrm{H}^s(\Omega)\hookrightarrow\mathrm{L}^4(\Omega)$, with $s\in(1/2,1]$, we get

$$I_5 \leq 2C_{\mathtt{reg}}\widehat{C_h}\|\mathbf{f}\|_{0,\Omega}|\psi-\psi_h|_{1,\Omega}\|\varphi\|_{2+t,\Omega} + Ch^{t+\min\{s,k-1\}}\|\psi\|_{2+s,\Omega}\|\varphi\|_{2+t,\Omega}.$$

By combining the above estimates we obtain the desired result. □

In what follows, we will consider the following additional small data assumption:

Assumption 4.4.2. *Let $\widehat{C_h}$ and $C_{\mathtt{reg}}$ are the constants in (4.4.5) and Assumption 4.4.1, respectively. We assume that $2C_{\mathtt{reg}}^2\widehat{C_h}\|\mathbf{f}\|_{0,\Omega}<1$.*

The following result provides error estimates in H^1 and L^2-norms of our numerical schemes.

Theorem 4.4.4. *Let $k\geq 2$ and $\mathbf{f}\in\mathbf{H}^{k-2}(\Omega_h)$. Under assumptions (4.2.5) and (4.4.6), let ψ and ψ_h be the unique solutions to the continuous and discrete problems (4.2.1) and (4.3.7), respectively. Moreover if Assumption 4.4.2 is satisfied, then there exists $\tilde{s}\in(1/2,1]$, such that*

$$|\psi-\psi_h|_{1,\Omega} \leq C(h^{\tilde{s}+\min\{s,k-1\}} + h^{2\min\{s,k-1\}})\,(|\mathbf{f}|_{k-2,h} + \|\psi\|_{2+s,\Omega})\,.$$

Moreover, we have the following estimates:

a) if $k=2$, $\mathbf{f}\in \mathbf{L}^2(\Omega)$ and (4.4.2) is satisfied, then there exists $\tilde{s}\in(1/2,1]$, such

$$\|\psi-\psi_h\|_{0,\Omega}\leq C(h^{\tilde{s}+\min\{s,1\}}+h^{2\min\{s,1\}})(\|\mathbf{f}\|_{0,\Omega}+\|\psi\|_{2+s,\Omega}),$$

b) if $k\geq 3$ and $\mathbf{f}\in\mathbf{H}^{k-2}(\Omega_h)$, then there exists $\gamma\in(1/2,2]$, such that

$$\|\psi-\psi_h\|_{0,\Omega}\leq C(h^{\gamma+\min\{s,k-1\}}+h^{2\min\{s,k-1\}})(|\mathbf{f}|_{k-2,h}+\|\psi\|_{2+s,\Omega}).$$

In all the above cases C is a positive constant independent of h.

Proof. Let $\phi\in\mathcal{W}$ be the solution of (4.4.9), with $\mathcal{L}:\mathrm{H}^1_0(\Omega)\to\mathbb{R}$ defined by:

$$\mathcal{L}(\varphi):=(\nabla(\psi-\psi_h),\nabla\varphi)_{0,\Omega}.$$

Then, using the additional regularity of problem (4.4.9) (see [111, Section 2]), there exists $\tilde{s}\in(1/2,1]$ such that $\phi\in\mathcal{W}\cap\mathrm{H}^{2+\tilde{s}}(\Omega)$ and

$$\|\phi\|_{2+\tilde{s},\Omega}\leq C_{\mathtt{reg}}|\psi-\psi_h|_{1,\Omega}. \tag{4.4.10}$$

Now, let $\phi_I\in\mathcal{W}_2^h$ be such that Proposition 4.4.3 holds true. Then, we have

$$\|\phi-\phi_I\|_{\mathcal{W}}\leq C_I h^{\tilde{s}}\|\phi\|_{2+\tilde{s},\Omega}\leq C_I C_{\mathtt{reg}} h^{\tilde{s}}|\psi-\psi_h|_{1,\Omega}. \tag{4.4.11}$$

Taking $\varphi:=(\psi-\psi_h)\in\mathcal{W}$ as test function in (4.4.9), and adding an subtracting several adequate terms, we have the following identity

$$\begin{aligned}|\psi-\psi_h|^2_{1,\Omega}&=\nu\mathcal{A}(\psi-\psi_h,\phi-\phi_I)+\nu[\mathcal{A}^h(\psi_h,\phi_I)-\mathcal{A}(\psi_h,\phi_I)]+[\mathcal{F}(\phi_I)-\mathcal{F}^h(\phi_I)]\\&+[\mathcal{B}^h(\psi_h;\psi_h,\phi_I-\phi)-\mathcal{B}(\psi;\psi,\phi_I-\phi)]+\mathcal{B}(\psi-\psi_h;\psi-\psi_h,\phi)\\&+[\mathcal{B}^h(\psi_h;\psi_h,\phi)-\mathcal{B}(\psi_h;\psi_h,\phi)]=:T_{\mathcal{A}1}+T_{\mathcal{A}2}+T_{\mathcal{F}}+T_{\mathcal{B}1}+T_{\mathcal{B}2}+T_{\mathcal{B}3}.\end{aligned} \tag{4.4.12}$$

By using standard arguments we obtain

$$T_{\mathcal{A}1}+T_{\mathcal{A}2}+T_{\mathcal{F}}\leq Ch^{\tilde{s}+\min\{s,k-1\}}\left(|\mathbf{f}|_{k-2,h}+\|\psi\|_{2+s,\Omega}\right)|\psi-\psi_h|_{1,\Omega}.$$

Moreover, the term $T_{\mathcal{B}1}$ is bounded by using the Lemmas 4.4.2 and 4.4.3, as follows:

$$\begin{aligned}|T_{\mathcal{B}1}|&\leq Ch^{\min\{s,k-1\}}(\|\psi\|_{2+s,\Omega}+\|\psi\|_{\mathcal{W}})\|\psi\|_{2+s,\Omega}\|\phi_I-\phi\|_{\mathcal{W}}\\&+\widehat{C_h}\|\psi-\psi_h\|_{\mathcal{W}}\|\phi-\phi_I\|_{\mathcal{W}}(\|\psi\|_{\mathcal{W}}+\|\psi_h\|_{\mathcal{W}})+\widehat{C_h}\|\phi-\phi_I\|^2_{\mathcal{W}}(2\|\psi_h\|_{\mathcal{W}}+\|\psi\|_{\mathcal{W}}).\end{aligned}$$

Now, using the above estimate, (4.4.11) and Theorem 4.4.3, we have that

$$\begin{aligned}|T_{\mathcal{B}1}|&\leq Ch^{\tilde{s}+\min\{s,k-1\}}(\|\psi\|_{2+s,\Omega}+\|\psi\|_{\mathcal{W}})\|\psi\|_{2+s,\Omega}|\psi-\psi_h|_{1,\Omega}\\&+Ch^{\tilde{s}+\min\{s,k-1\}}(\|\psi\|_{2+s,\Omega}+|\mathbf{f}|_{k-2,h})(\|\psi\|_{\mathcal{W}}+\|\psi_h\|_{\mathcal{W}})|\psi-\psi_h|_{1,\Omega}\\&+Ch^{2\tilde{s}+\min\{s,k-1\}}(\|\psi_h\|_{\mathcal{W}}+\|\psi\|_{\mathcal{W}})|\psi-\psi_h|_{1,\Omega},\end{aligned}$$

where we have used in the second term the estimate:

$$\|\phi-\phi_I\|^2_{\mathcal{W}}\leq C_I^2C^2_{\mathtt{reg}}h^{2\tilde{s}}|\psi-\psi_h|^2_{1,\Omega}\leq Ch^{2\tilde{s}}\|\psi-\psi_h\|_{\mathcal{W}}|\psi-\psi_h|_{1,\Omega}.$$

Next, we will continue with the remaining terms of (4.4.12). For the term $T_{\mathcal{B}2}$ we use the continuity of trilinear form $\mathcal{B}(\cdot;\cdot,\cdot)$, Theorem 4.4.3 and (4.4.10) to obtain

$$T_{\mathcal{B}2} \leq Ch^{2\min\{s,k-1\}}(\|\psi\|_{2+s,\Omega} + |\mathbf{f}|_{k-2,h})|\psi - \psi_h|_{1,\Omega}. \tag{4.4.13}$$

For the term $T_{\mathcal{B}3}$ we use Lemma 4.4.4 and (4.4.10) to obtain

$$\begin{aligned} T_{\mathcal{B}3} \leq C(h^{\tilde{s}+\min\{s,k-1\}} + h^{2\min\{s,k-1\}})\,(|\mathbf{f}|_{k-2,h} + \|\psi\|_{2+s,\Omega})\,|\psi - \psi_h|_{1,\Omega} \\ + 2C^2_{\mathtt{reg}}\widehat{C_h}\|\mathbf{f}\|_{0,\Omega}|\psi - \psi_h|^2_{1,\Omega}. \end{aligned} \tag{4.4.14}$$

Finally, the desired result is easily obtained by combining the estimates (4.4.12)–(4.4.14) and the fact that $(1 - 2C^2_{\mathtt{reg}}\widehat{C_h}\|\mathbf{f}\|_{0,\Omega}) > 0$ (cf. Assumption 4.4.2).

We continue with the L^2 estimates. Indeed, the bound *a*), follows from norms equivalence. To prove *b*), we consider the functional $\mathcal{L}(\varphi) := (\psi - \psi_h, \varphi)_{0,\Omega}$ $\forall\varphi \in \mathcal{W}$, then by repeating similar arguments above we obtain the result. □

4.5 Computing further variables of interest

In this section, by using the discrete stream-function obtained by solving the problem (4.3.7), we propose strategies to approximate further variables that are of great importance in fluid mechanics, namely; the velocity ($\mathbf{u}$), pressure (p) and vorticity (ω). Moreover, we write *a priori* error estimates for these variables.

4.5.1 The fluid velocity and vorticity recovery algorithm

We start by noticing that if $\psi \in \mathcal{W}$ is the unique solution of the continuous problem (4.2.1), then the velocity and vorticity fields of Navier–Stokes system (4.2.6) is given by:

$$\mathbf{u} = \mathbf{curl}\,\psi \qquad \text{and} \qquad \omega = \operatorname{rot}\mathbf{u} = \operatorname{rot}(\mathbf{curl}\,\psi) = -\Delta\psi. \tag{4.5.1}$$

At the discrete level, employing the projector $\boldsymbol{\Pi}_K^{k-1}$ and Π_K^{k-2}, we propose a fully computable approximation of the velocity and vorticity variables, given by:

$$\widehat{\mathbf{u}}_h := \boldsymbol{\Pi}_h^{k-1}\mathbf{curl}\,\psi_h \qquad \text{and} \qquad \widehat{\omega}_h := -\Pi_h^{k-2}(\Delta\psi_h), \tag{4.5.2}$$

where for all $\mathbf{v} \in \mathbf{L}^2(\Omega)$ and for all $\varphi \in \mathrm{L}^2(\Omega)$ we have used the notation

$$(\boldsymbol{\Pi}_h^{k-1}\mathbf{v})|_K = \boldsymbol{\Pi}_K^{k-1}(\mathbf{v}|_K) \quad \text{and} \quad (\Pi_h^{k-2}\varphi)|_K = \Pi_K^{k-2}(\varphi|_K) \qquad \forall K \in \Omega_h.$$

The following result establishes the accuracy for the velocity and vorticity fields.

Theorem 4.5.1. *Assume that the hypotheses of Theorem 4.4.3 hold true, then*

$$\begin{aligned} |\mathbf{u} - \widehat{\mathbf{u}}_h|_{1,h} + \|\omega - \widehat{\omega}_h\|_{0,\Omega} &\leq \widetilde{C}_1 h^{\min\{s,k-1\}}(\|\psi\|_{2+s,\Omega} + |\mathbf{f}|_{k-2,h}) \\ \|\mathbf{u} - \widehat{\mathbf{u}}_h\|_{0,\Omega} &\leq \widetilde{C}_2\big(h^{\tilde{s}+\min\{s,k-1\}} + h^{2\min\{s,k-1\}}\big)\,(\|\psi\|_{2+s,\Omega} + |\mathbf{f}|_{k-2,h})\,, \end{aligned}$$

where $\widetilde{C}_1$ and $\widetilde{C}_2$ are suitable constants independent of h.

Proof. The proof follows from identities (4.5.1) and (4.5.2), the triangle inequality and approximation and stability properties of the involved operators, together with Theorems 4.4.3 and 4.4.4. □

4.5.2 The fluid pressure recovery algorithm

In this subsection, we present a strategy to recover the fluid pressure of the Navier–Stokes system (4.2.6). We extend the ideas recently presented in [133]. In this work we propose a discrete virtual scheme of *high-order* $\ell := k-2$ (with $k \geq 3$), based on the enhanced C^0-VEM presented in [65] (see also [7]). From now, we assume that Ω is convex.

4.5.2.1 Continuous variational formulation

We start by introducing the following Hilbert space $\mathcal{H} := \{q \in \mathrm{H}^1(\Omega) : (q,1)_{0,\Omega} = 0\}$. Now, by using the identities $\Delta\mathbf{u} = -\mathbf{curl}(\mathrm{rot}\,\mathbf{u}) + \nabla(\mathrm{div}\,\mathbf{u})$ and $\mathrm{rot}(\mathbf{curl}\,\psi) = -\Delta\psi$ in the momentum equation of the Navier–Stokes problem (cf. (4.2.6) in Remark 4.2.1), we obtain

$$\nabla p = \mathbf{f} - (\mathbf{u}\cdot\boldsymbol{\nabla})\mathbf{u} + \nu(-\mathbf{curl}(\mathrm{rot}\,\mathbf{u}) + \nabla(\mathrm{div}\,\mathbf{u})) = \mathbf{f} - (\mathbf{curl}\,\psi\cdot\boldsymbol{\nabla})\mathbf{curl}\,\psi + \nu\,\mathbf{curl}(\Delta\psi), \quad (4.5.3)$$

where we have employed also the identities $\mathbf{u} = \mathbf{curl}\,\psi$ and $\mathrm{div}\,\mathbf{u} = 0$ in Ω (cf. system (4.2.6)).

Now, we proceed to test the equation (4.5.3) against ∇q, with $q \in \mathcal{H}$, then we get the following variational problem: seek $p \in \mathcal{H}$, such that

$$\mathcal{D}(p,q) = \mathcal{G}^{\psi}(q) \quad \forall q \in \mathcal{H}, \quad (4.5.4)$$

where the form $\mathcal{D} : \mathcal{H}\times\mathcal{H} \to \mathbb{R}$ is defined by

$$\mathcal{D}(p,q) := (\nabla p, \nabla q)_{0,\Omega} \qquad \forall p,q \in \mathcal{H},$$

and $\mathcal{G}^{\psi} : \mathcal{H} \to \mathbb{R}$ is the functional defined by

$$\mathcal{G}^{\psi}(q) := ((\mathbf{f} - (\mathbf{curl}\,\psi\cdot\boldsymbol{\nabla})\mathbf{curl}\,\psi + \nu\,\mathbf{curl}\,(\Delta\psi)), \nabla q)_{0,\Omega} \qquad \forall q \in \mathcal{H}.$$

The following result establishes that problem (4.5.4) is well-posed. The proof follows from the generalized Poincaré inequality and the Lax-Milgram Theorem.

Theorem 4.5.2. *Problem (4.5.4) have a unique solution $p \in \mathcal{H}$. Moreover, there exists $C > 0$ such that*

$$\|p\|_{1,\Omega} \leq C(\|\psi\|_{3,\Omega} + \|\mathbf{f}\|_{0,\Omega}) \leq C\|\mathbf{f}\|_{0,\Omega}.$$

4.5.2.2 C^0-VE approximation

From now on, we assume the C^1-VEM (4.3.7) has been solved with $k \geq 3$. Thus, we will introduce a C^0-VEM of high-order $\ell := k-2 \geq 1$, to discretize problem (4.5.4) (over the same mesh Ω_h).

First, we define the projector $\Pi_K^{\nabla,\ell} : \mathrm{H}^1(K) \to \mathbb{P}_\ell(K)$ for each $q_h \in \mathrm{H}^1(K)$ as the solution of the local problems:

$$\mathcal{D}_E(q_h - \Pi_K^{\nabla,\ell} q_h, r_\ell) = 0 \qquad \forall r_\ell \in \mathbb{P}_\ell(K), \quad \text{and} \quad \mathtt{P}_0(\Pi_K^{\nabla,\ell} q_h - q_h) = 0,$$

where the operator $\mathtt{P}_0(\cdot)$ is defined in (4.3.1). By employing this projection we introduce our local virtual space to approximate the fluid pressure:

$$\mathrm{H}_\ell^h(K) := \big\{q_h \in \mathrm{H}^1(K)\cap C^0(\partial K) : \Delta q_h \in \mathbb{P}_\ell(K),\ q_h|_e \in \mathbb{P}_\ell(e) \quad \forall e \subset \partial K$$
$$(r^*, q_h - \Pi_K^{\nabla,\ell} q_h)_{0,K} = 0 \quad \forall r^* \in \mathbb{M}_\ell^*(K) \cup \mathbb{M}_{\ell-1}^*(K)\big\}.$$

For each $q_h \in \widetilde{\mathrm{H}}_\ell^h(K)$ we consider the following set of linear operators:

$\mathbf{P_1}$: the values of $q_h(\mathbf{v}_i)$ for all vertex $\mathbf{v}_i$ of the polygon K;

$\mathbf{P_2}$: for $\ell \geq 2$, the moments: $h_e^{-1}(q_h, r)_{0,e} \quad \forall r \in \mathbb{M}_{\ell-2}(e), \quad \forall$ edge e;

$\mathbf{P_3}$: for $\ell \geq 2$, the moments: $h_K^{-2}(q_h, r)_{0,K} \quad \forall r \in \mathbb{M}_{\ell-2}(E) \quad \forall$ polygon E.

We have that the sets of linear operator $\mathbf{P_1} - \mathbf{P_3}$ constitutes a set of degrees of freedom for $\mathrm{H}_\ell^h(K)$. Moreover, the operator $\Pi_K^{\nabla,\ell} : \mathrm{H}_\ell^h(K) \to \mathbb{P}_\ell(K) \subseteq \mathrm{H}_\ell^h(K)$ is computable using only the information of the set of degrees of freedom $\mathbf{P_1}-\mathbf{P_3}$ (for further details, see for instance [7, 65]).

The global virtual space to approximate the fluid pressure of system (4.2.6), for each decomposition Ω_h of Ω is given by

$$\mathrm{H}_\ell^h := \left\{ q_h \in \mathcal{H} : q_h|_K \in \mathrm{H}_\ell^h(K) \quad \forall K \in \Omega_h \right\}.$$

In order to approximate the $\mathcal{D}(\cdot,\cdot)$, we set

$$\mathcal{D}_K^h(p_h, q_h) := (\boldsymbol{\Pi}_K^{\ell-1}\nabla p_h, \boldsymbol{\Pi}_K^{\ell-1}\nabla q_h)_{0,K} + \mathcal{S}_E^{\nabla}\big((\mathrm{I} - \Pi_K^{\nabla,\ell})p_h, (\mathrm{I} - \Pi_K^{\nabla,\ell})q_h\big),$$

where $\mathcal{S}_E^{\nabla}(\cdot,\cdot)$ given by the classical Euclidean scalar product associated to the degrees of freedom $\mathbf{P_1} - \mathbf{P_3}$ (see [27, 65]), which satisfies the stability properties. Using the above definition, we introduce the discrete problem for the pressure variable: seek $p_h \in \mathrm{H}_\ell^h$ such that

$$\mathcal{D}^h(p_h, q_h) = \sum_{K\in\Omega_h} \mathcal{D}_K^h(p_h, q_h) = \mathcal{G}^{\psi_h}(q_h) \qquad \forall q_h \in \mathrm{H}_\ell^h, \tag{4.5.5}$$

where the discrete linear functional is given by

$$\begin{aligned} \mathcal{G}^{\psi_h}(q_h) = \sum_{K\in\Omega_h} \mathcal{G}_K^{\psi_h}(q_h) := \sum_{K\in\Omega_h} \big(\mathbf{f} - (\boldsymbol{\Pi}_K^{k-1}\mathbf{curl}\,\psi_h \cdot \boldsymbol{\nabla})\boldsymbol{\Pi}_K^{k-1}\mathbf{curl}\,\psi_h \\ + \nu\mathbf{curl}\,(\Pi_K^{k-2}\Delta\psi_h), \boldsymbol{\Pi}_K^{\ell-1}\nabla q_h\big)_{0,K}. \end{aligned} \tag{4.5.6}$$

We have that the bilinear form $\mathcal{D}^h(\cdot,\cdot)$ is bounded and using the generalized Poincaré inequality we prove that $\mathcal{D}^h(\cdot,\cdot)$ is uniformly elliptic.

4.5.2.3 Theoretical analysis

Now, we develop the corresponding theoretical analysis for the VE scheme presented in Section 4.5.2.2. In particular, we establish that problem (4.5.5) is well-posed and we provide *a priori* error estimate for this scheme.

We start recalling the inverse inequalities for polynomials on polygons (see [35]).

Lemma 4.5.1. *There exist $\widehat{c}_1, \widehat{c}_2 > 0$, independent of h, such that for all $q \in \mathbb{P}_m(K)$, with $m \geq 0$ it holds*

$$|q|_{1,K} \leq \widehat{c}_1 h_K^{-1}\|q\|_{0,K}, \qquad \textit{and} \qquad \|q\|_{\mathrm{L}^4(K)} \leq \widehat{c}_2 h_K^{-1/2}\|q\|_{0,K}. \tag{4.5.7}$$

Thus, from the first inverse inequality in (4.5.7) and approximation property of projector $\boldsymbol{\Pi}_K^{k-1}$, we obtain the following stability property:

$$|\boldsymbol{\Pi}_K^{k-1}\mathbf{curl}\,\phi|_{1,K} \leq \widetilde{C}_{\mathtt{bd}}|\phi|_{2,K} \quad \forall K \in \Omega_h, \quad \forall \phi \in \mathrm{H}^2(K). \tag{4.5.8}$$

Henceforth, we will assume quasi-uniformity for the family of meshes Ω_h.

A3: For each $h>0$ and for each $K\in\Omega_h$, there exists an uniform constant $\widehat{c}>0$, independent of h, such that $h_K\geq \widehat{c}\,h$.

Proposition 4.5.1. *If the assumptions* **A1** $-$ **A3** *are satisfied,* $\psi\in \mathrm{H}^3(\Omega)\cap\mathcal{W}$ *and* $\mathbf{f}\in\mathbf{H}^1(\Omega_h)$, *then the lineal functional* $\mathcal{G}^{\psi_h}:\mathrm{H}^h_\ell\to\mathbb{R}$ *defined in* (4.5.6) *is bounded.*

Proof. Let $q_h\in\mathrm{H}^h_\ell$. Then, by using triangle inequality we get

$$\begin{aligned}|\mathcal{G}^{\psi_h}(q_h)|\leq C\|\mathbf{f}\|_{0,\Omega}\|q_h\|_{1,\Omega}&+\sum_{K\in\Omega_h}|((\mathbf{\Pi}^{k-1}_K\mathbf{curl}\,\psi_h\cdot\boldsymbol{\nabla})\mathbf{\Pi}^{k-1}_K\mathbf{curl}\,\psi_h,\mathbf{\Pi}^{\ell-1}_K\nabla q_h)_{0,K}|\\&+\nu|(\mathbf{curl}\,(\Pi^{k-2}_K\Delta\psi_h),\mathbf{\Pi}^{\ell-1}_K\nabla q_h)_{0,K}|=:C\|\mathbf{f}\|_{0,\Omega}\|q_h\|_{1,\Omega}+\mathcal{G}_2+\mathcal{G}_3.\end{aligned}\tag{4.5.9}$$

For the term $\mathcal{G}_2$, we add and subtract $(\mathbf{curl}\,\psi\cdot\boldsymbol{\nabla})\mathbf{curl}\,\psi\cdot\mathbf{\Pi}^{\ell-1}_K\nabla q_h$, then by employing triangle inequality and the stability of the projections Π^{k-2}_K and $\mathbf{\Pi}^{\ell-1}_K$ (cf. (4.4.1) and (4.4.2)), we obtain

$$\begin{aligned}\mathcal{G}_2\leq\sum_{K\in\Omega_h}&\big|\big((\mathbf{curl}\,\psi\cdot\boldsymbol{\nabla})\mathbf{curl}\,\psi-(\mathbf{\Pi}^{k-1}_K\mathbf{curl}\,\psi_h\cdot\boldsymbol{\nabla})\mathbf{\Pi}^{k-1}_K\mathbf{curl}\,\psi_h,\mathbf{\Pi}^{\ell-1}_K\nabla q_h\big)_{0,K}\big|\\&+\sum_{K\in\Omega_h}\big|((\mathbf{curl}\,\psi\cdot\boldsymbol{\nabla})\mathbf{curl}\,\psi,\mathbf{\Pi}^{\ell-1}_K\nabla q_h)_{0,K}\big|=:\mathcal{G}_{2a}+\mathcal{G}_{2b}.\end{aligned}\tag{4.5.10}$$

From the Cauchy-Schwarz inequality, we have that $\mathcal{G}_{2b}\leq C\|\psi\|_{\mathcal{W}}\|\psi\|_{3,\Omega}\|q_h\|_{1,\Omega}$. For the term $\mathcal{G}_{2a}$, we add and subtract $(\mathbf{\Pi}^{k-1}_K\mathbf{curl}\,\psi_h\cdot\boldsymbol{\nabla})\mathbf{curl}\,\psi\cdot\mathbf{\Pi}^{\ell-1}_K\nabla q_h$ and we apply triangle inequality to obtain

$$\begin{aligned}\mathcal{G}_{2a}\leq&\sum_{K\in\Omega_h}\|\mathbf{curl}\,\psi-\mathbf{\Pi}^{k-1}_K\mathbf{curl}\,\psi_h\|_{0,K}\|\boldsymbol{\nabla}\mathbf{curl}\,\psi\|_{\mathrm{L}^4(K)}\|\mathbf{\Pi}^{\ell-1}_K\nabla q_h\|_{\mathrm{L}^4(K)}\\&+\sum_{K\in\Omega_h}\|\mathbf{\Pi}^{k-1}_K\mathbf{curl}\,\psi_h\|_{\mathrm{L}^4(K)}\|\boldsymbol{\nabla}(\mathbf{curl}\,\psi-\mathbf{\Pi}^{k-1}_K\mathbf{curl}\,\psi_h)\|_{0,K}\|\mathbf{\Pi}^{\ell-1}_K\nabla q_h\|_{\mathrm{L}^4(K)}\\&\leq C\sum_{K\in\Omega_h}\|\mathbf{curl}\,\psi-\mathbf{\Pi}^{k-1}_K\mathbf{curl}\,\psi_h\|_{0,K}\|\mathbf{curl}\,\psi\|_{\mathrm{W}^1_4(K)}h_K^{-1/2}\|\nabla q_h\|_{0,K}\\&\quad+C\sum_{K\in\Omega_h}\|\mathbf{\Pi}^{k-1}_K\mathbf{curl}\,\psi_h\|_{\mathrm{L}^4(K)}|\mathbf{curl}\,\psi-\mathbf{\Pi}^{k-1}_K\mathbf{curl}\,\psi_h|_{1,K}h_K^{-1/2}\|\nabla q_h\|_{0,K}\\&=:T_1+T_2,\end{aligned}\tag{4.5.11}$$

where we have used the second inverse inequality in (4.5.7) and stability of projector $\mathbf{\Pi}^{\ell-1}_K$. Now, we will estimate the terms T_1 and T_2. For term T_1, first we add and subtract $\mathbf{\Pi}^{k-1}_K\mathbf{curl}\,\psi$, then applying approximation and stability properties of the projector $\mathbf{\Pi}^{k-1}_K$, along with Theorem 4.4.3, we obtain

$$\begin{aligned}T_1&\leq C\sum_{K\in\Omega_h}\left(\|(I-\mathbf{\Pi}^{k-1}_K)\mathbf{curl}\,\psi\|_K+\|\mathbf{\Pi}^{k-1}_K\mathbf{curl}\,(\psi-\psi_h)\|_K\right)\|\mathbf{curl}\,\psi\|_{\mathrm{W}^1_4(K)}\,h_K^{-1/2}\,\|\nabla q_h\|_K\\&\leq C\sum_{K\in\Omega_h}\left(\|\psi\|_{2,K}+(\|\psi\|_{3,\Omega}+|\mathbf{f}|_{1,h})\right)\|\mathbf{curl}\,\psi\|_{\mathrm{W}^1_4(K)}\,h_K^{1/2}\,\|\nabla q_h\|_{0,K}\\&\leq C\left(\|\psi\|_{2,\Omega}+(\|\psi\|_{3,\Omega}+|\mathbf{f}|_{1,h})\right)\sum_{K\in\Omega_h}\|\mathbf{curl}\,\psi\|_{\mathrm{W}^1_4(K)}\,\|1\|_{\mathrm{L}^4(E)}\,\|\nabla q_h\|_{0,K}\\&\leq C\left(\|\psi\|_{3,\Omega}+|\mathbf{f}|_{1,h}\right)\|1\|_{\mathrm{L}^4(\Omega)}\|\psi\|_{3,\Omega}\|q_h\|_{1,\Omega},\end{aligned}\tag{4.5.12}$$

where we have also used assumption **A3**, the relation $h_K^{1/2} \leq C\|1\|_{\mathrm{L}^4(E)}$, the Hölder inequality (for sequences) and Sobolev embedding $\mathrm{H}^2(\Omega) \hookrightarrow \mathrm{W}_4^1(\Omega)$.

For the term T_2, we use the same arguments as in (4.5.12), stability property (4.4.2) and Theorem 4.4.3, to get

$$T_2 \leq C\left(\|\psi\|_{3,\Omega} + |\mathbf{f}|_{1,h}\right)\|1\|_{\mathrm{L}^4(\Omega)}\|\psi_h\|_{\mathcal{W}}\|q_h\|_{1,\Omega}. \tag{4.5.13}$$

Next, inserting the estimates (4.5.12), (4.5.13) in (4.5.11), we obtain

$$\mathcal{G}_2 \leq \mathcal{G}_{2a} + \mathcal{G}_{2b} \leq C\left(\|\psi\|_{3,\Omega} + |\mathbf{f}|_{1,h}\right)\|q_h\|_{1,\Omega}. \tag{4.5.14}$$

To estimate the term $\mathcal{G}_3$ (cf. (4.5.9)), we observe that $\mathbf{curl}\,(\Pi_K^{k-2}\Delta\psi_h) \in \mathbf{P}_{k-3}(K)$, then using the first inverse inequality in (4.5.7) and repeating the arguments used in [133, Proposition 4.20], we get

$$\mathcal{G}_3 \leq C\left(\|\psi\|_{3,\Omega} + |\mathbf{f}|_{1,h}\right)\|q_h\|_{1,\Omega}, \tag{4.5.15}$$

where the constant $C > 0$ depends on the constant $\widehat{c}$ in assumption **A3**. Finally, from (4.5.9), (4.5.14) and (4.5.15) we obtain the desired result. $\square$

As a consequence of Proposition 4.5.1 and the Lax-Milgram Theorem, we have that problem (4.5.5) is well-posed. More precisely, we have the following result.

Theorem 4.5.3. *Under the same assumptions of Proposition 4.5.1, problem (4.5.5) admits a unique solution $p_h \in \mathrm{H}_\ell^h$ and there exists $C > 0$, independent to h, such that*

$$\|p_h\|_{1,\Omega} \leq C(\|\psi\|_{3,\Omega} + |\mathbf{f}|_{1,h}).$$

In what follows, we will establish the order of convergence of the VE scheme (4.5.5). We begin with the following Strang-type lemma, which proof is obtained from standard arguments in the VEM literature (see for instance [27, 65]).

Proposition 4.5.2. *Suppose that the assumptions of Proposition 4.5.1, are satisfied. Let p and p_h be the unique solutions of problems (4.5.4) and (4.5.5), respectively. Then, there exists $C > 0$, independent of h, such that*

$$\|p - p_h\|_{1,\Omega} \leq C\Big(\inf_{q_h \in \mathrm{H}_\ell^h}\|p - q_h\|_{1,\Omega} + \inf_{w_\ell \in \mathbb{P}_\ell(\Omega_h)}|p - w_\ell|_{1,h} + \|\mathcal{G}^\psi - \mathcal{G}^{\psi_h}\|\Big).$$

Next, in order to conclude the error estimate, we will bound the term $\|\mathcal{G}^\psi - \mathcal{G}^{\psi_h}\|$. With this end, we will require that $\psi \in \mathrm{H}^{k+1}(\Omega)$, with $k \geq 3$.

Proposition 4.5.3. *Let $k \geq 3$ and $\mathbf{f} \in \mathbf{H}^{k-2}(\Omega_h)$. Suppose that Assumptions **A1** – **A3** are satisfied and $\psi \in \mathrm{H}^{k+1}(\Omega)$, then we have the following estimate:*

$$\|\mathcal{G}^\psi - \mathcal{G}^{\psi_h}\| \leq \widehat{C}h^\ell\left(\|\psi\|_{k+1,\Omega} + |\mathbf{f}|_{k-2,h}\right).$$

Proof. Let $q_h \in \mathrm{H}_\ell^h$, then using the definition of the functionals $\mathcal{G}^\psi(\cdot)$ and $\mathcal{G}^{\psi_h}(\cdot)$ together with the triangle inequality and properties of $\boldsymbol{\Pi}_K^{\ell-1}$, we have that

$$\begin{aligned}
|\mathcal{G}^\psi(q_h) - \mathcal{G}^{\psi_h}(q_h)| &\leq \sum_{K \in \Omega_h} \left|(\mathbf{f} - \boldsymbol{\Pi}_K^{\ell-1}\mathbf{f}, \nabla q_h - \boldsymbol{\Pi}_K^{\ell-1}\nabla q_h)_{0,K}\right| \\
&+ \left|(\mathbf{curl}\,\psi \cdot \boldsymbol{\nabla})\mathbf{curl}\,\psi \cdot \nabla q_h - (\boldsymbol{\Pi}_K^{k-1}\mathbf{curl}\,\psi_h \cdot \boldsymbol{\nabla})\boldsymbol{\Pi}_K^{k-1}\mathbf{curl}\,\psi_h, \boldsymbol{\Pi}_K^{\ell-1}\nabla q_h)_{0,K}\right| \\
&+ \nu\left|(\mathbf{curl}\,(\Delta\psi) \cdot \nabla q_h - \mathbf{curl}\,(\Pi_K^{k-2}\Delta\psi), \boldsymbol{\Pi}_K^{\ell-1}\nabla q_h\big)_{0,K}\right| \\
&\leq Ch^\ell|\mathbf{f}|_{\ell,h}\|q_h\|_{1,\Omega} + T_1 + T_2.
\end{aligned} \tag{4.5.16}$$

To estimate T_1, we add and subtract suitable terms and employing the triangle inequality, we have that

$$\begin{aligned} T_1 = \sum_{K\in\Omega_h} & \left|((\mathbf{curl}\,\psi\cdot\boldsymbol{\nabla})\mathbf{curl}\,\psi,(I-\boldsymbol{\Pi}_K^{\ell-1})\nabla q_h)_{0,K}\right| \\ & + \left|(\mathbf{curl}\,\psi\cdot\boldsymbol{\nabla})(\mathbf{curl}\,\psi-\boldsymbol{\Pi}_K^{k-1}\mathbf{curl}\,\psi_h),\boldsymbol{\Pi}_K^{\ell-1}\nabla q_h)_{0,K}\right| \\ & + \left|\big(((\mathbf{curl}\,\psi-\boldsymbol{\Pi}_K^{k-1}\mathbf{curl}\,\psi_h)\cdot\boldsymbol{\nabla})\boldsymbol{\Pi}_K^{k-1}\mathbf{curl}\,\psi,\boldsymbol{\Pi}_K^{\ell-1}\nabla q_h\big)_{0,K}\right| =: T_{1a}+T_{1b}+T_{1c}. \end{aligned} \tag{4.5.17}$$

In that follows, we will establish bounds for the three terms above. We start with T_{1a}. By orthogonality and approximation properties of the projection $\boldsymbol{\Pi}_K^{\ell-1}$ and Cauchy-Schwarz inequality, we obtain

$$\begin{aligned} T_{1a} &\leq \sum_{K\in\Omega_h} \|(I-\boldsymbol{\Pi}_K^{\ell-1})((\mathbf{curl}\,\psi\cdot\boldsymbol{\nabla})\mathbf{curl}\,\psi)\|_{0,K}\|(I-\boldsymbol{\Pi}_K^{\ell-1})\nabla q_h\|_{0,K} \\ &\leq Ch^\ell|(\mathbf{curl}\,\psi\cdot\boldsymbol{\nabla})\mathbf{curl}\,\psi|_{\ell,\Omega}\|q_h\|_{1,\Omega} \leq Ch^\ell\|\psi\|_{k+1,\Omega}\|\psi\|_{k,\Omega}\|q_h\|_{1,\Omega}, \end{aligned} \tag{4.5.18}$$

where we have used Hölder inequality and the Sobolev inclusion $\mathrm{H}^{\ell+1}(\Omega)\hookrightarrow \mathrm{W}_4^\ell(\Omega)$. In order to bound the term T_{1b}, we use approximation property of the operator $\boldsymbol{\Pi}_K^{k-1}$ (cf. (4.4.2)), the second inverse inequality in (4.5.7) and stability property of $\boldsymbol{\Pi}_K^{\ell-1}$, as follows:

$$\begin{aligned} T_{1b} &\leq \sum_{K\in\Omega_h} \|\mathbf{curl}\,\psi\|_{\mathrm{L}^4(K)}|\mathbf{curl}\,\psi-\boldsymbol{\Pi}_K^{k-1}\mathbf{curl}\,\psi_h|_{1,K}\|\boldsymbol{\Pi}_K^{\ell-1}\nabla q_h\|_{\mathrm{L}^4(K)} \\ &\leq C\sum_{K\in\Omega_h} \|\mathbf{curl}\,\psi\|_{\mathrm{L}^4(K)}h^{k-1}(\|\psi\|_{k+1,\Omega}+|\mathbf{f}|_{k-2,h})h_K^{-1/2}\|\boldsymbol{\Pi}_K^{\ell-1}\nabla q_h\|_{0,K}, \end{aligned}$$

where in the last inequality, we have used stability property (4.5.8) and Theorem 4.4.3. Next, from the above inequality, using Hölder inequality, Sobolev inclusion and Assumption **A3**, we get

$$\begin{aligned} T_{1b} &\leq Ch^\ell\left(\|\psi\|_{k+1,\Omega}+|\mathbf{f}|_{k-2,h}\right)\sum_{K\in\Omega_h}\|\mathbf{curl}\,\psi\|_{\mathrm{L}^4(K)}\|1\|_{\mathrm{L}^4(K)}\|\nabla q_h\|_{0,K} \\ &\leq Ch^\ell\left(\|\psi\|_{k+1,\Omega}+|\mathbf{f}|_{k-2,h}\right)\|\psi\|_{3,\Omega}\|1\|_{\mathrm{L}^4(\Omega)}\|q_h\|_{1,\Omega}. \end{aligned} \tag{4.5.19}$$

Then, using similar arguments, we have the following bound fo the term T_{1c}:

$$\begin{aligned} T_{1c} &\leq \sum_{K\in\Omega_h} \|\mathbf{curl}\,\psi-\boldsymbol{\Pi}_K^{k-1}\mathbf{curl}\,\psi_h\|_{0,K}\|\boldsymbol{\nabla}\boldsymbol{\Pi}_K^{k-1}\mathbf{curl}\,\psi\|_{\mathrm{L}^4(K)}\|\boldsymbol{\Pi}_K^{\ell-1}\nabla q_h\|_{\mathrm{L}^4(K)} \\ &\leq Ch^\ell\left(\|\psi\|_{k+1,\Omega}+|\mathbf{f}|_{k-2,h}\right)\|1\|_{\mathrm{L}^4(\Omega)}\|\psi\|_{3,\Omega}\|q_h\|_{1,\Omega}. \end{aligned} \tag{4.5.20}$$

Next, inserting (4.5.18), (4.5.19) and (4.5.20) in (4.5.17), we have

$$T_1 \leq Ch^\ell\left(\|\psi\|_{k+1,\Omega}+|\mathbf{f}|_{k-2,h}\right)\|q_h\|_{1,\Omega}. \tag{4.5.21}$$

Now, repeating the arguments used in [133, Proposition 4.22], we obtain the same bound as in (4.5.21) for the term T_2. Finally, by combining the above fact, the estimates (4.5.16) and (4.5.21) we deduce the desired result. □

The following theorem provides the rate of convergence of our virtual scheme (4.5.5) in terms of $k\geq 3$, where k is the degree accuracy of the VE scheme (4.3.7).

Theorem 4.5.4. *Assume $p \in \mathrm{H}^{k-1}(\Omega) \cap \mathcal{H}$, then there exists $C > 0$, independent of h, such that*

$$\|p - p_h\|_{1,\Omega} \leq Ch^{k-2} \left(\|\psi\|_{k+1,\Omega} + \|p\|_{k-1,\Omega} + |\mathbf{f}|_{k-2,h} \right).$$

Proof. The proof follows by combining Propositions 4.5.2, 4.5.3, approximation properties in the polynomial and virtual element space H_ℓ^h (see [65, 134]). □

4.6 Extension to the boundary conditions on the pressure case

In this section we present a brief extension to the Navier–Stokes system with boundary conditions on the pressure formulated in terms of the stream-function.

Now, we assume that the boundary Γ admits a partition without overlap into two parts, as follows: $\Gamma = \overline{\Gamma}_1 \cup \overline{\Gamma}_2, \quad \Gamma_1 \cap \Gamma_2 = \emptyset$. Moreover, we assume that $|\Gamma_1| > 0$ in Γ and that each connected component of Γ_2 is flat. Next, we consider the Navier–Stokes problem (4.2.6), with the following boundary conditions (for further details, see [45, 48]):

$$\mathbf{u} = \mathbf{0} \quad \text{on } \Gamma_1, \quad \mathbf{u} \cdot \mathbf{t} = 0 \quad \text{and} \quad p + \frac{1}{2}|\mathbf{u}|^2 = p_0 \quad \text{on } \Gamma_2. \tag{4.6.1}$$

Let us consider the space

$$\mathbb{X} = \left\{ \mathbf{v} \in \mathbf{H}^1(\Omega) : \mathbf{v} \cdot \mathbf{n} = 0 \quad \text{on} \quad \Gamma_1 \quad \text{and} \quad \mathbf{v} \cdot \mathbf{t} = 0 \quad \text{on} \quad \Gamma \right\}.$$

We have that a variational formulation in terms of the primitive variables of problem (4.2.6) with boundary conditions (4.6.1), read as: given $\mathbf{f} \in \mathbf{L}^2(\Omega)$ and $p_0 \in \mathrm{H}_{00}^{\frac{1}{2}}(\Gamma_2)$, find $(\mathbf{u}, p) \in \mathbb{X} \times \mathrm{L}^2(\Omega)$ such that

$$\begin{aligned} \nu(\operatorname{rot} \mathbf{u}, \operatorname{rot} \mathbf{v})_{0,\Omega} + (\operatorname{rot} \mathbf{u} \times \mathbf{u}, \mathbf{v})_{0,\Omega} - (p + |\mathbf{u}|^2/2, \operatorname{div} \mathbf{v})_{0,\Omega} &= (\mathbf{f}, \mathbf{v})_{0,\Omega} - (p_0, (\mathbf{v} \cdot \mathbf{n}))_{0,\Gamma_2} \\ -(q, \operatorname{div} \mathbf{u})_{0,\Omega} &= 0, \end{aligned} \tag{4.6.2}$$

for all $(\mathbf{v}, q) \in \mathbb{X} \times \mathrm{L}^2(\Omega)$. The goal now is to obtain a formulation in terms of the stream-function, let us define the space $\mathbf{V} = \{\mathbf{v} \in \mathbb{X} : \operatorname{div} \mathbf{v} = 0 \quad \text{in} \quad \Omega\}$, and we note that given $\mathbf{v} \in \mathbf{V}$, there exists (the stream-function) $\phi \in \mathrm{H}^2(\Omega)/\mathbb{R}$, such that $\mathbf{v} = \mathbf{curl}\, \phi \in \mathbf{H}^1_{\Gamma_1}(\Omega)$. Motivated by the above facts, we consider the Hilbert space for the stream-function: $\widehat{\mathcal{W}} := \{\phi \in \mathcal{W} : \phi = 0 \quad \text{on} \quad \Gamma_1 \quad \text{and} \quad \partial_{\mathbf{n}}\phi = 0 \quad \text{on} \quad \Gamma\}$. Thus, by introducing the stream-function of the velocity field (i.e., $\mathbf{u} = \mathbf{curl}\, \psi$) and using some identities, we have

$$\operatorname{rot}(\mathbf{curl}\, \phi) = -\Delta\phi \quad \text{and} \quad (\operatorname{rot} \mathbf{u} \times \mathbf{u}) \cdot \mathbf{v} = (\Delta\psi\, \mathbf{curl}\, \psi) \cdot \nabla\phi. \tag{4.6.3}$$

Therefore, by combining (4.6.2) and (4.6.3), we obtain the following stream-function form: given $\mathbf{f} \in \mathbf{L}^2(\Omega)$ and $p_0 \in \mathrm{H}_{00}^{\frac{1}{2}}(\Gamma_2)$, seek $\psi \in \widehat{\mathcal{W}}$

$$\nu\widehat{\mathcal{A}}(\psi, \phi) + \mathcal{B}(\psi; \psi, \phi) = \mathcal{F}(\phi) - \mathcal{G}(\phi) \qquad \forall \phi \in \widehat{\mathcal{W}}, \tag{4.6.4}$$

with $\mathcal{B} : \widehat{\mathcal{W}}\times\widehat{\mathcal{W}}\times\widehat{\mathcal{W}} \to \mathbb{R}$ and $\mathcal{F} : \widehat{\mathcal{W}} \to \mathbb{R}$ are defined as before and the forms $\widehat{\mathcal{A}} : \widehat{\mathcal{W}}\times\widehat{\mathcal{W}} \to \mathbb{R}$, and $\mathcal{G} : \widehat{\mathcal{W}} \to \mathbb{R}$, are given by:

$$\widehat{\mathcal{A}}(\varphi,\phi) := (\Delta\varphi, \Delta\phi)_{0,\Omega}, \quad \text{and} \quad \mathcal{G}(\phi) := (p_0, \mathbf{curl}\,\phi\cdot\mathbf{n})_{0,\Gamma_2} \quad \forall\varphi,\phi\in\widehat{\mathcal{W}}.$$

From the generalized Poincaré inequality we have that $\|\varphi\|_{\widehat{\mathcal{W}}} := \widehat{\mathcal{A}}(\varphi,\varphi)^{1/2}$ is a norm in $\widehat{\mathcal{W}}$. Thus, we will endow the space $\widehat{\mathcal{W}}$ with this norm.

To discretize the new forms defined above, we set

$$\widehat{\mathcal{A}}^h(\varphi_h,\phi_h) := \sum_{K\in\Omega_h} (\Delta\Pi_K^{k,\mathrm{D}}\varphi_h, \Delta\Pi_K^{k,\mathrm{D}}\phi_h)_{0,K} + \mathcal{S}_K\big((\mathrm{I}-\Pi_K^{k,\mathrm{D}})\varphi_h, (\mathrm{I}-\Pi_K^{k,\mathrm{D}}\phi_h\big),$$
$$\mathcal{G}^h(\phi_h) := \sum_{e\in\Gamma_2} (p_0, \mathbf{curl}\,\phi_h\cdot\mathbf{n})_{0,\Gamma_2},$$

for all $\varphi_h,\phi_h \in \widehat{\mathrm{W}_k^h} := \left\{\phi_h\in\widehat{\mathcal{W}} :\ \phi_h|_K \in \mathrm{W}_k^h(K) \quad \forall K\in\Omega_h\right\}, \quad k\geq 2.$

We recall that the analysis developed in Sections 4.4.1 and 4.4.2.1 can be extended in order to obtain the well-posedness and optimal error estimate in H^2-norm for the scheme (4.6.4). Moreover, the velocity and vorticity are recovery by using the same algorithm presented in subsection 4.5.1. However, we observe that the extension to the pressure recovery technique (cf. Section(4.5.2)) to this type of boundary conditions does not follow directly due to the boundary and regularity conditions required for the pressure weak solution. We are going to test the scheme (4.6.4) in Test 4.7.6.

Finally, we observe that when $\Gamma_2 = \emptyset$ we recovery the standard Navier–Stokes system (4.2.6), with $\mathbf{g} = \mathbf{0}$.

4.7 Numerical experiments

In this section we present several numerical experiments to show the performance of our VEMs proposed in Sections 4.3 and 4.5. Moreover, we test the VEM (4.6.4).

4.7.1 Some aspects of the numerical implementation

In each example to solve the nonlinear system resulting from (4.3.7), we employ the Newton method, with a tolerance of $\mathrm{Tol} = 10^{-8}$. For the first and second tests we take as initial guess the solution of the associated linear Stokes problem, while for the other examples, we will specific later the initial guess taken. We test the C^1-VEM, with $k = 2,3$ and using different families of polygonal meshes (see Figure 4.1): i) Ω_h^1: quadrilateral meshes; ii) Ω_h^2: centroidal Voronoi meshes; iii) Ω_h^3: uniform triangular meshes; iv) Ω_h^4: concave rhombic meshes.

In order to verify the convergence of the proposed schemes, we introduce the following computable errors for $i = 0,1,2$ and $j = 0,1$:

$$\mathtt{E}_i(\psi) = \mathtt{Error}(\psi,\mathrm{H}^i) := |\psi - \Pi^{\mathrm{D},k}\psi_h|_{i,h}, \quad \mathtt{E}_1(\mathbf{u}) = \mathtt{Error}(\mathbf{u},\mathrm{H}^j) := |\mathbf{u}-\widehat{\mathbf{u}}_h|_{j,h},$$
$$\mathtt{E}_1(p) = \mathtt{Error}(p,\mathrm{H}^1) := |p - \Pi^{\nabla,\ell}p_h|_{1,h}, \quad \mathtt{E}_0(\omega) = \mathtt{Error}(\omega,\mathrm{L}^2) := \|\omega-\widehat{\omega}_h\|_{0,\Omega}.$$

The experimental rates of convergence for each variable are defined as follows:

$$\mathtt{r}_i(\cdot) := [\log(\mathtt{E}_i(\cdot)/\widehat{\mathtt{E}}_i(\cdot))][\log(h/\widehat{h})]^{-1}, \quad i = 0,1,2,$$

where $\mathtt{E}_i$ and $\widehat{\mathtt{E}}_i$ denote the error associated to two consecutive mesh sizes h, $\widehat{h}$.

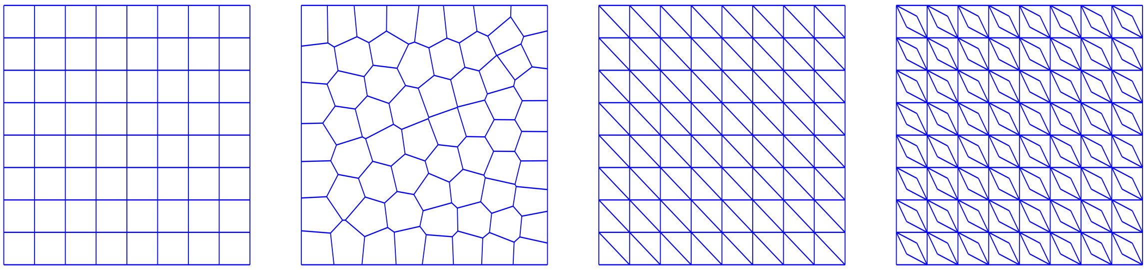

Figure 4.1: Sample meshes. Ω_h^1, Ω_h^2, Ω_h^3 and Ω_h^4.

4.7.2 Test 1. The exact solution of Kovasznay flow

This first numerical test illustrates the performance of the VE schemes (4.3.7) and (4.5.5) as a function of the viscosity ν. More precisely, we consider the domain $\Omega := (-0.5, 1.5) \times (0, 2)$ and the analytic solution to the Navier–Stokes system obtained by Kovasznay:

$$\psi(x,y) = y - \frac{1}{2\pi}\exp(\lambda x)\sin(2\pi y), \quad \mathbf{u}(x,y) = \mathbf{curl}\,\psi,$$
$$p(x,y) = -\frac{1}{2}\exp(2\lambda x) + \overline{p} \quad \text{and} \quad \omega = -\Delta\psi,$$

where $\lambda = \frac{\mathrm{Re}}{2} - \left(\frac{\mathrm{Re}^2}{4} + 4\pi^2\right)^{1/2}$, $\mathrm{Re} := \nu^{-1}$ is the Reynolds number and $\overline{p} \in \mathbb{R}$ is such that $(p,1)_{1,\Omega} = 0$. The load term $\mathbf{f}$ and non-homogeneous Dirichlet Boundary Conditions (BCs) are chosen so that they correspond to this exact solution. Table 4.1 shows the convergence history of the VEMs (4.3.7) and (4.5.5), with polynomial degrees $k = 3$ and $\ell = 1$, respectively, employing the meshes Ω_h^1 and different values of Re. We notice that the rates of convergence predicted in sections 4.4.2 and 4.5 are attained by the principal unknown stream-function and by all the postprocessed variables.

Next, in Table 4.2 we have reported the behavior of the Newton method as a function of the Reynolds number, considering different mesh sizes and the polynomial degrees $k = 2$ and $k = 3$. It can be seen that the larger Re more iterations are necessary to achieve the tolerance. Besides, we observe that when the polynomial degree increase, then the Newton method needs less iterations. The spaces with lines in Table 4.2 mean that the iterative method has taken more than 100 iterations. Figure 4.2 shows plots of the exact (top) and approximated (bottom) stream-function, pressure and vorticity, obtained with the VEMs (4.3.7), (4.5.5), and postprocess of Section 4.5.1, using the mesh Ω_h^1, with $h^{-1} = 64$, $k = 3$ and $\mathrm{Re} = 40$.

4.7.3 Test 2. No flow problem for the Navier–Stokes equations

In this numerical experiment we investigate the behaviour of our VE schemes considering the no flow problem adapted to the Navier–Stokes system (4.2.6) from [109, Example 1.1] in the square domain $\Omega := (0,1)^2$. For this example we take $\nu = 1$ and apply homogeneous Dirichlet BCs. The load term is taken to be $\mathbf{f} = (0, \mathrm{Ra}(3y^2 - y + 1))^T$. One finds that, the exact solution of this problem is given by: $\mathbf{u} = \mathbf{0}$ and $p = \mathrm{Ra}\left(y^3 - \frac{1}{2}y^2 + y - \frac{7}{12}\right)$, where $\mathrm{Ra} > 0$ is a parameter. In the simulations we will choose $\mathrm{Ra} = 1, 10^3, 10^6$.

Re	h^{-1}	$\mathtt{E}_0(\psi)$	$\mathtt{r}_0(\psi)$	$\mathtt{E}_1(\psi)$	$\mathtt{r}_1(\psi)$	$\mathtt{E}_2(\psi)$	$\mathtt{r}_2(\psi)$	$\mathtt{r}_1(\mathbf{u})$	$\mathtt{E}_1(\mathbf{u})$	$\mathtt{E}_0(\omega)$	$\mathtt{r}_0(\omega)$	$\mathtt{E}_1(p)$	$\mathtt{r}_1(p)$
1	8	6.4962e-2	—	1.5436e-1	—	2.7533e-1	—	5.6877e-1	—	2.5657e+0	—	6.7839e-1	—
	16	6.7143e-3	3.27	2.0444e-2	2.91	7.9373e-2	1.79	1.0121e-1	2.49	7.5775e-1	1.75	4.1231e-1	0.71
	32	6.0116e-4	3.48	2.1374e-3	3.25	1.9123e-2	2.05	1.9189e-2	2.39	1.6849e-1	2.16	2.1847e-1	0.91
	64	4.4368e-5	3.76	1.8703e-4	3.51	4.1140e-3	2.21	4.2898e-3	2.16	2.7603e-2	2.60	1.0726e-1	1.02
	128	2.9310e-6	3.92	1.7289e-5	3.43	9.2923e-4	2.14	1.0391e-3	2.04	3.9418e-3	2.80	5.2786e-2	1.02
40	8	9.7355e-4	—	1.3798e-2	—	9.9287e-2	—	1.2577e-1	—	9.9847e-2	—	1.4151e-1	—
	16	5.9194e-5	4.03	1.5460e-3	3.15	2.4605e-2	2.01	2.6913e-2	2.22	2.4661e-2	2.01	6.9705e-2	1.02
	32	3.7521e-6	3.97	1.8487e-4	3.06	6.1065e-3	2.01	6.2744e-3	2.10	6.1113e-3	2.01	3.4826e-2	1.00
	64	2.3312e-7	4.00	2.2728e-5	3.02	1.5215e-3	2.00	1.5368e-3	2.02	1.5219e-3	2.00	1.7398e-2	1.00
	128	1.4420e-8	4.01	2.8270e-6	3.00	3.7998e-4	2.00	3.8216e-4	2.00	3.8001e-4	2.00	8.6956e-3	1.00
10^2	8	9.1889e-4	—	1.2249e-2	—	9.1498e-2	—	1.1041e-1	—	9.1519e-2	—	7.3490e-2	—
	16	5.8013e-5	3.98	1.4705e-3	3.05	2.3104e-2	1.98	2.4958e-2	2.14	2.3105e-2	1.98	2.9005e-2	1.34
	32	3.6731e-6	3.98	1.8163e-4	3.01	5.7964e-3	1.99	5.9274e-3	2.07	5.7964e-3	1.99	1.4276e-2	1.02
	64	2.2908e-7	4.00	2.2614e-5	3.00	1.4503e-3	1.99	1.4593e-3	2.02	1.4503e-3	1.99	7.1074e-3	1.00
	128	1.4253e-8	4.00	2.8237e-6	3.00	3.6267e-4	1.99	3.6336e-4	2.00	3.6267e-4	1.99	3.5491e-3	1.00
10^3	8	8.6904e-4	—	1.2087e-2	—	8.9298e-2	—	9.1738e-2	—	8.9296e-2	—	2.2102e-1	—
	16	5.6880e-5	3.93	1.5601e-3	2.95	2.2869e-2	1.96	2.3986e-2	1.93	2.2869e-2	1.96	2.5378e-2	3.12
	32	3.7243e-6	3.93	1.9595e-4	2.99	5.7405e-3	1.99	5.8758e-3	2.02	5.7405e-3	1.99	3.1651e-3	3.00
	64	2.3621e-7	3.97	2.4484e-5	3.00	1.4364e-3	1.99	1.4456e-3	2.02	1.4364e-3	1.99	8.1697e-4	1.95
	128	1.4789e-8	3.99	3.0599e-6	3.00	3.5920e-4	1.99	3.5978e-4	2.00	3.5920e-4	1.99	3.6823e-4	1.14

Table 4.1: Test 1. Errors and experimental rates of convergence for the stream-function, velocity, vorticity and pressure, using the meshes Ω_h^1, $\mathrm{Re} = 1, 40, 10^2, 10^3$ and $k = 3$.

k	mesh	h^{-1}	dofs	Re = 1	Re = 10	Re = 40	Re = 10^2	Re = 10^3
2	Ω_h^2	8	294	3	4	5	—	—
		16	1371	3	4	5	5	—
		32	5796	3	4	5	5	—
		64	23874	3	4	5	5	6
		128	96855	3	4	5	5	6
3	Ω_h^1	8	259	3	4	5	5	7
		16	1155	3	4	5	5	6
		32	4867	3	4	5	5	6
		64	19971	3	4	5	5	6
		128	80899	3	4	5	5	6

Table 4.2: Test 1. Mesh sizes, degrees of freedom and number of iterations of the Newton method with respect to parameter Re.

We have approximated the stream-function employing the VEM (4.3.7), with $k = 3$ and using the polygonal meshes Ω_h^3 and Ω_h^4. Then, we have computed the fluid velocity employing the postprocess (4.5.2) described in Section 4.5.1. Furthermore, using the discrete stream-function we have approximated the fluid pressure through the virtual scheme developed in Section 4.5.2.2, with polynomial degree $\ell := k - 2 = 1$ and the same meshes Ω_h^3 and Ω_h^4. The

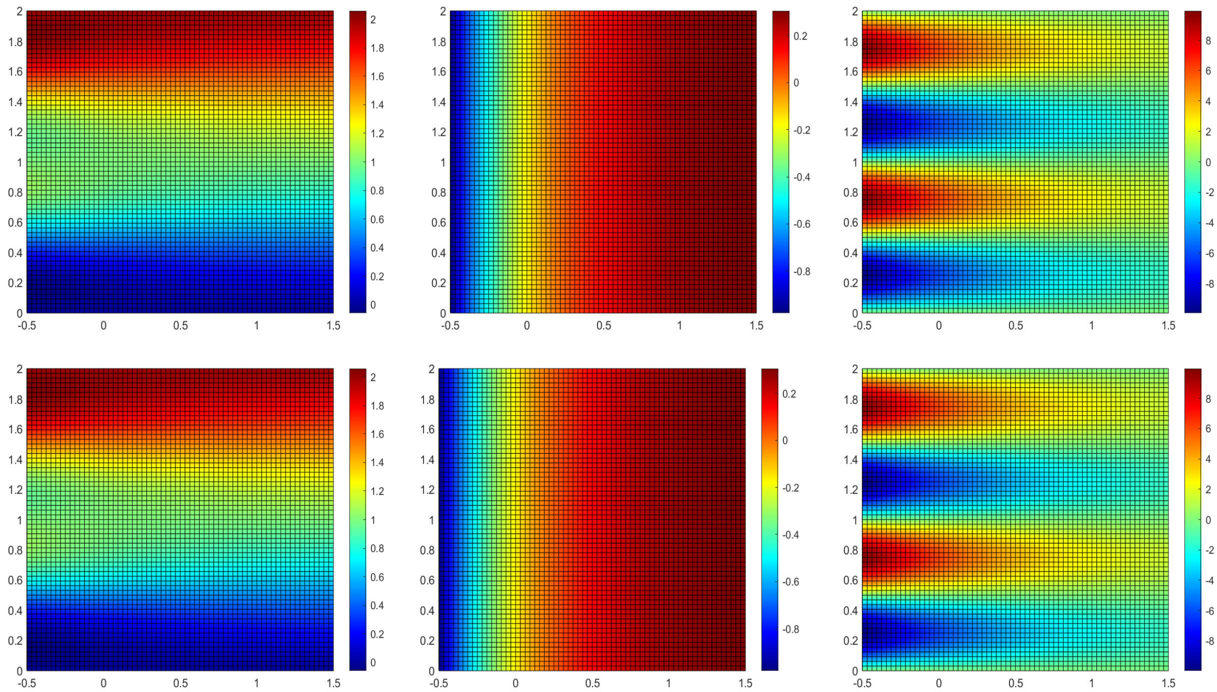

Figure 4.2: Test 1. Exact (top panels) and approximate (bottom panels) solutions stream-function, pressure and vorticity using the VEMs (4.3.7), (4.5.5) and postprocess (4.5.2), employing the mesh Ω_h^1, with $h^{-1} = 64$, $k = 3$ and $\mathrm{Re} = 40$.

maximum number of iterations that are required for the Newton method in this example is 3 for all the meshes.

In Figure 4.3(a) we plot the velocity errors in L^2-norm and it can be seen that is zero up to machine precision, regardless of mesh size. However, we notice that the velocity errors slightly increases as Ra increases, which is also observed in Galerkin schemes for fluid problems that are pressure robust; see for instance, [114, Example 1].

In Figure 4.3(b) we plot the pressure errors in H^1-norm and we observe that the errors converge optimally with the order predicted by our theory in Theorem 4.5.4. Moreover, we notice that the pressure errors increase as Ra increases, which is expected for this example (see [109, Example 1.1]).

We point out that our virtual scheme yields an hydrostatic velocity solution unlike the standard mixed FEMs, where the discrete velocity is far from being equal to zero, even for $\mathrm{Ra} = 1$ (see for instance [109, Figure 1.1]). We recall that our scheme is not pressure robust. However, this good performance can be attributed to the fact for the stream-function formulation the divergence-free constraint is satisfied automatically for the velocity field.

4.7.4 Test 3. The lid-driven cavity problem

In our third test, we consider the 2D lid-driven cavity problem for the Navier–Stokes equations, describing the behaviour of a viscous incompressible flow in a rectangular container whose upper lid is moving at a uniform velocity and fixed BCs on all other static walls. In particular,

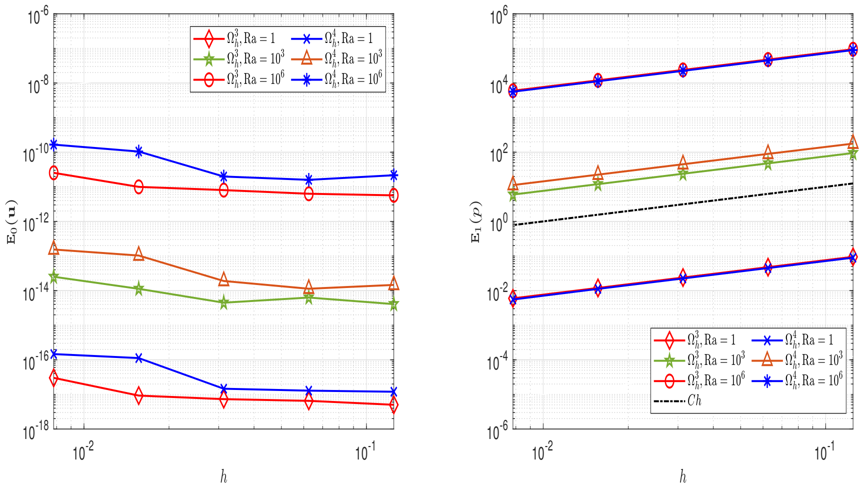

(a) Velocity errors (b) Pressure errors

Figure 4.3: Test 2. Velocity (a) and pressure (b) errors using the VEMs (4.3.7) and (4.5.5), with the meshes Ω_h^3 and Ω_h^4, $k = 3$, $\ell = 1$, $\nu = 1$ and taking different values for the parameter Ra.

we consider the unitary square domain $\Omega = (0,1)^2$, the uniform velocity is given by $\mathbf{u} := (1,0)^T$ and $\mathbf{u} = (0,0)^T$ is the BCs on the static walls. Thus, in terms of the stream-function the BCs are given by: $\psi_h = \partial_x \psi_h = 0$ and $\partial_y \psi_h = 1$ on the upper lid and $\psi_h = \partial_x \psi_h = \partial_y \psi_h = 0$ on the static walls. We have tested our VEMs (4.3.7) and (4.5.5), with $k = 3$ and $\ell = 1$, respectively, using Re $= 100, 400, 1000$, and setting the source term $\mathbf{f} = \mathbf{0}$. Moreover, we have compared our results with those obtained in [102] and [51]. For the Newton iteration, we follow the same procedure as in [143].

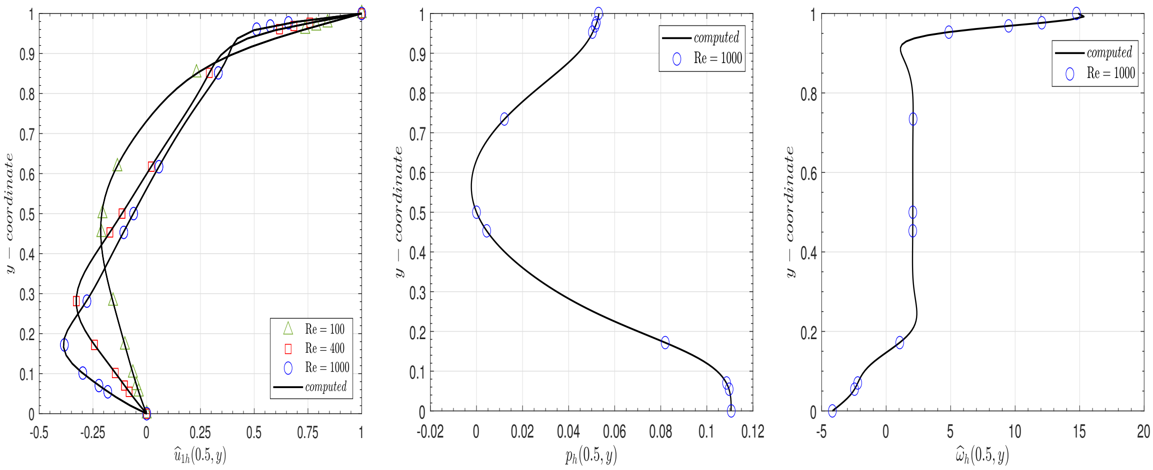

Figure 4.4: Test 3. Profiles of the velocity, pressure and vorticity (from left to right): $\widehat{u}_{1h}$-velocity component, using the mesh Ω_h^1, with $h^{-1} = 48$ and taking different values for Reynolds number Re; pressure and vorticity profiles along horizontal, with the mesh Ω_h^1, with $h^{-1} = 128$ and Re $= 1000$.

In Figure 4.4 we plot the $\widehat{u}_{1h}$-velocity component profile along the horizontal centre line in the 2D lid-driven cavity problem for $\mathrm{Re} = 100, 400$ and 1000, computed with uniform mesh Ω_h^1 of 48×48 elements. Here, the solid lines represent the solution obtained by our VEM (4.3.7) and the postprocess (4.5.2), while the symbols correspond to the values reported in reference [102]. Moreover in the same figure, we plot the pressure and vorticity profiles along horizontal center lines, for $\mathrm{Re} = 1000$, using an uniform mesh Ω_h^1, with $h^{-1} = 128$. Again, the solid lines represent the solution obtained by our VE scheme (4.5.5) and the postprocess (4.5.2), while the symbols correspond to the values reported by [51]. The agreement between these solutions is very good. In each case, no more than 8 iterations were sufficient to achieve tolerance Tol.

4.7.5 Test 4. Solution with less regularity

In this example, we are interesting to examine the accuracy of the scheme (4.3.7) with a exact solution having less regularity on a nonconvex L-shaped domain. We consider $\Omega = (-1,1)^2 \setminus ([0,1) \times (-1,0])$. The exact solution is given in polar coordinates by $\psi(r,\theta) = r^{4/3}\sin(\frac{4\theta}{3})$. The analytical solution contains a singularity at the re-entrant corner of Ω, we have $\psi \in \mathrm{H}^{7/3-\varepsilon}(\Omega)$ for all $\varepsilon > 0$. For this numerical experiment, we have taken $\psi_h^0 = 0$ as the initial guess. Table 4.3 shows the errors and experimental convergence rates in H^2-norm of our VE schemes on a mesh with squares elements (as in Ω_h^1), for $k = 2$ and $k = 3$. According to the regularity of ψ, for both polynomial degrees, we expect an order of convergence in H^2 as $\mathcal{O}(h^{1/3})$, which is predicted by Theorem 4.4.3.

k	h	dofs	$\mathtt{E}_2(\psi)$	$\mathtt{r}_2(\psi)$	iter	k	h	dofs	$\mathtt{E}_2(\psi)$	$\mathtt{r}_2(\psi)$	iter
	1/4	99	7.1728e-1	—	4		1/4	179	6.4424e-1	—	4
	1/8	483	5.7219e-1	0.32	4		1/8	835	5.1089e-1	0.33	4
2	1/16	2115	4.5318e-1	0.33	4	3	1/16	3587	4.0540e-1	0.33	4
	1/32	8835	3.5945e-1	0.33	4		1/32	14851	3.2176e-1	0.33	4
	1/64	36099	2.8526e-1	0.33	4		1/64	60419	2.5538e-1	0.33	4

Table 4.3: Test 4. Errors for the stream-function variable in H^2-norm on the L-shaped using with square elements Ω_h^1 and $k = 2, 3$.

4.7.6 Test 5. The Navier–Stokes system with BCs on the pressure

As last experiment, we test the scheme presented in Section 4.6. We consider the domain $\Omega := (0,1)^2$ and the analytic solution to the Navier–Stokes system given by:

$$\psi(x,y) = -\frac{1}{\pi^2}(1-x)^2\cos(2\pi x)\cos(2\pi y), \qquad \mathbf{u}(x,y) = \mathbf{curl}\,\psi,$$
$$p(x,y) = \sin((\pi/2)x)\cos(2\pi y) + \overline{p} \qquad \text{and} \qquad \omega = -\Delta\psi.$$

Table 4.4 shows the errors and convergence rates in H^2-norm for the stream-function, by using the VEM (4.6.4). Moreover, we show the errors and convergence rates in H^1, L^2-norm for the velocity and vorticity, respectively, employing the postprocess 4.5.1. For this experiment we have used the mesh Ω_h^4 and the polynomial degrees $k = 2$.

k	h	dofs	$\mathtt{E}_2(\psi)$	$\mathtt{r}_2(\psi)$	$\mathtt{E}_1(\mathbf{u})$	$\mathtt{r}_2(\mathbf{u})$	$\mathtt{E}_0(\omega)$	$\mathtt{r}_0(\omega)$	iter
	1/4	129	5.5066e-1	—	1.2499e+0	—	4.0096e-1	—	3
	1/8	545	2.8697e-1	0.94	6.6735e-1	0.90	1.4378e-1	1.47	4
2	1/16	2241	1.4295e-1	1.00	3.3722e-1	0.98	4.9535e-2	1.53	4
	1/32	9089	7.1421e-2	1.00	1.6863e-1	0.99	2.0831e-2	1.24	4
	1/64	36609	3.5710e-2	0.99	8.4213e-2	1.00	9.8326e-3	1.00	4

Table 4.4: Test 5. Errors in norm H^2- H^1- and L^2-norms for stream-function, velocity and vorticity fields, respectively, obtained with the VE scheme (4.6.4), the family mesh Ω_h^4 and $k = 2$.

Chapter 5

A fully-discrete virtual element method for the nonstationary Boussinesq equations in stream-function form

5.1 Introduction

The Boussinesq system is typically used to describe the natural convection in a viscous incompressible fluid, which consists of coupling between the Navier–Stokes equations with a convection-diffusion equation. Such coupling is done by means of a buoyancy term (in the momentum equation of the Navier–Stokes system) and convective heat transfer (in the energy equation). Applications of this fluid-thermal system appears in several engineering processes, such as, industrial ovens, cooling procedures (cooling of steel industries, electronic and electric equipments, nuclear reactors, etc). Moreover, this physical phenomena appears in oceanography and geophysics when studying oceanic flows and climate predictions.

Due its relevance and presence in different applications, several works have been devoted to study these equations (and some variants). For the analysis of existence, uniqueness and regularity of the solution, we refer to [140, 121]. Besides, over the last decades several discretizations have been employed to solve this system; see for instance [47, 50, 150, 161, 144, 9, 82, 85, 11] and the references therein, where the steady and unsteady regimens, temperature-dependent parameters problems have been studied, considering the classical velocity-pressure-temperature and pseudostress-velocity-temperature formulations.

Typically, in the existing literature, the majority of the discretizations for the fluid part involve the standard velocity–pressure formulation for the Boussinesq system. However, some researchers have developed numerical methods by using the stream-function–vorticity and pure stream-function approaches to approximate this system. For instance, in [148] a finite element discretization is considered to solve the problem in stream-function–vorticity–temperature form, numerical solutions are obtained for the natural convection in a square cavity and compared with some results available in the literature. In [152] a fourth-order compact finite difference scheme is formulated for solving the steady regimen, by using also the stream-function–vorticity–temperature formulation. Numerical experiments are also presented. More recently, in [120, 160], the authors present an analysis of stability and convergence for a fourth-order finite difference method for the unsteady regimen of Boussinesq equations with the stream-function–vorticity–temperature approach. Numerical results are provided in [120]. On the other hand, in [43], the authors employed a C^1 finite element method to approximate the stream-function variable. Numerical solution for the 2D natural convection in a square cavity are presented and compared with benchmark results [155].

For two dimensional fluid problems, the formulation in terms of the stream-function presents several attractive features, among these we can mention: the velocity vector and pressure fields are not present in the formulation, instead only one scalar variable (the stream-function) is the main unknown to approximate. By construction the incompressibility constraint is automatically satisfied. Moreover, the resulting trilinear form in the momentum equation is naturally skew-symmetric, which allows more direct stability and convergence arguments. On the other hand, in comparison with the stream-function–vorticity form, our approach avoid the difficulties related with the definition of the boundary values for the vorticity field, present in such formulation.

Nevertheless, the construction of subspaces of H^2 (space where the stream-function belongs) by using finite element method involve high order polynomials and a large number of degrees of freedom, which are considered a difficult task principally from the computational viewpoint, even for triangular decompositions. As an alternative to avoid the aforementioned drawback, we consider the approach presented in [58, 77] to introduce C^1-virtual element schemes of arbitrary order $k \geq 2$, to approximate the stream-function variable of the Boussinesq system.

The Virtual Element Method (VEM) were introduced in the seminal work [27] as an extension of Finite Elements Method (FEM) to polygonal or polyhedral decompositions. In this first work the Poisson equation is used to illustrate the main ideas of VEM approach. The virtual element spaces are constituted by polynomial and nonpolynomial functions, the degrees of freedom must be chosen appropriately so that the stiffness matrix and load term can be computed without computing these nonpolynomial functions. Later on, in [58] is introduced a new family of C^1-virtual element of high order $k \geq 2$, to solve Kirchhoff-Love plate problems, which in the lowest order polynomial degree employed only 3 degrees of freedom per mesh vertex (the function and its gradient values vertex). This fact represents a very significant advantage over C^1 schemes based on FEM. Moreover, in [36, 19], the authors discuss the application of VEM to construct finite dimensional spaces of arbitrarily regular C^α, with $\alpha \geq 1$, where promising results have been observed to solve equations involving high order PDEs. In the last year a wide variety of second- and fourth-order problems have been discretized by using VEM. Due to the large number of papers available in the literature, we here limit ourselves in citing some representative articles within the area of fluid mechanics, where several models have been addressed with the *conforming* VEM approach: the Stokes equations [17, 76, 34, 157], the Brinkman model [60, 133], Navier–Stokes and incompressible flows [35, 41, 97, 31, 42, 83], the Quasi-Geostrophic equations of the ocean [136] and Boussinesq system [99, 21], where different formulations have been considered.

According to the previously discussed, in the present contribution, we are interested in further exploring the ability of VEM to approximate coupled nonlinear fluid flow problems considering the stream-function approach. More precisely, we develop and analyze a fully-discrete VE scheme for solving the nonstationary Boussinesq system. Under assumption that the domain is simply connected and by using the incompressibility condition of the velocity field, we write a equivalent variational formulation in terms of the stream-function and temperature unknowns. The discretization for the spatial variables is based on the *coupling* of C^1- and C^0- conforming virtual element approaches [58, 27], for the stream-function and temperature fields, respectively, and we handle the time derivatives with a classical backward Euler implicit method. Employing the discretizations mentioned above, we propose a fully-discrete scheme of high order, which is fully-coupled, implicit in the nonlinear terms and unconditionally stable. By using the fixed point theory, we establish the corresponding existence of a discrete solution and, under a small time step assumption, we prove that such discrete solution is also unique. Moreover, employing the natural skew-symmetry property of the resulting discrete trilinear form (in the momentum equation) we provide optimal error estimates in H^2- and H^1-norms for the stream-function and temperature, respectively.

The remainder of this chapter has been organized as follows: In Section 5.2 we recall the unsteady Boussinesq equations in its standard velocity–pressure–temperature formulation. Moreover, we write a weak form of the system in terms of the stream-function and temperature variables. We finish this section by recalling the corresponding stability and well-posedness results for the continuous problem. In Section 5.3 we present the VE discretization, introducing the polygonal decomposition and mesh notations, the construction of stream-function and temperature VE spaces along with their corresponding degrees of freedom, the polynomial projections and the construction of the multilinear forms. In Section 5.4 we present the fully-discrete VE formulation and provide its stability and well-posedness. In Section 5.5 we derive error estimates for the stream-function and temperature fields. Finally, three numerical experiments, including the solution of the 2D natural convection benchmark problem, are presented in Section 5.6, to illustrate the good performance of the scheme and confirm our theoretical predictions.

5.2 The continuous problem

5.2.1 The time dependent Boussinesq system

In this work we are interested in approximating the solution of the nonstationary Boussinesq system, modeling incompressible nonisothermal fluid flows. The system consists of a coupling between the Navier–Stokes equations with a convection-diffusion equation for the temperature variable. The coupling is by means of a buoyancy term (in the momentum equation of the Navier–Stokes system) and convective heat transfer (in the energy equation). More precisely, given suitable initial data $(\mathbf{u}_0, \theta_0)$, the aforementioned system of equations are given by (see [140]):

$$\begin{aligned}
\partial_t \mathbf{u} - \nu\Delta\mathbf{u} + (\mathbf{u}\cdot\nabla)\mathbf{u} + \nabla p - \mathbf{g}\theta &= \mathbf{f}_\psi && \text{in} \quad \Omega\times(0,T),\\
\operatorname{div}\mathbf{u} &= 0 && \text{in} \quad \Omega\times(0,T),\\
\mathbf{u} &= \mathbf{0} && \text{on} \quad \Gamma\times(0,T),\\
\mathbf{u}(0) &= \mathbf{u}_0 && \text{in} \quad \Omega \text{ at } t=0,\\
(p,1)_{0,\Omega} &= 0 && \\
\partial_t\theta - \kappa\Delta\theta + \mathbf{u}\cdot\nabla\theta &= f_\theta && \text{in} \quad \Omega\times(0,T),\\
\theta &= 0 && \text{on} \quad \Gamma\times(0,T),\\
\theta(0) &= \theta_0 && \text{in} \quad \Omega \text{ at } t=0,
\end{aligned} \tag{5.2.1}$$

where $\mathbf{u}:\Omega\times(0,T)\to\mathbb{R}^2$, $p:\Omega\times(0,T)\to\mathbb{R}$ and $\theta:\Omega\times(0,T)\to\mathbb{R}$ denote the velocity, pressure and temperature fields. The parameters $\nu>0$ and $\kappa>0$ are the viscosity fluid and the thermal conductivity, respectively. The functions $\mathbf{f}_\psi : \Omega \times (0,T) \to \mathbb{R}^2$, $f_\theta : \Omega \times (0,T) \to \mathbb{R}$ is a set of external forces and $\mathbf{g} : \Omega \times (0,T) \to \mathbb{R}^2$ is a force per unit mass.

In next subsection, by using the incompressibility property of the velocity field, we will write an equivalent weak formulation of the system (5.2.1) in terms of the stream-function and temperature variables.

5.2.2 The time dependent stream-function–temperature formulation

Let us introduce the following space of functions belonging to $\mathbf{H}_0^1(\Omega)$ with vanishing divergence:

$$\mathbf{Z} := \left\{ \mathbf{v} \in \mathbf{H}_0^1(\Omega) : \operatorname{div} \mathbf{v} = 0 \quad \text{in} \quad \Omega \right\}.$$

Since $\Omega \subset \mathbb{R}^2$ is simply connected, a well known result states that a vector function $\mathbf{v} \in \mathbf{Z}$ if and only if there exists a scalar function $\varphi \in \mathrm{H}^2(\Omega)$ (called *stream-function*), such that

$$\mathbf{v} = \mathbf{curl}\, \varphi \in \mathbf{H}_0^1(\Omega).$$

The function φ is defined up to a constant (see [103]). Thus, we consider the following space

$$\mathrm{H}_0^2(\Omega) = \left\{ \varphi \in \mathrm{H}^2(\Omega) : \varphi = \partial_{\mathbf{n}} \varphi = 0 \quad \text{on} \quad \Gamma \right\}.$$

Then, choosing $\psi(t) \in \mathrm{H}_0^2(\Omega)$ the stream-function of the velocity field $\mathbf{u}(t) \in \mathbf{Z}$ (i.e. $\mathbf{u}(t) = \mathbf{curl}\, \psi(t)$) in the momentum equation of system (5.2.1), testing against a function $\mathbf{v} = \mathbf{curl}\, \phi$ with $\phi \in \mathrm{H}_0^2(\Omega)$ and applying twice an integration by parts, we have

$$\int_\Omega \mathbf{curl}\,(\partial_t \psi) \cdot \mathbf{curl}\, \phi + \nu \int_\Omega \mathrm{D}^2 \psi : \mathrm{D}^2 \phi + \int_\Omega \Delta \psi\, \mathbf{curl}\, \psi \cdot \nabla \phi - \int_\Omega \mathbf{g} \theta \cdot \mathbf{curl}\, \phi = \int_\Omega \mathbf{f}_\psi \cdot \mathbf{curl}\, \phi,$$

for all $\phi \in \mathrm{H}_0^2(\Omega)$. On other hand, multiplying by $v \in \mathrm{H}_0^1(\Omega)$ and integrating by parts in the energy equation of system (5.2.1), we obtain

$$\int_\Omega \partial_t \theta v + \kappa \int_\Omega \nabla \theta \cdot \nabla v + \int_\Omega (\mathbf{curl}\, \psi \cdot \nabla \theta) v = \int_\Omega f_\theta v \qquad \forall v \in \mathrm{H}_0^1(\Omega).$$

From the above identities, we obtain the following weak formulation for system (5.2.1): given $\psi_0 \in \mathrm{H}_0^1(\Omega)$, $\theta_0 \in \mathrm{L}^2(\Omega)$, $\mathbf{g} \in \mathrm{L}^\infty(0,T; \mathbf{L}^\infty(\Omega))$, and the external forces $\mathbf{f}_\psi \in \mathrm{L}^2(0,T; \mathbf{L}^2(\Omega))$, $f_\theta \in \mathrm{L}^2(0,T; \mathrm{L}^2(\Omega))$, find $(\psi, \theta) \in \mathrm{L}^2(0,T; \mathrm{H}_0^2(\Omega)) \times \mathrm{L}^2(0,T; \mathrm{H}_0^1(\Omega))$ such that

$$\begin{aligned} M_F(\partial_t \psi, \phi) + \nu A_F(\psi, \phi) + B_F(\psi; \psi, \phi) - C(\theta, \phi) &= F_\psi(\phi) \quad \forall \phi \in \mathrm{H}_0^2(\Omega), \\ M_T(\partial_t \theta, v) + \kappa A_T(\theta, v) + B_T(\psi; \theta, v) &= F_\theta(v) \quad \forall v \in \mathrm{H}_0^1(\Omega), \\ \psi(0) = \psi_0, \qquad \theta(0) &= \theta_0, \end{aligned} \tag{5.2.2}$$

for a.e. $t \in (0,T)$, where the bilinear forms $M_F(\cdot,\cdot)$, $M_T(\cdot,\cdot)$, $A_F(\cdot,\cdot)$ and $A_T(\cdot,\cdot)$ are given by

$$M_F(\cdot,\cdot) : \mathrm{H}_0^2(\Omega) \times \mathrm{H}_0^2(\Omega) \to \mathbb{R}, \qquad M_F(\varphi, \phi) := \int_\Omega \mathbf{curl}\, \varphi \cdot \mathbf{curl}\, \phi, \tag{5.2.3}$$

$$M_T(\cdot,\cdot) : \mathrm{H}_0^1(\Omega) \times \mathrm{H}_0^1(\Omega) \to \mathbb{R}, \qquad M_T(v, w) := \int_\Omega v w, \tag{5.2.4}$$

$$A_F : \mathrm{H}_0^2(\Omega) \times \mathrm{H}_0^2(\Omega) \to \mathbb{R}, \qquad A_F(\varphi, \phi) := \int_\Omega \mathrm{D}^2 \varphi : \mathrm{D}^2 \phi, \tag{5.2.5}$$

$$A_T : \mathrm{H}_0^1(\Omega) \times \mathrm{H}_0^1(\Omega) \to \mathbb{R}, \qquad A_T(v, w) := \int_\Omega \nabla v \cdot \nabla w, \tag{5.2.6}$$

whereas the convective trilinear forms $B_F(\cdot;\cdot,\cdot)$ and $B_T(\cdot;\cdot,\cdot)$ are defined by

$$B_F : \mathrm{H}_0^2(\Omega) \times \mathrm{H}_0^2(\Omega) \times \mathrm{H}_0^2(\Omega) \to \mathbb{R}, \quad B_F(\zeta;\varphi,\phi) := \int_\Omega \Delta\zeta \,\mathbf{curl}\,\varphi \cdot \nabla\phi, \tag{5.2.7}$$

$$B_T : \mathrm{H}_0^2(\Omega) \times \mathrm{H}_0^1(\Omega) \times \mathrm{H}_0^1(\Omega) \to \mathbb{R}, \quad B_T(\varphi;v,w) := \int_\Omega (\mathbf{curl}\,\varphi \cdot \nabla v)w. \tag{5.2.8}$$

The bilinear form $C(\cdot,\cdot)$ associated to the buoyancy term is given by

$$C : \mathrm{H}_0^1(\Omega) \times \mathrm{H}_0^2(\Omega) \to \mathbb{R}, \qquad C(v,\phi) := \int_\Omega \mathbf{g}v \cdot \mathbf{curl}\,\phi \tag{5.2.9}$$

and the functionals $F_\psi(\cdot)$ and $F_\theta(\cdot)$ are given by

$$F_\psi : \mathrm{H}_0^2(\Omega) \to \mathbb{R}, \qquad F_\psi(\phi) := \int_\Omega \mathbf{f}_\psi \cdot \mathbf{curl}\,\phi, \tag{5.2.10}$$

$$F_\theta : \mathrm{H}_0^1(\Omega) \to \mathbb{R}, \qquad F_\theta(v) := \int_\Omega f_\theta v. \tag{5.2.11}$$

We can observe by a direct computation that the trilinear form $B_T(\cdot;\cdot,\cdot)$ defined in (5.2.8) is skew-symmetric, i.e.,

$$B_T(\varphi;v,w) = -B_T(\varphi;w,v) \qquad \forall\varphi \in \mathrm{H}_0^2(\Omega) \quad \text{and} \quad \forall v,w \in \mathrm{H}_0^1(\Omega).$$

Therefore, the bilinear form $B_T(\cdot;\cdot,\cdot)$ is equal to its skew-symmetric part, defined by

$$B_{\mathrm{skew}}(\varphi;v,w) := \frac{1}{2}(B_T(\varphi;v,w) - B_T(\varphi;w,v)) \qquad \forall\varphi \in \mathrm{H}_0^2(\Omega) \quad \text{and} \quad \forall v,w \in \mathrm{H}_0^1(\Omega). \tag{5.2.12}$$

According with the above discussion, we rewrite system (5.2.2) in the following equivalent formulation: given the initial conditions $(\psi_0,\theta_0) \in \mathrm{H}_0^1(\Omega)\times\mathrm{L}^2(\Omega)$ and the forces $\mathbf{f}_\psi \in \mathrm{L}^2(0,T;\mathbf{L}^2(\Omega))$, $f_\theta \in \mathrm{L}^2(0,T;\mathrm{L}^2(\Omega))$ and $\mathbf{g} \in \mathrm{L}^\infty(0,T;\mathbf{L}^\infty(\Omega))$, find $(\psi,\theta) \in \mathrm{L}^2(0,T;\mathrm{H}_0^2(\Omega)) \times \mathrm{L}^2(0,T;\mathrm{H}_0^1(\Omega))$ such that, for a.e. $t \in (0,T)$

$$\begin{aligned}
M_F(\partial_t\psi,\phi) + \nu A_F(\psi,\phi) + B_F(\psi;\psi,\phi) - C(\theta,\phi) &= F_\psi(\phi) \quad \forall\phi \in \mathrm{H}_0^2(\Omega),\\
M_T(\partial_t\theta,v) + \kappa A_T(\theta,v) + B_{\mathrm{skew}}(\psi;\theta,v) &= F_\theta(v) \quad \forall v \in \mathrm{H}_0^1(\Omega),\\
\psi(0) = \psi_0, \qquad \theta(0) &= \theta_0,
\end{aligned} \tag{5.2.13}$$

5.2.3 Well-posedness of the weak formulation

In this subsection we recall some basic properties of the continuous forms and the existence and uniqueness properties of the solution to problem (5.2.13).

Lemma 5.2.1. *For all $\zeta,\varphi,\phi \in \mathrm{H}_0^2(\Omega)$ and for each $v,w \in \mathrm{H}_0^1(\Omega)$, the forms defined in (5.2.3)-*

(5.2.12) *satisfy the following properties:*

$$
\begin{aligned}
|M_F(\varphi,\phi)| &\leq C_{M_F}\|\varphi\|_{1,\Omega}\|\phi\|_{1,\Omega} \quad &&\textit{and} \quad M_F(\phi,\phi) \geq \|\phi\|^2_{1,\Omega},\\
|M_T(v,w)| &\leq C_{M_T}\|v\|_{0,\Omega}\|w\|_{0,\Omega} \quad &&\textit{and} \quad M_T(v,v) \geq \|v\|^2_{0,\Omega},\\
|A_F(\varphi,\phi)| &\leq C_{A_F}\|\varphi\|_{2,\Omega}\|\phi\|_{2,\Omega} \quad &&\textit{and} \quad A_F(\phi,\phi) \geq \alpha_{A_F}\|\phi\|^2_{2,\Omega},\\
|A_T(v,w)| &\leq C_{A_T}\|v\|_{1,\Omega}\|w\|_{1,\Omega} \quad &&\textit{and} \quad A_T(v,v) \geq \alpha_{A_T}\|v\|^2_{1,\Omega},\\
|B_F(\zeta;\varphi,\phi)| &\leq C_{B_F}\ \|\zeta\|_{2,\Omega}\|\varphi\|_{2,\Omega}\|\phi\|_{2,\Omega} \quad &&\textit{and} \quad B_F(\zeta;\phi,\phi) = 0,\\
|B_{\text{skew}}(\zeta;v,w)| &\leq C_{B_T}\ \|\zeta\|_{2,\Omega}\|v\|_{1,\Omega}\|w\|_{1,\Omega} \quad &&\textit{and} \quad B_{\text{skew}}(\zeta;v,v) = 0,\\
|C(v,\phi)| &\leq \|\mathbf{g}\|_{\infty,\Omega}\|v\|_{0,\Omega}\|\phi\|_{1,\Omega},\\
|F_\psi(\phi)| &\leq C_{F_\psi}\|\mathbf{f}_\psi\|_{0,\Omega}\|\phi\|_{1,\Omega}, \quad |F_\theta(v)| \leq C_{F_\theta}\|f_\theta\|_{0,\Omega}\|v\|_{0,\Omega}.
\end{aligned}
$$

The equivalence between the (weak form of) problem (5.2.1) and its stream-function formulation (5.2.13) is well known and easy to check. The couple (ψ,θ) satisfies (5.2.13) if and only if there exists a unique p such that the triple $(\mathbf{u},\theta,p)$ in $\mathrm{L}^2(0,T;\mathbf{H}^1_0(\Omega)) \times \mathrm{L}^2(0,T;\mathrm{H}^1_0(\Omega)) \times \mathrm{L}^2(0,T;\mathrm{L}^2_0(\Omega))$ solves (the variational formulation of) (5.2.1), where $\mathbf{u} = \mathbf{curl}\,\psi$. Therefore the existence result for problem (5.2.13) follow immediately from known results for (5.2.1) (see for instance [150]) and the uniqueness follow by combining the arguments used in [140].

Theorem 5.2.1. *Problem (5.2.13) admits a unique solution (ψ,θ), satisfying $\psi \in \mathrm{L}^2(0,T;\mathrm{H}^2_0(\Omega)) \cap \mathrm{L}^\infty(0,T;\mathrm{H}^1_0(\Omega))$ and $\theta \in \mathrm{L}^2(0,T;\mathrm{H}^1_0(\Omega)) \cap \mathrm{L}^\infty(0,T;\mathrm{L}^2(\Omega))$. Furthermore there exists a positive constant C, such that*

$$
\begin{aligned}
&\|\psi\|_{\mathrm{L}^\infty(0,T;\mathrm{H}^1_0(\Omega))} + \|\psi\|_{\mathrm{L}^2(0,T;\mathrm{H}^2_0(\Omega))} + \|\theta\|_{\mathrm{L}^\infty(0,T;\mathrm{L}^2(\Omega))} + \|\theta\|_{\mathrm{L}^2(0,T;\mathrm{H}^1_0(\Omega))}\\
&\qquad \leq C\left(\|\mathbf{f}_\psi\|_{\mathrm{L}^2(0,T;\mathbf{L}^2(\Omega))} + \|f_\theta\|_{\mathrm{L}^2(0,T;\mathrm{L}^2(\Omega))} + \|\theta_0\|_{0,\Omega} + |\psi_0|_{1,\Omega}\right).
\end{aligned}
$$

Now, we recall the Ladyzhenskaya inequality (see for instance [11, Lemma 2.2]), needed in the sequel:

$$
\|\mathbf{v}\|_{\mathrm{L}^4(\Omega)} \leq 2^{\frac{1}{4}}\|\mathbf{v}\|^{\frac{1}{2}}_{1,\Omega}\|\mathbf{v}\|^{\frac{1}{2}}_{0,\Omega} \qquad \forall \mathbf{v} \in \mathbf{H}^1_0(\Omega). \tag{5.2.14}
$$

We close this section with the following remark.

Remark 5.2.1. *For the bilinear form $A_F(\cdot,\cdot)$ defined in (5.2.5), we have the following classical identity:*

$$
A_F(\varphi,\phi) = \int_\Omega \Delta\varphi\Delta\phi \qquad \forall \varphi,\phi \in \mathrm{H}^2_0(\Omega). \tag{5.2.15}
$$

We recall that at discrete level the representations (5.2.5) and (5.2.15) will lead to different approximations, in general. In next section we will consider the representation (5.2.5), i.e., $A_F(\varphi,\phi) = \int_\Omega \mathrm{D}^2\varphi : \mathrm{D}^2\phi$, in order to construct the projection $\Pi^{k,\mathrm{D}}_K$ (see (5.3.2)). However, we also propose an alternative discretization inspired by (5.2.15) in Remark 5.3.2 below.

5.3 Virtual elements discretization

In this section we will introduce C^1- and C^0-conforming schemes of arbitrary order $k \geq 2$ and $\ell \geq 1$, for the numerical approximation of the stream-function and temperature unknowns of problem (5.2.13), respectively. First, we start by introducing some mesh notations together with the respective local and global virtual spaces and their degrees of freedom. Moreover, we introduce the classical VEM polynomial projections and we present the discrete multilinear forms.

5.3.1 Polygonal decompositions and notations

Henceforth, we will denote by K a general polygon, e a general edge of ∂K, h_K the diameter of the element K and by h_e the length of edge e. Let $\{\mathcal{T}_h\}_{h>0}$ be a sequence of decompositions of Ω into non-overlapping polygons K, where $h := \max_{K\in\mathcal{T}_h} h_K$. Moreover, N_K denotes the number of vertices of K and we define the unit normal vector $\mathbf{n}_K$, that points outside of K and the unit tangent vector $\mathbf{t}_K$ to K obtained by a counterclockwise rotation of $\mathbf{n}_K$.

For each integer $n \geq 0$, we define the discontinuous piecewise n-order polynomial by

$$\mathbb{P}_n(\mathcal{T}_h) := \left\{q \in \mathrm{L}^2(\Omega) : q|_K \in \mathbb{P}_n(K) \quad \forall K \in \mathcal{T}_h\right\}.$$

Besides, for $s > 0$, we consider the broken spaces

$$\mathrm{H}^s(\mathcal{T}_h) := \left\{\phi \in \mathrm{L}^2(\Omega) : \phi|_K \in \mathrm{H}^s(K) \quad \forall K \in \mathcal{T}_h\right\}$$

endowed with the following broken seminorm: $|\phi|_{s,h} := \left(\sum_{K\in\mathcal{T}_h} |\phi|^2_{s,K}\right)^{1/2}$.

For the theoretical convergence analysis, we suppose that for all h, each element K in the mesh family $\{\mathcal{T}_h\}_{h>0}$ satisfies the following assumptions [27, 77] for a uniform constant $\rho > 0$:

A1 : K is star-shaped with respect to every point of a ball of radius greater or equal to ρh_K;

A2 : every edge $e \in \partial K$ has the length greater or equal to ρh_K.

5.3.2 Virtual element space for the stream-function

In the present section we introduce a virtual space of order $k \geq 2$ used to approximate the stream-function unknown.

For each polygon $K \in \mathcal{T}_h$ and every integer $k \geq 2$, let $\widehat{k} := \max\{k, 3\}$ and $\widetilde{\mathrm{W}}^h_k(K)$ be the finite dimensional space introduced in [77]:

$$\begin{aligned}\widetilde{\mathrm{W}}^h_k(K) := \Big\{\phi_h \in \mathrm{H}^2(K) : \Delta^2\phi_h \in \mathbb{P}_{k-2}(K), \phi_h|_{\partial K} \in C^0(\partial K), \phi_h|_e \in \mathbb{P}_{\widehat{k}}(e),\\ \nabla\phi_h|_{\partial K} \in \boldsymbol{C}^0(\partial K), \partial_{\mathbf{n}^e_K}\phi_h \in \mathbb{P}_{k-1}(e) \quad \forall e \in \partial K\Big\}.\end{aligned}$$

Next, for $\phi_h \in \widetilde{\mathrm{W}}^h_k(K)$, we introduce the following set of linear operators:

- $\mathbf{D_W1}$: the values of $\phi_h(\mathbf{v}_i)$, for all vertex $\mathbf{v}_i$ of the polygon K;
- $\mathbf{D_W2}$: the values of $h_{\mathbf{v}_i}\nabla\phi_h(\mathbf{v}_i)$, for all vertex $\mathbf{v}_i$ of the polygon K;
- $\mathbf{D_W3}$: for $k \geq 3$, the moments on edges up to degree $k-3$:

$$(q, \partial_{\mathbf{n}^e_K}\phi_h)_{0,e} \qquad \forall q \in \mathbb{M}_{k-3}(e), \quad \forall \,\text{edge } e;$$

- $\mathbf{D_W4}$: for $k \geq 4$, the moments on edges up to degree $k-4$:

$$h_e^{-1}(q, \phi_h)_{0,e} \qquad \forall q \in \mathbb{M}_{k-4}(e), \quad \forall \,\text{edge } e;$$

- $\mathbf{D_W5}$: for $k \geq 4$, the moments on polygons up to degree $k-4$:

$$h_K^{-2}(q, \phi_h)_{0,K} \qquad \forall q \in \mathbb{M}_{k-4}(K), \quad \forall \,\text{polygon } K,$$

where for each vertex $\mathbf{v}_i$, we chose $h_{\mathbf{v}_i}$ as the average of the diameters of the elements having $\mathbf{v}_i$ as a vertex and $\mathbb{M}_n(K)$ denote the scaled monomials of degree n, for each $n \geq 0$ (for further details see [58]).

In order to construct an approximation for the bilinear form $A_F(\cdot,\cdot)$, we consider the operator $\mathsf{P}_0 : C^0(\partial K) \to \mathbb{P}_0(K)$ defined by the following average:

$$\mathsf{P}_0\phi_h = \frac{1}{N_K}\sum_{i=1}^{N_K}\phi_h(\mathbf{v}_i), \tag{5.3.1}$$

where $\mathbf{v}_i, 1 \leq i \leq N_K$, are the vertices of K. Then, for each polygon K, we define the projector:

$$\Pi_K^{k,\mathrm{D}} : \widetilde{\mathrm{W}}_k^h(K) \to \mathbb{P}_k(K) \subset \widetilde{\mathrm{W}}_k^h(K),$$

as the solution of the local problems

$$\begin{aligned}
&A_F^K(\phi_h - \Pi_K^{k,\mathrm{D}}\phi_h, q_k) = 0 \qquad \forall q_k \in \mathbb{P}_k(K),\\
&\mathsf{P}_0(\phi_h - \Pi_K^{k,\mathrm{D}}\phi_h) = 0, \quad \mathsf{P}_0(\nabla(\phi - \Pi_K^{k,\mathrm{D}}\phi_h)) = 0,
\end{aligned} \tag{5.3.2}$$

where $A_F^K(\cdot,\cdot)$ is the restriction of the global bilinear form $A_F(\cdot,\cdot)$ (cf. (5.2.5)) on each polygon K.

Remark 5.3.1. *The operator $\Pi_K^{k,\mathrm{D}} : \widetilde{\mathrm{W}}_k^h(K) \to \mathbb{P}_k(K)$ is explicitly computable for every $\phi_h \in \widetilde{\mathrm{W}}_k^h(K)$, using only the information of the linear operators* $\mathbf{D_W1} - \mathbf{D_W5}$*; see for instance [77, 133].*

Now, we will present the local stream-function virtual space. For any $K \in \mathcal{T}_h$ and each integer $k \geq 2$, we consider the following local enhanced virtual space

$$\mathrm{W}_k^h(K) := \left\{\phi_h \in \widetilde{\mathrm{W}}_k^h(K) : (q^*, \phi_h - \Pi_K^{k,\mathrm{D}}\phi_h)_{0,K} = 0 \quad \forall q^* \in \mathbb{M}_{k-3}^*(K) \cup \mathbb{M}_{k-2}^*(K)\right\}, \tag{5.3.3}$$

where $\mathbb{M}_{k-3}^*(K)$ and $\mathbb{M}_{k-2}^*(K)$ are scaled monomials of degree $k-3$ and $k-2$, respectively (see [7]), with the convention that $\mathbb{M}_{-1}^*(K) := \emptyset$. For further details, see for instance [77] (see also [58, 18, 133]).

For $k \geq 2$, we introduce an additional projector, which will be used to build an approximation of the bilinear form $M_F(\cdot,\cdot)$. Such projector $\Pi_K^{k,\nabla^\perp} : \widetilde{\mathrm{W}}_k^h(K) \to \mathbb{P}_k(K) \subset \widetilde{\mathrm{W}}_k^h(K)$ is defined as the solution of the local problems:

$$\begin{aligned}
&M_F^K(\phi_h - \Pi_K^{k,\nabla^\perp}\phi_h, q_k) = 0 \qquad \forall q_k \in \mathbb{P}_k(K),\\
&\mathsf{P}_0(\nabla(\phi_h - \Pi_K^{k,\nabla^\perp}\phi_h)) = 0,
\end{aligned}$$

where $M_F^K(\cdot,\cdot)$ is the restriction of the global bilinear form $M_F(\cdot,\cdot)$ (cf. (5.2.3)) on each polygon K.

We summarize the main properties of the local virtual space $\mathrm{W}_k^h(K)$ defined in (5.3.3) (for the proof, we refer to [7, 58, 77, 133]).

- $\mathbb{P}_k(K) \subset \mathrm{W}_k^h(K) \subset \widetilde{\mathrm{W}}_k^h(K)$;
- The sets of linear operators $\mathbf{D_W1} - \mathbf{D_W5}$ constitutes a set of degrees of freedom for $\mathrm{W}_k^h(K)$;

- The operators $\Pi_K^{k,\mathrm{D}} : \mathrm{W}_k^h(K) \to \mathbb{P}_k(K)$ and $\Pi_K^{k,\nabla^\perp} : \mathrm{W}_k^h(K) \to \mathbb{P}_k(K)$ are computable using only the degrees of freedom $\mathbf{D_W1} - \mathbf{D_W5}$.

Now, we present our global virtual space to approximate the stream-function of the Boussinesq system (5.2.13). For each decomposition $\mathcal{T}_h$ of Ω into simple polygons K, we define

$$\mathrm{W}_k^h := \left\{ \phi_h \in \mathrm{H}_0^2(\Omega) : \phi_h|_K \in \mathrm{W}_k^h(K) \quad \forall K \in \mathcal{T}_h \right\}.$$

5.3.3 Virtual element space for the temperature

In this subsection we will introduce a C^0-virtual element space of high order $\ell \geq 1$ to approximate the temperature field of problem (5.2.13). To this end, for each polygon $K \in \mathcal{T}_h$, we consider the following finite dimensional space (see [7, 28, 65]):

$$\widetilde{\mathrm{H}}_\ell^h(K) := \left\{ w_h \in \mathrm{H}^1(K) \cap C^0(\partial K) : \Delta w_h \in \mathbb{P}_\ell(K),\ w_h|_e \in \mathbb{P}_\ell(e) \quad \forall e \in \partial K \right\}.$$

For each $w_h \in \widetilde{\mathrm{H}}_\ell^h(K)$ we consider the following set of linear operators:

- $\mathbf{D_H1}$: the values of $w_h(\mathbf{v}_i)$, for all vertex $\mathbf{v}_i$ of the polygon K.
- $\mathbf{D_H2}$: for $\ell \geq 2$, the moments on edges up to degree $\ell - 2$:
$$h_e^{-1}(q, w_h)_{0,e} \qquad \forall q \in \mathbb{M}_{\ell-2}(e), \quad \forall\,\text{edge } e;$$
- $\mathbf{D_H3}$: for $\ell \geq 2$, the moments on element K up to degree $\ell - 2$:
$$h_K^{-2}(q, w_h)_{0,K} \qquad \forall q \in \mathbb{M}_{\ell-2}(E), \quad \forall\,\text{polygon } K,$$

where $\mathbb{M}_n(K)$ denote the scaled monomials of degree n, for each $n \geq 0$ (for further details see [7, 65]). Now, we define the projector $\Pi_K^{\nabla,\ell} : \widetilde{\mathrm{H}}_\ell^h(K) \to \mathbb{P}_\ell(K) \subset \widetilde{\mathrm{H}}_\ell^h(K)$, as the solution of the local problems:

$$\begin{aligned} A_T^K(w_h - \Pi_K^{\nabla,\ell} w_h, r_\ell) &= 0 \qquad \forall r_\ell \in \mathbb{P}_\ell(K), \\ \mathsf{P}_0(w_h - \Pi_K^{\nabla,\ell} w_h) &= 0, \end{aligned}$$

where $A_T^K(\cdot,\cdot)$ is the restriction of the global bilinear form $A_T(\cdot,\cdot)$ (cf. (5.2.6)) on each polygon K and the operator $\mathsf{P}_0(\cdot)$ is defined in (5.3.1). We have that the operator $\Pi_K^{\nabla,\ell} : \widetilde{\mathrm{H}}_\ell^h(K) \to \mathbb{P}_\ell(K)$ is computable using the set $\mathbf{D_H1} - \mathbf{D_H3}$ (see for instance, [7, 28, 65]). In addition, by using this projection and the definition of space $\widetilde{\mathrm{H}}_\ell^h(K)$, we introduce our local virtual space to approximate the temperature field:

$$\mathrm{H}_\ell^h(K) := \left\{ w_h \in \widetilde{\mathrm{H}}_\ell^h(K) : (r^*, w_h - \Pi_K^{\nabla,\ell} w_h)_{0,K} = 0 \qquad \forall r^* \in \mathbb{M}_\ell^*(K) \cup \mathbb{M}_{\ell-1}^*(K) \right\},$$

where $\mathbb{M}_\ell^*(K)$ and $\mathbb{M}_{\ell-1}^*(K)$ are scaled monomials of degree ℓ and $\ell - 1$, respectively, with the convention that $\mathbb{M}_{-1}^*(K) := \emptyset$ (see [7, 65]).

Now, we summarize the main properties of the local virtual spaces $\mathrm{H}_\ell^h(K)$ (for a proof we refer to [7, 28, 65]):

- $\mathbb{P}_\ell(K) \subset \mathrm{H}_\ell^h(K) \subset \widetilde{\mathrm{H}}_\ell^h(K)$;
- The sets of linear operators $\mathbf{D_H 1} - \mathbf{D_H 3}$ constitutes a set of degrees of freedom for $\mathrm{H}_\ell^h(K)$;
- The operator $\Pi_K^{\nabla,\ell} : \mathrm{H}_\ell^h(K) \to \mathbb{P}_\ell(K)$ is also computable using the degrees of freedom $\mathbf{D_H 1} - \mathbf{D_H 3}$.

Next, we present our global virtual space to approximate the fluid temperature of the Boussinesq system (5.2.13). For each decomposition $\mathcal{T}_h$ of Ω into simple polygons K, we define

$$\mathrm{H}_\ell^h := \left\{ w_h \in \mathrm{H}_0^1(\Omega) : w_h|_K \in \mathrm{H}_\ell^h(K) \quad \forall K \in \mathcal{T}_h \right\}.$$

5.3.4 L^2-projections and the discrete forms

In this subsection we introduce some functions built from the classical L^2-polynomial projections, which will be useful to construct an approximation for the continuous multilinear forms defined in Section 5.2.2. We start recalling the usual $\mathrm{L}^2(K)$-projection onto the scalar polynomial space $\mathbb{P}_n(K)$, with $n \in \mathbb{N} \cup \{0\}$: for each $\phi \in \mathrm{L}^2(K)$, the function $\Pi_K^n \phi \in \mathbb{P}_n(K)$ is defined as the unique function, such that

$$(q_n, \phi - \Pi_K^n \phi)_{0,K} = 0 \qquad \forall q_n \in \mathbb{P}_n(K). \tag{5.3.4}$$

An analogous definition holds for the $\mathbf{L}^2(K)$-projection onto the vectorial polynomial space $\mathbf{P}_n(K)$, which we will denote by $\boldsymbol{\Pi}_K^n$.

We recall that for all sufficiently regular ϕ (for the right hand side to make sense) there exists $C > 0$, independent of K and h_E, such that (see [35, Page 10]):

$$\|\Pi_K^n \phi\|_{\mathrm{L}^4(K)} \le C\|\phi\|_{\mathrm{L}^4(K)} \qquad \text{and} \qquad \|\Pi_K^n \phi\|_{0,K} \le \|\phi\|_{0,K}. \tag{5.3.5}$$

The same properties hold for the vectorial version.

The following lemma establishes that certain polynomial functions are computable on $\mathrm{W}_k^h(K)$, using only the information of the degrees of freedom $\mathbf{D_W 1} - \mathbf{D_W 5}$ (see for instance [77, 133]).

Lemma 5.3.1. *For $k \ge 2$, let $\Pi_K^{k-2} : \mathrm{L}^2(K) \to \mathbb{P}_{k-2}(K)$ and $\boldsymbol{\Pi}_K^{k-1} : \mathbf{L}^2(K) \to \mathbf{P}_{k-1}(K)$ be the operators defined by the relation (5.3.4) and by its vectorial version. Then, for each $\phi_h \in \mathrm{W}_k^h(K)$ the polynomial functions*

$$\Pi_K^{k-2}\phi_h, \quad \Pi_K^{k-2}\Delta\phi_h, \quad \boldsymbol{\Pi}_K^{k-1}\nabla\phi_h \quad \textit{and} \quad \boldsymbol{\Pi}_K^{k-1}\mathbf{curl}\,\phi_h$$

are computable using only the information of the degrees of freedom $\mathbf{D_W 1} - \mathbf{D_W 5}$.

For the space $\mathrm{H}_\ell^h(K)$ and its degrees of freedom $\mathbf{D_H 1} - \mathbf{D_H 3}$, we have the following result (see for instance [28, 65]).

Lemma 5.3.2. *For $\ell \ge 1$, let $\Pi_K^{\ell-1} : \mathrm{L}^2(K) \to \mathbb{P}_{\ell-1}(K)$, $\Pi_K^{\ell} : \mathrm{L}^2(K) \to \mathbb{P}_\ell(K)$ and $\boldsymbol{\Pi}_K^{\ell-1} : \mathbf{L}^2(K) \to \mathbf{P}_{\ell-1}(K)$ be the operators defined by the relation (5.3.4) and by its vectorial version, respectively. Then, for each $w_h \in \mathrm{H}_\ell^h(K)$ the polynomial functions*

$$\Pi_K^{\ell-1}w_h, \quad \Pi_K^{\ell}w_h \quad \textit{and} \quad \boldsymbol{\Pi}_K^{\ell-1}\nabla w_h$$

are computable using only the information of the degrees of freedom $\mathbf{D_H 1} - \mathbf{D_H 3}$.

Now, using the functions introduced above, we will construct the discrete version of the forms defined in Section 5.2.2. First, let $s_K^{\mathbf{c}} : \mathrm{W}_k^h(K) \times \mathrm{W}_k^h(K) \to \mathbb{R}$ and $s_K^{\mathrm{D}} : \mathrm{W}_k^h(K) \times \mathrm{W}_k^h(K) \to \mathbb{R}$ be any symmetric positive definite bilinear forms to be chosen to satisfy:

$$\begin{aligned} c_0 M_F^K(\phi_h, \phi_h) \leq s_K^{\mathbf{c}}(\phi_h, \phi_h) \leq c_1 M_F^K(\phi_h, \phi_h) \qquad & \forall \phi_h \in \mathrm{Ker}(\Pi_K^{k,\nabla^\perp}), \\ c_2 A_F^K(\phi_h, \phi_h) \leq s_K^{\mathrm{D}}(\phi_h, \phi_h) \leq c_3 A_F^K(\phi_h, \phi_h) \qquad & \forall \phi_h \in \mathrm{Ker}(\Pi_K^{k,\mathrm{D}}), \end{aligned} \tag{5.3.6}$$

with c_0, c_1, c_2 and c_3 are positive constants independent of h and K. We will choose the following representation satisfying (5.3.6) (see [133, Proposition 3.5]):

$$s_K^{\mathrm{D}}(\varphi_h, \phi_h) := h_K^{-2} \sum_{i=1}^{N_K^{\mathrm{dof}}} \mathrm{dof}_i^{\mathrm{W}_k^h(K)}(\varphi_h) \mathrm{dof}_i^{\mathrm{W}_k^h(K)}(\phi_h) \quad \text{and}$$

$$s_K^{\mathbf{c}}(\varphi_h, \phi_h) := \sum_{i=1}^{N_K^{\mathrm{dof}}} \mathrm{dof}_i^{\mathrm{W}_k^h(K)}(\varphi_h) \mathrm{dof}_i^{\mathrm{W}_k^h(K)}(\phi_h),$$

where $N_K^{\mathrm{dof}} := \dim(\mathrm{W}_k^h(K))$ and the operator $\mathrm{dof}_j^{\mathrm{W}_k^h(K)}(\phi)$ associates to each smooth enough function ϕ the jth local degree of freedom $\mathrm{dof}_j^{\mathrm{W}_k^h(K)}(\phi)$, with $1 \leq j \leq N_K^{\mathrm{dof}}$.

On each polygon K, for all $\varphi_h, \phi_h \in \mathrm{W}_k^h(K)$ we define the local discrete bilinear forms $M_F^{h,K}(\cdot,\cdot)$ and $A_F^{h,K}(\cdot,\cdot)$ as follows

$$M_F^{h,K}(\varphi_h, \phi_h) := M_F^K\big(\Pi_K^{k,\nabla^\perp} \varphi_h, \Pi_K^{k,\nabla^\perp} \phi_h\big) + s_K^{\mathbf{c}}\big((\mathrm{I} - \Pi_K^{k,\nabla^\perp})\varphi_h, (\mathrm{I} - \Pi_K^{k,\nabla^\perp})\phi_h\big) \tag{5.3.7}$$

$$A_F^{h,K}(\varphi_h, \phi_h) := A_F^K\big(\Pi_K^{k,\mathrm{D}} \varphi_h, \Pi_K^{k,\mathrm{D}} \phi_h\big) + s_K^{\mathrm{D}}\big((\mathrm{I} - \Pi_K^{k,\mathrm{D}})\varphi_h, (\mathrm{I} - \Pi_K^{k,\mathrm{D}})\phi_h\big), \tag{5.3.8}$$

For the approximation of the local trilinear form $B_F^K(\cdot;\cdot,\cdot)$, for all $\zeta_h, \varphi_h, \phi_h \in \mathrm{W}_k^h(K)$, we consider

$$B_F^{h,K}(\zeta_h; \varphi_h, \phi_h) := \int_K \big[(\Pi_K^{k-2} \Delta \zeta_h)\big(\boldsymbol{\Pi}_K^{k-1} \mathbf{curl}\, \varphi_h\big)\big] \cdot \boldsymbol{\Pi}_K^{k-1} \nabla \phi_h. \tag{5.3.9}$$

For the treatment of the right-hand side associate to the fluid equation, we set the following local load term:

$$F_\psi^{h,K}(\phi_h) = \int_K \mathbf{f}_\psi(t) \cdot \boldsymbol{\Pi}_K^{k-1} \mathbf{curl}\, \phi_h \qquad \forall \phi_h \in \mathrm{W}_k^h(K), \quad \text{for a.e. } t \in (0,T).$$

The following result establishes the usual k-consistency and stability properties for the discrete local forms $M_F^{h,K}(\cdot,\cdot)$ and $A_F^{h,K}(\cdot,\cdot)$.

Proposition 5.3.1. *The local bilinear forms defined in* (5.2.3), (5.2.5), (5.3.7) *and* (5.3.8), *satisfy the following properties:*

- *k-consistency: for all $K \in \mathcal{T}_h$, we have that*

$$\begin{aligned} M_F^{h,K}(q, \phi_h) &= M_F^K(q, \phi_h), \qquad & \forall q \in \mathbb{P}_k(K), \quad \forall \phi_h \in \mathrm{W}_k^h(K) \\ A_F^{h,K}(q, \phi_h) &= A_F^K(q, \phi_h) \qquad & \forall q \in \mathbb{P}_k(K), \quad \forall \phi_h \in \mathrm{W}_k^h(K). \end{aligned}$$

- *stability and boundedness: there exist positive constants $\alpha_i, i = 1, \dots, 4$, independent of K, such that:*

$$\begin{aligned} \alpha_1 M_F^K(\phi_h, \phi_h) \leq M_F^{h,K}(\phi_h, \phi_h) \leq \alpha_2 M_F^K(\phi_h, \phi_h) \qquad & \forall \phi_h \in \mathrm{W}_k^h(K), \\ \alpha_3 A_F^K(\phi_h, \phi_h) \leq A_F^{h,K}(\phi_h, \phi_h) \leq \alpha_4 A_F^K(\phi_h, \phi_h) \qquad & \forall \phi_h \in \mathrm{W}_k^h(K). \end{aligned}$$

Proof. The proof follows standard arguments in the VEM literature (see [18, 27, 28]). $\square$

Now, we continue with the construction of the forms associated to the energy equation. First, let $s_K^0(\cdot,\cdot)$ and $s_K^{\nabla}(\cdot,\cdot)$ be any symmetric positive definite bilinear forms such that

$$\begin{aligned} c_4 M_T^K(v_h,v_h) &\leq s_K^0(v_h,v_h) \leq c_5 M_T^K(v_h,v_h) && \forall v_h \in \mathrm{Ker}(\Pi_K^{\ell}),\\ c_6 A_T^K(v_h,v_h) &\leq s_K^{\nabla}(v_h,v_h) \leq c_7 A_T^K(v_h,v_h) && \forall v_h \in \mathrm{Ker}(\Pi_K^{\nabla,\ell}), \end{aligned} \tag{5.3.10}$$

for some positive constants c_4, c_5, c_6 and c_7, independent of h and K. We will choose the classical representation for these stabilizing forms satisfying property (5.3.10) (see [33, 55, 65]):

$$\begin{aligned} s_K^0(v_h,w_h) &:= h_K^2 \sum_{j=1}^{\dim(\mathrm{H}_\ell^h(K))} \mathrm{dof}_j^{\mathrm{H}_\ell^h(K)}(v_h)\mathrm{dof}_j^{\mathrm{H}_\ell^h(K)}(w_h),\\ s_K^{\nabla}(v_h,w_h) &:= \sum_{j=1}^{\dim(\mathrm{H}_\ell^h(K))} \mathrm{dof}_j^{\mathrm{H}_\ell^h(K)}(v_h)\mathrm{dof}_j^{\mathrm{H}_\ell^h(K)}(w_h), \end{aligned}$$

where the operator $\mathrm{dof}_j^{\mathrm{H}_\ell^h(K)}(v)$ associates to each smooth enough function v the jth local degree of freedom $\mathrm{dof}_j^{\mathrm{H}_\ell^h(K)}(v)$, with $1 \leq j \leq \dim(\mathrm{H}_\ell^h(K))$. Then, for all $v_h, w_h \in \mathrm{H}_\ell^h(K)$, we set the following approximation for the forms $M_T^K(\cdot,\cdot)$ and $A_T^K(\cdot,\cdot)$ (cf. (5.2.4) and (5.2.6))

$$\begin{aligned} M_T^{h,K}(v_h,w_h) &:= M_T^K\left(\Pi_K^{\ell} v_h, \Pi_K^{\ell} w_h\right) + s_K^0\big((\mathrm{I}-\Pi_K^{\ell})v_h, (\mathrm{I}-\Pi_K^{\ell})w_h\big)\\ A_T^{h,K}(v_h,w_h) &:= \int_K \boldsymbol{\Pi}_K^{\ell-1}\nabla v_h \cdot \boldsymbol{\Pi}_K^{\ell-1}\nabla w_h + s_K^{\nabla}\big((\mathrm{I}-\Pi_K^{\nabla,\ell})v_h, (\mathrm{I}-\Pi_K^{\nabla,\ell})w_h\big). \end{aligned}$$

We have that the bilinear forms $M_T^{h,K}(\cdot,\cdot)$ and $A_T^{h,K}(\cdot,\cdot)$ satisfy the classical ℓ-consistency and stability properties (analogous to Proposition (5.3.1)). For further details, see [27, 28, 65].

To approximate of bilinear form $C^K(\cdot,\cdot)$, we set

$$C^{h,K}(w_h,\phi_h) := \int_K \mathbf{g}\Pi_K^{\ell-1} w_h \cdot \boldsymbol{\Pi}_K^{k-1}\mathbf{curl}\,\phi_h \qquad \forall w_h \in \mathrm{H}_\ell^h(K),\ \forall \phi_h \in \mathrm{W}_k^h(K).$$

Now, for each $\varphi_h \in \mathrm{W}_k^h(K)$ and $w_h, v_h \in \mathrm{H}_\ell^h(K)$, we consider the following discrete trilinear form

$$B_T^{h,K}(\varphi_h; v_h, w_h) := \int_K \left(\boldsymbol{\Pi}_K^{k-1}\mathbf{curl}\,\varphi_h \cdot \boldsymbol{\Pi}_K^{\ell-1}\nabla v_h\right)\Pi_K^{\ell-1} w_h.$$

Then, for the skew-symmetric trilinear form $B_{\mathrm{skew}}^K(\cdot;\cdot,\cdot)$ (cf. (5.2.12)), we set the following approximation:

$$B_{\mathrm{skew}}^{h,K}(\varphi_h; v_h, w_h) := \frac{1}{2}(B_T^{h,K}(\varphi_h; v_h, w_h) - B_T^{h,K}(\varphi_h; w_h, v_h)).$$

For the treatment of the right-hand side associated to the temperature discretization, we set following local load term

$$F_\theta^{h,K}(v_h) := \int_K \Pi_K^{\ell-1} f_\theta(t) v_h \equiv \int_K f_\theta(t)\Pi_K^{\ell-1} v_h \qquad \forall v_h \in \mathrm{H}_\ell^h(K) \quad \text{for a.e. } t \in (0,T).$$

Thus, for all $\zeta_h, \varphi_h, \phi_h \in \mathrm{W}_k^h$, we define the associated global forms M_F^h, A_F^h, B_F^h, and F_ψ^h in the usual way, by summing the local forms on all mesh elements. Analogously, we define the associated global forms $M_T^h, C^h, B_{\text{skew}}^h, F_\theta^h$ for all $v_h, w_h \in \mathrm{H}_\ell^h$. For instance

$$M_F^h : \mathrm{W}_k^h \times \mathrm{W}_k^h \to \mathbb{R}, \qquad M_F^h(\varphi_h, \phi_h) := \sum_{K \in \mathcal{T}_h} M_F^{h,K}(\varphi_h, \phi_h).$$

We recall that the forms defined above are computable using the degrees of freedom. In addition, we have that the trilinear forms are immediately extendable to the whole continuous spaces.

In next result we summarize some properties of the discrete global forms defined above.

Lemma 5.3.3. *For each $\zeta_h, \varphi_h, \phi_h \in \mathrm{W}_k^h$ and each $v_h, w_h \in \mathrm{H}_\ell^h$, the global forms defined above satisfy the following properties:*

$$\begin{aligned}
|M_F^h(\varphi_h, \phi_h)| &\leq \widehat{C}_{M_F} \|\varphi_h\|_{1,\Omega} \|\phi_h\|_{1,\Omega} \quad \text{and} \quad M_F^h(\phi_h, \phi_h) \geq \widehat{\alpha}_{M_F} \|\phi_h\|_{1,\Omega}^2, \\
|M_T^h(v_h, w_h)| &\leq \widehat{C}_{M_T} \|v_h\|_{0,\Omega} \|w_h\|_{0,\Omega} \quad \text{and} \quad M_T^h(v_h, v_h) \geq \widehat{\alpha}_{M_T} \|v_h\|_{0,\Omega}^2, \\
|A_F^h(\varphi_h, \phi_h)| &\leq \widehat{C}_{A_F} \|\varphi_h\|_{2,\Omega} \|\phi_h\|_{2,\Omega} \quad \text{and} \quad A_F^h(\phi_h, \phi_h) \geq \widehat{\alpha}_{A_F} \|\phi_h\|_{2,\Omega}^2, \\
|A_T^h(v_h, w_h)| &\leq \widehat{C}_{A_T} \|v_h\|_{1,\Omega} \|w_h\|_{1,\Omega} \quad \text{and} \quad A_T^h(v_h, v_h) \geq \widehat{\alpha}_{A_T} \|v_h\|_{1,\Omega}^2, \\
|B_F^h(\zeta_h; \varphi_h, \phi_h)| &\leq \widehat{C}_{B_F} \|\zeta_h\|_{2,\Omega} \|\varphi_h\|_{2,\Omega} \|\phi_h\|_{2,\Omega} \quad \text{and} \quad B_F^h(\zeta_h; \phi_h, \phi_h) = 0, \\
|B_{\text{skew}}^h(\zeta_h; v_h, w_h)| &\leq \widehat{C}_{B_T} \|\zeta_h\|_{2,\Omega} \|v_h\|_{1,\Omega} \|w_h\|_{1,\Omega} \quad \text{and} \quad B_{\text{skew}}^h(\zeta_h; v_h, v_h) = 0, \\
|C^h(v_h, \phi_h)| &\leq \|\mathbf{g}\|_{\infty,\Omega} \|v_h\|_{0,\Omega} \|\phi_h\|_{1,\Omega}, \\
|F_\psi^h(\phi_h)| &\leq \widehat{C}_{F_\psi} \|\mathbf{f}_\psi\|_{0,\Omega} \|\phi_h\|_{1,\Omega} \quad \text{and} \quad |F_\theta^h(v_h)| \leq \widehat{C}_{F_\theta} \|f_\theta\|_{0,\Omega} \|v_h\|_{0,\Omega},
\end{aligned}$$

where all the constants involved are positive and independent of mesh size h.

We close this section with the following remarks.

Remark 5.3.2. *We can propose an alternative discretization inspired by (5.2.15), which is given by:*

$$A_F^h(\varphi_h, \phi_h) := \sum_{K \in \mathcal{T}_h} \int_K \Delta \Pi_K^{k,\mathrm{D}} \varphi_h \, \Delta \Pi_K^{k,\mathrm{D}} \phi_h + s_K^{\mathrm{D}}\big((\mathrm{I} - \Pi_K^{k,\mathrm{D}})\varphi_h, (\mathrm{I} - \Pi_K^{k,\mathrm{D}})\phi_h\big),$$

for all $\varphi_h, \phi_h \in \mathrm{W}_k^h$, which is also fully computable by using the degrees of freedom $\mathbf{D_W1} - \mathbf{D_W5}$. Nevertheless, in the present work we will stick to the choice (5.3.8).

Remark 5.3.3. *If $\mathbf{f}_\psi$ is given as an explicit function, then we can consider the following alternative discrete load term*

$$F_\psi^h(\phi_h) := \sum_{K \in \mathcal{T}_h} \int_K \operatorname{rot} \mathbf{f}_\psi(t) \Pi_K^{k-2} \phi_h \qquad \forall \phi_h \in \mathrm{W}_k^h,$$

which is also computable using the degrees of freedom $\mathbf{D_W1} - \mathbf{D_W5}$.

5.4 Fully-discrete formulation and its well posedness

In order to present a full discretization of problem (5.2.13) we introduce a sequence of time steps $t_n = n\Delta t$, $n = 0, 1, 2, \ldots, N$, where $\Delta t = T/N$ is the time step. Moreover, we consider the following approximations at each time t_n: $\psi_h^n \approx \psi_h(t_n)$ and $\theta_h^n \approx \theta_h(t_n)$. For the external forces, we introduce the following notation: $\mathbf{f}_\psi^n := \mathbf{f}_\psi(t_n)$, $f_\theta^n := f_\theta(t_n)$ and $\mathbf{g}^n := \mathbf{g}(t_n)$.

We consider the backward Euler method coupled with the VE discretization presented in Section 5.3, which read as follows: given (ψ_h^0, θ_h^0), find $\{(\psi_h^n, \theta_h^n)\}_{n=1}^N \in \mathrm{W}_k^h \times \mathrm{H}_\ell^h$, such that

$$\begin{aligned} M_F^h\left(\frac{\psi_h^n - \psi_h^{n-1}}{\Delta t}, \phi_h\right) + \nu A_F^h(\psi_h^n, \phi_h) + B_F^h(\psi_h^n; \psi_h^n, \phi_h) - C^h(\theta_h^n, \phi_h) &= F_\psi^h(\phi_h), \\ M_T^h\left(\frac{\theta_h^n - \theta_h^{n-1}}{\Delta t}, v_h\right) + \kappa A_T^h(\theta_h^n, v_h) + B_{\text{skew}}^h(\psi_h^n; \theta_h^n, v_h) &= F_\theta^h(v_h), \end{aligned} \tag{5.4.1}$$

for all $(\phi_h, v_h) \in \mathrm{W}_k^h \times \mathrm{H}_\ell^h$. The functions (ψ_h^0, θ_h^0) are initial approximations of (ψ_h, θ_h) at $t = 0$. For instance, we will consider $\psi_h^0 := \mathcal{S}_h\psi_0$ (see (5.5.1) below) and $\theta_h^0 := \mathcal{P}_h\theta_0$, with $\mathcal{P}_h(\cdot)$ being the energy operator associated to the H^1-inner product (for further details, see for instance [153, Equation (9)]). We now recall local inverse inequalities for the virtual spaces $\mathrm{W}_k^h(K)$ and $\mathrm{H}_\ell^h(K)$ (see [37, 74]), for all $\phi_h \in \mathrm{W}_k^h(K)$ and for all $v_h \in \mathrm{H}_\ell^h(K)$, we have

$$|\phi_h|_{2,K} \leq C_{\mathtt{inv}} h_K^{-1} |\phi_h|_{1,K} \quad \text{and} \quad |v_h|_{1,K} \leq C_{\mathtt{inv}} h_K^{-1} \|v_h\|_{0,K}. \tag{5.4.2}$$

In what follows, we will provide the well-posedness of the fully-discrete formulation (5.4.1).

Theorem 5.4.1. *Let $\widehat{\alpha} := \min\{\widehat{\alpha}_{M_F}, \widehat{\alpha}_{M_T}\}$ and $\gamma := \min\{\widehat{\alpha}_{A_F}\nu, \widehat{\alpha}_{A_T}\kappa\}$, where $\widehat{\alpha}_{M_F}, \widehat{\alpha}_{M_T}, \widehat{\alpha}_{A_F}$ and $\widehat{\alpha}_{A_T}$ are the constants in Lemma 5.3.3. Assume that*

$$\widehat{\alpha} + \Delta t\,(\gamma - C_{\mathbf{g}}) > 0, \tag{5.4.3}$$

where $C_{\mathbf{g}} := \|\mathbf{g}\|_{\mathrm{L}^\infty(0,T;\mathbf{L}^\infty(\Omega))}$. Then the fully-discrete scheme (5.4.1) admits at least one solution $(\psi_h^n, \theta_h^n) \in \mathrm{W}_k^h \times \mathrm{H}_\ell^h$ at every time step t_n, with $n = 1, \ldots, N$.

Proof. For simplicity we set $\mathrm{X}_{k,\ell}^h := \mathrm{W}_k^h \times \mathrm{H}_\ell^h$ and we endow this space with the following equivalent norm:

$$|||(\phi_h, w_h)||| := (\|\phi_h\|_{1,\Omega}^2 + \|w_h\|_{0,\Omega}^2)^{\frac{1}{2}} \qquad \forall (\phi_h, w_h) \in \mathrm{X}_{k,\ell}^h.$$

Next, for $1 \leq n \leq N$, let $(\psi_h^{n-1}, \theta_h^{n-1}) \in \mathrm{X}_{k,\ell}^h$. Thus, for any $(\psi_h, \theta_h) \in \mathrm{X}_{k,\ell}^h$, we consider the operator $\Phi : \mathrm{X}_{k,\ell}^h \to (\mathrm{X}_{k,\ell}^h)^*$ defined by

$$\begin{aligned} \langle \Phi(\psi_h, \theta_h), (\phi_h, w_h) \rangle &:= M_F^h(\psi_h, \phi_h) - M_F^h(\psi_h^{n-1}, \phi_h) + \nu\Delta t A_F^h(\psi_h, \phi_h) \\ &+ \Delta t B_F^h(\psi_h; \psi_h, \phi_h) - \Delta t F_\psi^h(\phi_h) + M_T^h(\theta_h, w_h) - M_T^h(\theta_h^{n-1}, w_h) + \kappa\Delta t A_T^h(\theta_h, w_h) \\ &+ \Delta t B_{\text{skew}}^h(\psi_h; \theta_h, w_h) - \Delta t F_\theta^h(w_h) - \Delta t C^h(\theta_h, \phi_h) \qquad \forall (\phi_h, w_h) \in \mathrm{X}_{k,\ell}^h. \end{aligned} \tag{5.4.4}$$

From the definition of operator Φ, we observe that for each $1 \leq n \leq N$ a solution $(\psi_h^n, \theta_h^n) \in \mathrm{X}_{k,\ell}^h$ of problem (5.4.1) is characterized by $\Phi(\psi_h^n, \theta_h^n) = \mathbf{0}$. Thus, we will prove that this operator satisfies the hypothesis of the fixed point result [103, Chap. IV, Corollary 1.1].

First we will prove its continuity. Indeed, by using of operator Φ and Lemma 5.3.3, for all $(\phi_h, w_h) \in \mathrm{X}^h_{k,\ell}$ have

$$\begin{aligned}
\langle \Phi(\psi_h,\theta_h) - \Phi(\psi_h^\star,\theta_h^\star),(\phi_h,w_h)\rangle &:= M_F^h(\psi_h-\psi_h^\star,\phi_h) + \nu\Delta t A_F^h(\psi_h-\psi_h^\star,\phi_h)\\
&\quad + \Delta t(B_F^h(\psi_h;\psi_h,\phi_h) - B_F^h(\psi_h^\star;\psi_h^\star,\phi_h))\\
&\quad + M_T^h(\theta_h-\theta_h^\star,w_h) + \kappa\Delta t A_T^h(\theta_h-\theta_h^\star,w_h)\\
&\quad + \Delta t(B^h_{\text{skew}}(\psi_h;\theta_h,w_h) - B^h_{\text{skew}}(\psi_h^\star;\theta_h^\star,w_h)) + \Delta t C^h(\theta_h^\star-\theta_h,\phi_h)\\
&\leq \widehat{C}_{M_F}\|\psi_h-\psi_h^\star\|_{1,\Omega}\|\phi_h\|_{1,\Omega} + \nu\Delta t\widehat{C}_{A_F}\|\psi_h-\psi_h^\star\|_{2,\Omega}\|\phi_h\|_{2,\Omega}\\
&\quad + \Delta t(B_F^h(\psi_h;\psi_h,\phi_h) - B_F^h(\psi_h^\star;\psi_h^\star,\phi_h))\\
&\quad + \widehat{C}_{M_T}\|\theta_h-\theta_h^\star\|_{0,\Omega}\|w_h\|_{0,\Omega} + \kappa\Delta t\widehat{C}_{A_T}\|\theta_h-\theta_h^\star\|_{1,\Omega}\|w_h\|_{1,\Omega}\\
&\quad + \Delta t(B^h_{\text{skew}}(\psi_h;\theta_h,w_h) - B^h_{\text{skew}}(\psi_h^\star;\theta_h^\star,w_h)) + \Delta t\|\mathbf{g}\|_{\infty,\Omega}\|\theta_h-\theta_h^\star\|_{0,\Omega}\|\phi_h\|_{1,\Omega}.
\end{aligned} \tag{5.4.5}$$

Now, we add and subtract the term $B_F^h(\psi_h^\star;\psi_h,\phi_h)$, then by using the linearity in each entry and the continuity of the trilinear form $B_F^h(\cdot;\cdot,\cdot)$ (cf. Lemma 5.3.3), we obtain

$$\begin{aligned}
B_F^h(\psi_h;\psi_h,\phi_h) - B_F^h(\psi_h^\star;\psi_h^\star,\phi_h) &= B_F^h(\psi_h-\psi_h^\star;\psi_h,\phi_h) + B_F^h(\psi_h^\star;\psi_h-\psi_h^\star,\phi_h)\\
&\leq \widehat{C}_{B_F}(\|\psi_h-\psi_h^\star\|_{2,\Omega}\|\psi_h\|_{2,\Omega} + \|\psi_h^\star\|_{2,\Omega}\|\psi_h-\psi_h^\star\|_{2,\Omega})\|\phi_h\|_{2,\Omega}.
\end{aligned}$$

Following analogous steps, we get

$$\begin{aligned}
B^h_{\text{skew}}(\psi_h;\theta_h,w_h) - B^h_{\text{skew}}(\psi_h^\star;\theta_h^\star,w_h) &= B^h_{\text{skew}}(\psi_h-\psi_h^\star;\theta_h,w_h) + B^h_{\text{skew}}(\psi_h^\star;\theta_h-\theta_h^\star,w_h)\\
&\leq \widehat{C}_{B_T}(\|\psi_h-\psi_h^\star\|_{2,\Omega}\|\theta_h\|_{1,\Omega} + \|\psi_h^\star\|_{2,\Omega}\|\theta_h-\theta_h^\star\|_{1,\Omega})\|w_h\|_{1,\Omega}.
\end{aligned}$$

By combining (5.4.5), the above estimates, the inverse inequalities (5.4.2) and the Cauchy-Schwarz inequality, for all $(\phi_h, w_h) \in \mathrm{X}^h_{k,\ell}$, it holds

$$|\langle \Phi(\psi_h,\theta_h) - \Phi(\psi_h^\star,\theta_h^\star),(\phi_h,w_h)\rangle| \leq C(1+\Delta t h_{\min}^{-2} + \Delta t h_{\min}^{-3})|||(\psi_h-\psi_h^\star,\theta_h-\theta_h^\star)|||\;|||(\phi_h,w_h)|||.$$

Therefore, we deduce that for h and Δt fixed

$$\|\Phi(\psi_h,\theta_h) - \Phi(\psi_h^\star,\theta_h^\star)\|_{(\mathrm{X}^h_{k,\ell})^*} \longrightarrow 0, \quad \text{when} \quad (\psi_h,\theta_h) \xrightarrow{|||\cdot|||} (\psi_h^\star,\theta_h^\star),$$

i.e., Φ is continuous.

On the other hand, by employing again Lemma 5.3.3 and the Young inequality, for all

$(\psi_h, \theta_h) \in \mathrm{X}_{k,\ell}^h$, we obtain

$$\begin{aligned}
\langle \Phi(\psi_h,\theta_h),(\psi_h,\theta_h)\rangle &\geq \widehat{\alpha}_{M_F}\|\psi_h\|_{1,\Omega}^2 - \frac{\widehat{C}_{M_F}^2}{2\widehat{\alpha}_{M_F}}\|\psi_h^{n-1}\|_{1,\Omega}^2 - \frac{\widehat{\alpha}_{M_F}}{2}\|\psi_h\|_{1,\Omega}^2 \\
&\quad + \widehat{\alpha}_{A_F}\nu\Delta t\|\psi_h\|_{2,\Omega}^2 - \frac{\widehat{C}_{F_\psi}^2\Delta t}{2\widehat{\alpha}_{A_F}\nu}\|\mathbf{f}_\psi^n\|_{0,\Omega}^2 - \frac{\widehat{\alpha}_{A_F}\nu\Delta t}{2}\|\psi_h\|_{2,\Omega}^2 + \widehat{\alpha}_{M_T}\|\theta_h\|_{0,\Omega}^2 \\
&\quad - \frac{\widehat{C}_{M_T}^2}{2\widehat{\alpha}_{M_T}}\|\theta_h^{n-1}\|_{0,\Omega}^2 - \frac{\widehat{\alpha}_{M_T}}{2}\|\theta_h\|_{0,\Omega}^2 + \widehat{\alpha}_{A_T}\kappa\Delta t\|\theta_h\|_{1,\Omega}^2 \\
&\quad - \frac{\widehat{C}_{F_\theta}^2\Delta t}{2\widehat{\alpha}_{A_T}\kappa}\|f_\theta^n\|_{0,\Omega}^2 - \frac{\widehat{\alpha}_{A_T}\kappa\Delta t}{2}\|\theta_h\|_{1,\Omega}^2 - \frac{\Delta t C_{\mathbf{g}}}{2}(\|\psi_h\|_{1,\Omega}^2 + \|\theta_h\|_{0,\Omega}^2) \\
&\geq \frac{1}{2}\min\{\widehat{\alpha}_{M_F},\widehat{\alpha}_{M_T}\}(\|\psi_h\|_{1,\Omega}^2 + \|\theta_h\|_{0,\Omega}^2) \\
&\quad + \frac{\Delta t}{2}\min\{\widehat{\alpha}_{A_F}\nu,\widehat{\alpha}_{A_T}\kappa\}(\|\psi_h\|_{2,\Omega}^2 + \|\theta_h\|_{1,\Omega}^2) \\
&\quad - \frac{\Delta t C_{\mathbf{g}}}{2}(\|\psi_h\|_{1,\Omega}^2 + \|\theta_h\|_{0,\Omega}^2) - \frac{\widehat{C}_{M_F}^2}{2\widehat{\alpha}_{M_F}}\|\psi_h^{n-1}\|_{1,\Omega}^2 - \frac{\widehat{C}_{M_T}^2}{2\widehat{\alpha}_{M_T}}\|\theta_h^{n-1}\|_{0,\Omega}^2 \\
&\quad - \frac{\widehat{C}_{F_\psi}^2\Delta t}{2\widehat{\alpha}_{A_F}\nu}\|\mathbf{f}_\psi^n\|_{0,\Omega}^2 - \frac{\widehat{C}_{F_\theta}^2\Delta t}{2\widehat{\alpha}_{A_T}\kappa}\|f_\theta^n\|_{0,\Omega}^2 \\
&\geq \frac{1}{2}(\widehat{\alpha} + \Delta t(\gamma - C_{\mathbf{g}}))(\|\psi_h\|_{1,\Omega}^2 + \|\theta_h\|_{0,\Omega}^2) - \frac{\widehat{C}_{M_F}^2}{2\widehat{\alpha}_{M_F}}\|\psi_h^{n-1}\|_{1,\Omega}^2 - \frac{\widehat{C}_{M_T}^2}{2\widehat{\alpha}_{M_T}}\|\theta_h^{n-1}\|_{0,\Omega}^2 \\
&\quad - \frac{\widehat{C}_{F_\psi}^2\Delta t}{2\widehat{\alpha}_{A_F}\nu}\|\mathbf{f}_\psi^n\|_{0,\Omega}^2 - \frac{\widehat{C}_{F_\theta}^2\Delta t}{2\widehat{\alpha}_{A_T}\kappa}\|f_\theta^n\|_{0,\Omega}^2,
\end{aligned}$$

where we have used the facts that $\|\psi_h\|_{1,\Omega} \leq \|\psi_h\|_{2,\Omega}$, $\|\theta_h\|_{0,\Omega} \leq \|\theta_h\|_{1,\Omega}$ and

$$\frac{\Delta t}{2}\min\{\widehat{\alpha}_{A_F}\nu,\widehat{\alpha}_{A_T}\kappa\}(\|\psi_h\|_{2,\Omega}^2 + \|\theta_h\|_{1,\Omega}^2) \geq 0.$$

Thus, from assumption (5.4.3), we can set

$$\rho := (\widehat{\alpha} + \Delta t(\gamma - C_{\mathbf{g}}))^{-\frac{1}{2}}\left(\frac{\widehat{C}_{M_F}^2}{\widehat{\alpha}_{M_F}}\|\psi_h^{n-1}\|_{1,\Omega}^2 + \frac{\widehat{C}_{M_T}^2}{\widehat{\alpha}_{M_T}}\|\theta_h^{n-1}\|_{0,\Omega}^2 + \frac{\widehat{C}_{F_\psi}^2\Delta t}{\widehat{\alpha}_{A_F}\nu}\|\mathbf{f}_\psi^n\|_{0,\Omega}^2 + \frac{\widehat{C}_{F_\theta}^2\Delta t}{\widehat{\alpha}_{A_T}\kappa}\|f_\theta^n\|_{0,\Omega}^2\right)^{\frac{1}{2}}$$

and $\mathcal{S} := \left\{(\varphi_h, w_h) \in \mathrm{X}_{k,\ell}^h : |||(\varphi_h, w_h)||| \leq \rho\right\}$. Then, we have that

$$\langle \Phi(\psi_h,\theta_h),(\psi_h,\theta_h)\rangle \geq 0 \quad \text{for any} \quad (\psi_h,\theta_h) \in \partial\mathcal{S}.$$

Then, by employing the fixed point Theorem [103, Chap. IV, Corollary 1.1], there exists $(\psi_h^n, \theta_h^n) \in \mathcal{S}$, such that $\Phi(\psi_h^n, \theta_h^n) = \mathbf{0}$, i.e., the fully-discrete problem (5.4.1) admits at least one solution $(\psi_h^n, \theta_h^n) \in \mathcal{S}$ at every time step t_n. □

Remark 5.4.1. *From assumption (5.4.3) it follows that if $C_{\mathbf{g}} \leq \gamma$ then the condition (5.4.3) is always satisfied. Instead, if $C_{\mathbf{g}} > \gamma$, that is when the buoyancy term is strong when compared to the diffusion terms, a "small time step condition" $\Delta t < \widehat{\alpha}/(C_{\mathbf{g}} - \gamma)$ is needed in order to guarantee the existence of a discrete solution.*

The following result establishes that the fully-discrete scheme (5.4.1) is unconditionally stable.

Theorem 5.4.2. *Assume that* $\mathbf{f}_\psi \in \mathrm{L}^2(0,T;\mathbf{L}^2(\Omega))$, $f_\theta \in \mathrm{L}^2(0,T;\mathrm{L}^2(\Omega))$, $\mathbf{g} \in \mathrm{L}^\infty(0,T;\mathbf{L}^\infty(\Omega))$. *Moreover, suppose that the initial data satisfy* $\psi_0 \in \mathrm{H}_0^2(\Omega)$ *and* $\theta_0 \in \mathrm{H}_0^1(\Omega)$. *Then, the fully-discrete scheme* (5.4.1) *is unconditionally stable and satisfy the following estimate for any* $0 < m \leq N$

$$\|(\psi_h^m,\theta_h^m)\|_{\mathrm{H}^1(\Omega)\times\mathrm{L}^2(\Omega)} + \Big(\Delta t\sum_{n=1}^m \|(\psi_h^n,\theta_h^n)\|^2_{\mathrm{H}^2(\Omega)\times\mathrm{H}^1(\Omega)}\Big)^{\frac{1}{2}}$$
$$\leq C\Big(\Big(\Delta t\sum_{n=1}^m \|(\mathbf{f}_\psi^n,f_\theta^n)\|^2_{\mathbf{L}^2(\Omega)\times\mathrm{L}^2(\Omega)}\Big)^{\frac{1}{2}} + \|(\psi_0,\theta_0)\|_{\mathrm{H}^2(\Omega)\times\mathrm{H}^1(\Omega)}\Big) =: \delta,$$

where $C>0$ *is independent of* h *and* Δt.

Proof. Let $(\psi_h^n,\theta_h^n) \in \mathrm{W}_k^h \times \mathrm{H}_\ell^h$ be a solution of fully-discrete problem (5.4.1). We consider the following equivalent norms:

$$|||\phi_h|||_{F,h} := (M_F^h(\phi_h,\phi_h))^{1/2}, \quad |||v_h|||_{T,h} := (M_T^h(v_h,v_h))^{1/2} \quad \phi_h \in \mathrm{W}_k^h,\ \forall v_h \in \mathrm{H}_\ell^h. \tag{5.4.6}$$

Taking $v_h = \theta_h^n \in \mathrm{H}_\ell^h$ in the second equation of (5.4.1), using Lemma 5.3.3, the Young inequality and some identities of real numbers, we obtain

$$\frac{1}{2\Delta t}(|||\theta_h^n|||^2_{T,h} - |||\theta_h^{n-1}|||^2_{T,h}) + \widehat{\alpha}_{A_T}\kappa\|\theta_h^n\|^2_{1,\Omega} \leq C\|f_\theta^n\|^2_{0,\Omega} + \frac{1}{2}\widehat{\alpha}_{A_T}\kappa\|\theta_h^n\|^2_{1,\Omega}.$$

Then, multiplying by $2\Delta t$, using the equivalence of norms and summing for $n = 1,\dots,m$, we have that

$$\|\theta_h^m\|^2_{0,\Omega} + \Delta t\sum_{n=1}^m \|\theta_h^n\|^2_{1,\Omega} \leq C\Big(\Delta t\sum_{n=1}^m \|f_\theta^n\|^2_{0,\Omega} + \|\theta_h^0\|^2_{0,\Omega}\Big). \tag{5.4.7}$$

Analogously, taking $\phi_h = \psi_h^n \in \mathrm{W}_k^h$ in the first equation of (5.4.1) and repeating the same arguments, we obtain

$$|||\psi_h^n|||^2_{F,h} - |||\psi_h^{n-1}|||^2_{F,h} + \widehat{\alpha}_{A_F}\nu\Delta t\|\psi_h^n\|^2_{2,\Omega} \leq C\Delta t C_{\mathbf{g}}\|\theta_h^n\|^2_{0,\Omega} + C\Delta t\|\mathbf{f}_\psi^n\|^2_{0,\Omega}, \tag{5.4.8}$$

where the constant $C_{\mathbf{g}}$ is defined in Theorem 5.4.1.

Now, summing for $n = 1,\dots,m$, inserting (5.4.7) in (5.4.8) and using the equivalence of norms and, we get

$$\|\psi_h^m\|^2_{1,\Omega} + \Delta t\sum_{n=1}^m \|\psi_h^n\|^2_{2,\Omega} \leq C\Big(\Delta t\sum_{n=1}^m \big(\|\mathbf{f}_\psi^n\|^2_{0,\Omega} + \|f_\theta^n\|^2_{0,\Omega}\big) + \|\psi_h^0\|^2_{1,\Omega} + \|\theta_h^0\|^2_{0,\Omega}\Big), \tag{5.4.9}$$

where the constant $C_{\mathbf{g}}$ was included in the constant C to shorten the bound.

Finally, the desired result follows adding (5.4.7) and (5.4.9). $\square$

The following result establishes that the solution of scheme (5.4.1) is unique for small values of Δt.

Theorem 5.4.3. *Let $\widehat{\alpha}_{M_F}, \widehat{\alpha}_{M_T}, \widehat{C}_{B_F}$ and $\widehat{C}_{B_T}$ be the constants in Lemma 5.3.3. Moreover, let δ be the upper bound in Theorem 5.4.2, $C_{\mathtt{g}}$ be the constant defined in Theorem 5.4.1 and $C_{\mathtt{inv}}$ be the constant in (5.4.2). Assume that*

$$\Delta t < \min\{\widehat{\alpha}_{M_F}, \widehat{\alpha}_{M_T}\} \min\left\{ \frac{h_{\min}^2}{2C_{\mathtt{inv}}^2(\widehat{C}_{B_F} + \widehat{C}_{B_T})\delta}, \frac{1}{2C_{\mathtt{g}}} \right\}. \tag{5.4.10}$$

Then, for each $n = 1, \ldots, N$ the solution of the fully-discrete scheme (5.4.1) is unique.

Proof. Let $1 \leq n \leq N$ and $(\psi_{h1}^n, \theta_{h1}^n), (\psi_{h2}^n, \theta_{h2}^n) \in \mathrm{W}_k^h \times \mathrm{H}_\ell^h$ be two solutions of problem (5.4.1). Then, setting $\widetilde{\psi_h^n} := \psi_{h1}^n - \psi_{h2}^n$, $\widetilde{\theta_h^n} := \theta_{h1}^n - \theta_{h2}^n$ and using the definition of operator (5.4.4), for all $(\phi_h, v_h) \in \mathrm{W}_k^h \times \mathrm{H}_\ell^h$, we have that

$$\begin{aligned} &M_F^h(\widetilde{\psi_h^n}, \phi_h) + M_T^h(\widetilde{\theta_h^n}, v_h) + \nu\Delta t A_F^h(\widetilde{\psi_h^n}, \phi_h) + \kappa\Delta t A_T^h(\widetilde{\theta_h^n}, v_h) - \Delta t C^h(\widetilde{\theta_h^n}, \phi_h) \\ &\quad + \Delta t(B_F^h(\psi_{h1}^n; \psi_{h1}^n, \phi_h) - B_F^h(\psi_{h2}^n; \psi_{h2}^n, \phi_h)) \\ &\quad + \Delta t(B_{\text{skew}}^h(\psi_{h1}^n; \theta_{h1}^n, v_h) - B_{\text{skew}}^h(\psi_{h2}^n; \theta_{h2}^n, v_h)) = 0. \end{aligned} \tag{5.4.11}$$

Adding and subtracting $B_F^h(\psi_{h2}^n; \psi_{h1}^n, \phi_h)$ and $B_{\text{skew}}^h(\psi_{h2}^n; \theta_{h1}^n, v_h)$ we obtain

$$\begin{aligned} B_F^h(\psi_{h1}^n; \psi_{h1}^n, \phi_h) - B_F^h(\psi_{h2}^n; \psi_{h2}^n, \phi_h) &= B_F^h(\widetilde{\psi_h^n}; \psi_{h1}^n, \phi_h) + B_F^h(\psi_{h2}^n; \widetilde{\psi_h^n}, \phi_h) \\ B_{\text{skew}}^h(\psi_{h1}^n; \theta_{h1}^n, v_h) - B_{\text{skew}}^h(\psi_{h2}^n; \theta_{h2}^n, v_h) &= B_{\text{skew}}^h(\widetilde{\psi_h^n}; \theta_{h1}^n, v_h) + B_{\text{skew}}^h(\psi_{h2}^n; \widetilde{\theta_h^n}, v_h). \end{aligned}$$

Next, taking $\phi_h = \widetilde{\psi_h^n}$ and $v_h = \widetilde{\theta_h^n}$ in (5.4.11), from the above identities, the skew-symmetry of trilinear forms, the continuity and coercivity properties of the multilinear forms involved (cf. Lemma 5.3.3), it follows

$$\begin{aligned} &\widehat{\alpha}_{M_F}\|\widetilde{\psi_h^n}\|_{1,\Omega}^2 + \widehat{\alpha}_{M_T}\|\widetilde{\theta_h^n}\|_{0,\Omega}^2 + \widehat{\alpha}_{A_F}\nu\Delta t\|\widetilde{\psi_h^n}\|_{2,\Omega}^2 + \widehat{\alpha}_{A_T}\kappa\Delta t\|\widetilde{\theta_h^n}\|_{1,\Omega}^2 \\ &\leq \Delta t\widehat{C}_{B_F}\|\widetilde{\psi_h^n}\|_{2,\Omega}\|\psi_{h1}^n\|_{2,\Omega}\|\widetilde{\psi_h^n}\|_{2,\Omega} + \Delta t\widehat{C}_{B_T}\|\widetilde{\psi_h^n}\|_{2,\Omega}\|\theta_{h1}^n\|_{1,\Omega}\|\widetilde{\theta_h^n}\|_{1,\Omega} + \Delta t C_{\mathtt{g}}\|\widetilde{\theta_h^n}\|_{0,\Omega}\|\widetilde{\psi_h^n}\|_{1,\Omega} \\ &\leq \Delta t\big(\widehat{C}_{B_F}\|\psi_{h1}^n\|_{2,\Omega} + \widehat{C}_{B_T}\|\theta_{h1}^n\|_{1,\Omega}\big)\|(\widetilde{\psi_h^n}, \widetilde{\theta_h^n})\|_{\mathrm{H}^2(\Omega)\times\mathrm{H}^1(\Omega)}^2 + \Delta t C_{\mathtt{g}}\|(\widetilde{\psi_h^n}, \widetilde{\theta_h^n})\|_{\mathrm{H}^1(\Omega)\times\mathrm{L}^2(\Omega)}^2. \end{aligned}$$

Now, employing local inverse inequalities (5.4.2) in the above estimate and Theorem 5.4.2, we get

$$\begin{aligned} &\min\{\widehat{\alpha}_{M_F}, \widehat{\alpha}_{M_F}\}\|(\widetilde{\psi_h^n}, \widetilde{\theta_h^n})\|_{\mathrm{H}^1(\Omega)\times\mathrm{L}^2(\Omega)}^2 \\ &\leq \Big[C_{\mathtt{inv}}h_{\min}^{-1}\Delta t\big((\widehat{C}_{B_F} + \widehat{C}_{B_T})C_{\mathtt{inv}}h_{\min}^{-1}\delta\big) + \Delta t C_{\mathtt{g}}\Big]\|(\widetilde{\psi_h^n}, \widetilde{\theta_h^n})\|_{\mathrm{H}^1(\Omega)\times\mathrm{L}^2(\Omega)}^2. \end{aligned}$$

From the assumption (5.4.10), we have that

$$\frac{1}{\min\{\widehat{\alpha}_{M_F}, \widehat{\alpha}_{M_F}\}}\big(C_{\mathtt{inv}}h_{\min}^{-1}(\widehat{C}_{B_F} + \widehat{C}_{B_T})C_{\mathtt{inv}}h_{\min}^{-1}\delta + C_{\mathtt{g}}\big) < 1. \tag{5.4.12}$$

Thus, $\widetilde{\psi_h^n} = 0$ and $\widetilde{\theta_h^n} = 0$, which implies $\psi_{h1}^n = \psi_{h2}^n$ and $\theta_{h1}^n = \theta_{h2}^n$. The proof is complete. □

Remark 5.4.2. *Exploiting the fact that we are in the two dimensional case and using sharper Sobolev bounds for the convective terms (i.e., employing the Hölder inequality, Sobolev bounds with adequate exponents and an inverse inequality), we could get a power $h_{\min}^{-\epsilon}$, for all $\epsilon > 0$, instead of $h_{\min}^{-1}$ in the term $h_{\min}^{-1}\delta$ (see equation (5.4.12)).*

5.5 Convergence analysis

This section is devoted to the convergence analysis of the fully-discrete formulation (5.4.1) introduced in the previous section. We start recalling some preliminary results of approximation in the polynomial and virtual spaces. Moreover, we introduce an energy operator associated to the H^2-inner product with its corresponding approximation properties. Later on, we state technical results, which will be useful to provide the convergence result of our fully-discrete virtual scheme.

5.5.1 Preliminary results

First, we recall the following polynomial approximation result (see for instance [54]). Here below E represents as usual a generic element of $\{\Omega_h\}_{h>0}$, which we recall satisfies assumptions **A1**, **A2** in Section 5.3.1.

Proposition 5.5.1. *Let $m \in \mathbb{R}$ and $n \in \mathbb{N} \cup \{0\}$. Then, for each $\phi \in \mathrm{H}^m(K)$, there exist $\phi_\pi \in \mathbb{P}_n(K)$, and $C > 0$ independent of h_K, such that*

$$\|\phi - \phi_\pi\|_{t,K} \leq C h_K^{m-t} |\phi|_{m,K}, \quad 0 \leq m \leq n+1,\ t = 0, \ldots, [m],$$

with $[m]$ denoting the largest integer equal or smaller than m.

Standard arguments and (5.3.5) lead easily to following approximation properties for the projectors Π_K^n (an analogous result can be obtained the vectorial version).

Proposition 5.5.2. *Let $m \in \mathbb{R}$, $n \in \mathbb{N} \cup \{0\}$ and let Π_K^n be the projection defined in (2.3.5). Then, for each $\phi \in \mathrm{H}^m(K)$, there exists a constant C, independent of K and h_K, such that*

$$\|\phi - \Pi_K^n \phi\|_{t,K} \leq C h_K^{m-t} |\phi|_{m,K}, \quad 0 \leq m \leq n+1,\ t = 0, \ldots, [m],$$

with $[m]$ denoting the largest integer equal or smaller than m.

Now, we continue with the following approximation for the stream-function and temperature virtual element spaces, which can be found in [105, 38, 58] and [134, 65, 28], respectively.

Proposition 5.5.3. *Let $m \in \mathbb{R}$. Then, for each $\phi \in \mathrm{H}^m(\Omega)$, there exist $\phi_I \in \mathrm{W}_k^h$ and $C_I > 0$, independent of h, such that*

$$\|\phi - \phi_I\|_{t,\Omega} \leq C_I h^{m-t} |\phi|_{m,\Omega}, \quad t = 0, 1, 2, \quad 2 < m \leq k+1, \quad k \geq 2.$$

For the temperature variable, we present local and global approximation properties.

Proposition 5.5.4. *Let $m \in \mathbb{R}$. Then, for each $v \in \mathrm{H}^m(\Omega)$, there exist $v_I \in \mathrm{H}_\ell^h$ and $C_I > 0$, independent of h, such that*

$$\|v - v_I\|_{t,K} \leq C_I h_K^{m-t} |v|_{m,K} \quad \forall K \in \mathcal{T}_h; \quad \|v - v_I\|_{t,\Omega} \leq C_I h^{m-t} |v|_{m,\Omega},$$

with $t = 0, 1$, $1 < m \leq \ell + 1$, $\ell \geq 1$.

Now, we will introduce the following discrete biharmonic projection associated with the stream-function discretization. For each $\varphi \in \mathrm{H}_0^2(\Omega)$, we consider the operator $\mathcal{S}_h : \mathrm{H}_0^2(\Omega) \to \mathrm{W}_k^h$, defined as the solution of problem:

$$A_F^h(\mathcal{S}_h\varphi, \phi_h) = A_F(\varphi, \phi_h) \qquad \forall \phi_h \in \mathrm{W}_k^h, \tag{5.5.1}$$

where $A_F(\cdot,\cdot)$ was defined in (5.2.5) and we recall that $A_F^h(\cdot,\cdot)$ is the global version of the form defined in (5.3.8). By using the ellipticity and continuity of the bilinear form $A_F^h(\cdot,\cdot)$ (cf. Lemma 5.3.3) and the Lax-Milgram Lemma, we have that the above problem (5.5.1) is well-posed.

By using Propositions 5.3.1, 5.5.1 and 5.5.3, the following approximation result for the energy projection $\mathcal{S}_h(\cdot)$ holds true (see [3, Lemma 5.3]).

Proposition 5.5.5. *For each $\varphi \in \mathrm{H}_0^2(\Omega)$, there exists a unique function $\mathcal{S}_h\varphi \in \mathrm{W}_k^h$ satisfying (5.5.1). Moreover, if $\varphi \in \mathrm{H}^{2+s}(\Omega)$, with $\frac{1}{2} < s \leq k-1$, then the following approximation property holds:*

$$\|\varphi - \mathcal{S}_h\varphi\|_{1,\Omega} + h^{\tilde{s}}\|\varphi - \mathcal{S}_h\varphi\|_{2,\Omega} \leq C h^{\tilde{s}+s}|\varphi|_{2+s,\Omega},$$

where C is a positive constant, independent of h and $\tilde{s} \in (\frac{1}{2}, 1]$ depends on the largest re-entrant angle of the domain Ω. In particular, when Ω is a convex domain it holds $\tilde{s} = 1$.

In what follows, we will establish four technical lemmas involving the trilinear forms associated to transport/convection and the bilinear form associated to the buoyancy term; these results will be useful in subsection 5.5.2.

Lemma 5.5.1. *For all $\zeta_h; \varphi_h, \phi_h \in \mathrm{W}_k^h$, there exists $\widehat{C}_{B_F} > 0$, independent of h, such that*

$$|B_F^h(\zeta_h; \varphi_h, \phi_h)| \leq \widehat{C}_{B_F}\, \|\zeta_h\|_{2,\Omega}\|\varphi_h\|_{2,\Omega}\|\phi_h\|_{2,\Omega}^{\frac{1}{2}}\|\phi_h\|_{1,\Omega}^{\frac{1}{2}}.$$

Proof. We use the definition of the trilinear form $B_F^h(\cdot;\cdot,\cdot)$ (cf. (5.3.9)), the Hölder inequality, the continuity of the operators Π_K^{k-2} and $\boldsymbol{\Pi}_K^{k-1}$ with respect to the L^2- and L^4-norms, respectively (cf. properties (5.3.5)), and the Hölder inequality for sequences, to obtain

$$\begin{aligned} B_F^h(\zeta_h; \varphi_h, \phi_h) &\leq \sum_{K \in \mathcal{T}_h} \|\Pi_K^{k-2}\Delta\zeta_h\|_{0,K}\|\boldsymbol{\Pi}_K^{k-1}\mathbf{curl}\,\varphi_h\|_{\mathrm{L}^4(K)}\|\boldsymbol{\Pi}_K^{k-1}\nabla\phi_h\|_{\mathrm{L}^4(K)} \\ &\leq C\|\Delta\zeta_h\|_{0,\Omega}\|\mathbf{curl}\,\varphi_h\|_{\mathrm{L}^4(\Omega)}\|\nabla\phi_h\|_{\mathrm{L}^4(\Omega)} \\ &\leq C\|\Delta\zeta_h\|_{0,\Omega}\|\varphi_h\|_{2,\Omega}\|\nabla\phi_h\|_{\mathrm{L}^4(\Omega)}, \end{aligned}$$

where we have used the Sobolev inclusion $\mathrm{H}^1(\Omega) \hookrightarrow \mathrm{L}^4(\Omega)$. Now, applying the Ladyzhenskaya inequality (5.2.14) with $\mathbf{v} = \nabla\phi_h$ we obtain the desired result. □

Lemma 5.5.2. *For all $\zeta, \varphi, \phi \in \mathrm{H}_0^2(\Omega)$, we have that*

$$B_F^h(\varphi; \varphi, \phi) - B_F^h(\zeta; \zeta, \phi) = B_F^h(\varphi; \varphi - \zeta + \phi, \phi) + B_F^h(\varphi - \zeta + \phi; \zeta, \phi) - B_F^h(\phi; \zeta, \phi).$$

Proof. The proof follows by adding and subtracting suitable terms, and using the trilineality and skew-symmetry properties of the form $B_F^h(\cdot;\cdot,\cdot)$. □

Next lemmas give us the measure of the variational crime in the discretization of the trilinear forms $B_F(\cdot;\cdot,\cdot)$ and $B_{\text{skew}}(\cdot;\cdot,\cdot)$ and the bilinear form $C(\cdot,\cdot)$.

Lemma 5.5.3. *Let $\varphi(t) \in \mathrm{H}_0^2(\Omega) \cap \mathrm{H}^{2+s}(\Omega)$, with $\frac{1}{2} < s \leq k-1$, for almost all $t \in (0,T)$. Then, there exists $C > 0$, independent of mesh size h, such that*

$$|B_F(\varphi;\varphi,\phi_h) - B_F^h(\varphi;\varphi,\phi_h)| \leq Ch^s\big(\|\varphi\|_{1+s,\Omega} + \|\varphi\|_{2,\Omega}\big)\|\varphi\|_{2+s,\Omega}\|\phi_h\|_{2,\Omega} \quad \forall \phi_h \in \mathrm{W}_k^h.$$

Proof. The proof has been established in [3, Lemma 5.4]. □

Lemma 5.5.4. *Let $\frac{1}{2} < \gamma \leq \min\{k-1,\ell\}$. Assume that $\varphi(t) \in \mathrm{H}_0^2(\Omega) \cap \mathrm{H}^{2+\gamma}(\Omega)$ and $v(t) \in \mathrm{H}_0^1(\Omega) \cap \mathrm{H}^{1+\gamma}(\Omega)$, for almost all $t \in (0,T)$. Then, there exists $C > 0$, independent of mesh size h, such that, a.e. $t \in (0,T)$,*

$$|B_{\text{skew}}(\varphi;v,w_h) - B_{\text{skew}}^h(\varphi;v,w_h)| \leq Ch^\gamma\|\varphi\|_{1+\gamma,\Omega}\|v\|_{1+\gamma,\Omega}\|w_h\|_{1,\Omega} \quad \forall w_h \in \mathrm{H}_\ell^h. \tag{5.5.2}$$

Moreover, assume that $\mathbf{g}(t) \in \mathbf{H}^\gamma(\Omega) \cap \mathbf{L}^\infty(\Omega)$, for almost all $t \in (0,T)$. Then, a.e. $t \in (0,T)$,

$$|C(v,\phi_h) - C^h(v,\phi_h)| \leq Ch^\gamma \max\{\|\mathbf{g}\|_{\gamma,\Omega}, \|\mathbf{g}\|_{\infty,\Omega}\}\|v\|_{1+\gamma,\Omega}\|\phi_h\|_{1,\Omega} \quad \forall \phi_h \in \mathrm{W}_k^h. \tag{5.5.3}$$

Proof. To prove estimate (5.5.2), we split the consistency error as

$$B_{\text{skew}}(\varphi;v,w_h) - B_{\text{skew}}^h(\varphi;v,w_h) = \frac{1}{2}\left(\beta_1(w_h) + \beta_2(w_h)\right), \tag{5.5.4}$$

where

$$\beta_1(w_h) := \sum_{K\in\mathcal{T}_h}\Big(B_T^K(\varphi;v,w_h) - B_T^{h,K}(\varphi;v,w_h)\Big),$$
$$\beta_2(w_h) := \sum_{K\in\mathcal{T}_h}\Big(B_T^K(\varphi;w_h,v) - B_T^{h,K}(\varphi;w_h,v)\Big).$$

In what follows, we will establish bounds for the terms $\beta_1(w_h)$ and $\beta_2(w_h)$. Indeed, for the term $\beta_1(w_h)$ we have

$$\begin{aligned}
&\beta_1(w_h) = \sum_{K\in\mathcal{T}_h}\int_K(\mathbf{curl}\,\varphi\cdot\nabla v)w_h - \int_K(\boldsymbol{\Pi}_K^{k-1}\mathbf{curl}\,\varphi\cdot\boldsymbol{\Pi}_K^{\ell-1}\nabla v)\Pi_K^{\ell-1}w_h \\
&= \sum_{K\in\mathcal{T}_h}\int_K(\mathbf{curl}\,\varphi\cdot\nabla v)(w_h - \Pi_K^{\ell-1}w_h) + \sum_{K\in\mathcal{T}_h}\int_K\left(\mathbf{curl}\,\varphi\cdot(\nabla v - \boldsymbol{\Pi}_K^{\ell-1}\nabla v)\right)\Pi_K^{\ell-1}w_h \\
&\quad + \sum_{K\in\mathcal{T}_h}\int_K\left((\mathbf{curl}\,\varphi - \boldsymbol{\Pi}_K^{k-1}\mathbf{curl}\,\varphi)\cdot\boldsymbol{\Pi}_K^{\ell-1}\nabla v\right)\Pi_K^{\ell-1}w_h \\
&=: T_1 + T_2 + T_3.
\end{aligned} \tag{5.5.5}$$

In order to bound the terms T_1, first we consider the case $1/2 < \gamma \leq 1$. Then, by using approximation property of $\Pi_K^{\ell-1}$ and the Hölder inequality, it follows

$$\begin{aligned}
T_1 &\leq \sum_{K\in\mathcal{T}_h}\|\mathbf{curl}\,\varphi\|_{\mathrm{L}^4(K)}\|\nabla v\|_{\mathrm{L}^4(K)}\|w_h - \Pi_K^{\ell-1}w_h\|_{0,K} \\
&\leq C\sum_{K\in\mathcal{T}_h}\|\mathbf{curl}\,\varphi\|_{\mathrm{L}^4(K)}\|\nabla v\|_{\mathrm{L}^4(K)}h_K|w_h|_{1,K} \\
&\leq Ch^\gamma\|\varphi\|_{1+\gamma,\Omega}\|v\|_{1+\gamma,\Omega}\|w_h\|_{1,\Omega}.
\end{aligned}$$

On the other hand, for the case $1 < \gamma \leq \ell$, we use orthogonality property of $\Pi_K^{\ell-1}$, the Hölder inequality (for sequences), to obtain

$$T_1 = \sum_{K\in\mathcal{T}_h} \int_K (\mathbf{curl}\,\varphi \cdot \nabla v - \Pi_K^{\ell-1}(\mathbf{curl}\,\varphi \cdot \nabla v))(w_h - \Pi_K^{\ell-1} w_h).$$

Now, we apply [26, Theorem 7.4], with $s = \gamma - 1$, $s_1 = s_2 = \gamma$ and $p = p_1 = p_2 = 2$ to obtain $\mathbf{curl}\,\varphi \cdot \nabla v \in \mathrm{H}^{\gamma-1}(\Omega)$ and $|\mathbf{curl}\,\varphi \cdot \nabla v|_{\gamma-1,\Omega} \leq C\|\varphi\|_{1+\gamma,\Omega}\|v\|_{1+\gamma,\Omega}$.

Thus, by using Proposition 5.5.2 and the above facts, we arrive

$$T_1 \leq Ch^{\gamma-1}|\mathbf{curl}\,\varphi \cdot \nabla v|_{\gamma-1,\Omega} h\|w_h\|_{1,\Omega} \leq Ch^{\gamma}\|\varphi\|_{1+\gamma,\Omega}\|v\|_{1+\gamma,\Omega}\|w_h\|_{1,\Omega}.$$

Collecting the above inequalities, for $\frac{1}{2} < \gamma \leq \ell$, we have

$$T_1 \leq Ch^{\gamma}\|\varphi\|_{1+\gamma,\Omega}\|v\|_{1+\gamma,\Omega}\|w_h\|_{1,\Omega}. \tag{5.5.6}$$

Now, for the term T_2 we proceed as follows. First, we apply the Hölder inequality, then by using stability and approximation properties of the L^2-projectors (cf. properties (5.3.5) and Proposition 5.5.2), Sobolev embedding and the Hölder inequality for sequences, we get

$$\begin{aligned} T_2 &\leq \sum_{K\in\mathcal{T}_h} \|\mathbf{curl}\,\varphi\|_{\mathrm{L}^4(K)}\|\nabla v - \boldsymbol{\Pi}_K^{\ell-1}\nabla v\|_{0,K}\|\Pi_K^{\ell-1}w_h\|_{\mathrm{L}^4(K)} \\ &\leq Ch^{\gamma}\|\varphi\|_{1+\gamma,\Omega}\|v\|_{1+\gamma,\Omega}\|w_h\|_{1,\Omega}. \end{aligned} \tag{5.5.7}$$

For the term T_3, we follow similar arguments, to obtain

$$T_3 \leq Ch^{\gamma}\|\varphi\|_{1+\gamma,\Omega}\|v\|_{1+\gamma,\Omega}\|w_h\|_{1,\Omega}. \tag{5.5.8}$$

From the bounds (5.5.5), (5.5.6), (5.5.7) and (5.5.8), we conclude that

$$\beta_1(w_h) \leq Ch^{\gamma}\|\varphi\|_{1+\gamma,\Omega}\|v\|_{1+\gamma,\Omega}\|w_h\|_{1,\Omega}. \tag{5.5.9}$$

Now, we will focus on the term $\beta_2(w_h)$. To estimate this term, first we add and subtract suitable expressions to obtain

$$\begin{aligned} \beta_2(w_h) &= \sum_{K\in\mathcal{T}_h} \int_K (\mathbf{curl}\,\varphi \cdot \nabla w_h)v - \int_K (\boldsymbol{\Pi}_K^{k-1}\mathbf{curl}\,\varphi \cdot \boldsymbol{\Pi}_K^{\ell-1}\nabla w_h)\Pi_K^{\ell-1}v \\ &= \sum_{K\in\mathcal{T}_h} \int_K v(\mathbf{curl}\,\varphi)\cdot(\nabla w_h - \boldsymbol{\Pi}_K^{\ell-1}\nabla w_h) \\ &\quad + \sum_{K\in\mathcal{T}_h} \int_K \left(\mathbf{curl}\,\varphi - \boldsymbol{\Pi}_K^{k-1}\mathbf{curl}\,\varphi\right)\cdot v\boldsymbol{\Pi}_K^{\ell-1}\nabla w_h \\ &\quad + \sum_{K\in\mathcal{T}_h} \int_K \left(\boldsymbol{\Pi}_K^{k-1}\mathbf{curl}\,\varphi \cdot \boldsymbol{\Pi}_K^{\ell-1}\nabla w_h\right)(v - \Pi_K^{\ell-1}v) \\ &=: I_1 + I_2 + I_3. \end{aligned}$$

Applying orthogonality and approximation properties of $\boldsymbol{\Pi}_K^{\ell-1}$, we have

$$\begin{aligned} I_1 &= \sum_{K\in\mathcal{T}_h} \int_K (v(\mathbf{curl}\,\varphi) - \boldsymbol{\Pi}_K^{\ell-1}(v(\mathbf{curl}\,\varphi)))\cdot(\nabla w_h - \boldsymbol{\Pi}_K^{\ell-1}\nabla w_h) \\ &\leq C\sum_{K\in\mathcal{T}_h} h_K^{\gamma}|v(\mathbf{curl}\,\varphi)|_{\gamma,K}|w_h|_{1,K} \leq Ch^{\gamma}|v(\mathbf{curl}\,\varphi)|_{\gamma,\Omega}\|w_h\|_{1,\Omega}. \end{aligned}$$

Then, applying again [26, Theorem 7.4], now with $s = \gamma$, $s_1 = \gamma + 1$, $s_2 = \gamma$ and $p = p_1 = p_2 = 2$, we get

$$|v(\mathbf{curl}\, \varphi)|_{\gamma,\Omega} \leq C\|v\|_{1+\gamma,\Omega}\|\varphi\|_{1+\gamma,\Omega}.$$

From the two bounds above, we obtain

$$I_1 \leq Ch^\gamma\|\varphi\|_{1+\gamma,\Omega}\|v\|_{1+\gamma,\Omega}\|w_h\|_{1,\Omega}.$$

The terms I_2 and I_3 can be estimated using similar arguments. We conclude that

$$\beta_2(w_h) \leq Ch^\gamma\|\varphi\|_{2+\gamma,\Omega}\|v\|_{1+\gamma,\Omega}\|w_h\|_{1,\Omega}. \tag{5.5.10}$$

The proof of (5.5.2) follows from (5.5.4), (5.5.9) and (5.5.10).

Next, we will prove property (5.5.3). Let $\phi_h \in \mathrm{W}_k^h$, then adding and subtracting the term $\mathbf{g}v \cdot \mathbf{\Pi}_K^{k-1}\mathbf{curl}\,\phi_h$ and by using orthogonality, stability and approximations properties of the L^2-projections, we have

$$\begin{aligned}
C(v, \phi_h) - C^h(v, \phi_h) &= \sum_{K\in\mathcal{T}_h} \int_K (\mathbf{g}v - \mathbf{\Pi}_K^{k-1}(\mathbf{g}v)) \cdot (\mathbf{curl}\,\phi_h - \mathbf{\Pi}_K^{k-1}\mathbf{curl}\,\phi_h) \\
&\quad + \int_K \mathbf{g}(v - \Pi_K^{\ell-1}v) \cdot \mathbf{\Pi}_K^{k-1}\mathbf{curl}\,\phi_h \\
&\leq C \sum_{K\in\mathcal{T}_h} (h_K^\gamma|\mathbf{g}v|_{\gamma,K}\|\mathbf{curl}\,\phi_h\|_{0,K} + h_K^\gamma\|\mathbf{g}\|_{\mathrm{L}^\infty(K)}\|v\|_{\gamma,K}\|\mathbf{curl}\,\phi_h\|_{0,K}) \\
&\leq Ch^\gamma(\|\mathbf{g}\|_{\gamma,\Omega}\|v\|_{1+\gamma,\Omega}\|\phi_h\|_{1,\Omega} + h_K^\gamma\|\mathbf{g}\|_{\infty,\Omega}\|v\|_{\gamma,\Omega}\|\phi_h\|_{1,\Omega}),
\end{aligned}$$

where we have used analogous step to those used to bound I_1. The proof is complete. □

We finish this subsection recalling a discrete Gronwall inequality, which will be useful to derive the error estimate of the fully-discrete virtual scheme (5.4.1).

Lemma 5.5.5. *Let $D \geq 0$, a_j, b_j, c_j and λ_j be non negative numbers for any integer $j \geq 0$, such that*

$$a_n + \Delta t\sum_{j=0}^n b_j \leq \Delta t\sum_{j=0}^n \lambda_j a_j + \Delta t\sum_{j=0}^n c_j + D, \quad n \geq 0.$$

Suppose that $\Delta t\lambda_j < 1$ for all j, and set $\sigma_j := (1 - \Delta t\lambda_j)^{-1}$. Then, the following bound holds

$$a_n + \Delta t\sum_{j=0}^n b_j \leq \exp\Big(\Delta t\sum_{j=0}^n \sigma_j\lambda_j\Big)\Big(\Delta t\sum_{j=0}^n c_j + D\Big).$$

5.5.2 Error estimates for the fully-discrete scheme

In this subsection we will provide a convergence result for the fully-discrete problem (5.4.1) under suitable regularity conditions for the exact solution.

We start denoting $(\psi(t_n), \theta(t_n))$ as (ψ^n, θ^n) at each time level t_n, and splitting the stream-function error as follows:

$$\psi^n - \psi_h^n = (\psi^n - \mathcal{S}_h\psi^n) - (\psi_h^n - \mathcal{S}_h\psi^n) =: \eta_\psi^n - \varphi_\psi^n.$$

For the temperature variable we will exploit the virtual interpolant presented in Proposition 5.5.4, to split the error as:

$$\theta^n - \theta_h^n = (\theta^n - \theta_I^n) - (\theta_h^n - \theta_I^n) =: \eta_\theta^n - \varphi_\theta^n,$$

where θ_I^n is the interpolant of θ^n in the virtual space H_ℓ^h.

Error estimates for the terms η_θ^n and η_ψ^n are given by Propositions 5.5.4 and 5.5.5, respectively. Therefore, we will focus on the terms φ_ψ^n and φ_θ^n.

We start establishing error equations of the momentum and energy identities. Indeed, by using the fully-discrete scheme (5.4.1), the continuous weak formulation (5.2.13) and the biharmonic energy projection $\mathcal{S}_h$ defined in (5.5.1), we have the following error equation for the momentum identity (where we have taken $\phi_h = \varphi_\psi^n \in \mathrm{W}_k^h$)

$$\begin{aligned}
M_F^h\left(\frac{\varphi_\psi^n - \varphi_\psi^{n-1}}{\Delta t}, \varphi_\psi^n\right) + \nu A_F^h(\varphi_\psi^n, \varphi_\psi^n) &= \Big(F_\psi^h(\varphi_\psi^n) - F_\psi(\varphi_\psi^n)\Big) \\
&+ \Big(B_F(\psi^n; \psi^n, \varphi_\psi^n) - B_F^h(\psi_h^n; \psi_h^n, \varphi_\psi^n)\Big) \\
&+ \left(M_F(\partial_t\psi^n, \varphi_\psi^n) - M_F^h\Big(\frac{\mathcal{S}_h\psi^n - \mathcal{S}_h\psi^{n-1}}{\Delta t}, \varphi_\psi^n\Big)\right) \\
&+ \Big(C^h(\theta_h^n, \varphi_\psi^n) - C(\theta^n, \varphi_\psi^n)\Big) \\
&=: T_F + T_B + T_M + T_C.
\end{aligned} \tag{5.5.11}$$

Analogously, recalling that $\varphi_\theta^n = \theta_h^n - \theta_I^n$, and using the definition of the continuous and discrete problems (cf. (5.2.13) and (5.4.1), respectively) for the energy equation, we have that

$$\begin{aligned}
&M_T^h\left(\frac{\varphi_\theta^n - \varphi_\theta^{n-1}}{\Delta t}, \varphi_\theta^n\right) + \kappa A_T^h(\varphi_\theta^n, \varphi_\theta^n) = \Big(F_\theta^h(\varphi_\theta^n) - F_\theta(\varphi_\theta^n)\Big) \\
&+ \Big(B_{\text{skew}}(\psi^n; \theta^n, \varphi_\theta^n) - B_{\text{skew}}^h(\psi_h^n; \theta_h^n, \varphi_\theta^n)\Big) \\
&+ \left(M_T(\partial_t\theta^n, \varphi_\theta^n) - M_T^h\Big(\frac{\theta_I^n - \theta_I^{n-1}}{\Delta t}, \varphi_\theta^n\Big)\right) + \kappa\left(A_T(\theta^n, \varphi_\theta^n) - A_T^h(\theta_I^n, \varphi_\theta^n)\right) \\
&=: I_F + I_B + I_M + I_A.
\end{aligned} \tag{5.5.12}$$

The next step is to establish error estimates for the momentum and energy equations (5.5.11) and (5.5.12). The following two lemmas provide such bounds and will be useful to obtain the convergence result for the fully-discrete problem (5.4.1).

Lemma 5.5.6 (Error estimate for the momentum equation)**.** *Suppose that the external forces satisfy* $\mathbf{f}_\psi \in \mathrm{L}^\infty(0,T;\mathbf{H}^s(\Omega))$ *and* $\mathbf{g} \in \mathrm{L}^\infty(0,T;\mathbf{H}^{\min\{s,r\}}(\Omega) \cap \mathbf{L}^\infty(\Omega))$*, with* $\frac{1}{2} < s \leq k-1$ *and* $1 \leq r \leq \ell$*. Let* $(\psi^n, \theta^n) \in \mathrm{H}_0^2(\Omega) \times \mathrm{H}_0^1(\Omega)$ *be the solution of problem* (5.2.13) *at time* $t = t_n$*. Moreover, assume that*

$$\begin{aligned}
&\psi \in \mathrm{L}^\infty(0,T;\mathrm{H}^{2+s}(\Omega)), \quad \partial_t\psi \in \mathrm{L}^1(0,T;\mathrm{H}^{1+s}(\Omega)), \\
&\partial_{tt}\psi \in \mathrm{L}^1(0,T;\mathrm{H}^1(\Omega)), \quad \theta \in \mathrm{L}^\infty(0,T;\mathrm{H}^r(\Omega)).
\end{aligned}$$

Let $(\psi_h^n, \theta_h^n) \in \mathrm{W}_k^h \times \mathrm{H}_\ell^h$ be the virtual element solution generated by scheme (5.4.1). Then, the following error estimate holds

$$\begin{aligned}
&\frac{1}{2\Delta t}\left(|||\varphi_\psi^n|||_{F,h}^2 - |||\varphi_\psi^{n-1}|||_{F,h}^2\right) + \frac{\widehat{\alpha}_{A_F}\nu}{2}\|\varphi_\psi^n\|_{2,\Omega}^2 \\
&\quad\leq C\left[1+\nu^{-3}\left(\|\eta_\psi^n\|_{2,\Omega}^4 + \|\psi^n\|_{2,\Omega}^4\right)\right]|||\varphi_\psi^n|||_{F,h}^2 \\
&\quad + C\left[\nu^{-1}(\|\psi^n\|_{2,\Omega}^2 + \|\eta_\psi^n\|_{2,\Omega}^2)\right]\|\eta_\psi^n\|_{2,\Omega}^2 + \|\mathbf{g}^n\|_{\infty,\Omega}^2(\|\eta_\theta^n\|_{0,\Omega}^2 + \|\varphi_\theta^n\|_{0,\Omega}^2) \\
&\quad + Ch^{2s}\left(\|\mathbf{f}_\psi\|_{\mathrm{L}^\infty(t_{n-1},t_n;\mathrm{H}^s(\mathcal{T}_h))}^2 + \nu^{-1}\|\psi^n\|_{2+s,\Omega}^2\right) \\
&\quad + Ch^{2\min\{s,r\}}\max\{\|\mathbf{g}^n\|_{\min\{s,r\},\Omega}^2, \|\mathbf{g}^n\|_{\infty,\Omega}^2\}\|\theta^n\|_{r,\Omega}^2 \\
&\quad + C\|\partial_{tt}\psi\|_{\mathrm{L}^1(t_{n-1},t_n;\mathrm{H}^1(\Omega))}|||\varphi_\psi^n|||_{F,h} + \frac{C}{\Delta t}h^s\|\partial_t\psi\|_{\mathrm{L}^1(t_{n-1},t_n;\mathrm{H}^{1+s}(\Omega))}|||\varphi_\psi^n|||_{F,h}.
\end{aligned} \tag{5.5.13}$$

Proof. We will estimate each terms in (5.5.11). Indeed, by using the definition of the functionals $F_\psi(\cdot)$ and $F_\psi^h(\cdot)$, the Cauchy-Schwarz and Young inequalities for the term T_F holds

$$T_F \leq \frac{C}{2c}h^{2s}\|\mathbf{f}_\psi\|_{\mathrm{L}^\infty(t_{n-1},t_n;\mathrm{H}^s(\mathcal{T}_h))}^2 + \frac{c}{2}\|\varphi_\psi^n\|_{1,\Omega}^2. \tag{5.5.14}$$

For the term T_M, we proceed similarly as in [3, Theorem 5.6] to obtain

$$\begin{aligned}
T_M &:= M_F(\partial_t\psi^n, \varphi_\psi^n) - M_F^h\left(\frac{\mathcal{S}_h\psi^n - \mathcal{S}_h\psi^{n-1}}{\Delta t}, \varphi_\psi^n\right) = M_F\left(\partial_t\psi^n - \frac{\psi^n - \psi^{n-1}}{\Delta t}, \varphi_\psi^n\right) \\
&\quad + \sum_{K\in\mathcal{T}_h} M_F^K\left(\frac{\psi^n - \psi^{n-1}}{\Delta t} - \left(\frac{\Pi_K^{\mathrm{D}}(\psi^n - \psi^{n-1})}{\Delta t}\right), \varphi_\psi^n\right) \\
&\quad + \sum_{K\in\mathcal{T}_h} M_F^{K,h}\left(\left(\frac{\Pi_K^{\mathrm{D}}(\psi^n - \psi^{n-1})}{\Delta t}\right) - \frac{\mathcal{S}_h\psi^n - \mathcal{S}_h\psi^{n-1}}{\Delta t}, \varphi_\psi^n\right) \\
&\leq C\|\partial_{tt}\psi\|_{\mathrm{L}^1(t_{n-1},t_n;\mathrm{H}^1(\Omega))}\|\varphi_\psi^n\|_{1,\Omega} + \frac{C}{\Delta t}h^s\|\partial_t\psi\|_{\mathrm{L}^1(t_{n-1},t_n;\mathrm{H}^{1+s}(\Omega))}\|\varphi_\psi^n\|_{1,\Omega}.
\end{aligned} \tag{5.5.15}$$

Next, to estimate T_C, we add and subtract the term $C^h(\theta^n, \varphi_\psi^n)$ to get

$$\begin{aligned}
T_C &:= C^h(\theta_h^n, \varphi_\psi^n) - C(\theta^n, \varphi_\psi^n) = C^h(\theta_h^n - \theta^n, \varphi_\psi^n) + (C^h(\theta^n, \varphi_\psi^n) - C(\theta^n, \varphi_\psi^n)) \\
&= (C^h(\varphi_\theta^n, \varphi_\psi^n) - C^h(\eta_\theta^n, \varphi_\psi^n)) + (C^h(\theta^n, \varphi_\psi^n) - C(\theta^n, \varphi_\psi^n)) \\
&\leq \|\mathbf{g}^n\|_{\infty,\Omega}\left(\|\varphi_\theta^n\|_{0,\Omega} + \|\eta_\theta^n\|_{0,\Omega}\right)\|\varphi_\psi^n\|_{1,\Omega} \\
&\quad + Ch^{\min\{s,r\}}\max\{\|\mathbf{g}^n\|_{\min\{s,r\},\Omega}, \|\mathbf{g}^n\|_{\infty,\Omega}\}\|\theta^n\|_{r,\Omega}\|\varphi_\psi^n\|_{1,\Omega} \\
&\leq C\|\mathbf{g}^n\|_{\infty,\Omega}^2(\|\varphi_\theta^n\|_{0,\Omega}^2 + \|\varphi_\psi^n\|_{1,\Omega}^2) \\
&\quad + Ch^{2\min\{s,r\}}\max\{\|\mathbf{g}^n\|_{\min\{s,r\},\Omega}^2, \|\mathbf{g}^n\|_{\infty,\Omega}^2\}\|\theta^n\|_{r,\Omega}^2 + c\|\varphi_\psi^n\|_{1,\Omega}^2,
\end{aligned} \tag{5.5.16}$$

where we have used the Hölder inequality, bound (5.5.3) (with $\gamma = \min\{s,r\}$) and the Young inequality.

For the term T_B, we have

$$\begin{aligned}
T_B &:= B_F(\psi^n;\psi^n, \varphi_\psi^n) - B_F^h(\psi_h^n;\psi_h^n, \varphi_\psi^n) = \left(B_F(\psi^n;\psi^n, \varphi_\psi^n) - B_F^h(\psi^n;\psi^n, \varphi_\psi^n)\right) \\
&\quad + \left(B_F^h(\psi^n;\psi^n, \varphi_\psi^n) - B_F^h(\psi_h^n;\psi_h^n, \varphi_\psi^n)\right) =: T_{B1} + T_{B2}.
\end{aligned} \tag{5.5.17}$$

Now, we will bound the terms T_{B1} and T_{B2}. Indeed, from Lemma 5.5.3 and the Young inequality we have that

$$\begin{aligned} T_{B1} &:= B_F(\psi^n;\psi^n,\varphi_\psi^n) - B_F^h(\psi^n;\psi^n,\varphi_\psi^n) \\ &\leq C\, h^s(\|\psi^n\|_{2+s,\Omega} + \|\psi^n\|_{2,\Omega})\|\psi^n\|_{2+s,\Omega}\|\varphi_\psi^n\|_{2,\Omega} \\ &\leq \frac{4C_\psi}{\widehat{\alpha}_{A_F}\nu} h^{2s}\|\psi^n\|^2_{2+s,\Omega} + \frac{\widehat{\alpha}_{A_F}\nu}{8}\|\varphi_\psi^n\|^2_{2,\Omega} \\ &\leq C_\psi \nu^{-1} h^{2s}\|\psi^n\|^2_{2+s,\Omega} + \frac{\widehat{\alpha}_{A_F}\nu}{8}\|\varphi_\psi^n\|^2_{2,\Omega}, \end{aligned} \tag{5.5.18}$$

where we have included the term $(\|\psi^n\|_{2+s,\Omega} + \|\psi^n\|_{2,\Omega})$ in the constant C_ψ in order to shorten the inequality.

On the other hand, to bound the expression T_{B2}, we apply Lemma 5.5.2, recall that $\varphi_\psi^n = \psi_h^n - \mathcal{S}_h\psi^n$ and $\eta_\psi^n = \psi^n - \mathcal{S}_h\psi^n$, to arrive

$$\begin{aligned} T_{B2} &:= B_F^h(\psi^n;\psi^n,\varphi_\psi^n) - B_F^h(\psi_h^n;\psi_h^n,\varphi_\psi^n) \\ &= B_F^h(\psi^n;\psi^n - \psi_h^n + \varphi_\psi^n,\varphi_\psi^n) + B_F^h(\psi^n - \psi_h^n + \varphi_\psi^n;\psi_h^n,\varphi_\psi^n) - B_F^h(\varphi_\psi^n;\psi_h^n,\varphi_\psi^n) \\ &= B_F^h(\psi^n;\eta_\psi^n,\varphi_\psi^n) + B_F^h(\eta_\psi^n;\psi_h^n,\varphi_\psi^n) - B_F^h(\varphi_\psi^n;\psi_h^n,\varphi_\psi^n). \end{aligned} \tag{5.5.19}$$

By using Lemma 5.3.3, together with the Young inequality, we have

$$B_F^h(\psi^n;\eta_\psi^n,\varphi_\psi^n) \leq \frac{\widehat{\alpha}_{A_F}\nu}{8}\|\varphi_\psi^n\|^2_{2,\Omega} + C\nu^{-1}\|\psi^n\|^2_{2,\Omega}\|\eta_\psi^n\|^2_{2,\Omega}.$$

Now, adding and subtracting suitable terms, and employing Lemma 5.3.3 along with the Young inequality, we obtain

$$\begin{aligned} B_F^h(\eta_\psi^n;\psi_h^n,\varphi_\psi^n) &= B_F^h(\eta_\psi^n;\psi^n + (\psi_h^n - \psi^n),\varphi_\psi^n) \\ &= B_F^h(\eta_\psi^n;\psi^n,\varphi_\psi^n) + B_F^h(\eta_\psi^n;\varphi_\psi^n - \eta_\psi^n,\varphi_\psi^n) \\ &= B_F^h(\eta_\psi^n;\psi^n,\varphi_\psi^n) - B_F^h(\eta_\psi^n;\eta_\psi^n,\varphi_\psi^n) \\ &\leq \widehat{C}_{B_F}\left(\|\psi^n\|_{2,\Omega} + \|\eta_\psi^n\|_{2,\Omega}\right)\|\eta_\psi^n\|_{2,\Omega}\|\varphi_\psi^n\|_{2,\Omega} \\ &\leq \frac{\widehat{\alpha}_{A_F}\nu}{8}\|\varphi_\psi^n\|^2_{2,\Omega} + C\nu^{-1}(\|\psi^n\|^2_{2,\Omega} + \|\eta_\psi^n\|^2_{2,\Omega})\|\eta_\psi^n\|^2_{2,\Omega}. \end{aligned}$$

Once again adding and subtracting adequate terms, using Lemma 5.5.1 and the Young inequality, we get

$$\begin{aligned} -B_F^h(\varphi_\psi^n;\psi_h^n,\varphi_\psi^n) &= B_F^h(\varphi_\psi^n;(\psi^n - \psi_h^n) - \psi^n,\varphi_\psi^n) = B_F^h(\varphi_\psi^n;\eta_\psi^n,\varphi_\psi^n) - B_F^h(\varphi_\psi^n;\psi^n,\varphi_\psi^n) \\ &\leq \widehat{C}_{B_F}\|\varphi_\psi^n\|_{2,\Omega}\left(\|\eta_\psi^n\|_{2,\Omega} + \|\psi^n\|_{2,\Omega}\right)\|\varphi_\psi^n\|^{\frac{1}{2}}_{2,\Omega}\|\varphi_\psi^n\|^{\frac{1}{2}}_{1,\Omega} \\ &\leq \frac{\widehat{\alpha}_{A_F}\nu}{16}\|\varphi_\psi^n\|^2_{2,\Omega} + 2C\nu^{-1}\left(\|\eta_\psi^n\|^2_{2,\Omega} + \|\psi^n\|^2_{2,\Omega}\right)\|\varphi_\psi^n\|_{2,\Omega}\|\varphi_\psi^n\|_{1,\Omega} \\ &\leq \frac{\widehat{\alpha}_{A_F}\nu}{16}\|\varphi_\psi^n\|^2_{2,\Omega} + 2\nu^{-2}C_4\nu^{-1}\left(\|\eta_\psi^n\|^2_{2,\Omega} + \|\psi^n\|^2_{2,\Omega}\right)^2\|\varphi_\psi^n\|^2_{1,\Omega} + \frac{\widehat{\alpha}_{A_F}\nu}{16}\|\varphi_\psi^n\|^2_{2,\Omega} \\ &\leq \frac{\widehat{\alpha}_{A_F}\nu}{8}\|\varphi_\psi^n\|^2_{2,\Omega} + 4C_4\nu^{-3}\left(\|\eta_\psi^n\|^4_{2,\Omega} + \|\psi^n\|^4_{2,\Omega}\right)\|\varphi_\psi^n\|^2_{1,\Omega}. \end{aligned}$$

Combining the estimates (5.5.17)-(5.5.19) and the three previous inequalities, we have

$$
\begin{aligned}
T_B \leq C_1\nu^{-1}h^{2s}\|\psi^n\|^2_{2+s,\Omega}\|\psi^n\|^2_{2,\Omega} + \frac{\widehat{\alpha}_{A_F}\nu}{2}\|\varphi^n_\psi\|^2_{2,\Omega} + C\nu^{-1}\|\psi^n\|^2_{2,\Omega}\|\eta^n_\psi\|^2_{2,\Omega} \\
+ C\nu^{-1}(\|\psi^n\|^2_{2,\Omega} + \|\eta^n_\psi\|^2_{2,\Omega})\|\eta^n_\psi\|^2_{2,\Omega} + C_4\nu^{-3}\left(\|\eta^n_\psi\|^4_{2,\Omega} + \|\psi^n\|^4_{2,\Omega}\right)\|\varphi^n_\psi\|^2_{1,\Omega}.
\end{aligned}
\tag{5.5.20}
$$

Now, from estimates (5.5.11), (5.5.14)-(5.5.16) and (5.5.20), the definition and equivalence of the norm $|||\cdot|||_{F,h}$ (cf. (5.4.6)), together with the coercivity of bilinear form $A^h_F(\cdot,\cdot)$ we obtain the desired estimate.

□

Lemma 5.5.7 (Error estimate for the energy equation)**.** *Let $\frac{1}{2} < s \leq k-1$ and $1 \leq r \leq \ell$. Suppose that $f_\theta \in \mathrm{L}^\infty(0,T;\mathrm{H}^r(\Omega))$. Moreover, let $(\psi^n,\theta^n) \in \mathrm{H}^2_0(\Omega)\times\mathrm{H}^1_0(\Omega)$ be the solution of problem (5.2.13) at time $t = t_n$ and assume that*

$$
\begin{aligned}
&\theta \in \mathrm{L}^\infty(0,T;\mathrm{H}^{1+r}(\Omega)\cap \mathrm{W}^1_\infty(\Omega)), \quad \partial_t\theta \in \mathrm{L}^1(0,T;\mathrm{H}^r(\Omega)),\\
&\partial_{tt}\theta \in \mathrm{L}^1(0,T;\mathrm{L}^2(\Omega)) \quad \text{and} \quad \psi \in \mathrm{L}^\infty(0,T;\mathrm{H}^{2+s}(\Omega)).
\end{aligned}
$$

Let $(\psi^n_h,\theta^n_h) \in \mathrm{W}^h_k \times \mathrm{H}^h_\ell$ be the virtual element solution generated by scheme (5.4.1). Then, the following error estimate holds

$$
\begin{aligned}
\frac{1}{2\Delta t}\left(|||\varphi^n_\theta|||^2_{T,h} - |||\varphi^{n-1}_\theta|||^2_{T,h}\right) + \frac{\widehat{\alpha}_{A_T}\kappa}{2}\|\varphi^n_\theta\|^2_{1,\Omega} \leq C\|\varphi^n_\theta\|^2_{0,\Omega} + \kappa^{-1}\|\theta^n\|^2_{1,\Omega}\|\eta^n_\psi\|^2_{2,\Omega} \\
+ C\left[\kappa^{-1}(\|\psi^n\|^2_{2,\Omega} + \|\eta^n_\psi\|^2_{2,\Omega})\right]\|\eta^n_\theta\|^2_{1,\Omega} + C|||\varphi^n_\theta|||^2_{T,h} \\
+ Ch^{2r}\|f_\theta\|^2_{\mathrm{L}^\infty(t_{n-1},t_n;\mathrm{H}^r(\mathcal{T}_h))} + C\kappa^{-1}h^{2\min\{s,r\}}\|\psi^n\|^2_{2+s,\Omega}\|\theta^n\|^2_{2+r,\Omega} \\
+ C\|\partial_{tt}\theta\|_{\mathrm{L}^1(t_{n-1},t_n;\mathrm{L}^2(\Omega))}|||\varphi^n_\theta|||_{T,h} + \frac{C}{\Delta t}h^r\|\partial_t\theta\|_{\mathrm{L}^1(t_{n-1},t_n;\mathrm{H}^r(\Omega))}|||\varphi^n_\theta|||_{T,h}.
\end{aligned}
\tag{5.5.21}
$$

Proof. We will establish estimates for each terms in the error equation (5.5.12). We start with the term I_F, which is bounded by using the Cauchy-Schwarz inequality and approximation properties of projection Π^ℓ_K, as follows:

$$
I_F := F^h_\theta(\varphi^n_\theta) - F_\theta(\varphi^n_\theta) \leq \frac{C}{2c}h^{2r}\|f_\theta\|^2_{\mathrm{L}^\infty(t_{n-1},t_n;\mathrm{H}^r(\mathcal{T}_h))} + \frac{c}{2}\|\varphi^n_\theta\|^2_{0,\Omega}. \tag{5.5.22}
$$

For the term I_M, we proceed similarly as in [153, Theorem 3.3] to obtain

$$
\begin{aligned}
I_M &:= M_T(\partial_t\theta^n,\varphi^n_\theta) - M^h_F\Big(\frac{\theta^n_I - \theta^{n-1}_I}{\Delta t},\varphi^n_\theta\Big)\\
&\leq C\|\partial_{tt}\theta\|_{\mathrm{L}^1(t_{n-1},t_n;\mathrm{L}^2(\Omega))}\|\varphi^n_\theta\|_{0,\Omega} + \frac{C}{\Delta t}h^r\|\partial_t\theta\|_{\mathrm{L}^1(t_{n-1},t_n;\mathrm{H}^r(\Omega))}\|\varphi^n_\theta\|_{0,\Omega}.
\end{aligned}
\tag{5.5.23}
$$

Analogously, as in (5.5.17) we split the term I_B as follows:

$$
\begin{aligned}
I_B := B_{\text{skew}}(\psi^n;\theta^n,\varphi^n_\theta) - B^h_{\text{skew}}(\psi^n_h;\theta^n_h,\varphi^n_\psi) = \Big(B_{\text{skew}}(\psi^n;\theta^n,\varphi^n_\theta) - B^h_{\text{skew}}(\psi^n;\theta^n,\varphi^n_\theta)\Big)\\
+ \Big(B^h_{\text{skew}}(\psi^n;\theta^n,\varphi^n_\theta) - B^h_{\text{skew}}(\psi^n_h;\theta^n_h,\varphi^n_\theta)\Big) =: I_{B1} + I_{B2}.
\end{aligned}
\tag{5.5.24}
$$

Now, applying the bound (5.5.2), with $\gamma = \min\{s,r\}$ and using the Young inequality, we obtain

$$\begin{aligned} I_{B1} &:= B_{\text{skew}}(\psi^n;\theta^n,\varphi_\theta^n) - B_{\text{skew}}^h(\psi^n;\theta^n,\varphi_\theta^n) \le Ch^{\min\{s,r\}}\|\psi^n\|_{2+s,\Omega}\|\theta^n\|_{1+r,\Omega}\|\varphi_\theta^n\|_{1,\Omega} \\ &\le C\kappa^{-1}h^{2\min\{s,r\}}\|\psi^n\|_{2+s,\Omega}^2\|\theta^n\|_{1+r,\Omega}^2 + \frac{\widehat{\alpha}_{A_T}\kappa}{10}\|\varphi_\theta^n\|_{1,\Omega}^2. \end{aligned} \tag{5.5.25}$$

On the other hand, similarly as in (5.5.19) and (5.5.20), we can derive

$$\begin{aligned} I_{B2} &= B_{\text{skew}}^h(\psi^n;\eta_\theta^n,\varphi_\theta^n) + B_{\text{skew}}^h(\eta_\psi^n;\theta_h^n,\varphi_\theta^n) - B_{\text{skew}}^h(\varphi_\psi^n;\theta_h^n,\varphi_\theta^n) \\ &\le \frac{\widehat{\alpha}_{A_T}\kappa}{10}\|\varphi_\theta^n\|_{1,\Omega}^2 + C\kappa^{-1}\|\psi^n\|_{2,\Omega}^2\|\eta_\theta^n\|_{1,\Omega}^2 + \frac{\widehat{\alpha}_{A_T}\kappa}{10}\|\varphi_\theta^n\|_{1,\Omega}^2 \\ &\quad + C\kappa^{-1}(\|\theta^n\|_{1,\Omega}^2 + \|\eta_\theta^n\|_{1,\Omega}^2)\|\eta_\psi^n\|_{2,\Omega}^2 - B_{\text{skew}}^h(\varphi_\psi^n;\theta_h^n,\varphi_\theta^n). \end{aligned} \tag{5.5.26}$$

However, since the discrete trilinear form $B_{\text{skew}}^h(\cdot;\cdot,\cdot)$ does not satisfy an analogous property to Lemma 5.5.1, we will bound the last term in (5.5.26) by a different way. Indeed, adding and subtracting adequate terms, using the definition of trilinear form, the Hölder inequality and employing the continuity of the L^2-projections involved (cf. (5.3.5)), we obtain

$$\begin{aligned} &- B_{\text{skew}}^h(\varphi_\psi^n;\theta_h^n,\varphi_\theta^n) = B_{\text{skew}}^h(\varphi_\psi^n;\eta_\theta^n,\varphi_\theta^n) + B_{\text{skew}}^h(\varphi_\psi^n;-\theta^n,\varphi_\theta^n) \\ &= \frac{1}{2}\big(B_T^h(\varphi_\psi^n;\eta_\theta^n,\varphi_\theta^n) - B_T^h(\varphi_\psi^n;\varphi_\theta^n,\eta_\theta^n)\big) + B_{\text{skew}}^h(\varphi_\psi^n;-\theta^n,\varphi_\theta^n) \\ &\le C\sum_{K\in\mathcal{T}_h}\|\boldsymbol{\Pi}_K^{\ell-1}\nabla\eta_\theta^n\|_{\mathrm{L}^\infty(K)}\|\mathbf{curl}\,\varphi_\psi^n\|_{0,K}\|\varphi_\theta^n\|_{0,K} \\ &\quad + C\sum_{K\in\mathcal{T}_h}\|\Pi_K^{\ell-1}\eta_\theta^n\|_{\mathrm{L}^\infty(K)}\|\mathbf{curl}\,\varphi_\psi^n\|_{0,K}\|\nabla\varphi_\theta^n\|_{0,K} + B_{\text{skew}}^h(\varphi_\psi^n;-\theta^n,\varphi_\theta^n). \end{aligned} \tag{5.5.27}$$

Now, applying an inverse inequality for polynomials, the continuity of $\boldsymbol{\Pi}_K^{\ell-1}$, and Proposition 5.5.4, for $r\ge 1$ we get

$$\|\boldsymbol{\Pi}_K^{\ell-1}\nabla\eta_\theta^n\|_{\mathrm{L}^\infty(K)} \le Ch_K^{-1}\|\boldsymbol{\Pi}_K^{\ell-1}\nabla\eta_\theta^n\|_{0,K} \le Ch_K^{-1}\|\eta_\theta^n\|_{1,K} \le C\|\theta^n\|_{1+r,K} \le C_{\mathtt{reg}}.$$

Analogously, we have that

$$\|\Pi_K^{\ell-1}\eta_\theta^n\|_{\mathrm{L}^\infty(K)} \le C\|\theta^n\|_{1+r,K} \le C_{\mathtt{reg}}.$$

Next, under assumption $\theta^n \in \mathrm{W}_\infty^1(\Omega)$, the definition of the form $B_{\text{skew}}^h(\cdot;\cdot,\cdot)$ and the Cauchy-Schwarz inequality, we get

$$B_{\text{skew}}^h(\varphi_\psi^n;-\theta^n,\varphi_\theta^n) \le C_1\|\theta^n\|_{\mathrm{W}_\infty^1(\Omega)}\|\varphi_\psi^n\|_{1,\Omega}\|\varphi_\theta^n\|_{0,\Omega} \le C_{\mathtt{reg}}\|\varphi_\psi^n\|_{1,\Omega}\|\varphi_\theta^n\|_{0,\Omega}.$$

Inserting the above estimates in (5.5.27), and applying the Cauchy-Schwarz and Young inequalities, it follows

$$-B_{\text{skew}}^h(\varphi_\psi^n;\theta_h^n,\varphi_\theta^n) \le 3C_{\mathtt{reg}}\|\varphi_\psi^n\|_{1,\Omega}\|\varphi_\theta^n\|_{1,\Omega} \le C\kappa^{-1}\|\varphi_\psi^n\|_{1,\Omega}^2 + \frac{\widehat{\alpha}_{A_T}\kappa}{10}\|\varphi_\theta^n\|_{1,\Omega}^2. \tag{5.5.28}$$

Then, combining the estimates (5.5.24), (5.5.25), (5.5.26) and (5.5.28), we obtain

$$\begin{aligned} I_B &\le C\kappa^{-1}h^{2\min\{s,r\}}\|\psi^n\|_{2+s,\Omega}^2\|\theta^n\|_{1+r,\Omega}^2 + C\kappa^{-1}\|\psi^n\|_{2,\Omega}^2\|\eta_\theta^n\|_{1,\Omega}^2 \\ &\quad + C\kappa^{-1}(\|\theta^n\|_{1,\Omega}^2 + \|\eta_\theta^n\|_{1,\Omega}^2)\|\eta_\psi^n\|_{2,\Omega}^2 + \frac{4\widehat{\alpha}_{A_T}\kappa}{10}\|\varphi_\theta^n\|_{1,\Omega}^2 + C(\kappa^{-1}+1)\|\varphi_\psi^n\|_{1,\Omega}^2. \end{aligned} \tag{5.5.29}$$

Now, for the term I_A, we add and subtract $\theta_\pi^n \in \mathbb{P}_\ell(K)$ such that Proposition 5.5.1 holds true, then applying the consistency property of $A_T^{h,K}(\cdot,\cdot)$, the triangle inequality and Proposition 5.5.4, we have that

$$\begin{aligned} I_A &= \kappa \sum_{K\in\mathcal{T}_h} \Big(A_T^K(\theta^n,\varphi_\theta^n) - A_T^{h,K}(\theta_I^n,\varphi_\theta^n)\Big) \\ &= \kappa \sum_{K\in\mathcal{T}_h} \Big(A_T^K(\theta^n-\theta_\pi^n,\varphi_\theta^n) + A_T^{h,K}(\theta_\pi^n-\theta_I^n,\varphi_\theta^n)\Big) \\ &\leq C\kappa h^r \|\theta^n\|_{1+r,\Omega}\|\varphi_\theta^n\|_{1,\Omega} \\ &\leq Ch^{2r}\|\theta^n\|_{1+r,\Omega}^2 + \frac{\widehat{\alpha}_{A_T}\kappa}{10}\|\varphi_\theta^n\|_{1,\Omega}^2. \end{aligned} \tag{5.5.30}$$

Now, from bounds (5.5.12), (5.5.22), (5.5.23), (5.5.29) and (5.5.30), the definition and equivalence of the norms $|||\cdot|||_{T,h}$ (cf. (5.4.6)) and $\|\cdot\|_{0,\Omega}$, together with the coercivity of bilinear form $A_T^h(\cdot,\cdot)$, we obtain the estimate (5.5.21).

□

The following result establishes an error estimate for the fully-discrete virtual scheme (5.4.1).

Theorem 5.5.1. *Suppose that the external forces satisfy $\mathbf{f}_\psi \in \mathrm{L}^\infty(0,T;\mathbf{H}^s(\Omega))$, $f_\theta \in \mathrm{L}^\infty(0,T;\mathrm{H}^r(\Omega))$ and $\mathbf{g} \in \mathrm{L}^\infty(0,T;\mathbf{H}^{\min\{s,r\}}(\Omega)\cap\mathbf{L}^\infty(\Omega))$, with $\frac{1}{2} < s \leq k-1$ and $1 \leq r \leq \ell$. Let $(\psi^n,\theta^n) \in \mathrm{H}_0^2(\Omega)\times\mathrm{H}_0^1(\Omega)$ be the solution of problem (5.2.13) at time $t = t_n$. Moreover, assume that*

$$\begin{aligned} \psi &\in \mathrm{L}^\infty(0,T;\mathrm{H}^{2+s}(\Omega)), & \partial_t\psi &\in \mathrm{L}^1(0,T;\mathrm{H}^{1+s}(\Omega)), & \partial_{tt}\psi &\in \mathrm{L}^1(0,T;\mathrm{H}^1(\Omega)), \\ \theta &\in \mathrm{L}^\infty(0,T;\mathrm{H}^{1+r}(\Omega)\cap\mathrm{W}_\infty^1(\Omega)), & \partial_t\theta &\in \mathrm{L}^1(0,T;\mathrm{H}^r(\Omega)), & \partial_{tt}\theta &\in \mathrm{L}^1(0,T;\mathrm{L}^2(\Omega)). \end{aligned}$$

Let $(\psi_h^n,\theta_h^n) \in \mathrm{W}_k^h \times \mathrm{H}_\ell^h$ be the virtual element solution generated by scheme (5.4.1). Then, the following estimate holds

$$\|(\psi^n-\psi_h^n,\theta^n-\theta_h^n)\|_{\mathrm{H}^1(\Omega)\times\mathrm{L}^2(\Omega)}^2 + \Delta t\sum_{j=1}^n \|(\psi^j-\psi_h^j,\theta^j-\theta_h^j)\|_{\mathrm{H}^2(\Omega)\times\mathrm{H}^1(\Omega)}^2 \leq C(h^{2\min\{s,r\}}+\Delta t^2),$$

where the constant C is positive and depends on the physical parameters ν,κ, final time T, mesh regularity parameter, the regularity of the Boussinesq solution fields (ψ,θ) and the external forces $\mathbf{f}_\psi, f_\theta, \mathbf{g}$, but is independent of mesh size h and time steps Δt.

Proof. The desired estimate will follow combining Lemmas 5.5.6 and 5.5.7 with the discrete Gronwall inequality. Indeed, we proceed to multiply by $2\Delta t$ the estimates (5.5.13) and (5.5.21), then by employing the Young inequality to the resulting bounds and iterating $j = 0,\ldots,n$, we have

$$
\begin{aligned}
&|||\varphi_\psi^n|||_{F,h}^2 + |||\varphi_\theta^n|||_{T,h}^2 + \Delta t \sum_{j=0}^{n} \|\varphi_\psi^j\|_{2,\Omega}^2 + \Delta t \sum_{j=0}^{n} \|\varphi_\theta^j\|_{1,\Omega}^2 \\
&\leq C\Delta t \sum_{j=0}^{n} \left[1 + \nu^{-3}\left(\|\eta_\psi^j\|_{2,\Omega}^4 + \|\psi^j\|_{2,\Omega}^4\right)\right] |||\varphi_\psi^j|||_{F,h}^2 + C\Delta t \sum_{j=0}^{n} \left[1 + \|\mathbf{g}^j\|_{\infty,\Omega}^2\right] |||\varphi_\theta^j|||_{T,h}^2 \\
&\quad + C\Delta t \sum_{j=0}^{n} \left[\nu^{-1}(\|\psi^j\|_{2,\Omega}^2 + \|\eta_\psi^j\|_{2,\Omega}^2) + \kappa^{-1}\|\theta^j\|_{1,\Omega}^2\right] \|\eta_\psi^j\|_{2,\Omega}^2 \\
&\quad + C\Delta t \sum_{j=0}^{n} \left[\kappa^{-1}(\|\psi^j\|_{2,\Omega}^2 + \|\eta_\psi^j\|_{2,\Omega}^2) + \|\mathbf{g}^j\|_{\infty,\Omega}^2\right] \|\eta_\theta^j\|_{1,\Omega}^2 \\
&\quad + C\Delta t h^{2s} \left(\|\mathbf{f}_\psi\|_{\mathrm{L}^\infty(0,t_n;\mathrm{H}^s(\mathcal{T}_h))}^2 + \|\partial_t \psi\|_{\mathrm{L}^1(0,t_n;\mathrm{H}^{1+s}(\Omega))}^2 + \nu^{-1}\|\psi\|_{\mathrm{L}^\infty(0,t_n;\mathrm{H}^{2+s}(\Omega))}^2\right) \\
&\quad + \Delta t h^{2\min\{s,r\}} \max\{\|\mathbf{g}\|_{\mathrm{L}^\infty(0,t_n;\mathbf{H}^{\min\{s,r\}}(\Omega))}^2, \|\mathbf{g}\|_{\mathrm{L}^\infty(0,t_n;\mathbf{L}^\infty(\Omega))}^2\} \|\theta\|_{\mathrm{L}^\infty(0,t_n;\mathrm{H}^r(\Omega))}^2 \\
&\quad + C\Delta t h^{2r} \left(\|f_\theta\|_{\mathrm{L}^\infty(0,t_n;\mathrm{H}^r(\mathcal{T}_h))}^2 + \|\partial_t \theta\|_{\mathrm{L}^1(0,t_n;\mathrm{H}^r(\Omega))}^2\right) \\
&\quad + C\Delta t \kappa^{-1} h^{2\min\{s,r\}} \left(\|\psi\|_{\mathrm{L}^\infty(0,t_n;\mathrm{H}^{2+s}(\Omega))}^2 + \|\theta\|_{\mathrm{L}^\infty(0,t_n;\mathrm{H}^{1+r}(\Omega))}^2\right) \\
&\quad + C\Delta t^2 \left(\|\partial_{tt}\theta\|_{\mathrm{L}^1(0,t_n;\mathrm{L}^2(\Omega))}^2 + \|\partial_{tt}\psi\|_{\mathrm{L}^1(0,t_n;\mathrm{H}^1(\Omega))}^2\right) + \widehat{\alpha}_{M_F}\|\varphi_\psi^0\|_{1,\Omega}^2 + \widehat{\alpha}_{M_T}\|\varphi_\theta^0\|_{0,\Omega}^2.
\end{aligned}
$$

Thus, applying the discrete Gronwall inequality (cf. Lemma 5.5.5), choosing $(\psi_h^0, \theta_h^0) = (\psi_I(0), \theta_I(0))$ and using Propositions 5.5.3 and 5.5.4 along with the equivalence of norms, we have

$$
(\|\varphi_\psi^n\|_{1,\Omega}^2 + \|\varphi_\theta^n\|_{0,\Omega}^2) + \Delta t \sum_{j=1}^{n} (\|\varphi_\psi^j\|_{2,\Omega}^2 + \|\varphi_\theta^j\|_{1,\Omega}^2) \leq C(h^{2\min\{s,r\}} + \Delta t^2),
$$

with $\frac{1}{2} < s \leq k-1$, $1 \leq r \leq \ell$ and $C > 0$ is independent of mesh size h and time step Δt.

Finally, the desired result follows from the above estimate, triangular inequality, together with Propositions 5.5.4 and 5.5.5. $\square$

Remark 5.5.1. *In the present framework, the main advantage of using an energy projector $\mathcal{S}_h\psi^n$, as we do for the stream-function space, is to obtain a shorter proof. Nevertheless, for the temperature variable we do not use an energy projector, but resort to a standard interpolant θ_I^n. The reason is that we need also some local approximation properties for the temperature field that the energy projection operator, being global in nature, would not have.*

5.6 Numerical results

In this section we carry out numerical experiments in order to support our analytical results and illustrate the performance of the proposed fully-discrete virtual scheme (5.4.1) for the Boussinesq system. In all examples, we use the lowest order virtual element spaces W_2^h and H_1^h, for the stream-function and temperature fields, respectively. At each discrete time, the nonlinear fully-discrete system (5.4.1) is linearized by using the Newton method. For the first time step, we take as initial guess $(\psi_h^{\mathtt{in}}, \theta_h^{\mathtt{in}}) = (0,0)$, and for all $n \geq 1$ we take $(\psi_h^{\mathtt{in}}, \theta_h^{\mathtt{in}}) = (\psi_h^{n-1}, \theta_h^{n-1})$.

The iterations are finalized when the ℓ^∞-norm of the global incremental discrete solution drop below a fixed tolerance of $\mathrm{Tol} = 10^{-8}$.

The domain Ω is partitioned using the following sequences of polygonal meshes (an example for each family is shown in Figure 5.1):

- $\mathcal{T}_h^1$: Distorted quadrilaterals meshes;
- $\mathcal{T}_h^2$: Triangular meshes;
- $\mathcal{T}_h^3$: Voronoi meshes;
- $\mathcal{T}_h^4$: Distorted concave rhombic quadrilaterals.

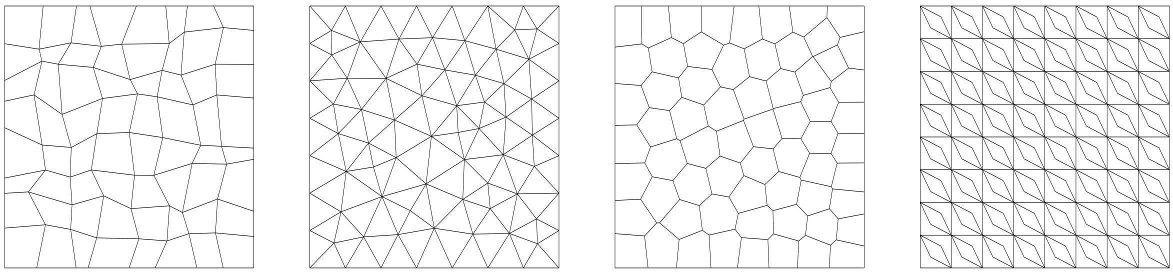

(a) mesh $\mathcal{T}_h^1$ (b) mesh $\mathcal{T}_h^2$ (c) mesh $\mathcal{T}_h^3$ (d) mesh $\mathcal{T}_h^4$

Figure 5.1: Domain discretized with different meshes.

In order to test the convergence properties of the proposed VEM, we measure some errors as the difference between the exact solutions (ψ, θ) and adequate projections of the numerical solution (ψ_h^n, θ_h^n). More precisely, we consider the following quantities:

$$\begin{aligned}
\mathtt{E}(\psi, \mathrm{L}^2, \mathrm{H}^2) &:= \left(\Delta t \sum_{n=1}^{N} |\psi(t_n) - \Pi^{\mathrm{D},2}\psi_h^n|_{2,h}^2\right)^{1/2}, \\
\mathtt{E}(\theta, \mathrm{L}^2, \mathrm{H}^1) &:= \left(\Delta t \sum_{n=1}^{N} |\theta(t_n) - \Pi^{\nabla,1}\theta_h^n|_{1,h}^2\right)^{1/2},
\end{aligned} \tag{5.6.1}$$

for the temperature we have

$$\begin{aligned}
\mathtt{E}(\psi, \mathrm{L}^\infty, \mathrm{H}^1) &:= |\psi(T) - \Pi^{\mathrm{D},2}\psi_h^N|_{1,h}, \\
\mathtt{E}(\theta, \mathrm{L}^\infty, \mathrm{L}^2) &:= \|\theta(T) - \Pi^{\nabla,1}\theta_h^N\|_{0,\Omega}.
\end{aligned} \tag{5.6.2}$$

Accordingly to Theorem 5.5.1, the expected convergence rate for the sum of the above norms is $\mathcal{O}(h + \Delta t)$.

5.6.1 Accuracy assessment

In our first example, we illustrate the accuracy in space and time of the proposed VEM (5.4.1), considering a manufactured exact solution on the square domain $\Omega := (0,1)^2$, the time interval $[0,1]$ and force per unit mass $\mathbf{g} = (0,-1)^T$. We solve the Boussinesq system (5.2.1), taking the load terms $\mathbf{f}_\psi$ and f_θ, boundary and initial conditions in such a way that the analytical solution is given by:

$$\mathbf{u}(x,y,t) = \begin{pmatrix} u_1(x,y,t) \\ u_2(x,y,t) \end{pmatrix} = \begin{pmatrix} (e^{10(t-1)} - e^{-10})\, x^2(1-x)^2(2y-6y^2+4y^3) \\ -(e^{10(t-1)} - e^{-10}) y^2(1-y)^2(2x-6x^2+4x^3) \end{pmatrix},$$

$$p(x,y,t) = (e^{10(t-1)} - e^{-10})(\sin(x)\cos(y) + (\cos(1)-1)\sin(1)),$$

$$\psi(x,y,t) = (e^{10(t-1)} - e^{-10}) x^2(1-x)^2 y^2(1-y)^2 \qquad \text{and} \qquad \theta(x,y,t) = u_1(x,y,t) + u_2(x,y,t).$$

In order to see the linear trend of the stream-function and temperature errors (5.6.1), predicted by Theorem 5.5.1, we refine simultaneously in space and time. More precisely, for each mesh family we consider the mesh refinements with $h = 1/4, 1/8, 1/16, 1/32$, and we use the same uniform refinements for the time variable. In particular, for the mesh $\mathcal{T}_h^1$, it can be seen along the diagonal of Table 5.1, the expected first order convergence for the stream-function and temperature errors (5.6.1).

In Figure 5.2, we display the errors (5.6.1) for the same simultaneous time and space refinements ($h = \Delta t = 2^{-i}$, with $i = 2, \ldots, 5$), using the four mesh families. We notice that the rates of convergence predicted in Theorem 5.5.1 are attained by both unknowns.

dofs	h \ Δt	1/4	1/8	1/16	1/32	1/64
				$\mathtt{E}(\psi, \mathrm{L}^2; \mathrm{H}^2)$		
36	1/4	$\boxed{1.88912\text{e-}2}$	1.42183e-2	1.16131e-2	1.02912e-2	$\boxed{9.63665\text{e-}3}$
196	1/8	1.11333e-2	$\boxed{8.42107\text{e-}3}$	6.91546e-3	6.15400e-3	$\boxed{5.77765\text{e-}3}$
900	1/16	4.92223e-3	3.53363e-3	$\boxed{2.85747\text{e-}3}$	2.54826e-3	$\boxed{2.40427\text{e-}3}$
3844	1/32	3.61175e-3	2.11884e-3	1.46063e-3	$\boxed{1.21158\text{e-}3}$	$\boxed{1.11670\text{e-}3}$
15876	1/64	$\boxed{3.21002\text{e-}3}$	$\boxed{1.64565\text{e-}3}$	$\boxed{9.22443\text{e-}4}$	6.49802e-4	$\boxed{5.59824\text{e-}4}$
				$\mathtt{E}(\theta, \mathrm{L}^2; \mathrm{H}^1)$		
36	1/4	$\boxed{1.74892\text{e-}2}$	1.34200e-2	1.11391e-2	9.96756e-3	$\boxed{9.38232\text{e-}3}$
196	1/8	1.02277e-2	$\boxed{7.88174\text{e-}3}$	6.66404e-3	6.05736e-3	$\boxed{5.75702\text{e-}3}$
900	1/16	5.32067e-3	3.65373e-3	$\boxed{2.93777\text{e-}3}$	2.64415e-3	$\boxed{2.51594\text{e-}3}$
3844	1/32	3.80377e-3	2.18463e-3	1.49484e-3	$\boxed{1.24874\text{e-}3}$	$\boxed{1.16084\text{e-}3}$
15876	1/64	$\boxed{3.37157\text{e-}3}$	$\boxed{1.71644\text{e-}3}$	$\boxed{9.52229\text{e-}4}$	6.64250e-4	$\boxed{5.69713\text{e-}4}$

Table 5.1: Accuracy assessment. Errors (5.6.1) using the VEM (5.4.1), with polynomial degrees $(k,\ell) = (2,1)$, physical parameters $\nu = \kappa = 1$ and the mesh family mesh $\mathcal{T}_h^1$.

In order to study the trend of the stream-function and temperature errors (5.6.2), we show in Table 5.2 the results considering again the mesh $\mathcal{T}_h^1$, with $h = \Delta t = 2^{-i}$, with $i = 2, \ldots, 5$. In particular, we can observe that the rate of convergence in the mesh size h seems higher than one; this is not fully surprising, since standard interpolation estimates (in space) for the norms in (5.6.2) indicate that, potentially, the discrete space could approximate the exact solution with order $\mathcal{O}(h^2)$. In order to better investigate this aspect, in Figure 5.3 we display the

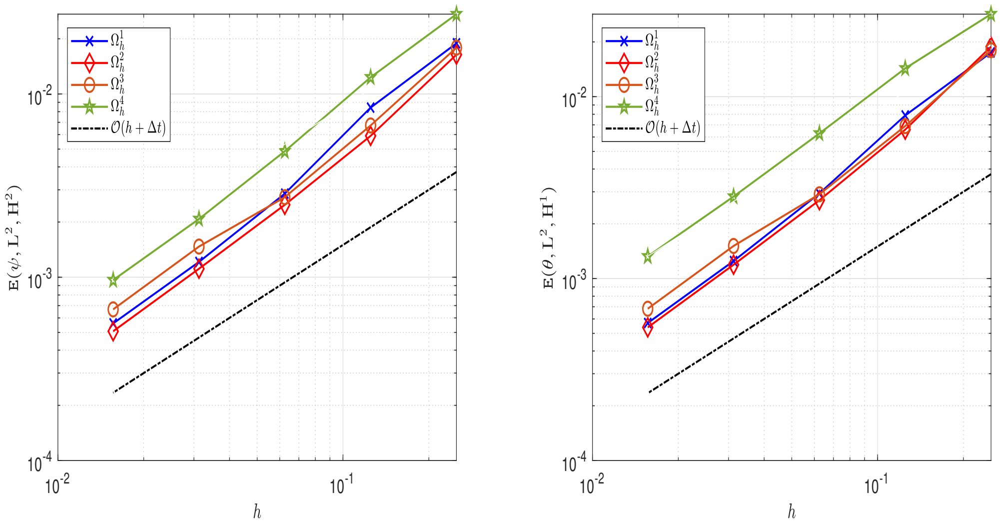

(a) Stream-function errors (b) Temperature errors

Figure 5.2: Accuracy assessment. Errors (5.6.1) for simultaneous space and time refinements, using the VEM (5.4.1) with polynomial degrees $(k, \ell) = (2, 1)$, physical parameters $\nu = \kappa = 1$ and the mesh families $\mathcal{T}_h^i$, $i = 1, \ldots, 4$.

errors (5.6.2) for space and time refinements given by $h = 2^{-i}$ and $\Delta t = 4^{-i}$, with $i = 2, \ldots, 5$, respectively, using the four mesh families. We notice that the rates of convergence seem indeed quadratic with respect to h.

				$\mathtt{E}(\psi, \mathrm{L}^\infty; \mathrm{H}^1)$		
dofs	h \ Δt	1/4	1/8	1/16	1/32	1/64
36	1/4	4.30301e-3	4.50090e-3	4.65255e-3	4.74590e-3	4.79749e-3
196	1/8	2.03865e-3	2.20110e-3	$\boxed{2.33234\text{e-}3}$	2.41662e-3	2.46443e-3
900	1/16	2.38767e-4	2.11074e-4	3.61809e-4	4.80109e-4	$\boxed{5.49619\text{e-}4}$
3844	1/32	7.26027e-4	4.35284e-4	2.05347e-4	6.71747e-5	4.99331e-5
15876	1/64	8.16241e-4	5.20174e-4	2.84604e-4	1.34953e-4	5.10645e-5
				$\mathtt{E}(\theta, \mathrm{L}^\infty; \mathrm{L}^2)$		
36	1/4	3.44760e-3	3.94792e-3	4.28939e-3	4.48462e-3	4.58811e-3
196	1/8	9.85211e-4	1.44875e-3	$\boxed{1.82900\text{e-}3}$	2.06308e-3	2.19159e-3
900	1/16	5.96219e-4	2.98014e-4	3.26274e-4	4.64998e-4	$\boxed{5.57065\text{e-}4}$
3844	1/32	8.26668e-4	4.90632e-4	2.31786e-4	9.52686e-5	9.44396e-5
15876	1/64	8.90387e-4	5.68492e-4	3.13988e-4	1.53393e-4	6.48063e-5

Table 5.2: Accuracy assessment. Errors (5.6.2) using the VEM (5.4.1), with polynomial degrees $(k, \ell) = (2, 1)$, the physical parameters $\nu = \kappa = 1$ and the mesh family $\mathcal{T}_h^1$.

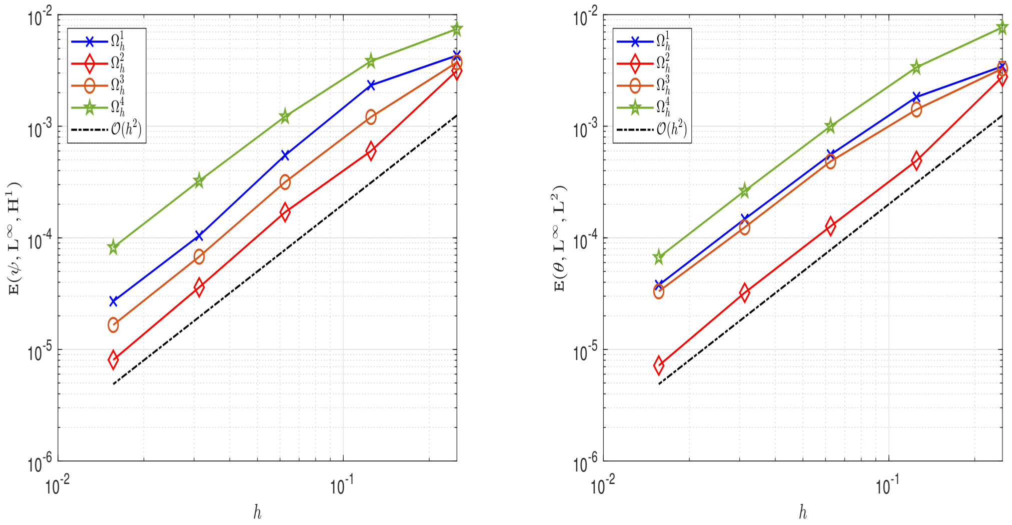

(a) Stream-function errors (b) Temperature errors

Figure 5.3: Accuracy assessment. Errors (5.6.2), using the VEM (5.4.1) with polynomial degrees $(k, \ell) = (2, 1)$, the physical parameters $\nu = \kappa = 1$ and the mesh families $\mathcal{T}_h^i$, $i = 1, \ldots, 4$.

5.6.2 Performance of the VEM for small viscosity

In this test we consider the square domain $\Omega := (0,1)^2$, the time interval $[0,1]$ and force per unit mass $\mathbf{g} = (0,-1)^T$. We solve the Boussinesq system (5.2.1), taking the load terms $\mathbf{f}_\psi$ and f_θ, boundary and initial conditions in such a way that the analytical solution is given by:

$$\mathbf{u}(x,y,t) = \begin{pmatrix} u_1(x,y,t) \\ u_2(x,y,t) \end{pmatrix} = \begin{pmatrix} -\cos(t)\sin(\pi x)\sin(\pi y) \\ -\cos(t)\cos(\pi x)\cos(\pi y) \end{pmatrix},$$

$$p(x,y,t) = \cos(t)(\sin(\pi x) + \cos(\pi y) - 2/\pi),$$

$$\psi(x,y,t) = \frac{1}{\pi}\cos(t)\sin(\pi x)\cos(\pi y) \qquad \text{and} \qquad \theta(x,y,t) = u_1(x,y,t) + u_2(x,y,t).$$

The purpose of this experiment is to investigate the performance of the VEM (5.4.1) for small viscosity parameters. In Figure 5.4, we post the errors (5.6.1) of the stream-function variable obtained with the mesh sizes $h = 1/4, 1/8, 1/16$ of $\mathcal{T}_h^2$, considering different values of ν and fixing the time step Δt as $1/8$ and $1/16$ (see Figure 5.4(a) and Figure 5.4(b), respectively). It can be observed that the solutions of our VEM are accurate even for small values of ν. Larger stream-function errors appear for very small viscosity values.

We observe that this results are in accordance with the general observation that exactly divergence-free Galerkin methods are more robust with respect to small diffusion parameters, see for instance [147] (and also [35] in the VEM context). On the other hand, note that the scheme proposed here has no explicit stabilization of the convection term since this is not the focus of the present work (for instance, the natural norm associated to the stability of the discrete problem does not guarantee a robust control on the convection).

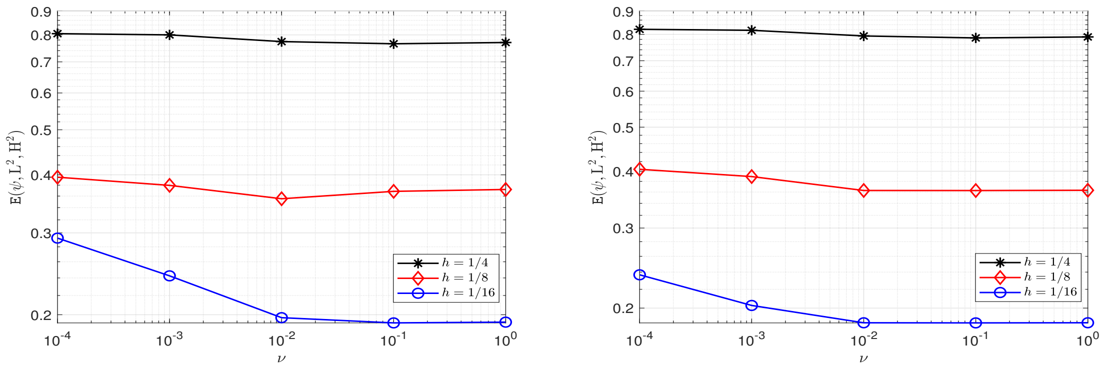

(a) Stream-function errors with $\Delta t = 1/8$ (b) Stream-function errors with $\Delta t = 1/16$

Figure 5.4: Small viscosity test. Errors (5.6.1) of the VEM (5.4.1), for different values of ν and $\kappa = 1$, using the meshes $\mathcal{T}_h^2$, polynomial degrees $(k, \ell) = (2, 1)$.

5.6.3 Natural convection in a cavity with the left wall heating

In this last example we consider the 2D natural convection benchmark problem, describing the behaviour of a incompressible flow in a squared cavity, which is heated at the left wall (see [161, 155, 128, 125, 158]). In particular, we consider the unitary square domain $\Omega = (0,1)^2$. The boundary conditions are given as follows: the temperature in the left and right walls are $\theta_L = 1$ and $\theta_R = 0$, respectively, while in the horizontal walls is $\partial_{\boldsymbol{n}}\theta = 0$ (i.e., insulated, there is no heat transfer through these walls), no-slip boundary conditions are imposed for the fluid flow at all walls. In terms of the stream-function these conditions are given by: $\psi = \partial_x\psi = \partial_y\psi = 0$ on $\Gamma \times (0,T)$, as shown in Figure 5.5. The initial conditions are chosen as $\psi_0 = -x + y$ and $\theta_0 = 1$ (so that the initial data does not satisfy the boundary conditions).

We consider the forces $\mathbf{f}_\psi = \mathbf{0}$, $f_\theta = 0$ and $\mathbf{g} = \mathrm{PrRa}(0,1)^T$, where Pr and Ra denote the Prandtl and Rayleigh numbers, respectively. For the numerical experiment, we set the physical parameters as: $\nu = \mathrm{Pr} = 0.71$, $\mathrm{Ra} \in [10^3, 10^6]$ and $\kappa = 1$.

In order to compare our results with the existing bibliographic, we decompose the domain Ω using mesh $\mathcal{T}_h^5$ conformed by uniform squares (see Figure 5.5(b)). Moreover, the time step is $\Delta t = 10^{-3}$ and final time $T = 1$.

Streamlines and isotherms of the discrete solution obtained with our VEM (5.4.1) are posted in Figure 5.6, using $\mathrm{Ra} = 10^3, 10^4, 10^5, 10^6$ and mesh size $h = 1/64$. The results show well agreement with the results presented in the benchmark solutions in [161, 155, 128, 125, 158].

Tables 5.3 and 5.4 present a quantitative comparison between our results and those obtained by the benchmark solutions in the above papers. Table 5.3 shows the maximum vertical velocity at $y = 0.5$, for $\mathrm{Ra} = 10^4, 10^5$ and 10^6, while Table 5.4 shows the maximum horizontal velocity at $x = 0.5$, using the same values of the Rayleigh number. Here the numbers in the parenthesis denotes the numbers of elements along each edge of the domain, and is therefore an indication on the mesh finesse. We can observe that the results show good agreement, even for higher Rayleigh numbers.

Finally, for the natural convection problem we investigate the heat transfer coefficient along the vertical walls of the cavity in terms of the local Nusselt number (Nu_{local}), which is defined by: $\mathrm{Nu}_{local}(x,y) := -\partial_{\boldsymbol{n}}\theta(x,y)$. Figure 5.7 describes the variation of local Nusselt number at hot wall and cold wall, for different values of the Rayleigh number. It can be seen that the

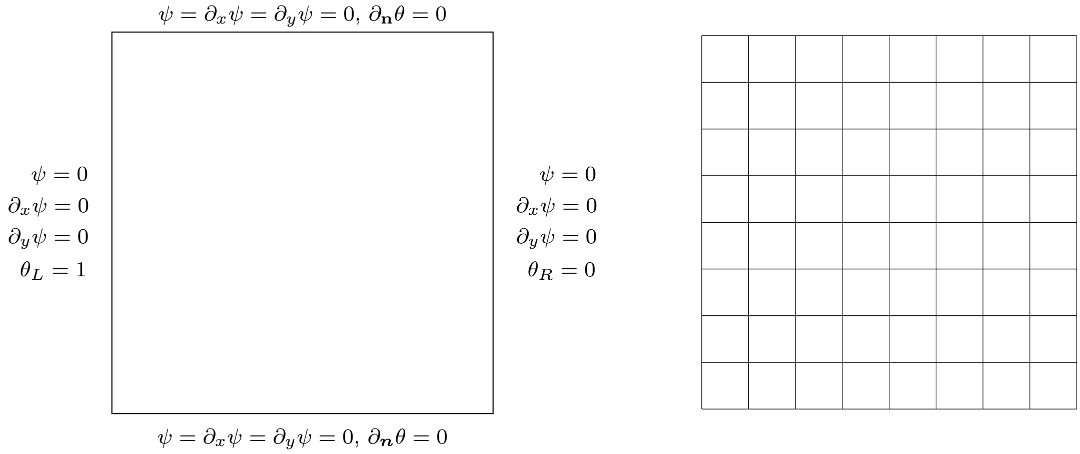

(a) Boundary conditions

(b) mesh $\mathcal{T}_h^5$ with $h = 1/8$

Figure 5.5: Natural convection cavity. Boundary conditions and domain discretized with mesh $\mathcal{T}_h^5$.

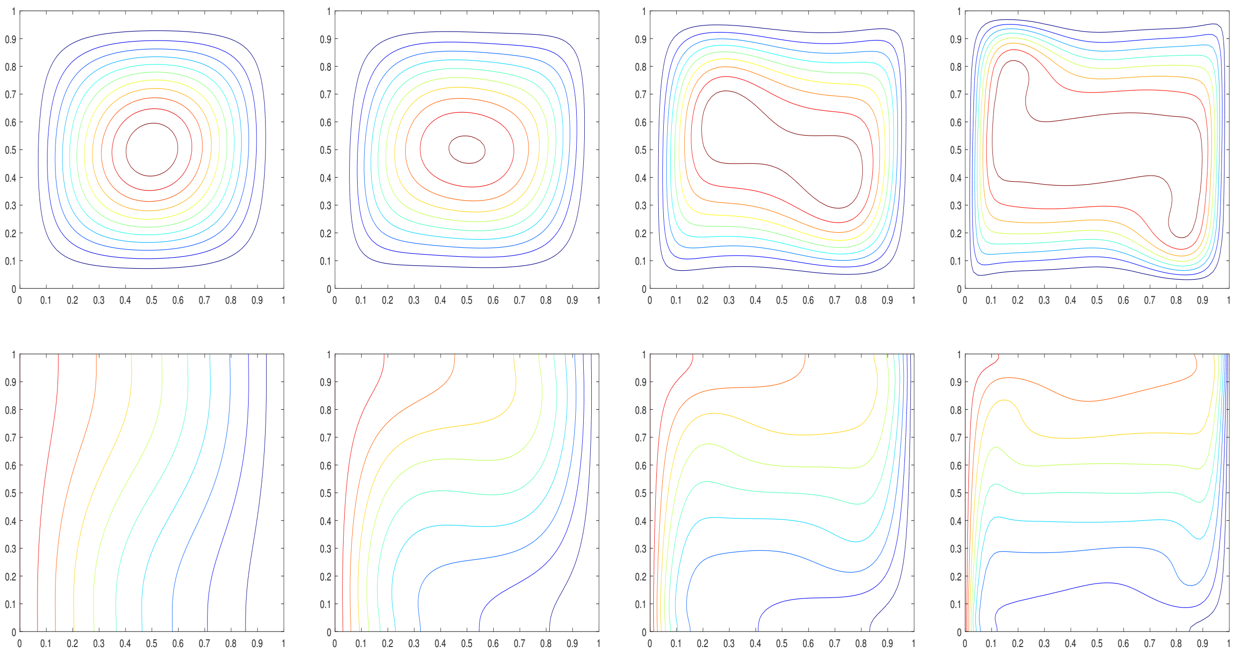

Figure 5.6: Natural convection cavity: streamlines (top panels) and isotherms (bottom panels), for $\mathrm{Ra} = 10^3, 10^4, 10^5$ and 10^6, respectively (from left to right), using the mesh $\mathcal{T}_h^5$ $(h = 1/64)$.

results show good agreement with the results presented in [161, 155, 128, 125, 158].

Ra	VEM	Ref [161]	Ref [155]	Ref [128]	Ref [125]	Ref [158]
10^4	19.56(64)	19.63(64)	19.51(41)	19.63(71)	19.90(71)	19.79(101)
10^5	68.46(64)	68.48(64)	68.22(81)	68.85(71)	70.00(71)	70.63(101)
10^6	216.37(64)	220.46(64)	216.75(81)	221.6(71)	228.0(71)	227.11(101)

Table 5.3: Natural convection cavity. Comparison of maximum vertical velocity $u_{1h} := \Pi_h^1 \partial_y \psi$ at $y = 0.5$ with the VEM (5.4.1) and mesh $\mathcal{T}_h^5$ ($h = 1/64$).

Ra	VEM	Ref [161]	Ref [155]	Ref [125]	Ref [158]
10^4	16.15(64)	16.19(64)	16.18(41)	16.10(71)	16.10(101)
10^5	34.80(64)	34.74(64)	34.81(81)	34.0(71)	34.00(101)
10^6	65.91(64)	64.81(64)	65.33(81)	65.40(71)	65.40(101)

Table 5.4: Natural convection cavity. Comparison of maximum horizontal velocity $u_{2h} := -\Pi_h^1 \partial_x \psi$ at $x = 0.5$ with the VEM (5.4.1) and mesh $\mathcal{T}_h^5$ ($h = 1/64$).

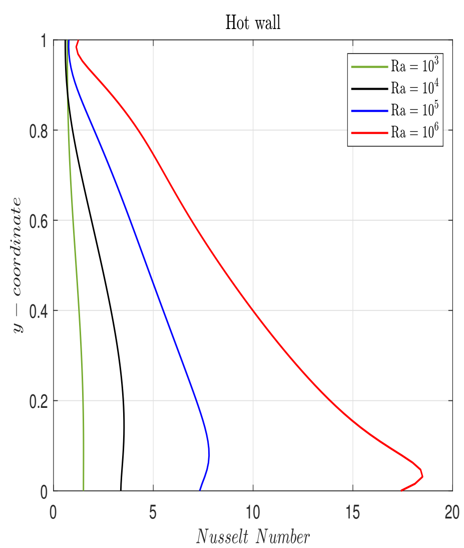

(a) Nusselt in the hot wall

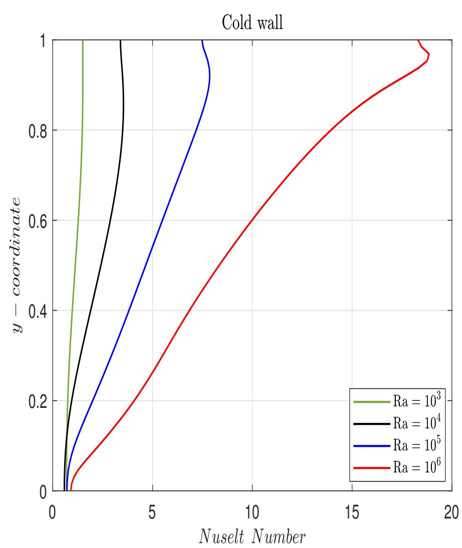

(b) Nusselt in the cold wall

Figure 5.7: Natural convection cavity. Nusselt number along the hot wall (left) and the cold wall (right) for varying Rayleigh numbers, using the VEM (5.4.1) and mesh $\mathcal{T}_h^5$, with $h = 1/64$.

Chapter 6

The Morley-type virtual element method for the Navier–Stokes equations in stream-function form

6.1 Introduction

The two dimensional steady Navier-Stokes equations in its standard velocity-pressure form reads as: given a sufficiently smooth force density $\mathbf{f} : \Omega \to \mathbb{R}^2$, find $(\mathbf{u}, p)$ such that

$$\begin{aligned} -\nu\boldsymbol{\Delta}\mathbf{u} + (\boldsymbol{\nabla}\mathbf{u})\mathbf{u} + \nabla p = \mathbf{f}, \qquad \operatorname{div}\mathbf{u} = 0 \qquad \text{in} \quad \Omega, \\ \mathbf{u} = \mathbf{0} \qquad \text{on} \quad \Gamma := \partial\Omega, \qquad (p, 1)_{0,\Omega} = 0, \end{aligned} \tag{6.1.1}$$

where $\mathbf{u} : \Omega \to \mathbb{R}^2$ is the velocity field, $p : \Omega \to \mathbb{R}$ is the pressure field and $\nu > 0$ represents the fluid viscosity. This system models the behaviour of a viscous incompressible fluid in the domain Ω. The first and second equations in (6.1.1) dictates the momentum and mass conservation of the fluid, while the third identity indicates non-slip boundary conditions for the velocity field and the last equation represents the mean value of p over Ω vanishing, which is used for the uniqueness of the pressure solution. Due to the important role it plays in the study of viscous incompressible flows, several numerical schemes have been developed to efficiently approximate the Navier–Stokes system. In particular, we are interested in discretizing this system by using general polygonal decompositions and introducing the *stream-function* of the velocity field.

In the last years, numerical methods for PDEs on polytopal meshes have received substantial attention. Different approaches have been proposed (see for instance [149, 62, 86, 32, 80, 87, 108, 70] and the references therein), offering significant flexibility in terms of dealing with complicated domains. Among them, we can find the Virtual Element Method (VEM), which was presented for first time in [27], as an evolution of mimetic finite differences and a generalization of the Finite Element Method (FEM). The approach of VEM allows to avoid an explicit construction of the discrete shape functions and this fact implies a high flexibility of the method, which is reflected, for instance in the ability to construct numerical schemes of high-order on general polygonal meshes (including "hanging vertexes" and nonconvex shapes). Moreover, in the construction of discrete spaces with high-regularity and of schemes with the divergence-free property (in the context of fluid problems). In virtue of these features, the VEM technology has enjoyed extensive success in numerical modeling and engineering applications, both in its conforming and *nonconforming* approaches (see for instance [58, 65, 29, 18, 39, 22, 126, 127, 66]).

In particular, many works have been devoted to solving problems in fluid mechanics by using the VEM. Below are two list of representative works in the conforming and nonconforming cases; [17, 98, 35, 41, 3, 131] and [64, 118, 164, 119], respectively. For a current state of the art on VEM, we refer to book [16].

In [20, 163] the authors have introduced fully-nonconforming VEMs of high-order, independently and by using different approaches to solve biharmonic problems. In particular, the lowest-order configuration (i.e., $k = 2$) of these VEMs, can be consider as the extension of the popular Morley FE [141] to general polygonal meshes. Since then, several schemes and analysis based on these VEMs have been developed for linear problems; see for instance [116, 159, 81, 107, 67, 4]. In the present work we are interesting to extend the Morley-type VEM to solve the nonlinear fourth-order Navier-Stokes equations in stream-function form on simply connected domains (not necessarily convex) by using general polygonal decompositions.

Typically, the velocity-pressure formulation (6.2.1) is the most used to discretize the Navier-Stokes problem. However, the stream-function formulation has shown to be a competitive alternative to discretize fluid flow problems in two dimensions, which has been the focus of study in the last decades. In particular, we can highlight the following features: the system is reduced in a singular scalar weak formulation, with automatic satisfaction of the incompressibility condition (the velocity field is equal to the curl of the stream-function), the possibility to recover further variables of interest such as the velocity, vorticity and pressure fields by postprocessing from the stream-function. Besides, for nonlinear problems, the resulting trilinear form is naturally skew-symmetric (without adding additional terms), allowing more direct stability and convergence arguments. On the other hand, the stream-function approach avoids the difficulties related with the boundary values for the vorticity field, which are present in stream-function–vorticity formulation. Due to the attractive features discussed above, over last decades the stream-function formulation has received great attention from many researchers. In particular, in the area of Numerical Analysis several works have been devoted to the development and study of efficient numerical schemes to approximate this system. For instance; conforming and nonconforming FEMs in [71, 72, 91, 68], bivariate spline [115], *hp*-version discontinuous FE [143], NURBS-based Isogeometric Analysis in [151]. Moreover, in [111] the nonconforming Morley FEM have been used to solve the steady Quasi-Geostrophic equations, which can be seen as an extension (in form) of the two dimensional Navier-Stokes equations in stream-function formulation.

In the present contribution, we configure the Stokes complex structure of the nonconforming VEM introduced in [164] to solve the fourth-order nonlinear Navier-Stokes equations in stream-function form on domains not necessarily convex and employing general polygonal partitions of the domain, allowing additionally the reconstruction of the pressure field. By using the enhancement technique, we introduce a discrete Stokes complex structure associate to the Morley- and Crouzeix-Raviart-type Virtual Element (VE) spaces. Then, we construct suitable projections useful to build the discrete trilinear form, which mimics the interesting and *naturally skew-symmetry* property of the continuous version (see below Remark 6.3.2). In order to establish the well-posedness of the discrete nonconforming formulation, it is necessary to prove the continuity of the resulting discrete trilinear form with respect to the natural norm in the Morley-type VE space $\mathcal{M}_h$. However, this fact does not follow directly, since it involves a discrete Sobolev inclusion (namely, $\mathcal{M}_h \subset \mathrm{W}^1_4(\Omega)$). The derivation of the Sobolev embeddings require particular attention for the nonconforming approach, which is usually considered a challenging task. To the best of our knowledge, this is the first work where Sobolev embeddings for the Morley-type VE space are established. More precisely, with the aim of achieving such purpose, we introduce a novel *enriching operator*, which is a special kind of quasi-interpolation operator that maps the elements of the sum space between the continuous and nonconforming spaces (namely, $\Phi + \mathcal{M}_h$) to the conforming counterpart of the nonconforming space. Then, by using this operator and its approximation properties, we provide new discrete Sobolev embeddings for the sum space $\Phi + \mathcal{M}_h$ and we prove the well-posedness of the discrete problem by using the Banach fixed-point Theorem. Moreover, this inclusion is strongly used to obtain the error estimates of the method (see Remark 6.4.2).

It well know that due to nonconformity of the space increases the technicalities in the demonstrations of error estimates in the nonconforming approach, implying in some cases high-regularity of the solution, which are not realistic. Furthermore, for nonlinear problems these difficulties increase remarkably. In the present work, by employing the naturally skew-symmetry property of the discrete trilinear form and the discrete Sobolev inclusion, we write an abstract convergence result for the nonlinear VE scheme. Then, by exploiting again the enriching operator, we establish key approximation properties involving the bilinear and trilinear forms, together with the consistency errors, allowing the derivation of an optimal error estimate in broken H^2-norm under the *minimal regularity* condition on the weak stream-function solution (see below Theorem 6.2.2). In addition, by using duality arguments and the enriching operator we also provided new optimal error estimates in the H^1- and L^2-norm under the same regularity conditions on the stream-function and the force density.

On the other hand, by exploiting the stream-function approach, we present techniques to recover further variables of physical interest, such as, the primitive velocity and pressure variables, along with the important vorticity field. More precisely, we recover the velocity and vorticity fields through a postprocess of the discrete stream-function by using adequate polynomial projections, which are directly computable from the degrees of freedom. The pressure recovery procedure require a special attention. Indeed, we approximate the fluid pressure by employing the Stokes complex sequence associate to the Morley- and Crouzeix-Raviart-type VE spaces, and solving an additional Stokes-like system with right hand side coming from the virtual stream-function solution and the force density $\mathbf{f}$. For all the postprocessed variables, we provide optimal a priori error estimates. Furthermore, the numerical method is tested with several benchmark tests, including the Kovasznay and cavity problems, where the theoretical accuracy and the good performance of the scheme are corroborated.

We summarize the highlight of this article as follows:

- The development of a Stokes complex sequence associate to the Morley- and Crouzeix-Raviart-type VE spaces allowing not only the approximation of the stream-function but also the pressure recovery of the Navier-Stokes problem on simply connected polygonal domains (not necessarily convex).

- The construction of a new enriching operator, which allows to prove novel discrete Sobolev embeddings in the space sum $\Phi + \mathcal{M}_h$. Moreover, by using this operator, we develop a rigorous analysis obtaining optimal error estimates in broken H^i-norms ($i = 0, 1, 2$) under *minimal regularity* condition on the weak solution.

- Velocity, vorticity and pressure postprocessing algorithms with optimal error estimates and performed numerical experiments that justify the theoretical error bounds and show the good performance of the numerical scheme.

The results presented in this study mark a significant milestone towards advancing the development and analysis of novel numerical schemes based on the nonconforming Morley-type VEM for solving fourth-order problems in more complicated situations, such as, nonlinear coupled and/or time dependent systems present in the fluid and solid mechanics, and in large scale driven ocean circulation. In particular, we note that the discrete Sobolev inclusion (see below Theorem 6.4.1) can be used to establish a well-posedness analysis for the natural convection problems in stream-function–temperature form, the von Karmán plate system and the multi-layer Quasi-Geostrophic equations of the ocean, among others.

The outline of the remaining parts of this chapter reads as follows: in Section 6.2 we introduce some preliminary notations and the stream-function weak formulation of the Navier-Stokes problem (6.1.1). Moreover, we recall its well-posedness and regularity property. The Morley-type VE discretization, together with the Crouzeix-Raviart VE space are described in Section 6.3. In Section 6.4 we introduce the enriching operator, provide the discrete Sobolev embeddings and the well-posedness of the discrete problem by using a fixed-point strategy. In Section 6.5 we develop the error analysis of the scheme under minimal regularity condition on the weak solution. In Section 6.6 we describe the recovery techniques for the velocity, vorticity and pressure fields by using the discrete stream-function solution. Finally, several numerical tests on different polygonal meshes are reported in Section 6.7.

6.2 Preliminaries and continuous weak form

The Navier-Stokes in velocity-pressure weak form. The standard variational formulation of problem (6.1.1) reads as: find $(\mathbf{u}, p) \in \mathrm{H} \times Q$, such that

$$\begin{aligned} \nu(\boldsymbol{\nabla}\mathbf{u}, \boldsymbol{\nabla}\mathbf{v})_{0,\Omega} + ((\boldsymbol{\nabla}\mathbf{u})\mathbf{u}, \mathbf{v})_{0,\Omega} - (p, \operatorname{div}\mathbf{v})_{0,\Omega} &= (\mathbf{f}, \mathbf{v})_{0,\Omega} \qquad \forall \mathbf{v} \in \mathrm{H}, \\ -(g, \operatorname{div}\mathbf{u})_{0,\Omega} &= 0 \qquad\quad\;\; \forall g \in Q, \end{aligned} \tag{6.2.1}$$

where the Hilbert spaces H and Q are defined by:

$$\mathbf{H} := \left\{\mathbf{v} \in \mathbf{H}^1(\Omega) : \mathbf{v} = \mathbf{0} \quad \text{on} \quad \Gamma\right\} \qquad \text{and} \qquad Q := \left\{g \in \mathrm{L}^2(\Omega) : (g, 1)_{0,\Omega} = 0\right\}. \tag{6.2.2}$$

It is well known that problem (6.2.1) admits a unique solution (see [103]) under smallness assumption on the data. Moreover, several works have been devoted to develop numerical schemes to approximate this formulation. For instance, see [35, 97, 118, 162] in the VEM context.

In this work, we will study the Navier-Stokes equations with a different approach. More precisely, under assumption that the domain is simply connected and by using the incompressibility condition of the velocity field (i.e., $\operatorname{div}\mathbf{u} = 0$), we write an equivalent variational formulation in terms of the *stream-function* of the velocity field.

6.2.1 The stream-function weak form

Since $\Omega \subset \mathbb{R}^2$ is simply connected, is well known that a vector function $\mathbf{v} \in \mathbf{Z} := \{\mathbf{v} \in \mathbf{H} : \operatorname{div}\mathbf{v} = 0 \quad \text{in} \quad \Omega\}$ if and only if there exists a function $\varphi \in \mathrm{H}^2(\Omega)$ (called *stream-function*), such that $\mathbf{v} = \mathbf{curl}\,\varphi$.

Let us consider the following Hilbert space $\Phi := \{\varphi \in \mathrm{H}^2(\Omega) : \varphi = 0,\, \partial_{\mathbf{n}}\varphi = 0 \quad \text{on} \quad \Gamma\}$, and we endow this space with the norm $\|\varphi\|_{2,\Omega} := (\mathrm{D}^2\varphi, \mathrm{D}^2\varphi)_{0,\Omega}^{1/2} \quad \forall \varphi \in \Phi$. Then, we have that a variational formulation of problem (6.1.1), formulated in terms of stream-function, read as (see for instance [146, Section 10.4]): given $\mathbf{f} \in \mathbf{L}^2(\Omega)$, find $\psi \in \Phi$, such that

$$\nu A(\psi, \phi) + B(\psi; \psi, \phi) = F(\phi) \qquad \forall \phi \in \Phi, \tag{6.2.3}$$

where the forms $A : \Phi \times \Phi \to \mathbb{R}$, $B : \Phi \times \Phi \times \Phi \to \mathbb{R}$ and $F : \Phi \to \mathbb{R}$ are defined by:

$$A(\psi, \phi) := (\mathrm{D}^2\psi, \mathrm{D}^2\phi)_{0,\Omega}, \tag{6.2.4}$$
$$B(\zeta; \psi, \phi) := (\Delta\zeta\, \mathbf{curl}\, \psi, \nabla\phi)_{0,\Omega}, \tag{6.2.5}$$
$$F(\phi) := (\mathbf{f}, \mathbf{curl}\, \phi)_{0,\Omega}. \tag{6.2.6}$$

From the definition of the bilinear form $A(\cdot, \cdot)$ and equivalence of norms, we obtain its Φ-ellipticity. Moreover, by using the Cauchy-Schwarz inequality we easily obtain:

$$\begin{aligned} |A(\varphi, \phi)| &\leq \|\varphi\|_{2,\Omega}\|\phi\|_{2,\Omega} \qquad && \forall \varphi, \phi \in \Phi, \\ |F(\phi)| &\leq C_F\|\mathbf{f}\|_{0,\Omega}\|\phi\|_{2,\Omega} && \forall \phi \in \Phi, \end{aligned}$$

where C_F is a positive constant. Now, we recall the following continuous Sobolev inclusion: for all $\mathbf{v} \in \mathrm{H}^1(\Omega)^2$, there exists $\widetilde{C}_{\mathrm{sob}} > 0$ such that

$$\|\mathbf{v}\|_{\mathrm{L}^4(\Omega)} \leq \widetilde{C}_{\mathrm{sob}}\|\mathbf{v}\|_{1,\Omega}. \tag{6.2.7}$$

Then, by using the Hölder inequality and the above inclusion, there exists $\widehat{C_B} := \widetilde{C}^2_{\mathrm{sob}} > 0$, such that

$$|B(\zeta; \varphi, \phi)| \leq \widehat{C_B}\, \|\zeta\|_{2,\Omega}\|\varphi\|_{2,\Omega}\|\phi\|_{2,\Omega} \qquad \forall \zeta, \varphi, \phi \in \Phi.$$

From the above properties and the fixed-point Banach theorem, we can prove that problem (6.2.3) is well-posed. More precisely, we have the following existence and uniqueness result (see for instance, [103, Chapter IV, Section 2.2]).

Theorem 6.2.1. *If $\widehat{C_B} C_F \nu^{-2}\|\mathbf{f}\|_{0,\Omega} < 1$, then there exists a unique $\psi \in \Phi$ solution to problem (6.2.3), which satisfies the following continuous dependence on the data*

$$\|\psi\|_{2,\Omega} \leq C_F\nu^{-1}\|\mathbf{f}\|_{0,\Omega}.$$

Now, we state an additional regularity result for the solution of problem (6.2.3) (see for instance [49]).

Theorem 6.2.2. *Let $\psi \in \Phi$ be the unique solution of problem (6.2.3). Then, there exist $\gamma \in (1/2, 1]$ and $C_{\mathrm{reg}} > 0$, such that $\psi \in \mathrm{H}^{2+\gamma}(\Omega)$ and*

$$\|\psi\|_{2+\gamma,\Omega} \leq C_{\mathrm{reg}}\|\mathbf{f}\|_{0,\Omega}.$$

6.3 Morley-type virtual element approximation

This section is devoted to the construction of a VEM to solve problem (6.2.3). We will introduce a Morley-type VE space by using some auxiliaries local virtual spaces and the enhancement technique. More precisely, the present framework is based on the discrete Stokes complex sequence for the *Morley-* and *Crouzeix-Raviart*-type VE spaces presented in [164]. This Stokes complex structure will allow us to approximate the main unknown in problem (6.2.3) and as an important topic, also it will allow to compute the pressure variable of the Navier-Stokes system (6.1.1) as a postprocess, by solving a Stokes-like problem with right hand side coming from the discrete-stream function solution and force density $\mathbf{f}$ (cf. Subsection 6.6.3).

We start with a subsection introducing the polygonal decompositions and some useful notations, these preliminaries are followed by a subsection on the local and global nonconforming virtual spaces, their degrees of freedom and the classical VEM local projectors. Later on, we introduce other polynomial projections useful to build the discrete trilinear form.

The polygonal decompositions and basic setting

Let $\{\mathcal{T}_h\}_{h>0}$ be a sequence of decompositions of Ω into general non-overlapping simple polygons K, where $h := \max_{K\in\mathcal{T}_h} h_K$ and h_K is the diameter of K. We will denote by ∂K, N_K and $|K|$ the boundary, the number of vertices and area of each polygon K, respectively.

For each element K we denote by $\mathscr{E}_h^K$ the set of its edges, while the set of all the edges in $\mathcal{T}_h$ will be denote by $\mathscr{E}_h$. We decompose this set as the following union: $\mathscr{E}_h := \mathscr{E}_h^{\text{int}} \cup \mathscr{E}_h^{\text{bdry}}$, where $\mathscr{E}_h^{\text{int}}$ and $\mathscr{E}_h^{\text{bdry}}$ are the set of interior and boundary edges, respectively. For the set of all the vertices we have an analogous notation. More precisely, we will denote by $\mathscr{V}_h := \mathscr{V}_h^{\text{int}} \cup \mathscr{V}_h^{\text{bdry}}$ the set of vertices in $\mathcal{T}_h$, where $\mathscr{V}_h^{\text{int}}$ and $\mathscr{V}_h^{\text{bdry}}$ are the set of interior and boundary vertices, respectively. In addition, we denote by e a generic edge of $\mathscr{E}_h$ and by h_e its length.

Besides, for each $K \in \mathcal{T}_h$, we denote by $\mathbf{n}_K$ its unit outward normal vector and by $\mathbf{t}_K$ its tangential vector along the boundary ∂K. Moreover, we will adopt the notation $\mathbf{n}_e$ and $\mathbf{t}_e$ for a unit normal and tangential vector of an edge $e \in \mathscr{E}_h$, respectively.

For every $\ell > 0$ and $q \in [1, +\infty)$, we define the following broken Sobolev spaces

$$\mathrm{W}_q^\ell(\mathcal{T}_h) := \{\phi \in \mathrm{L}^2(\Omega) : \phi|_K \in \mathrm{W}_q^\ell(K) \quad \forall K \in \mathcal{T}_h\},$$

and we endow these spaces with the following broken seminorm:

$$|\phi|_{\ell,q,h} := \Big(\sum_{K\in\mathcal{T}_h} |\phi|_{\ell,q,K}^q \Big)^{1/q},$$

where $|\cdot|_{\ell,q,K}$ is the usual seminorm in $\mathrm{W}^{\ell,q}(K)$. When $q = 2$, we omit the index q and write $\mathrm{H}^\ell(\mathcal{T}_h)$ instead $\mathrm{W}_2^\ell(\mathcal{T}_h)$, with the corresponding seminorm denoted by $|\cdot|_{\ell,h}$.

Next, we will define the jump operator across an edge e. First, for each $\phi_h \in H^2(\mathcal{T}_h)$, we denote by $\phi_h^\pm$ the trace of $\phi_h|_{K^\pm}$, with $e \subset \partial K^+ \cap \partial K^-$. Then, the jump operator $[\![\cdot]\!]$ is defined as follows:

$$[\![\phi_h]\!] := \begin{cases} \phi_h^+ - \phi_h^- & \text{for every } e \in \mathscr{E}_h^{\text{int}}, \\ \phi_h|_e & \text{for every } e \in \mathscr{E}_h^{\text{bdry}}. \end{cases}$$

The same notation is adopted for vectorial fields. Let us define a subspace of $\mathrm{H}^2(\mathcal{T}_h)$ with certain continuity:

$$\begin{aligned}\mathrm{H}^{2,\mathrm{NC}}(\mathcal{T}_h) := \Big\{\phi_h \in \mathrm{H}^2(\mathcal{T}_h) : \phi_h \in C^0(\mathscr{V}_h^{\text{int}}), \quad \phi_h(\mathbf{v}_i) = 0 \quad \forall \mathbf{v}_i \in \mathscr{V}_h^{\text{bdry}}, \\ ([\![\partial_{\mathbf{n}_e}\phi_h]\!], 1)_{0,e} = 0 \quad \forall e \in \mathscr{E}_h\Big\},\end{aligned}$$

where $C^0(\mathscr{V}_h^{\text{int}})$ is the set of functions continuous at internal vertexes.

Finally, for every integer $\ell \geq 0$, the piecewise ℓ-order polynomial space is defined by:

$$\mathbb{P}_\ell(\mathcal{T}_h) := \{\chi \in \mathrm{L}^2(\Omega) : \chi|_K \in \mathbb{P}_\ell(K) \quad \forall K \in \mathcal{T}_h\}.$$

In what follows, we will introduce some preliminary spaces, which are useful to construct the Morley-type VE space to approximate the solution of problem (6.2.3).

6.3.1 Some auxiliary spaces

For every polygon $K \in \mathcal{T}_h$, first we consider the following auxiliary finite dimensional space [20, 163, 116]:

$$\widetilde{\mathcal{M}}_h(K) := \left\{\phi_h \in \mathrm{H}^2(K) : \Delta^2\phi_h \in \mathbb{P}_2(K),\ \ \phi_h|_e \in \mathbb{P}_2(e),\ \ \Delta\phi_h|_e \in \mathbb{P}_0(e) \quad \forall e \in \partial K\right\}.$$

Next, for a given $\phi_h \in \widetilde{\mathcal{M}}_h(K)$, we introduce the following sets:

- $\mathbf{D}_{\mathcal{M}}1$: the values of $\phi_h(\mathbf{v}_i)$ for all vertex $\mathbf{v}_i$ of the polygon K;
- $\mathbf{D}_{\mathcal{M}}2$: the edge moments $(\partial_{\mathbf{n}_e}\phi_h, 1)_{0,e}$ $\quad\forall$ edge $e \in \mathscr{E}_h^K$.

For each polygon K, we define the following projector $\Pi_K^{\mathrm{D}} : \widetilde{\mathcal{M}}_h(K) \to \mathbb{P}_2(K) \subseteq \widetilde{\mathcal{M}}_h(K)$, as the solution of the local problems:

$$\begin{aligned} A^K(\Pi_K^{\mathrm{D}}\phi_h, \chi) &= A^K(\phi_h, \chi) \quad \forall \chi \in \mathbb{P}_2(K), \\ \langle\langle\, \Pi_K^{\mathrm{D}}\phi_h, \chi \,\rangle\rangle_K &= \langle\langle \phi_h, \chi \rangle\rangle_K \quad \forall \chi \in \mathbb{P}_1(K), \end{aligned}$$

where $\langle\langle \varphi_h, \phi_h \rangle\rangle_K$ is defined as follows:

$$\langle\langle \varphi_h, \phi_h \rangle\rangle_K := \sum_{i=1}^{N_K} \varphi_h(\mathbf{v}_i)\phi_h(\mathbf{v}_i),$$

with $\mathbf{v}_i$, $1 \leq i \leq N_K$, being the vertices of K and $A^K(\cdot,\cdot)$ is the restriction of the continuous form $A(\cdot,\cdot)$ (cf. (6.2.4)) on the element K.

The operator $\Pi_K^{\mathrm{D}} : \widetilde{\mathcal{M}}_h(K) \to \mathbb{P}_2(K)$ is explicitly computable for every $\phi_h \in \widetilde{\mathcal{M}}_h(K)$, using only the information of the linear operators $\mathbf{D}_{\mathcal{M}}1 - \mathbf{D}_{\mathcal{M}}2$ (for further details, we refer to [163]).

Now, we will introduce another auxiliary local spaces. Indeed, following [164] we define the spaces:

$$\widehat{\boldsymbol{\mathcal{U}}}(K) := \left\{\mathbf{v}_h \in \mathbf{H}^1(K) : \operatorname{div}\mathbf{v}_h \in \mathbb{P}_0(K),\ \operatorname{rot}\mathbf{v}_h \in \mathbb{P}_0(K),\ \mathbf{v}_h \cdot \mathbf{n}_e \in \mathbb{P}_1(e) \quad \forall e \in \mathscr{E}_h^K\right\},$$

and

$$\widetilde{\mathcal{Z}}(K) := \left\{\phi_h \in \mathrm{H}^2(K) : \Delta^2\phi_h = 0 \quad \text{in } K,\ \phi_h|_e = 0,\ \Delta\phi_h|_e \in \mathbb{P}_0(e) \quad \forall e \in \mathscr{E}_h^K\right\}.$$

By adding $\widehat{\boldsymbol{\mathcal{U}}}(K)$ and $\mathbf{curl}$ of the functions belongs to $\widetilde{\mathcal{Z}}(K)$, we define the space

$$\boldsymbol{\mathcal{U}}_0(K) := \widehat{\boldsymbol{\mathcal{U}}}(K) + \mathbf{curl}\,(\widetilde{\mathcal{Z}}(K)).$$

Then, for each $\mathbf{v}_h \in \boldsymbol{\mathcal{U}}_0(K)$ we introduce the set of vector-valued, bounded linear functional

- $\mathbf{D}_{\boldsymbol{\mathcal{U}}}$: the edge moments $h_e^{-1}(\mathbf{v}_h, \mathbf{1})_{0,e} \qquad \forall e \in \mathscr{E}_h^K$.

We observe that $\mathbf{P}_1(K) \subset \boldsymbol{\mathcal{U}}_0(K)$, and we introduce the grad projection operator $\boldsymbol{\Pi}_K^{\boldsymbol{\nabla}} : \boldsymbol{\mathcal{U}}_0(K) \to \mathbf{P}_1(K)$ as the solution of the following problem:

$$\begin{aligned}&(\boldsymbol{\nabla}(\boldsymbol{\Pi}_K^{\boldsymbol{\nabla}}\mathbf{v}_h - \mathbf{v}_h), \boldsymbol{\nabla}\boldsymbol{\chi})_{0,K} = 0 \quad \forall \boldsymbol{\chi} \in \mathbb{P}_1(K)^2,\\ &(\boldsymbol{\Pi}_K^{\boldsymbol{\nabla}}\mathbf{v}_h - \mathbf{v}_h, 1)_{0,\partial K} = 0.\end{aligned} \tag{6.3.1}$$

By using an integration by parts, we can deduce that the polynomial $\boldsymbol{\Pi}_K^{\boldsymbol{\nabla}}\mathbf{v}_h$ is computable for all $\mathbf{v}_h \in \boldsymbol{\mathcal{U}}_0(K)$ from the set of values $\mathbf{D}_{\boldsymbol{\mathcal{U}}}$ (see [164]).

Next, by employing the grad projection operator $\boldsymbol{\Pi}_K^{\boldsymbol{\nabla}}$, we define the local Crouzeix-Raviart-like VE space by:

$$\boldsymbol{\mathcal{U}}_h(K) := \Big\{\mathbf{v}_h \in \boldsymbol{\mathcal{U}}_0(K) : (\mathbf{v}_h \cdot \mathbf{n}_e - \boldsymbol{\Pi}_K^{\boldsymbol{\nabla}}\mathbf{v}_h \cdot \mathbf{n}_e, \chi)_{0,e} \quad \forall \chi \in \mathbb{P}_1(e) \setminus \mathbb{P}_0(e), \quad \forall e \in \mathscr{E}_h^K\Big\}.$$

Further, from [164] we have that the set $\mathbf{D}_{\boldsymbol{\mathcal{U}}}$ characterize uniquely the functions of $\boldsymbol{\mathcal{U}}_h(K)$. Moreover, for each $\phi_h \in \widetilde{\mathcal{M}}_h(K)$, the function $\boldsymbol{\Pi}_K^{\boldsymbol{\nabla}}\mathbf{curl}\,\phi_h$ is computable using the sets $\mathbf{D}_{\mathcal{M}}1$ and $\mathbf{D}_{\mathcal{M}}2$.

The global Crouzeix-Raviart-like space is defined as follows [164]:

$$\boldsymbol{\mathcal{U}}_h := \Big\{\mathbf{v}_h \in \mathbf{L}^2(\Omega) : \mathbf{v}_h|_K \in \boldsymbol{\mathcal{U}}_h(K) \quad \forall K \in \mathcal{T}_h, \quad ([\![\mathbf{v}_h]\!], \mathbf{1})_{0,e} = 0 \quad \forall e \in \mathscr{E}_h\Big\}. \tag{6.3.2}$$

We have that the dimension of the space $\boldsymbol{\mathcal{U}}_h$ is equal to $2N^{\mathscr{E}_h}$, where $N^{\mathscr{E}_h}$ is the total number of mesh edges of the discretization $\mathcal{T}_h$. This space will be useful in subsection 6.6.3 to present the pressure recovery technique.

Remark 6.3.1. *The nonconforming VE space defined in (6.3.2) coincides with the Crouzeix-Raviart finite element space when the polygon K is a triangle. Therefore, this space can be seen as an extension of the classical Crouzeix-Raviart space from triangle to polygonal element in the nonconforming VEM context. For further details of this discussion, see [164, Remark 8].*

6.3.2 The Morley-type nonconforming virtual element space

By using the auxiliary spaces defined in the above subsection, for each $K \in \mathcal{T}_h$ we introduce the local Morley-type VE space [164]:

$$\begin{aligned}\mathcal{M}_h(K) :=\Big\{&\phi_h \in \widetilde{\mathcal{M}}_h(K) : (\mathbf{curl}\,\phi_h \cdot \mathbf{n}_e - \boldsymbol{\Pi}_K^{\boldsymbol{\nabla}}(\mathbf{curl}\,\phi_h \cdot \mathbf{n}_e), \chi)_{0,e} = 0\\ &\forall \chi \in \mathbb{P}_1(e) \setminus \mathbb{P}_0(e) \quad \forall e \in \mathscr{E}_h^K, \quad (\phi_h - \Pi_K^{\mathrm{D}}\phi_h, \chi)_{0,K} = 0 \quad \forall \chi \in \mathbb{P}_2(K)\Big\}.\end{aligned} \tag{6.3.3}$$

In the next result we summarize the main properties of the local Morley-type VE space.

Lemma 6.3.1. *For each polygons K, the space $\mathcal{M}_h(K)$ defined in (6.3.3), we have $\mathbb{P}_2(K) \subseteq \mathcal{M}_h(K)$. Moreover, we can deduce the following properties:*

- *The linear operators $\mathbf{D}_{\mathcal{M}}1 - \mathbf{D}_{\mathcal{M}}2$ constitutes a set of degrees of freedom for $\mathcal{M}_h(K)$;*
- *The operator $\Pi_K^{\mathrm{D}} : \mathcal{M}_h(K) \to \mathbb{P}_2(K)$ is computable using the sets $\mathbf{D}_{\mathcal{M}}1 - \mathbf{D}_{\mathcal{M}}2$;*

- *For each $\phi_h \in \mathcal{M}_h(K)$, the function $\mathbf{\Pi}_K^{\boldsymbol{\nabla}}\mathbf{curl}\phi_h$ is computable using the degrees of freedom $\mathbf{D}_{\mathcal{M}}1 - \mathbf{D}_{\mathcal{M}}2$.*

With the above preliminaries we can introduce the global Morley-type VE space to the numerical approximation of the problem (6.2.3). Indeed, for every decomposition $\mathcal{T}_h$ of Ω into polygons K, the global nonconforming VE space is given by:

$$\mathcal{M}_h := \left\{\phi_h \in \mathrm{H}^{2,\mathrm{NC}}(\mathcal{T}_h) : \phi_h|_K \in \mathcal{M}_h(K) \quad \forall K \in \mathcal{T}_h\right\}. \tag{6.3.4}$$

We have that $\mathcal{M}_h \subset \mathrm{H}^{2,\mathrm{NC}}(\mathcal{T}_h)$, but $\mathcal{M}_h \nsubseteq \Phi$. Moreover, we observe that the nonconforming VE does not require C^0-continuity over Ω. This space can be seen as an extension of the popular Morley FE [141] to general polygonal meshes. For further details about this discussion, we refer to [164, Remark 20] and [163, Remark 4.1].

For the continuous bilinear form $A(\cdot,\cdot)$, we adopt the following notation:

$$A(\varphi_h, \phi_h) := \sum_{K\in\mathcal{T}_h} A^K(\varphi_h, \phi_h) \qquad \forall \varphi_h, \phi_h \in \Phi + \mathcal{M}_h.$$

We also adopt the same notation by the continuous forms $B(\cdot;\cdot,\cdot)$ and $F(\cdot)$.

6.3.3 Polynomial projection operators and discrete forms

This subsection is dedicated to the presentation of other important polynomial projections, along with the construction of the trilinear form and the load term, by using such projections. Moreover, we build the bilinear discrete form.

For each $m \in \mathbb{N} \cup \{0\}$, we consider the usual L^2-projection, $\Pi_K^m : \mathrm{L}^2(K) \to \mathbb{P}_m(K)$, defined by the function such that

$$(\phi - \Pi_K^m\phi, \chi)_{0,K} = 0 \qquad \forall \chi \in \mathbb{P}_m(K). \tag{6.3.5}$$

Moreover, we define its vectorial $\mathbf{\Pi}_K^m$ version in an analogous way. For the projection previously defined we have the following result.

We recall that there exists $C_{\mathtt{bd}} > 0$ such that (see [35]):

$$\|\Pi_K^m\phi\|_{\mathrm{L}^4(K)} \le C_{\mathtt{bd}}\|\phi\|_{\mathrm{L}^4(K)} \qquad \text{and} \qquad \|\Pi_K^m\phi\|_{0,K} \le \|\phi\|_{0,K} \quad \forall \phi \in \mathrm{L}^2(K). \tag{6.3.6}$$

Lemma 6.3.2. *Let Π_K^2, Π_K^0 and $\mathbf{\Pi}_K^1$ be the operators defined by relation (6.3.5) and by its vectorial version. Then, for each $\phi_h \in \mathcal{M}_h(K)$, the polynomial functions $\Pi_K^2\phi_h, \Pi_K^0\Delta\phi_h, \mathbf{\Pi}_K^1\mathbf{curl}\,\phi_h$ and $\mathbf{\Pi}_K^1\nabla\phi_h$ are computable using only the information of the degrees of freedom $\mathbf{D}_{\mathcal{M}}1 - \mathbf{D}_{\mathcal{M}}2$.*

Proof. Let $\phi_h \in \mathcal{M}_h(K)$, the proof of the function $\Pi_K^2\phi_h$ follows from the definition of the space $\mathcal{M}_h(K)$ (cf. (6.3.3)). Moreover, using an integration by parts we obtain

$$(\mathbf{curl}\,\phi_h, \boldsymbol{\chi})_{0,K} = \mathrm{rot}\,\boldsymbol{\chi}(\Pi_K^2\phi_h, 1)_{0,K} - (\phi_h, \boldsymbol{\chi}\cdot\mathbf{t}_K)_{0,e} \qquad \forall \boldsymbol{\chi} \in \mathbb{P}_1(K)^2,$$

then we also conclude that the $\mathbf{\Pi}_K^1\mathbf{curl}\,\phi_h$ is fully computable from the degrees of freedom. Similarly, we prove that the function $\mathbf{\Pi}_K^1\nabla\phi_h$ is computable from the degrees of freedom $\mathbf{D}_{\mathcal{M}}1 - \mathbf{D}_{\mathcal{M}}2$.

Next, we will prove that the polynomial function $\Pi_K^0 \Delta\phi_h$ is also computable. Indeed, using integration by parts, we have

$$\Pi_K^0 \Delta\phi_h = |K|^{-1}(\partial_{\mathbf{n}_K}\phi_h, 1)_{0,\partial K} = |K|^{-1}\sum_{e\in\partial K}(\partial_{\mathbf{n}_e}\phi_h, 1)_{0,e},$$

and note that the above integral is computable using the output values of the set $\mathbf{D}_{\mathcal{M}}2$. □

Now, we will build the discrete version of the continuous forms defined in (6.2.4), (6.2.5) and (6.2.6) using the operators introduced previously. First, we consider the following discrete local bilinear form, $A_h^K : \mathcal{M}_h(K) \times \mathcal{M}_h(K) \to \mathbb{R}$ approximating the continuous form $A(\cdot,\cdot)$:

$$A_h^K(\varphi_h, \phi_h) := A^K\left(\Pi_K^{\mathrm{D}}\varphi_h, \Pi_K^{\mathrm{D}}\phi_h\right) + S_{\mathrm{D}}^K\left((\mathrm{I}-\Pi_K^{\mathrm{D}})\varphi_h, (\mathrm{I}-\Pi_K^{\mathrm{D}})\phi_h\right) \quad \forall \varphi_h, \phi_h \in \mathcal{M}_h(K), \tag{6.3.7}$$

where $S_{\mathrm{D}}^K(\cdot,\cdot)$ is any symmetric positive definite bilinear form to be chosen as to satisfy:

$$c_* A^K(\phi_h, \phi_h) \le S_{\mathrm{D}}^K(\phi_h, \phi_h) \le c^* A^K(\phi_h, \phi_h) \qquad \forall \phi_h \in \mathrm{Ker}(\Pi_K^{\mathrm{D}}), \tag{6.3.8}$$

with c_* and c^* positive constants independent of K. More precisely, we choose the following computable representation satisfying property (6.3.8) (see [67, Lemma 5.1]):

$$S_{\mathrm{D}}^K(\varphi_h, \phi_h) := h_K^{-2}\sum_{i=1}^{N_{\mathrm{dof}}^K} \mathrm{dof}_i(\varphi_h)\mathrm{dof}_i(\phi_h) \qquad \forall \varphi_h, \phi_h \in \mathcal{M}_h(K),$$

where N_{dof}^K denote the number of degrees freedom of $\mathcal{M}_h(K)$ and $\mathrm{dof}_i(\cdot)$ is the operator that to each smooth enough function ϕ associates the ith local degree of freedom $\mathrm{dof}_i(\phi)$, with $1 \le i \le N_{\mathrm{dof}}^K$.

To approximate the local trilinear form $B^K(\cdot;\cdot,\cdot)$, we consider the following expression:

$$B_h^K(\zeta_h; \varphi_h, \phi_h) := \left(\Pi_K^0\Delta\zeta_h\, \mathbf{\Pi}_K^1 \mathbf{curl}\,\varphi_h, \mathbf{\Pi}_K^1\nabla\phi_h\right)_{0,K} \qquad \forall \zeta_h, \varphi_h, \phi_h \in \mathcal{M}_h(K). \tag{6.3.9}$$

Finally, for the functional (6.2.6) we consider the following local approximation:

$$F_h^K(\phi_h) := (\mathbf{\Pi}_K^1\mathbf{f}, \mathbf{curl}\,\phi_h)_{0,K} \equiv (\mathbf{f}, \mathbf{\Pi}_K^1\mathbf{curl}\,\phi_h)_{0,K} \qquad \forall \phi_h \in \mathcal{M}_h(K).$$

Thus, for all $\zeta_h, \varphi_h, \phi_h \in \mathcal{M}_h$, we define the global multilineal forms, as follows:

$$A_h : \mathcal{M}_h \times \mathcal{M}_h \to \mathbb{R}, \quad A_h(\varphi_h, \phi_h) := \sum_{K\in\mathcal{T}_h} A_h^K(\varphi_h, \phi_h), \tag{6.3.10}$$

$$B_h : \mathcal{M}_h \times \mathcal{M}_h \times \mathcal{M}_h \to \mathbb{R}, \quad B_h(\zeta_h; \varphi_h, \phi_h) := \sum_{K\in\mathcal{T}_h} B_h^K(\zeta_h; \varphi_h, \phi_h), \tag{6.3.11}$$

$$F_h : \mathcal{M}_h \to \mathbb{R}, \quad F_h(\phi_h) := \sum_{K\in\mathcal{T}_h} F_h^K(\phi_h). \tag{6.3.12}$$

We recall that all the forms defined above are computable using the degrees of freedom and the trilinear form $B_h(\cdot;\cdot,\cdot)$ is extendable to the whole space Φ.

The following result establishes the classical consistency and stability VEM properties (see for instance [27, 22, 65, 164]).

Lemma 6.3.3. *The local bilinear forms $A^K(\cdot,\cdot)$ and $A_h^K(\cdot,\cdot)$ satisfy the following properties:*

- *consistency: for all $h > 0$ and for all $K \in \mathcal{T}_h$, we have that*

$$A_h^K(\chi,\phi_h) = A^K(\chi,\phi_h) \qquad \forall \chi \in \mathbb{P}_2(K), \qquad \forall \phi_h \in \mathcal{M}_h(K), \tag{6.3.13}$$

- *stability and boundedness: there exist positive constants α_1 and α_2, independent of h and K, such that:*

$$\alpha_1 A^K(\phi_h,\phi_h) \le A_h^K(\phi_h,\phi_h) \le \alpha_2 A^K(\phi_h,\phi_h) \qquad \forall \phi_h \in \mathcal{M}_h(K). \tag{6.3.14}$$

Remark 6.3.2. *We observe that the discrete trilinear form $B_h(\cdot;\cdot,\cdot)$, defined in (6.3.11) (see also (6.3.9)), preserves the natural skew-symmetry property of the continuous trilinear form $B(\cdot;\cdot,\cdot)$ defined in (6.2.5). Thus, we do not need to add any additional term in order to guarantee such property, unlike velocity-pressure virtual element formulations, where a transpose term is added (see [162] in the nonconforming approach). This important fact has also advantages from the computational viewpoint.*

6.4 Discrete formulation and its well-posedness

In this section we write the nonconforming discrete VE formulation and we provide its well-posedness by using a fixed-point strategy.

The nonconforming VE problem reads as: find $\psi_h \in \mathcal{M}_h$, such that

$$\nu A_h(\psi_h,\phi_h) + B_h(\psi_h;\psi_h,\phi_h) = F_h(\phi_h) \qquad \forall \phi_h \in \mathcal{M}_h, \tag{6.4.1}$$

where the multilineal forms $A_h(\cdot,\cdot)$, $B_h(\cdot;\cdot,\cdot)$ and $F_h(\cdot)$ are defined in (2.3.12), (2.3.13) and (2.3.15), respectively.

In order to prove that problem (6.4.1) is well-posed, in next section, we will introduce an *enriching operator* $\widetilde{E}_h$, from the sum space $\Phi + \mathcal{M}_h$ into the conforming counterpart of the space $\mathcal{M}_h$. Moreover, we establish some approximation properties for this operator, and by using such estimates we provide novel embedding results for the sum space $\Phi + \mathcal{M}_h$, which will be useful to establish the well-posedness of discrete problem and the error estimates.

We remark that the operator $\widetilde{E}_h$ constructed here can be seen as an extension of the enriching operator defined in [107] and the quasi-interpolation operator constructed in [75].

6.4.1 A new enriching operator

With the aim of introducing the aforementioned operator and establishing its approximation properties, we start by assuming the classical assumptions on the polygonal decomposition. There exists a uniform number $\rho > 0$ independent of $\mathcal{T}_h$, such that for every $K \in \mathcal{T}_h$ it holds [27]:

$\mathbf{A_1}$: K is star-shaped with respect to every point of a ball of radius $\ge \rho h_K$;

A2 : the length h_e of every edge $e \in \partial K$, satisfies $h_e \ge \rho h_K$.

From reference [74] we have that if the mesh $\mathcal{T}_h$ fulfilling the assumptions $\mathbf{A_1}$ and $\mathbf{A_2}$, then the mesh also satisfy the following property:

$\mathbf{P_1}$: For each $K \in \mathcal{T}_h$, there exists a virtual triangulation $\mathcal{T}_h^K$ of K such that $\mathcal{T}_h^K$ is uniformly shape regular and quasi-uniform. The corresponding mesh size h_T of $\mathcal{T}_h^K$ is proportional to h_K. Every edge of K is a side of a certain triangle in $\mathcal{T}_h^K$.

Remark 6.4.1. *From property $\mathbf{P_1}$, we have that the number of triangles of each virtual triangulation $\mathcal{T}_h^K$ is uniformly bounded by a number L and the size of each triangle is comparable to that of the polygon (for further details, see [74]).*

Now, for the sake of completeness, we will recall the construction of the H^2-conforming virtual space [18].

Conforming virtual local and global space. For every polygon $K \in \mathcal{T}_h$, we introduce the following preliminary finite dimensional space [18]:

$$\widetilde{\mathcal{W}}_h^{\mathrm{C}}(K) := \big\{\phi_h \in \mathrm{H}^2(K) : \Delta^2\phi_h \in \mathbb{P}_2(K), \phi_h|_{\partial K} \in C^0(\partial K), \phi_h|_e \in \mathbb{P}_3(e)\ \forall e \subseteq \partial K, \\ \nabla\phi_h|_{\partial K} \in \mathbf{C}^0(\partial K), \partial_{\mathbf{n}_e}\phi_h|_e \in \mathbb{P}_1(e)\ \forall e \subseteq \partial K\big\},$$

Next, for a given $\phi_h \in \widetilde{\mathcal{W}}_h^{\mathrm{C}}(K)$, we introduce two sets $\mathbf{D}_{\mathbf{v}}^{\mathrm{C}}$ and $\mathbf{D}_{\nabla}^{\mathrm{C}}$ of linear operators from the local virtual space $\widetilde{\mathcal{W}}_h^{\mathrm{C}}(K)$ into $\mathbb{R}$:

- $\mathbf{D}_{\mathbf{v}}^{\mathrm{C}}$: the values of $\phi_h(\mathbf{v})$ for all vertex $\mathbf{v}$ of the polygon K;
- $\mathbf{D}_{\nabla}^{\mathrm{C}}$: the values of $h_{\mathbf{v}}\nabla\phi_h(\mathbf{v})$ for all vertex $\mathbf{v}$ of the polygon K,

where $h_{\mathbf{v}}$ is a characteristic length attached to each vertex $\mathbf{v}$, for instance to the average of the diameters of the elements with $\mathbf{v}$ as a vertex.

Now, we consider the operator $\Pi_K^{\mathrm{D,C}} : \widetilde{\mathcal{W}}_h^{\mathrm{C}}(K) \longrightarrow \mathbb{P}_2(K) \subseteq \widetilde{\mathcal{W}}_h^{\mathrm{C}}(K)$ associated to the conforming approach, which is computable using the sets $\mathbf{D}_{\mathbf{v}}^{\mathrm{C}}$ and $\mathbf{D}_{\nabla}^{\mathrm{C}}$ (for further details see [18, Lemma 2.1]).

Next, for each $K \in \mathcal{T}_h$, we consider the conforming local virtual space given by:

$$\mathcal{W}_h^{\mathrm{C}}(K) := \Big\{\phi_h \in \widetilde{\mathcal{W}}_h^{\mathrm{C}}(K) : (\phi_h - \Pi_K^{\mathrm{D,C}}\phi_h, \chi)_{0,K} = 0 \quad \forall \chi \in \mathbb{P}_2(K)\Big\}.$$

For every decomposition $\mathcal{T}_h$ of Ω into polygons K, we define the conforming virtual spaces $\mathcal{W}_h^{\mathrm{C}}$:

$$\mathcal{W}_h^{\mathrm{C}} := \big\{\phi_h \in \Phi :\ \phi_h|_K \in \mathcal{W}_h^{\mathrm{C}}(K) \qquad \forall K \in \mathcal{T}_h\big\}.$$

We recall that the global degrees of freedom are defined by $\mathbf{D}_{\mathbf{v}}^{\mathrm{C}}$ and $\mathbf{D}_{\nabla}^{\mathrm{C}}$ excluding the degrees of freedom on the boundary Γ.

Construction of the enriching operator. We will extend the ideas of [107, 75]. First, we will introduce some additional notations. Indeed, for each vertex $\mathbf{v} \in \mathscr{V}_h$ and for all $e \in \mathscr{E}_h$ we define the following sets (*patches*):

$$\omega(\mathbf{v}) := \bigcup\big\{K \in \mathcal{T}_h : \mathbf{v} \in K\big\} \quad \text{and} \quad \omega(e) := \bigcup\big\{K \in \mathcal{T}_h : e \in \partial K\big\}.$$

Moreover, for each $K \in \mathcal{T}_h$ we define

$$\omega(K) := \bigcup\big\{\widehat{K} \in \mathcal{T}_h : K \cap \widehat{K} \neq \emptyset\big\},$$

and for a function $\phi_h \in \mathrm{H}^2(\mathcal{T}_h)$, we defined the following broken seminorm

$$|\phi_h|_{2,\omega(K),h} := \Big(\sum_{\widehat{K}\in\omega(K)} |\phi_h|^2_{2,\widehat{K}}\Big)^{1/2}.$$

We will denote by $N(\mathbf{v})$ and by $N(e)$ the number of elements in $\omega(\mathbf{v})$ and $\omega(e)$, respectively. In addition, for any $\varphi_h \in \Phi + \mathcal{M}_h$, we introduce the piecewise L^2-projection Π^2, as $\Pi^2\varphi_h|_K = \Pi^2_K(\varphi_h|_K)$, where Π^2_K is the usual L^2-projection onto $\mathbb{P}_2(K)$ defined in (6.3.5).

Let $N^{\mathrm{C}}_{\mathrm{dof}} := \dim(\mathcal{W}^{\mathrm{C}}_h)$, then as in [107, 75] we can relabel the degrees of freedom using a single subindex $j = 1, \ldots, N^{\mathrm{C}}_{\mathrm{dof}}$ and will denote the degrees of freedom by $\{\mathbf{D}^{\mathrm{C}}_j\}_{j=1}^{N^{\mathrm{C}}_{\mathrm{dof}}}$, which are associated with the shape basis functions $\{\zeta_j\}_{j=1}^{N^{\mathrm{C}}_{\mathrm{dof}}}$ of the space $\mathcal{W}^{\mathrm{C}}_h$. Employing this notation the enriching operator $\widetilde{E}_h : \Phi + \mathcal{M}_h \to \mathcal{W}^{\mathrm{C}}_h$ is defined by:

$$\widetilde{E}_h\varphi_h(x) = \sum_{j=1}^{N^{\mathrm{C}}_{\mathrm{dof}}} \mathbf{D}^{\mathrm{C}}_j(\widetilde{E}_h\varphi_h)\zeta_j(x),$$

where the degrees of freedom for $\widetilde{E}_h\varphi_h$ are determined by:

1. $\mathbf{D}^{\mathrm{C}}_{1,\mathbf{v}}(\widetilde{E}_h\varphi_h) = \widetilde{E}_h\varphi_h(\mathbf{v}) := \varphi_h(\mathbf{v}) \qquad \forall \mathbf{v} \in \mathscr{V}^{\mathrm{int}}_h$;

2. $\mathbf{D}^{\mathrm{C}}_{2,\mathbf{v}}(\widetilde{E}_h\varphi_h) := \frac{1}{N(\mathbf{v})}\sum_{\widehat{K}\in\omega(\mathbf{v})} h_{\mathbf{v}}\nabla(\Pi^2\varphi_h|_{\widehat{K}}(\mathbf{v})) \qquad \forall \mathbf{v} \in \mathscr{V}^{\mathrm{int}}_h$.

The following result establishes approximation properties of the enriching operator $\widetilde{E}_h$.

Proposition 6.4.1. *For all $\phi_h \in \Phi + \mathcal{M}_h$, there exists $C > 0$ independent of h, such that*

$$\sum_{j=0}^{2} h_K^{2j}|\phi_h - \widetilde{E}_h\phi_h|^2_{j,K} \le Ch_K^4|\phi_h|^2_{2,\omega(K),h} \qquad \forall K \in \mathcal{T}_h.$$

Proof. First, we note that using the same arguments used in [107, Lemma 4.2] and [75, Lemma 4.1] (see also [4]), for all $\phi_h \in \Phi + \mathcal{M}_h$, we have that

$$\|\phi_h - \widetilde{E}_h\phi_h\|_{0,K} \le Ch_K^2|\phi_h|_{2,\omega(K),h} \quad \text{and} \quad |\phi_h - \widetilde{E}_h\phi_h|_{2,K} \le C|\phi_h|_{2,\omega(K),h}. \tag{6.4.2}$$

Now, by using standard inequality and (6.4.2), there exists a constant $C > 0$, independent to h_K, such that

$$\begin{aligned}|\phi_h - \widetilde{E}_h\phi_h|_{1,K} &\le C(h_K|\phi_h - \widetilde{E}_h\phi_h|_{2,K} + h_K^{-1}\|\phi_h - \widetilde{E}_h\phi_h\|_{0,K})\\ &\le C(h_K|\phi_h|_{2,\omega(K),h} + h_K^2h_K^{-1}|\phi_h|_{2,\omega(K),h})\\ &\le Ch_K|\phi_h|_{2,\omega(K),h}.\end{aligned} \tag{6.4.3}$$

The desired result follows from (6.4.2) and (6.4.3). □

6.4.2 Discrete Sobolev embeddings and properties of the discrete forms

In this subsection we establish two important estimates, which are useful to prove the continuity of the discrete multilineal forms. We start presenting the main result of this section, which establishes discrete Sobolev embeddings for the space $\Phi + \mathcal{M}_h$.

Theorem 6.4.1. *For any $2 \leq q < \infty$ there exists a positive constant C, independent of h, such that*

$$|\phi_h|_{1,q,h} \leq C_{\mathtt{sob}} |\phi_h|_{2,h} \qquad \forall \phi_h \in \Phi + \mathcal{M}_h.$$

Proof. Let $2 \leq q < \infty$, $\phi_h \in \Phi + \mathcal{M}_h$ and $\widetilde{E}_h : \Phi + \mathcal{M}_h \to \mathcal{W}_h^{\mathrm{C}}$ be the enriching operator defined in the above subsection. Then, by using the triangle inequality, the embedding of $\mathrm{H}^2(\Omega)$ into $W_q^1(\Omega)$ and stability property in Proposition 6.4.1, we have that

$$\begin{aligned} |\phi_h|_{1,q,h} &\leq |\phi_h - \widetilde{E}_h\phi_h|_{1,q,h} + |\widetilde{E}_h\phi_h|_{1,q,\Omega} \\ &\leq |\phi_h - \widetilde{E}_h\phi_h|_{1,q,h} + C|\widetilde{E}_h\phi_h|_{2,\Omega} \\ &\leq |\phi_h - \widetilde{E}_h\phi_h|_{1,q,h} + C|\phi_h|_{2,h}. \end{aligned} \tag{6.4.4}$$

In what follows we will estimate the term $|\phi_h - \widetilde{E}_h\phi_h|_{1,q,h}$ in the right-hand side of (6.4.4). To do that, for each $K \in \mathcal{T}_h$, we consider the sub-triangulation $\mathcal{T}_h^K$ of property $\mathbf{P_1}$. Next, let $\varphi := \nabla(\phi_h - \widetilde{E}_h\phi_h)|_K$ and $\widehat{\varphi}$ be the image of φ under the affine transformation from T to the reference triangle $\widehat{T}$. Then, by using scaling arguments and the embedding of $\mathrm{H}^1(\widehat{T})$ into $\mathrm{L}^q(\widehat{T})$, there is $C > 0$ independent of K, such that

$$\begin{aligned} |\phi_h - \widetilde{E}_h\phi_h|_{1,q,T} = \|\varphi\|_{\mathrm{L}^q(T)} &\leq C|T|^{1/q}\|\widehat{\varphi}\|_{\mathrm{L}^q(\widehat{T})} \leq C|T|^{1/q}\|\widehat{\varphi}\|_{1,\widehat{T}} \\ &\leq C|T|^{(2-q)/2q}(\|\varphi\|_{0,T}^2 + h_T^2|\varphi|_{1,T}^2)^{1/2} \\ &\leq C(h_T^2)^{(2-q)/2q}(|\phi_h - \widetilde{E}_h\phi_h|_{1,T}^2 + h_T^2|\phi_h - \widetilde{E}_h\phi_h|_{2,T}^2)^{1/2} \\ &\leq Ch_K^{(2-q)/q}(|\phi_h - \widetilde{E}_h\phi_h|_{1,K}^2 + h_K^2|\phi_h - \widetilde{E}_h\phi_h|_{2,K}^2)^{1/2}, \end{aligned}$$

where we have used the relation $|T| \approx h_T^2$ and that the size of each triangle in $\mathcal{T}_h^K$ is comparable with the polygon mesh size h_K (see Remark 6.4.1).

Now, from the above estimate and Proposition 6.4.1 it holds

$$|\phi_h - \widetilde{E}_h\phi_h|_{1,q,T} \leq Ch_K^{(2-q)/q}h_K|\phi_h|_{2,\omega(K),h} \leq Ch_K^{2/q}|\phi_h|_{2,\omega(K),h}. \tag{6.4.5}$$

From bound (6.4.5) and since the number of triangles of each virtual triangulation $\mathcal{T}_h^K$ is uniformly bounded by a number L (see again Remark 6.4.1), we obtain

$$|\phi_h - \widetilde{E}_h\phi_h|_{1,q,K}^q = \sum_{T\in K}|\phi_h - \widetilde{E}_h\phi_h|_{1,q,T}^q \leq C\sum_{T\in K}h_K^2|\phi_h|_{2,\omega(K),h}^q \leq CLh_K^2|\phi_h|_{2,\omega(K),h}^q.$$

Summing over each $K \in \mathcal{T}_h$, using the fact that $q \geq 2$ and a ℓ^q-norms inequality, along with $0 < h \leq C < 1$, we obtain

$$\begin{aligned} |\phi_h - \widetilde{E}_h\phi_h|_{1,q,h} = \Big(\sum_{K\in\mathcal{T}_h}|\phi_h - \widetilde{E}_h\phi_h|_{1,q,K}^q\Big)^{1/q} &\leq Ch^{2/q}\Big(\sum_{K\in\mathcal{T}_h}|\phi_h|_{2,\omega(K),h}^q\Big)^{1/q} \\ &\leq Ch^{2/q}\Big(\sum_{K\in\mathcal{T}_h}|\phi_h|_{2,\omega(K),h}^2\Big)^{1/2} \leq Ch^{2/q}|\phi_h|_{2,h} \leq C|\phi_h|_{2,h}, \end{aligned} \tag{6.4.6}$$

where the constant $C>0$ is independent of h.

Finally, combining the estimates (6.4.4) and (6.4.6) we conclude the proof. □

The next result has been established in [163, Lemma 5.1] and allows to show that the application $|\cdot|_{2,h}$ is a norm in $\mathcal{M}_h$.

Lemma 6.4.1. *For all $\phi_h \in \mathcal{M}_h$, is holds:*

$$\|\phi_h\|_{0,\Omega} + |\phi_h|_{1,h} \leq C|\phi_h|_{2,h},$$

where $C>0$ is a constant independent of h.

The following lemma summarize other properties of the discrete forms defined in (2.3.12)-(2.3.15), which will be used to establish the well-posedness of the discrete problem.

Lemma 6.4.2. *There exist positive constants $C_{A_h}, \widetilde{\alpha}, \widehat{C_h}, C_{F_h}$, independent of h, such that for all $\zeta_h, \varphi_h, \phi_h \in \mathcal{M}_h$ the forms defined in (2.3.12)-(2.3.15) satisfies the following properties:*

$$|A_h(\varphi_h,\phi_h)| \leq C_{A_h}|\varphi_h|_{2,h}|\phi_h|_{2,h} \qquad \textit{and} \qquad A^h(\phi_h,\phi_h) \geq \widetilde{\alpha}|\phi_h|^2_{2,h}, \tag{6.4.7}$$

$$B_h(\zeta_h;\varphi_h,\phi_h) \leq \widehat{C_h}|\zeta_h|_{2,h}|\varphi_h|_{2,h}|\phi_h|_{2,h}, \tag{6.4.8}$$

$$B_h(\zeta_h;\phi_h,\phi_h) = 0, \qquad \textit{and} \qquad B_h(\zeta_h;\varphi_h,\phi_h) = -B_h(\zeta_h;\phi_h,\varphi_h), \tag{6.4.9}$$

$$|F_h(\phi_h)| \leq C_{F_h}\|\mathbf{f}\|_{0,\Omega}|\phi_h|_{2,h}. \tag{6.4.10}$$

Proof. Properties in (6.4.7) are obtained from the definition of bilinear form $A_h(\cdot,\cdot)$ and the stability property (6.3.14). To prove (6.4.8), we use the definition of trilinear form $B_h(\cdot;\cdot,\cdot)$ and Hölder inequality to obtain

$$\begin{aligned}
B_h(\zeta_h;\varphi_h,\phi_h) &\leq C^2_{\mathtt{bd}}\Big(\sum_{K\in\mathcal{T}_h}\|\Delta\zeta_h\|^2_{0,K}\Big)^{1/2}\Big(\sum_{K\in\mathcal{T}_h}\|\mathbf{curl}\,\varphi_h\|^4_{\mathrm{L}^4(K)}\Big)^{1/4}\Big(\sum_{K\in\mathcal{T}_h}\|\nabla\phi_h\|^4_{\mathrm{L}^4(K)}\Big)^{1/4}\\
&\leq C^2_{\mathtt{bd}}|\zeta_h|_{2,h}|\varphi_h|_{1,4,h}|\phi_h|_{1,4,h}\\
&\leq \widehat{C_h}|\zeta_h|_{2,h}|\varphi_h|_{2,h}|\phi_h|_{2,h},
\end{aligned}$$

where $\widehat{C_h} := (C_{\mathtt{bd}}C_{\mathtt{sob}})^2 > 0$, and $C_{\mathtt{bd}}$, $C_{\mathtt{sob}}$ are the constants in (6.3.6) and Theorem 6.4.1, respectively.

Finally, the proof of properties (6.4.9) and (6.4.10) are obtained from the definition of forms $B_h(\cdot;\cdot,\cdot)$ and $F_h(\cdot)$. □

6.4.3 A fixed-point strategy

In this subsection we will develop a fixed-point strategy to establish the well-posedness of discrete problem (6.4.1). Indeed, for a given $\xi_h \in \mathcal{M}_h$, we define the operator

$$\begin{aligned}
T^h : \mathcal{M}_h &\longrightarrow \mathcal{M}_h\\
\xi_h &\longmapsto T^h(\xi_h) = \varphi_h,
\end{aligned}$$

where φ_h is the solution of the following linear problem: find $\varphi_h \in \mathcal{M}_h$, such that

$$\nu A_h(\varphi_h,\phi_h) + B_h(\xi_h;\varphi_h,\phi_h) = F_h(\phi_h) \qquad \forall\phi_h \in \mathcal{M}_h.$$

Next, we consider the ball $Y_h := \{\phi_h \in \mathcal{M}_h : |\phi_h|_{2,h} \leq C_{F_h}(\widetilde{\alpha}\nu)^{-1}\|\mathbf{f}\|_{0,\Omega}\}$. Then, we have the following result for the operator T^h.

Lemma 6.4.3. *The operator T^h is well defined. Moreover, if*

$$\lambda_h := \widehat{C}_h C_{F_h} (\widetilde{\alpha}\nu)^{-2} \|\mathbf{f}\|_{0,\Omega} < 1. \tag{6.4.11}$$

Then, $T^h : Y_h \to Y_h$ is a contraction mapping.

Proof. The proof follows from the definition of operator T^h, Lemma 6.4.2 and the Lax-Milgram Theorem.

□

We finish this section with the following result, which establishes that the discrete problem is well-posed.

Theorem 6.4.2. *If condition (6.4.11) is satisfied, then there exists a unique $\psi_h \in \mathcal{M}_h$ solution to problem (6.4.1) satisfying the following dependence of the data*

$$|\psi_h|_{2,h} \leq C_{F_h} (\widetilde{\alpha}\nu)^{-1} \|\mathbf{f}\|_{0,\Omega}. \tag{6.4.12}$$

Proof. The proof follows from Lemma 6.4.3 and the Banach fixed-point theorem.

□

Remark 6.4.2. *We observe that to prove the well-posedness of the discrete problem (6.4.1) is enough that the Sobolev embedding in Theorem 6.4.1 holds true just for the discrete space $\mathcal{M}_h$ (see Lemma 6.4.2 and Theorem 6.4.2). However, to prove the error estimates in H^2-, H^1- and L^2-norms we need that the Sobolev inclusion holds true for the sum space $\Phi + \mathcal{M}_h$ (see below Lemmas 6.5.2 and 6.5.6). For this reason we have built a new operator and provided a more general result considering the sum space in Theorem 6.4.1.*

Remark 6.4.3. *We recall that the main motivation for considering the lowest order case is that we can derive optimal error estimates under minimal condition on the weak stream-function solution, i.e., $\psi \in \mathrm{H}^{2+\gamma}(\Omega)$, with $\gamma \in (1/2, 1]$ (cf. Theorem 6.2.2 and Section 6.5). However, by combining the strategies presented here and the construction of the Stokes complex sequence of high order developed in [164, Section 6.2], we can design a VE scheme of arbitrary order $k \geq 3$ to approximate problem (6.2.3) (and recovery the pressure field by using the algorithm presented in Section 6.6.3). Moreover, by employing similar arguments used in the present work and the ideas developed in [107, 75], we can extend the construction of an enriching operator $\widetilde{E}_h^k$ for the high-order case (see Subsection 6.4.1), which allow us to prove the well-posedness of the high-order discrete problem. On the other hand, we observe that to obtain error estimates the weak stream-function solution must have high regularity, i.e., $\psi \in \mathrm{H}^{2+\gamma}(\Omega)$, with $\gamma \geq 1$.*

6.5 Error analysis

In this section we will develop an error analysis for the VEM proposed in (6.4.1). By exploiting the naturally skew-symmetry property of the discrete trilinear form, and the consistency and boundedness properties of discrete bilinear form, we write an abstract convergence result for the nonlinear VE scheme. Then, by using the enriching operator, we establish key approximation properties involving the bilinear and trilinear forms, together with the consistency errors, which allow the derivation of an optimal error estimate in broken H^2-norm under the minimal regularity condition on the weak solution (cf. Theorem 6.2.2). Moreover, by employing duality arguments and the enriching operator we also establish optimal error estimates in the broken H^1- and L^2-norm under the same regularity condition on the stream-function ψ and the force density $\mathbf{f}$.

6.5.1 An abstract convergence result

We start with two technical lemmas involving the continuous and discrete forms $B(\cdot,\cdot,\cdot)$ and $B_h(\cdot,\cdot,\cdot)$ defined in (6.2.5) and (6.3.11), respectively.

Lemma 6.5.1. *Let $B(\cdot;\cdot,\cdot)$ be the trilinear form defined in (6.2.5). Then, for all $\zeta \in \mathrm{H}^{2+t}(\Omega)$, with $t \in (1/2, 1]$, and for all $\varphi \in \mathrm{H}^2(\Omega)$ and $\phi_h \in \mathrm{H}^1(\mathcal{T}_h)$, it holds:*

$$B(\zeta;\varphi,\phi_h) \leq C\|\zeta\|_{2+t,\Omega}\|\varphi\|_{2,\Omega}|\phi_h|_{1,h}.$$

Proof. By using the Hölder inequality, for each $\zeta \in \mathrm{H}^{2+t}(\Omega)$, with $t \in (1/2, 1]$, for all $\varphi \in \mathrm{H}^2(\Omega)$ and for all $\phi_h \in \mathrm{H}^1(\mathcal{T}_h)$, we have

$$\begin{aligned} B(\zeta;\varphi,\phi_h) &\leq \Big(\sum_{K\in\mathcal{T}_h}\|\Delta\zeta\|^4_{\mathrm{L}^4(K)}\Big)^{1/4}\Big(\sum_{K\in\mathcal{T}_h}\|\nabla\varphi\|^4_{\mathrm{L}^4(K)}\Big)^{1/4}\Big(\sum_{K\in\mathcal{T}_h}\|\nabla\phi_h\|^2_{0,K}\Big)^{1/2} \\ &\leq |\zeta|_{2,4,\Omega}|\varphi|_{1,4,\Omega}|\phi_h|_{1,h}. \end{aligned}$$

Then, from the Sobolev embeddings $\mathrm{H}^2(\Omega) \hookrightarrow \mathrm{W}^1_4(\Omega)$ and $\mathrm{H}^{2+t}(\Omega) \hookrightarrow \mathrm{W}^2_4(\Omega)$, with $t \in (1/2, 1]$, we obtain

$$B(\zeta;\varphi,\phi_h) \leq C\|\zeta\|_{2+t,\Omega}\|\varphi\|_{2,\Omega}|\phi_h|_{1,h},$$

where C depends only on Ω. The proof is complete. □

Remark 6.5.1. *Following the above arguments, we can also prove that for all $\zeta \in \mathrm{H}^{2+t}(\Omega)$, with $t \in (1/2, 1]$, and for all $\varphi_h \in \mathrm{H}^1(\mathcal{T}_h)$ and $\phi \in \mathrm{H}^2(\Omega)$, it holds*

$$B(\zeta;\varphi_h,\phi) \leq C\|\zeta\|_{2+t,\Omega}|\varphi_h|_{1,h}|\phi|_{2,\Omega}.$$

The following lemma is a consequence of the Sobolev embedding result for the sum space $\Phi + \mathcal{M}_h$ (see Theorem 6.4.1).

Lemma 6.5.2. *Let $\varphi \in \Phi$ and $\varphi_h \in \mathcal{M}_h$. Then, for each $\phi_h \in \mathcal{M}_h$, it holds*

$$|B_h(\varphi;\varphi,\phi_h) - B_h(\varphi_h;\varphi_h,\phi_h)| \leq \widehat{C}_h\Big(|\varphi_h|_{2,h}|\phi_h|_{2,h} + |\varphi-\varphi_h+\phi_h|_{2,h}(\|\varphi\|_{2,\Omega} + |\varphi_h|_{2,h})\Big)|\phi_h|_{2,h}.$$

Proof. By adding and subtracting adequate terms together with property (6.4.9) we obtain

$$\begin{aligned} &B_h(\varphi;\varphi,\phi_h) - B_h(\varphi_h;\varphi_h,\phi_h) \\ &\quad= B_h(\varphi;\varphi-\varphi_h,\phi_h) + B_h(\varphi-\varphi_h;\varphi_h,\phi_h) \\ &\quad= B_h(\varphi;\varphi-\varphi_h+\phi_h,\phi_h) - B_h(\varphi;\phi_h,\phi_h) + B_h(\varphi-\varphi_h+\phi_h;\varphi_h,\phi_h) - B_h(\phi_h;\varphi_h,\phi_h) \\ &\quad= B_h(\varphi;\varphi-\varphi_h+\phi_h,\phi_h) + B_h(\varphi-\varphi_h+\phi_h;\varphi_h,\phi_h) - B_h(\phi_h;\varphi_h,\phi_h). \end{aligned}$$

Thus, by employing Theorem 6.4.1 (with $q = 4$), we conclude the proof. □

In order to derive the abstract error estimate for the nonlinear VE scheme, we will introduce the following consistency errors. Let $\psi \in \Phi$ be the solution of continuous problem (6.2.3), then we define:

$$\mathcal{N}_h(\psi;\phi_h) := \nu A(\psi,\phi_h) + B(\psi;\psi,\phi_h) - F(\phi_h) \qquad \forall \phi_h \in \mathcal{M}_h, \tag{6.5.1}$$

$$\mathcal{C}_h(\psi;\phi_h) := B(\psi;\psi,\phi_h) - B_h(\psi;\psi,\phi_h) \qquad \forall \phi_h \in \mathcal{M}_h. \tag{6.5.2}$$

The first term above measures to what extent the continuous solution ψ does not satisfy the nonconforming virtual element formulation (6.4.1) and the second term measure of the variational crime perpetrated in the discretization of the trilinear form $B(\cdot;\cdot,\cdot)$. In addition, we define the following quantity:

$$\|F - F_h\| := \sup_{\substack{\phi_h \in \mathcal{M}_h \\ \phi_h \neq 0}} \frac{|F(\phi_h) - F_h(\phi_h)|}{|\phi_h|_{2,h}}. \tag{6.5.3}$$

In Subsection 6.5.2 we will establish approximation properties for the above terms. Next, we provide the following Strang-type result for our nonlinear VE scheme.

Theorem 6.5.1 (Abstract convergence result)**.** *Let ψ and ψ_h be the unique solutions to problems (6.2.3) and (6.4.1), respectively. There exists a positive constant C, independent of h, such that*

$$|\psi-\psi_h|_{2,h} \leq C\Big(\inf_{\phi_h \in \mathcal{M}_h} |\psi-\phi_h|_{2,h} + \inf_{\chi \in \mathbb{P}_2(\mathcal{T}_h)} |\psi-\chi|_{2,h} + \|F-F_h\| + \sup_{\substack{\phi_h \in \mathcal{M}_h \\ \phi_h \neq 0}} \Big(\frac{|\mathcal{N}_h(\psi;\phi_h)|}{|\phi_h|_{2,h}} + \frac{|\mathcal{C}_h(\psi;\phi_h)|}{|\phi_h|_{2,h}} \Big)\Big),$$

where $\mathcal{N}_h(\psi;\cdot)$ and $\mathcal{C}_h(\psi;\cdot)$ are the consistency errors defined in (6.5.1) and (6.5.2), respectively.

Proof. Let $\phi_h \in \mathcal{M}_h$ and set $\delta_h := \phi_h - \psi_h$. Then, by using triangle inequality we obtain

$$|\psi - \psi_h|_{2,h} \leq |\psi - \phi_h|_{2,h} + |\delta_h|_{2,h}. \tag{6.5.4}$$

Now, from the property (6.4.7), the consistence of bilinear forms $A_h^K(\cdot,\cdot)$ (cf. (6.3.13)), we have

$$\begin{aligned}
\nu\widetilde{\alpha}|\delta_h|_{2,h}^2 &\leq \nu A_h(\delta_h,\delta_h) = \nu A_h(\phi_h,\delta_h) - \nu A_h(\psi_h,\delta_h) \\
&= \nu A_h(\phi_h,\delta_h) - F_h(\delta_h) + B_h(\psi_h;\psi_h,\delta_h) \\
&= \nu \sum_{K\in\mathcal{T}_h} \big(A_h^K(\phi_h-\chi,\delta_h) + A^K(\chi-\psi,\delta_h)\big) + \nu \sum_{K\in\mathcal{T}_h} A^K(\psi,\delta_h) - F_h(\delta_h) + B_h(\psi_h;\psi_h,\delta_h) \\
&= \nu \sum_{K\in\mathcal{T}_h} \big(A_h^K(\phi_h-\chi,\delta_h) + A^K(\chi-\psi,\delta_h)\big) + (\nu A(\psi,\delta_h) - F_h(\delta_h) + B_h(\psi_h;\psi_h,\delta_h)) \\
&= \nu \sum_{K\in\mathcal{T}_h} \big(A_h^K(\phi_h-\chi,\delta_h) + A^K(\chi-\psi,\delta_h)\big) + \mathcal{N}_h(\psi;\delta_h) \\
&\quad + [F(\delta_h) - F_h(\delta_h)] + [B_h(\psi_h;\psi_h,\delta_h) - B(\psi;\psi,\delta_h)],
\end{aligned} \tag{6.5.5}$$

where we have added and subtracted adequate terms and χ is an arbitrary element of $\mathbb{P}_2(\mathcal{T}_h)$.

From the continuity of bilinear forms $A^K(\cdot,\cdot)$, $A_h^K(\cdot,\cdot)$, and by using the triangular inequality, we have

$$\sum_{K\in\mathcal{T}_h}\big(A_h^K(\phi_h-\chi,\delta_h)+A^K(\chi-\psi,\delta_h)\big)\leq C(|\phi_h-\psi|_{2,h}+|\psi-\chi|_{2,h})|\delta_h|_{2,h}. \tag{6.5.6}$$

Now, we add and subtract the term $B_h(\psi;\psi,\delta_h)$, then applying Lemma 6.5.2, we obtain

$$\begin{aligned}|B_h(\psi_h;\psi_h,\delta_h)-B(\psi;\psi,\delta_h)|&\leq|B_h(\psi_h;\psi_h,\delta_h)-B_h(\psi;\psi,\delta_h)|+|B_h(\psi;\psi,\delta_h)-B(\psi;\psi,\delta_h)|\\&\leq\widehat{C_h}\big(|\psi_h|_{2,h}|\delta_h|_{2,h}+|\psi-\phi_h|_{2,h}(\|\psi\|_{2,\Omega}+|\psi_h|_{2,h})\big)|\delta_h|_{2,h}+|\mathcal{C}_h(\psi;\delta_h)|.\end{aligned} \tag{6.5.7}$$

Therefore, combining (6.5.5)-(6.5.7), we get

$$\begin{aligned}\nu\widetilde{\alpha}|\delta_h|_{2,h}\leq C(|\psi-\phi_h|_{2,h}+|\psi-\chi|_{2,h})+\widehat{C_h}|\psi_h|_{2,h}|\delta_h|_{2,h}\\+\frac{|F(\delta_h)-F_h(\delta_h)|}{|\delta_h|_{2,h}}+\frac{|\mathcal{N}_h(\psi;\delta_h)|}{|\delta_h|_{2,h}}+\frac{|\mathcal{C}_h(\psi;\delta_h)|}{|\delta_h|_{2,h}}.\end{aligned}$$

From the inequality above, we obtain

$$\begin{aligned}\nu\widetilde{\alpha}(1-\widehat{C_h}(\nu\widetilde{\alpha})^{-1}|\psi_h|_{2,h})|\delta_h|_{2,h}\leq C\Big(|\psi-\phi_h|_{2,h}+|\psi-\chi|_{2,h}+\frac{|F(\delta_h)-F_h(\delta_h)|}{|\delta_h|_{2,h}}\\+\frac{|\mathcal{N}_h(\psi;\delta_h)|}{|\delta_h|_{2,h}}+\frac{|\mathcal{C}_h(\psi;\delta_h)|}{|\delta_h|_{2,h}}\Big).\end{aligned}$$

By using (6.4.12) and condition (6.4.11) we have that $(1-\widehat{C_h}(\nu\widetilde{\alpha})^{-1}|\psi_h|_{2,h})\geq 1-\lambda_h>0$. Therefore, from above inequality, we have

$$|\delta_h|_{2,h}\leq C\Big(|\psi-\phi_h|_{2,h}+|\psi-\chi|_{2,h}+\|F-F_h\|+\sup_{\substack{\phi_h\in\mathcal{M}_h\\\phi_h\neq0}}\Big(\frac{|\mathcal{N}_h(\psi;\phi_h)|}{|\phi_h|_{2,h}}+\frac{|\mathcal{C}_h(\psi;\phi_h)|}{|\phi_h|_{2,h}}\Big)\Big).$$

Finally, the desired result follows from (6.5.4) and the above estimate.

□

The next step is to provide approximation properties that can be used in Theorem 6.5.1. In next subsection we will establish such properties.

6.5.2 Approximation results and a priori error estimate

We have the following approximation result for polynomials on star-shaped domains.

Proposition 6.5.1. *For every $\phi\in\mathrm{H}^{2+t}(K)$, with $t\in[0,1]$, there exist $\phi_\pi\in\mathbb{P}_2(K)$ and $C>0$, independent of h, such that*

$$\|\phi-\phi_\pi\|_{\ell,K}\leq Ch_K^{2+t-\ell}|\phi|_{2+t,K},\qquad \ell=0,1,2.$$

For the virtual space $\mathcal{M}_h$ we have the following approximation result (see [20, 163, 116, 67]).

Proposition 6.5.2. *For each $\phi \in \mathrm{H}^{2+t}(\Omega)$, with $t \in [0,1]$, there exist $\phi_I \in \mathcal{M}_h$ and $C > 0$, independent of h, such that*

$$\|\phi - \phi_I\|_{\ell,K} \le C h_K^{2+t-\ell} |\phi|_{2+t,K}, \qquad \ell = 0,1,2.$$

Let $E_h : \mathcal{M}_h \to \mathcal{W}_h^{\mathrm{C}}$ be the restriction of the operator $\widetilde{E}_h$ to the space $\mathcal{M}_h$, i.e., $E_h := \widetilde{E}_h|_{\mathcal{M}_h}$. We note that this operator satisfies the approximation properties in Proposition 6.4.1. Then, by using the operator E_h, we will establish an error estimate involving the bilinear form $A(\cdot,\cdot)$, which will be useful to obtain an error estimate in broken H^2-norm under minimal regularity condition on the exact stream-function ψ (cf. Theorem 6.2.2).

Lemma 6.5.3. *Let $\varphi \in \mathrm{H}^{2+t}(\Omega)$, with $t \in [0,1]$. Then, for all $\phi_h \in \mathcal{M}_h$ there exists a positive constant C, independent of h, such that*

$$A(\varphi, \phi_h - E_h\phi_h) \le C h^t \|\varphi\|_{2+t,\Omega} |\phi_h|_{2,h}.$$

Proof. The proof has been established in [4, Lemma 4.10]. □

The following result establishes error estimates for the consistence errors $\mathcal{N}_h(\psi;\cdot)$ and $\mathcal{C}_h(\psi;\cdot)$ defined in (6.5.1) and (6.5.2), respectively.

Lemma 6.5.4. *Let $\psi \in \mathrm{H}^{2+\gamma}(\Omega) \cap \Phi$ be the solution of problem (6.2.3). Then, for all $\phi_h \in \mathcal{M}_h$, there exists a constant $C > 0$, independent to h, such that*

$$\begin{aligned} |\mathcal{N}_h(\psi;\phi_h)| &\le C h^\gamma (\|\psi\|_{2+\gamma,\Omega} + \|\mathbf{f}\|_{0,\Omega}) |\phi_h|_{2,h}, \\ |\mathcal{C}_h(\psi;\phi_h)| &\le C h^\gamma (\|\psi\|_{1+\gamma,\Omega} + \|\psi\|_{2,\Omega}) \|\psi\|_{2+\gamma,\Omega} |\phi_h|_{2,h}. \end{aligned}$$

Proof. Let $\phi_h \in \mathcal{M}_h$. Then, we can take $E_h\phi_h \in \mathcal{W}_h^{\mathrm{C}} \subset \Phi$ as test function in (6.2.3) to obtain

$$\nu A(\psi, E_h\phi_h) + B(\psi;\psi, E_h\phi_h) = F(E_h\phi_h). \tag{6.5.8}$$

Thus, from (6.5.1) and (6.5.8), we get

$$\begin{aligned} \mathcal{N}_h(\psi;\phi_h) &= \nu A(\psi,\phi_h) + B(\psi;\psi,\phi_h) - F(\phi_h - E_h\phi_h) - F(E_h\phi_h) \\ &= \nu A(\psi, \phi_h - E_h\phi_h) + B(\psi;\psi,\phi_h - E_h\phi_h) - F(\phi_h - E_h\phi_h). \end{aligned} \tag{6.5.9}$$

By using the identity (6.5.9), the Cauchy-Schwarz inequality, Lemmas 6.5.1, 6.5.3 along with Proposition 6.4.1, we get

$$\begin{aligned} |\mathcal{N}_h(\psi;\phi_h)| &\le C\nu h^\gamma \|\psi\|_{2+\gamma,\Omega} |\phi_h|_{2,h} + C|\psi|_{2+\gamma,\Omega}|\psi|_{2,\Omega}|\phi_h - E_h\phi_h|_{1,h} + C_F\|\mathbf{f}\|_{0,\Omega}|\phi_h - E_h\phi_h|_{1,h} \\ &\le C h^\gamma (\|\psi\|_{2+\gamma,\Omega} + \|\mathbf{f}\|_{0,\Omega}) |\phi_h|_{2,h}, \end{aligned}$$

where $C > 0$ is independent of h.

The proof of second property follows by adapting the arguments used in [136, Lemma 4.2] to the nonconforming case and using Theorem 6.4.1. □

For the consistence error in the approximation defined in (6.5.3), we have the following result.

Lemma 6.5.5. *Let* $\mathbf{f} \in \mathbf{L}^2(\Omega)$*,* $F(\cdot)$ *and* $F_h(\cdot)$ *be the functionals defined in* (6.2.6) *and* (6.3.12)*, respectively. Then, we have the following estimate:*

$$\|F - F_h\| \leq Ch\|\mathbf{f}\|_{0,\Omega}.$$

Proof. The proof follows from the definition of the functionals $F(\cdot)$ and $F_h(\cdot)$, together with approximation properties of the projector $\mathbf{\Pi}_K^1$. □

The following result provides the rate of convergence of our virtual element scheme in broken H^2-norm.

Theorem 6.5.2. *Let* $\psi \in \Phi \cap \mathrm{H}^{2+\gamma}(\Omega)$ *and* $\psi_h \in \mathcal{M}_h$ *be the unique solutions of problem* (6.2.3) *and problem* (6.4.1)*, respectively. Then, there exists a positive constant* C*, independent of* h*, such that*

$$|\psi - \psi_h|_{2,h} \leq Ch^{\gamma}(\|\psi\|_{2+\gamma,\Omega} + \|\mathbf{f}\|_{0,\Omega}).$$

Proof. The proof follows from Theorem 6.5.1, Propositions 6.5.1 and 6.5.2, together with Lemmas 6.5.4 and 6.5.5. □

6.5.3 Error estimates in broken H^1 and L^2

In this section we provide new optimal error estimates in broken H^1- and L^2-norms for the stream-function by using duality arguments and employing the enriching operator E_h, under same regularity of the weak solution ψ and data $\mathbf{f}$, considered in Theorem 6.5.2.

We start establishing the following key preliminary result involving the forms $B(\cdot;\cdot,\cdot)$ and $B_h(\cdot;\cdot,\cdot)$, which will be useful to provide the error estimates in the weak norms. This term will deal with the consistency error associate to the trilinear form present in the VEM approach and as we will observe, its manipulation is not direct, so it will require special attention due to the nonlinearity involved.

Lemma 6.5.6. *Let* $\psi \in \Phi \cap \mathrm{H}^{2+\gamma}(\Omega)$ *and* $\psi_h \in \mathcal{M}_h$ *be the unique solutions of problems* (6.2.3) *and* (6.4.1)*, respectively. Assuming that* $\mathbf{f} \in \mathbf{L}^2(\Omega)$ *and let* $\varphi \in \mathrm{H}^{2+t}(\Omega)$*, with* $t \in (1/2, 1]$*. Then, it holds*

$$\begin{aligned} T_B(\varphi) := B_h(\psi_h;\psi_h,\varphi) - B(\psi_h;\psi_h,\varphi) \leq C\left(h^{\gamma+t} + h^{2\gamma}\right)(\|\mathbf{f}\|_{0,\Omega} + \|\psi\|_{2+\gamma,\Omega})\,\|\varphi\|_{2+t,\Omega} \\ + 2C_{\mathtt{reg}}\widetilde{C}_{\mathrm{sob}}^2 C_{\mathtt{bd}}\|\mathbf{f}\|_{0,\Omega}|\psi - \psi_h|_{1,h}\|\varphi\|_{1+t,\Omega}, \end{aligned}$$

where $C > 0$ *is a constant independent of* h*, and* $\widetilde{C}_{\mathrm{sob}}$*,* $C_{\mathtt{reg}}$ *and* $C_{\mathtt{bd}}$ *are the constants in* (6.2.7)*, Theorem 6.2.2 and* (5.3.5)*, respectively.*

Proof. By using the definition of trilinear forms $B(\cdot;\cdot,\cdot)$ and $B_h(\cdot;\cdot,\cdot)$, adding and subtracting suitable terms and using the orthogonality property of the L^2-projections, we have the following identity

$$
\begin{aligned}
T_B(\varphi) = \sum_{K\in\mathcal{T}_h} & ((\Delta\psi_h - \Pi_K^0\Delta\psi_h)(\mathbf{curl}\,\psi_h - \mathbf{curl}\,\psi), \nabla\varphi)_{0,K} \\
& + (\Pi_K^0(\Delta\psi_h - \Delta\psi)(\mathbf{curl}\,\psi_h - \mathbf{\Pi}_K^1\mathbf{curl}\,\psi_h), \nabla\varphi)_{0,K} \\
& + (\Pi_K^0(\Delta(\psi_h - \psi))\mathbf{\Pi}_K^1\mathbf{curl}\,\psi_h, \nabla\varphi - \mathbf{\Pi}_K^1\nabla\varphi)_{0,K} \\
& + (\Pi_K^0\Delta\psi\mathbf{\Pi}_K^1(\mathbf{curl}\,(\psi_h - \psi)), \nabla\varphi - \mathbf{\Pi}_K^1\nabla\varphi)_{0,K} \\
& + (\Pi_K^0\Delta\psi(\mathbf{curl}\,\psi_h - \mathbf{\Pi}_K^1\mathbf{curl}\,\psi_h), \nabla\varphi)_{0,K} + ((\Delta\psi_h - \Pi_K^0\Delta\psi_h)\mathbf{curl}\,\psi, \nabla\varphi)_{0,K} \\
& + (\Pi_K^0\Delta\psi\,\mathbf{\Pi}_K^1\mathbf{curl}\,\psi, \nabla\varphi - \mathbf{\Pi}_K^1\nabla\varphi)_{0,K} \\
=: & \, T_1 + T_2 + T_3 + T_4 + T_5 + T_6 + T_7.
\end{aligned}
$$

In what follows, we will establish estimates for each terms on the right hand side of the previous identity. For the term T_1 we use the Hölder and triangle inequalities, along with approximations properties of Π_K^0, to obtain

$$
\begin{aligned}
T_1 &\leq \sum_{K\in\mathcal{T}_h} \|\Delta\psi_h - \Pi_K^0\Delta\psi_h\|_{0,K}\|\mathbf{curl}\,\psi_h - \mathbf{curl}\,\psi\|_{\mathrm{L}^4(K)}\|\nabla\varphi\|_{\mathrm{L}^4(K)} \\
&\leq \sum_{K\in\mathcal{T}_h} (2\|\Delta\psi_h - \Delta\psi\|_{0,K} + \|\Delta\psi - \Pi_K^0\Delta\psi\|_{0,K})\|\mathbf{curl}\,(\psi_h - \psi)\|_{\mathrm{L}^4(K)}\|\nabla\varphi\|_{\mathrm{L}^4(K)} \\
&\leq C(|\psi - \psi_h|_{2,h} + h^\gamma\|\psi\|_{2+\gamma,\Omega})|\psi - \psi_h|_{1,4,h}\|\nabla\varphi\|_{\mathrm{L}^4(\Omega)} \\
&\leq Ch^{2\gamma}(\|\mathbf{f}\|_{0,\Omega} + \|\psi\|_{2+\gamma,\Omega})\|\varphi\|_{2+t,\Omega},
\end{aligned}
$$

where we have used the Hölder inequality (for sequences), continuous Sobolev inclusion, along with Theorems 6.4.1 and 6.5.2.

Now, for T_2 we follow similar arguments to obtain

$$
T_2 \leq Ch^{2\gamma}(\|\mathbf{f}\|_{0,\Omega} + \|\psi\|_{2+\gamma,\Omega})\|\varphi\|_{2+t,\Omega}.
$$

For the term T_3 we employ again the Hölder inequality, the continuity of the projector $\mathbf{\Pi}_K^1$, along with Theorems 6.4.1 and 6.5.2, to obtain:

$$
\begin{aligned}
T_3 &\leq \sum_{K\in\mathcal{T}_h} \|\Pi_K^0(\Delta\psi_h - \Delta\psi)\|_{0,K}\|\mathbf{\Pi}_K^1\mathbf{curl}\,\psi_h\|_{\mathrm{L}^4(K)}\|\nabla\varphi - \mathbf{\Pi}_K^1\nabla\varphi\|_{\mathrm{L}^4(K)} \\
&\leq C|\psi - \psi_h|_{2,h}|\psi_h|_{1,4,h}h^t|\nabla\varphi|_{W_4^t(\Omega)} \\
&\leq Ch^{\gamma+t}(\|\mathbf{f}\|_{0,\Omega} + \|\psi\|_{2+\gamma,\Omega})\|\varphi\|_{2+t,\Omega}.
\end{aligned}
$$

For the term T_4, we follow similar steps to those used above, to get

$$
\begin{aligned}
T_4 &\leq \sum_{K\in\mathcal{T}_h} \|\Pi_K^0\Delta\psi\|_{0,K}\|\mathbf{\Pi}_K^1\mathbf{curl}\,(\psi_h - \psi)\|_{\mathrm{L}^4(K)}\|\nabla\varphi - \mathbf{\Pi}_K^1\nabla\varphi\|_{\mathrm{L}^4(K)} \\
&\leq Ch^{\gamma+t}(\|\mathbf{f}\|_{0,\Omega} + \|\psi\|_{2+\gamma,\Omega})\|\varphi\|_{2+t,\Omega}.
\end{aligned}
$$

Next, for the term T_5, we add and subtract suitable terms, use the Hölder inequality, properties of the L^2-projections $\mathbf{\Pi}_K^1$ and Π_K^0, together with continuous Sobolev embeddings to obtain

$$
\begin{aligned}
T_5 &\leq \sum_{K\in\mathcal{T}_h} \|\Pi_K^0\Delta\psi\|_{\mathrm{L}^4(K)}\|\mathbf{curl}\,\psi_h - \mathbf{\Pi}_K^1\mathbf{curl}\,\psi_h\|_{0,K}\|\nabla\varphi\|_{\mathrm{L}^4(K)} \\
&\leq \left(2|\psi - \psi_h|_{1,h} + Ch^{1+\gamma}\|\psi\|_{2+\gamma,\Omega}\right)\left(C_{\mathtt{bd}}\|\Delta\psi\|_{\mathrm{L}^4(\Omega)}\|\nabla\varphi\|_{\mathrm{L}^4(\Omega)}\right) \\
&\leq 2C_{\mathtt{reg}}\widetilde{C}_{\mathrm{sob}}^2C_{\mathtt{bd}}\|\mathbf{f}\|_{0,\Omega}|\psi - \psi_h|_{1,h}\|\varphi\|_{1+t,\Omega} + Ch^{\gamma+t}\|\psi\|_{2+\gamma,\Omega}\|\varphi\|_{2+t,\Omega}.
\end{aligned}
$$

Repeating the same arguments, we obtain the following bounds for the terms T_6 and T_7:

$$T_6 + T_7 \leq Ch^{\gamma+t}(\|\mathbf{f}\|_{0,\Omega} + \|\psi\|_{2+\gamma,\Omega})\|\varphi\|_{2+t,\Omega}.$$

Finally, by combining the above bounds we obtain the desired result. □

Moreover, for the bilinear form $A(\cdot,\cdot)$ we have the following auxiliary result [4, Lemma 4.11].

Lemma 6.5.7. *For $\varphi \in \mathrm{H}^{2+t}(\Omega)$ and $\phi \in \Phi \cap \mathrm{H}^{2+t}(\Omega)$, with $t \in [0,1]$, it holds:*

$$A(\varphi, \phi - \phi_I) \leq Ch^{2t}\|\varphi\|_{2+t,\Omega}\|\phi\|_{2+t,\Omega},$$

where $\phi_I \in \mathcal{M}_h$ is the interpolant of ϕ in the virtual space $\mathcal{M}_h$ (cf. Proposition 6.5.2).

In order to establish the desired error estimates, we consider the following assumption:

$$2C_{\mathtt{reg}}^2 \widetilde{C}_{\mathrm{sob}}^2 C_{\mathtt{bd}}\|\mathbf{f}\|_{0,\Omega} < 1, \tag{6.5.10}$$

where $\widetilde{C}_{\mathrm{sob}}$, and $C_{\mathtt{reg}}$ and $C_{\mathtt{bd}}$ are the constants in (6.2.7), Theorem 6.2.2 and (5.3.5), respectively.

The following theorem establish the main result of this subsection.

Theorem 6.5.3. *Let $\psi \in \Phi \cap \mathrm{H}^{2+\gamma}(\Omega)$ and $\psi_h \in \mathcal{M}_h$ be the unique solutions of problems (6.2.3) and (6.4.1), respectively. Then, under assumption (6.5.10) there exists a positive constant C, independent of h, such that*

$$\|\psi - \psi_h\|_{0,\Omega} + |\psi - \psi_h|_{1,h} \leq Ch^{2\gamma}(\|\psi\|_{2+\gamma,\Omega} + \|\mathbf{f}\|_{0,\Omega}). \tag{6.5.11}$$

Proof. First we will prove the H^1 estimate in (6.5.11). With this aim, let $\psi_I \in \mathcal{M}_h$ be the interpolant of ψ such that Proposition 6.5.2 holds true. We set $\delta_h := (\psi_h - \psi_I) \in \mathcal{M}_h$. Then, we write

$$\psi_h - \psi = (\psi_h - \psi_I) + (\psi_I - \psi) = (\psi_I - \psi) + (\delta_h - E_h\delta_h) + E_h\delta_h.$$

Thus, by using the triangle inequality together with Propositions 6.4.1 and 6.5.2, along with Theorem 6.5.2, we obtain

$$|\psi - \psi_h|_{1,h} \leq |\psi - \psi_I|_{1,h} + |\delta_h - E_h\delta_h|_{1,h} + |E_h\delta_h|_{1,h} \leq Ch^{2\gamma}\|\psi\|_{2+\gamma,\Omega} + \|\nabla E_h\delta_h\|_{0,\Omega}. \tag{6.5.12}$$

Now, the goal is to estimate the term $\|\nabla E_h\delta_h\|_{0,\Omega}$. To do that, we consider the following dual problem: given $\psi \in \Phi$ (the unique solution of the formulation (6.2.3)), find $\phi \in \Phi$, such that

$$\mathcal{A}^{DP}(\psi;\varphi,\phi) := \nu A(\varphi,\phi) + B(\psi;\varphi,\phi) + B(\varphi;\psi,\phi) = (\nabla(E_h\delta_h), \nabla\varphi)_{0,\Omega} \qquad \forall \varphi \in \Phi, \tag{6.5.13}$$

where $A(\cdot,\cdot)$ and $B(\cdot;\cdot,\cdot)$ are the continuous forms defined in (6.2.4) and (6.2.5), respectively. Following the same arguments in [111], we have that problem (6.5.13) is well-posed and from Theorem 6.2.2, we obtain that $\phi \in \Phi \cap \mathrm{H}^{2+\gamma}(\Omega)$ and

$$\|\phi\|_{2+\gamma,\Omega} \leq C_{\mathtt{reg}}\|\nabla E_h\delta_h\|_{0,\Omega}, \tag{6.5.14}$$

where $C > 0$ is a constant independent of h. Taking $\varphi = E_h\delta_h \in \mathcal{W}_h^{\mathrm{C}} \subset \Phi$ as test function, adding and subtracting δ_h in problem (6.5.13), we get

$$\|\nabla E_h\delta_h\|_{0,\Omega}^2 = \mathcal{A}^{DP}(\psi; E_h\delta_h, \phi) = \mathcal{A}^{DP}(\psi; E_h\delta_h - \delta_h, \phi) + \mathcal{A}^{DP}(\psi; \delta_h, \phi) =: I_1 + I_2. \tag{6.5.15}$$

Now, we will obtain bounds for the terms I_1 and I_2 in the above identity. For I_1, we apply Lemma 6.5.3, Remark 6.5.1, Propositions 6.4.1 and 6.5.2 to obtain

$$\begin{aligned}
I_1 &:= \mathcal{A}^{DP}(\psi; E_h\delta_h - \delta_h, \phi) \\
&= \nu A(E_h\delta_h - \delta_h, \phi) + B(\psi; E_h\delta_h - \delta_h, \phi) + B(E_h\delta_h - \delta_h; \psi, \phi) \\
&\leq C\nu h^\gamma |\delta_h|_{2,h} \|\phi\|_{2+\gamma,\Omega} + C\|\psi\|_{2+\gamma,\Omega} |E_h\delta_h - \delta_h|_{1,h} \|\phi\|_{2,\Omega} + B(E_h\delta_h - \delta_h; \psi, \phi) \\
&\leq C\nu h^{2\gamma} \|\psi\|_{2+\gamma,\Omega} \|\phi\|_{2+\gamma,\Omega} + Ch^{2\gamma} \|\psi\|_{2+\gamma,\Omega} \|\phi\|_{2,\Omega} + B(E_h\delta_h - \delta_h; \psi, \phi).
\end{aligned} \tag{6.5.16}$$

To estimate the term $B(E_h\delta_h - \delta_h; \psi, \phi)$, we start recalling that $\psi, \phi \in \mathrm{H}^{2+\gamma}(\Omega)$, with $\gamma \in (1/2, 1]$, then by using the Sobolev inclusion $\mathrm{H}^{2+\gamma}(\Omega) \hookrightarrow W_4^1(\Omega)$, we have

$$|\mathbf{curl}\, \psi \cdot \nabla\phi|_{1,\Omega} \leq \|\mathbf{curl}\, \psi\|_{1,4,\Omega} \|\nabla\phi\|_{1,4,\Omega} \leq C_{\mathtt{sob}}^2 \|\psi\|_{2+\gamma,\Omega} \|\phi\|_{2+\gamma,\Omega} < +\infty.$$

Therefore, $\mathbf{curl}\, \psi \cdot \nabla\phi \in \mathrm{H}^1(\Omega)$ (hence belongs to $\mathrm{H}^1(K)$ for each $K \in \mathcal{T}_h$). Thus, by using the definition of $B(\cdot;\cdot,\cdot)$ we have

$$\begin{aligned}
B(E_h\delta_h - \delta_h; \psi, \phi) &= \sum_{K\in\mathcal{T}_h} (\Delta(E_h\delta_h - \delta_h), \mathbf{curl}\, \psi \cdot \nabla\phi)_{0,K} \\
&\leq \sum_{K\in\mathcal{T}_h} \|\Delta(E_h\delta_h - \delta_h)\|_{-1,K} \|\mathbf{curl}\, \psi \cdot \nabla\phi\|_{1,K}.
\end{aligned}$$

Now, by using the definition of the dual norm and an integration by parts, we obtain

$$\begin{aligned}
\|\Delta(E_h\delta_h - \delta_h)\|_{-1,K} &= \sup_{\varphi\in H_0^1(K)} \frac{(\Delta(E_h\delta_h - \delta_h), \varphi)_{0,K}}{|\varphi|_{1,K}} = \sup_{\varphi\in H_0^1(K)} \frac{(\nabla(E_h\delta_h - \delta_h), \nabla\varphi)_{0,K}}{|\varphi|_{1,K}} \\
&\leq |E_h\delta_h - \delta_h|_{1,K}.
\end{aligned}$$

From the two estimates above, the Hölder inequality for sequences, Proposition 6.4.1 and estimate (6.5.14), we have

$$\begin{aligned}
B(E_h\delta_h - \delta_h; \psi, \phi) &\leq \sum_{K\in\mathcal{T}_h} |E_h\delta_h - \delta_h|_{1,K} \|\mathbf{curl}\, \psi \cdot \nabla\phi\|_{1,K} \leq |E_h\delta_h - \delta_h|_{1,h} \|\mathbf{curl}\, \psi \cdot \nabla\phi\|_{1,\Omega} \\
&\leq Ch^{2\gamma} \|\psi\|_{2+\gamma,\Omega} \|\phi\|_{2+\gamma,\Omega} \leq Ch^{2\gamma} \|\psi\|_{2+\gamma,\Omega} \|\nabla E_h\delta_h\|_{0,\Omega}.
\end{aligned}$$

Consequently, inserting the above inequality in (6.5.16), we arrive to

$$I_1 \leq Ch^{2\gamma} \|\psi\|_{2+\gamma,\Omega} \|\nabla E_h\delta_h\|_{0,\Omega}. \tag{6.5.17}$$

Now, we will estimate the remaining term I_2. Indeed, we split again $\delta_h := (\psi_h - \psi) + (\psi - \psi_I)$, then

$$I_2 = -\mathcal{A}^{DP}(\psi; \psi - \psi_h, \phi) + \mathcal{A}^{DP}(\psi; \psi - \psi_I, \phi) =: -I_{21} + I_{22}. \tag{6.5.18}$$

By using analogous arguments as those employed to bound the term I_1 and applying Proposition 6.5.2 and Lemma 6.5.7, we obtain

$$I_{22} \leq Ch^{2\gamma} \|\psi\|_{2+\gamma,\Omega} \|\nabla E_h\delta_h\|_{0,\Omega}. \tag{6.5.19}$$

Next, adding and subtracting ϕ_I, $B(\psi;\psi,\phi_I)$ and other suitable terms together with the definition of the continuous and discrete problems (cf. (6.2.3) and (6.4.1), respectively), we get

$$\begin{aligned}
I_{21} &= \nu A(\psi-\psi_h,\phi) + B(\psi;\psi-\psi_h,\phi) + B(\psi-\psi_h;\psi,\phi)\\
&= \nu A(\psi-\psi_h,\phi-\phi_I) + \nu A(\psi-\psi_h,\phi_I) + B(\psi;\psi-\psi_h,\phi) + B(\psi-\psi_h;\psi,\phi)\\
&= \nu A(\psi-\psi_h,\phi-\phi_I) + F(\phi_I) - F_h(\phi_I) + \nu A_h(\psi_h,\phi_I) + B_h(\psi_h;\psi_h,\phi_I)\\
&\quad\; - B(\psi;\psi,\phi_I) - \nu A(\psi_h,\phi_I) + B(\psi;\psi-\psi_h,\phi) + B(\psi-\psi_h;\psi,\phi)\\
&= \nu A(\psi-\psi_h,\phi-\phi_I) + \nu[A_h(\psi_h,\phi_I) - A(\psi_h,\phi_I)] + [F(\phi_I) - F_h(\phi_I)]\\
&\quad + [B_h(\psi_h;\psi_h,\phi_I-\phi) - B(\psi;\psi,\phi_I-\phi)]\\
&\quad + B(\psi-\psi_h;\psi-\psi_h,\phi) + [B_h(\psi_h;\psi_h,\phi) - B(\psi_h;\psi_h,\phi)]\\
&=: T_{A1} + T_{A2} + T_F + T_{B1} + T_{B2} + T_{B3},
\end{aligned} \tag{6.5.20}$$

where we have used also the identity

$$\begin{aligned}
B(\psi;\psi-\psi_h,\phi) + B(\psi-\psi_h;\psi,\phi) + B_h(\psi_h;\psi_h,\phi) - B(\psi;\psi,\phi)&\\
= B(\psi-\psi_h;\psi-\psi_h,\phi) + [B_h(\psi_h;\psi_h,\phi) - B(\psi_h;\psi_h,\phi)]&.
\end{aligned}$$

Applying standard arguments and (6.5.14), we obtain that

$$T_{A1} + T_{A2} + T_F + T_{B2} \leq Ch^{2\gamma}\left(\|\mathbf{f}\|_{0,\Omega} + \|\psi\|_{2+\gamma,\Omega}\right)\|\nabla E_h\delta_h\|_{0,\Omega}. \tag{6.5.21}$$

For the remaining term T_{B1}, we employ Lemmas 6.5.2 and 6.5.4, to obtain

$$\begin{aligned}
|T_{B1}| &\leq |B(\psi;\psi,\phi_I-\phi) - B(\psi;\psi,\phi_I-\phi)| + |B_h(\psi;\psi,\phi_I-\phi) - B_h(\psi_h;\psi_h,\phi_I-\phi)|\\
&\leq Ch^{\gamma}(\|\psi\|_{1+\gamma,\Omega} + \|\psi\|_{2,\Omega})\|\psi\|_{2+\gamma,\Omega}|\phi_I-\phi|_{2,h}\\
&\quad + \widehat{C_h}\left(|\psi_h|_{2,h}|\phi_I-\phi|_{2,h} + |(\psi-\psi_h)+(\phi_I-\phi)|_{2,h}(\|\psi\|_{2,\Omega} + |\psi_h|_{2,h})\right)|\phi_I-\phi|_{2,h}\\
&\leq Ch^{2\gamma}(\|\psi\|_{1+\gamma,\Omega} + \|\psi\|_{2,\Omega})\|\psi\|_{2+\gamma,\Omega}\|\nabla E_h\delta_h\|_{0,\Omega}\\
&\quad + Ch^{2\gamma}(\|\psi\|_{2+\gamma,\Omega} + \|\mathbf{f}\|_{0,\Omega})(\|\psi\|_{2,\Omega} + |\psi_h|_{2,h})\|\nabla E_h\delta_h\|_{0,\Omega}\\
&\quad + Ch^{2\gamma}(\|\psi\|_{2,\Omega} + |\psi_h|_{2,h})\|\nabla E_h\delta_h\|_{0,\Omega},
\end{aligned} \tag{6.5.22}$$

where we have used Theorem 6.5.2 and (6.5.14). For the term T_{B3}, we observe that $T_{B3} = T_B(\phi)$, then by using Lemma 6.5.6 and (6.5.14) we get

$$\begin{aligned}
T_{B3} &\leq Ch^{2\gamma}(\|\psi\|_{2+\gamma,\Omega} + \|\mathbf{f}\|_{0,\Omega})\|\phi\|_{2+\gamma,\Omega} + 2C_{\mathtt{reg}}\widetilde{C}^2_{\mathrm{sob}}C_{\mathtt{bd}}\|\mathbf{f}\|_{0,\Omega}|\psi-\psi_h|_{1,h}\|\phi\|_{2+\gamma,\Omega}\\
&\leq Ch^{2\gamma}(\|\psi\|_{2+\gamma,\Omega} + \|\mathbf{f}\|_{0,\Omega})\|\nabla E_h\delta_h\|_{0,\Omega} + 2C^2_{\mathtt{reg}}\widetilde{C}^2_{\mathrm{sob}}C_{\mathtt{bd}}\|\mathbf{f}\|_{0,\Omega}|\psi-\psi_h|_{1,h}\|\nabla E_h\delta_h\|_{0,\Omega}.
\end{aligned} \tag{6.5.23}$$

Combining (6.5.18)-(6.5.23), we have

$$|I_2| \leq C(\|\psi\|_{2+\gamma,\Omega} + \|\mathbf{f}\|_{0,\Omega})\|\nabla E_h\delta_h\|_{0,\Omega} + 2C^2_{\mathtt{reg}}\widetilde{C}^2_{\mathrm{sob}}C_{\mathtt{bd}}\|\mathbf{f}\|_{0,\Omega}|\psi-\psi_h|_{1,h}\|\nabla E_h\delta_h\|_{0,\Omega}. \tag{6.5.24}$$

The H^1 error estimate follows by combining the estimates (6.5.12), (6.5.15), (6.5.17) and (6.5.24) together with the fact that $(1 - 2C^2_{\mathtt{reg}}\widetilde{C}^2_{\mathrm{sob}}C_{\mathtt{bd}}\|\mathbf{f}\|_{0,\Omega}) > 0$ (see assumption (6.5.10)).

Finally, the L^2 estimate in (6.5.11) is obtained from the triangle inequality, Propositions 6.4.1 and 6.5.2, Lemma 6.5.7 together with Theorem 6.5.2, as follows:

$$\begin{aligned}\|\psi-\psi_h\|_{0,\Omega} &\leq \|\psi-\psi_I\|_{0,\Omega}+\|\delta_h-E_h\delta_h\|_{0,\Omega}+\|E_h\delta_h\|_{0,\Omega}\\ &\leq Ch^{2+\gamma}\|\psi\|_{2+\gamma,\Omega}+Ch^2(|\psi_h-\psi|_{2,h}+|\psi-\psi_I|_{2,h})+C|E_h\delta_h|_{1,\Omega}\\ &\leq Ch^{2\gamma}(\|\psi\|_{2+\gamma,\Omega}+\|\mathbf{f}\|_{0,\Omega}),\end{aligned}$$

where we have used norm equivalence in Φ. The proof is complete. □

We finish this section establishing the following remark.

Remark 6.5.2. *If* $\mathbf{f}$ *is a smooth function, then applying an integration by parts and the boundary conditions in (6.2.6), we have that* $(\mathbf{f},\mathbf{curl}\,\phi)_{0,\Omega}=(\mathrm{rot}\,\mathbf{f},\phi)_{0,\Omega}\quad\forall\phi\in\Phi$. *Inspired by this identity, we can consider an alternative right hand side to write a discrete problem, as follows:*

$$\widetilde{F}_h(\phi_h):=\sum_{K\in\mathcal{T}_h}(\mathrm{rot}\,\mathbf{f},\Pi_K^2\phi_h)_{0,K}\qquad\forall\phi_h\in\mathcal{M}_h. \tag{6.5.25}$$

We note that $\widetilde{F}_h(\cdot)$ *is fully computable using the degrees of freedom* $\mathbf{D}_{\mathcal{M}}1-\mathbf{D}_{\mathcal{M}}2$, *since* Π_K^2 *is computable (cf. Lemma (3.3.2)).*

For the VE scheme (6.4.1) considering the alternative load term (6.5.25), we can provide an analogous analysis as the one developed in the above sections. Therefore, we can obtain rate of convergences as in Theorems 6.5.2 and 6.5.3 (with the minimal regularity condition on the force density $\mathbf{f}$, *i.e.,* $\mathbf{f}\in\mathrm{H}(\mathrm{rot};\mathcal{T}_h)$*). We will present a numerical test to confirm the error estimates in this case (cf. Subsection 6.7.4). Moreover, we observe that if the load term is irrotational, i.e.,* $\mathbf{f}=\nabla\varphi$ *(for some* φ*), it is possible improve the error estimate in Theorem 6.5.2 by removing the dependence of the error by the load term* $\mathbf{f}$.

6.6 Postprocessing of further fields of interest

In this section we propose postprocessing techniques that allow us to obtain approximations of the velocity, vorticity and pressure fields from the discrete stream-function ψ_h. Moreover, we provide optimal error estimates for all the postprocessed variables.

6.6.1 Postprocessing the velocity field

In order to propose an approximation for the velocity field, we recall that if $\psi\in\Phi$ is the unique solution of continuous problem (6.2.3), then

$$\mathbf{u}=\mathbf{curl}\,\psi. \tag{6.6.1}$$

At the discrete level, we define a piecewise linear approximation of the velocity field $\mathbf{u}$ as

$$\widetilde{\mathbf{u}}_h|_K:=\boldsymbol{\Pi}_K^1\mathbf{curl}\,\psi_h, \tag{6.6.2}$$

where $\psi_h\in\mathcal{M}_h$ is discrete virtual solution delivered by solving problem (6.4.1) and the operator $\boldsymbol{\Pi}_K^1$ is defined by the vectorial version of (6.3.5).

We have the following result for velocity vector $\widetilde{\mathbf{u}}_h$.

Theorem 6.6.1. *The discrete velocity field $\widetilde{\mathbf{u}}_h$ defined by the relation (6.6.2) is computable from the degrees of freedom $\mathbf{D}_{\mathcal{M}}1 - \mathbf{D}_{\mathcal{M}}2$. Moreover, under the hypotheses of Theorem 6.5.2, there exists a positive constant C, independent of h, such that*

$$\|\mathbf{u} - \widetilde{\mathbf{u}}_h\|_{0,\Omega} + h^{\gamma}|\mathbf{u} - \widetilde{\mathbf{u}}_h|_{1,h} \leq Ch^{2\gamma}(\|\psi\|_{2+\gamma,\Omega} + \|\mathbf{f}\|_{0,\Omega}).$$

Proof. From Lemma 6.3.2 we have immediately the computability of $\widetilde{\mathbf{u}}_h$ by using $\mathbf{D}_{\mathcal{M}}1-\mathbf{D}_{\mathcal{M}}2$. On the other hand, the error estimates, follow from (6.6.1), (6.6.2), the triangular inequality, stability property of $\mathbf{\Pi}^1_K$, together with Theorems 6.5.2 and 6.5.3.

□

6.6.2 Postprocessing the vorticity field

Due its importance and applications in fluid mechanics, different works have been devoted to approximate the vorticity field of the incompressible Navier-Stokes equations; see for instance [44, 102, 13] and the references therein. By solving the nonconforming discrete problem (6.4.1), we only obtain an approximation for the stream-function. Nevertheless, in this subsection we propose an approximation for the vorticity field ω via postprocessing formula through the discrete stream-function ψ_h and the projection Π^0_K defined by the relation (6.3.5).

First, we recall that $\omega = \operatorname{rot}\mathbf{u}$, then using the identity $\mathbf{u} = \mathbf{curl}\,\psi$, we have obtain $\omega = \operatorname{rot}\mathbf{u} = \operatorname{rot}(\mathbf{curl}\,\psi) = -\Delta\psi$. Then, at discrete level we define the following approximation for the vorticity:

$$\widetilde{\omega}_h|_K := -\Pi^0_K(\Delta\psi_h), \tag{6.6.3}$$

where $\psi_h \in \mathcal{M}_h$ is the unique solution of problem (6.4.1) and Π^0_K is defined in (6.3.5).

We have the following result for the discrete vorticity.

Theorem 6.6.2. *The discrete vorticity field $\widetilde{\omega}_h$ defined by the relation (6.6.3) is computable from the degrees of freedom $\mathbf{D}_{\mathcal{M}}1 - \mathbf{D}_{\mathcal{M}}2$. Moreover, under the hypotheses of Theorem 6.5.2, there exists a positive constant C, independent of h, such that*

$$\|\omega - \widetilde{\omega}_h\|_{0,\Omega} \leq Ch^{\gamma}(\|\psi\|_{2+\gamma,\Omega} + \|\mathbf{f}\|_{0,\Omega}).$$

Proof. The proof follows by using the same arguments in Theorem 6.6.1.

□

6.6.3 Postprocessing the pressure field

This subsection is devoted to developing a strategy to recover the pressure variable form the discrete stream-function solution ψ_h of problem (6.4.1), which is based on the algorithm presented in [72] and extended to the nonconforming VE approach.

We start by recalling that if $\psi \in \Phi$ is the unique solution of the weak formulation (6.2.3), then the velocity field is given by $\mathbf{u} = \mathbf{curl}\,\psi$. Thus, we can write

$$\begin{aligned} b(\mathbf{v}, p) := (p, \operatorname{div}\mathbf{v})_{0,\Omega} &= \nu(\boldsymbol{\nabla}\mathbf{u}, \boldsymbol{\nabla}\mathbf{v})_{0,\Omega} + ((\boldsymbol{\nabla}\mathbf{u})\mathbf{u}, \mathbf{v})_{0,\Omega} - (\mathbf{f}, \mathbf{v})_{0,\Omega} \\ &= \nu(\boldsymbol{\nabla}\mathbf{curl}\,\psi, \boldsymbol{\nabla}\mathbf{v})_{0,\Omega} + ((\boldsymbol{\nabla}\mathbf{curl}\,\psi)\mathbf{curl}\,\psi, \mathbf{v})_{0,\Omega} - (\mathbf{f}, \mathbf{v})_{0,\Omega} \qquad \forall \mathbf{v} \in \mathbf{H}. \end{aligned} \tag{6.6.4}$$

Now, we consider the functional $\mathcal{F}(\psi, \mathbf{f})(\cdot) : \mathbf{H} \to \mathbb{R}$ given by

$$\mathcal{F}(\psi, \mathbf{f})(\mathbf{v}) := \nu(\boldsymbol{\nabla}\mathbf{curl}\,\psi, \boldsymbol{\nabla}\mathbf{v})_{0,\Omega} + ((\boldsymbol{\nabla}\mathbf{curl}\,\psi)\mathbf{curl}\,\psi, \mathbf{v})_{0,\Omega} - (\mathbf{f}, \mathbf{v})_{0,\Omega} \qquad \forall \mathbf{v} \in \mathbf{H}. \tag{6.6.5}$$

By using (6.6.4) and (6.6.5), we reformulate (6.2.1) as a variational problem for the pressure variable: given $\psi \in \Phi$ the unique solution of problem (6.2.3) and $\mathbf{f} \in \mathbf{L}^2(\Omega)$, find $p \in Q$ such that

$$b(\mathbf{v}, p) = \mathcal{F}(\psi, \mathbf{f})(\mathbf{v}) \qquad \forall \mathbf{v} \in \mathbf{H}, \tag{6.6.6}$$

where $\mathbf{H}$ and Q are the spaces defined in (6.2.2). From an equivalence of problems and the LBB theory we have that problem (6.6.6) has a unique solution $p \in Q$ (see [103]).

The difficulties to discretize directly problem (6.6.6) have been discussed in [71, Section 9]. Thus, inspired in this work we consider the following equivalent problem: find $(\mathbf{w}, p) \in \mathbf{H} \times Q$, such that

$$\begin{aligned} a(\mathbf{w}, \mathbf{v}) + b(\mathbf{v}, p) &= \mathcal{F}(\psi, \mathbf{f})(\mathbf{v}) \qquad && \forall \mathbf{v} \in \mathrm{H} \\ b(\mathbf{w}, q) &= 0 && \forall q \in Q, \end{aligned} \tag{6.6.7}$$

where $a(\widetilde{\mathbf{v}}, \mathbf{v}) := (\boldsymbol{\nabla} \widetilde{\mathbf{v}}, \boldsymbol{\nabla} \mathbf{v})_{0,\Omega} \quad \forall \widetilde{\mathbf{v}}, \mathbf{v} \in \mathbf{H}$. We have that this Stokes-like problem is well-posed. Moreover, $\mathbf{w} = 0$. Now the goal is to discretize problem (6.6.7).

Nonconforming Crouzeix-Raviart-type VE discretization

In this subsection we will present a VE scheme to solve problem (6.6.7). First, we recall that the Morley-type VE space $\mathcal{M}_h$ is in a Stokes-complex relation with the Crouzeix-Raviart type VE space $\boldsymbol{\mathcal{U}}_h$, defined in (6.3.4) and (6.3.2), respectively. Apart from the previously mentioned spaces, we introduce the space for pressure approximation as

$$Q_h := \{q_h \in Q : q_h|_K \in \mathbb{P}_0(K) \quad \forall K \in \mathcal{T}_h\}. \tag{6.6.8}$$

At last, we introduce the auxiliary space

$$\widehat{\boldsymbol{\mathcal{U}}}_h := \Big\{\mathbf{v}_h \in \boldsymbol{\mathcal{U}}_h : \sum_{K \in \mathcal{T}_h} (q_h, \operatorname{div} \mathbf{v}_h)_{0,K} = 0 \quad \forall q_h \in Q_h\Big\}, \tag{6.6.9}$$

where $\boldsymbol{\mathcal{U}}_h$ is the Crouzeix-Raviart-type VE space defined in (6.3.2).

Lemma 6.6.1. *Let $\mathcal{M}_h$ and $\widehat{\boldsymbol{\mathcal{U}}}_h$ be the spaces defined in (6.3.4) and (6.6.9), respectively. Then, it holds that*

$$\mathbf{curl}\ \mathcal{M}_h = \widehat{\boldsymbol{\mathcal{U}}}_h,$$

Proof. The proof can be followed from [2, Lemma 6.1]. □

By employing the projection operator $\boldsymbol{\Pi}_K^{\boldsymbol{\nabla}}$ defined in (6.3.1), we discretize the bilinear form $a(\cdot, \cdot)$ through the bilinear form $a_h : \boldsymbol{\mathcal{U}}_h \times \boldsymbol{\mathcal{U}}_h \to \mathbb{R}$, which is such that

$$a_h(\mathbf{w}_h, \mathbf{v}_h) := \sum_{K \in \mathcal{T}_h} a_h^K(\mathbf{w}_h, \mathbf{v}_h) = \sum_{K \in \mathcal{T}_h} \Big(a^K\big(\boldsymbol{\Pi}_K^{\boldsymbol{\nabla}} \mathbf{u}_h, \boldsymbol{\Pi}_K^{\boldsymbol{\nabla}} \mathbf{v}_h\big) + S_{\boldsymbol{\nabla}}^K\big((\mathbf{I} - \boldsymbol{\Pi}_K^{\boldsymbol{\nabla}})\mathbf{u}_h, (\mathbf{I} - \boldsymbol{\Pi}_K^{\boldsymbol{\nabla}})\mathbf{v}_h\big)\Big),$$

where $S_{\boldsymbol{\nabla}}^K(\cdot, \cdot)$ is a symmetric and positive definite bilinear form satisfying the stability condition

$$c_{\#} a^K(\mathbf{v}_h, \mathbf{v}_h) \le S_{\boldsymbol{\nabla}}^K(\mathbf{v}_h, \mathbf{v}_h) \le c^{\#} a^K(\mathbf{v}_h, \mathbf{v}_h) \qquad \forall \mathbf{v}_h \in \operatorname{Ker}(\boldsymbol{\Pi}_K^{\boldsymbol{\nabla}}),$$

for some pair of strictly positive, real constants $c_{\#}$ and $c^{\#}$, independent of h. Then, we define the bilinear form $b_h : \boldsymbol{\mathcal{U}}_h \times Q_h \to \mathbb{R}$ as

$$b_h(\mathbf{v}_h, q_h) := \sum_{K\in\mathcal{T}_h} (q_h, \operatorname{div} \mathbf{v}_h)_{0,K}. \tag{6.6.10}$$

The next step is the construction of a discrete version of the lineal functional defined in (6.6.5). To do that, first we consider the constant vector field $\boldsymbol{\Pi}_K^0 : \boldsymbol{\mathcal{U}}_h(K) \to \mathbb{P}_0(K)^2$, defined on $\boldsymbol{\mathcal{U}}_h(K)$. Then, we consider the following discrete functional $\mathcal{F}_h(\psi_h, \mathbf{f})(\cdot) : \boldsymbol{\mathcal{U}}_h \to \mathbb{R}$

$$\mathcal{F}_h(\psi_h, \mathbf{f})(\mathbf{v}_h) := \sum_{K\in\mathcal{T}_h} \Big(a^K\big(\boldsymbol{\Pi}_K^{\boldsymbol{\nabla}}\mathbf{curl}\,\psi_h, \boldsymbol{\Pi}_K^{\boldsymbol{\nabla}}\mathbf{v}_h\big) + ((\boldsymbol{\nabla}\boldsymbol{\Pi}_K^1\mathbf{curl}\,\psi_h)\boldsymbol{\Pi}_K^1\mathbf{curl}\,\psi_h - \mathbf{f}, \boldsymbol{\Pi}_K^0\mathbf{v}_h)_{0,K}\Big). \tag{6.6.11}$$

From the stability properties of projectors $\boldsymbol{\Pi}_K^{\boldsymbol{\nabla}}$, $\boldsymbol{\Pi}_K^1$ and $\boldsymbol{\Pi}_K^0$, we have that the $\mathcal{F}_h(\psi_h, \mathbf{f})(\cdot)$ is continuous. Moreover, the projection $\boldsymbol{\Pi}_K^0$ is computable by using the degrees of freedom $\mathbf{D}_{\boldsymbol{\mathcal{U}}}$. Then, from this fact and Lemma 6.3.1, we conclude that this functional is fully computable.

Now, we present the nonconforming VE discretization of the Stokes problem (6.6.7) that reads as: find $(\mathbf{w}_h, p_h) \in \boldsymbol{\mathcal{U}}_h \times Q_h$ such that

$$\begin{aligned} a_h(\mathbf{w}_h, \mathbf{v}_h) + b_h(\mathbf{v}_h, p_h) &= \mathcal{F}_h(\psi_h, \mathbf{f})(\mathbf{v}_h) \qquad &&\forall \mathbf{v}_h \in \boldsymbol{\mathcal{U}}_h, \\ b_h(\mathbf{w}_h, q_h) &= 0 &&\forall q_h \in Q_h, \end{aligned} \tag{6.6.12}$$

where Q_h is the space defined in (6.6.8).

The scheme (6.6.12) is well-posed since $a_h(\cdot,\cdot)$ is coercive and continuous, the bilinear form $b_h(\cdot,\cdot)$ is continuous and satisfies a discrete inf-sup condition on the pair of functional spaces $\boldsymbol{\mathcal{U}}_h$-$Q_h$ (see [164]) and $\mathbf{curl}\,\mathcal{M}_h = \widehat{\boldsymbol{\mathcal{U}}}_h$. We summarize this fact in the following result.

Theorem 6.6.3. *Let $b_h(\cdot,\cdot)$ be the discrete bilinear form defined in (6.6.10). Then, there exists a strictly positive, real constant $\beta > 0$ such that*

$$\sup_{\mathbf{v}_h\in \boldsymbol{\mathcal{U}}_h\setminus\{\mathbf{0}\}} \frac{b_h(\mathbf{v}_h, q_h)}{|\mathbf{v}_h|_{1,h}} \geq \beta\|q_h\|_{0,\Omega} \qquad \forall q_h \in Q_h.$$

Moreover, there exists a unique $(\mathbf{w}_h, p_h) \in \boldsymbol{\mathcal{U}}_h \times Q_h$, solution of problem (6.6.12).

Error estimate for the pressure scheme

In this subsection we develop an abstract error result for the VEM presented above. Moreover, we provide error estimates involving some consistent errors. Finally, by combining these results we derive an optimal error estimate for the pressure field.

First, we focus on deriving a bound on the difference between the functional (6.6.11) applied to the stream-function ψ solving the continuous variational formulation (6.2.3) and its virtual element approximation solving problem (6.4.1).

Lemma 6.6.2. *Let $\psi \in \Phi$ and $\psi_h \in \mathcal{M}_h$ be the solution to problems (6.2.3) and (6.4.1), respectively. Moreover, let $\mathcal{F}_h(\psi, \mathbf{f})(\cdot)$ and $\mathcal{F}_h(\psi_h, \mathbf{f})(\cdot)$ be the functionals defined in (6.6.11) (applied to ψ and ψ_h, respectively). Then, there exists positive constant $C_{\mathcal{F}_h}$, independent of h, such that*

$$\big|\mathcal{F}_h(\psi, \mathbf{f})(\mathbf{v}_h) - \mathcal{F}_h(\psi_h, \mathbf{f})(\mathbf{v}_h)\big| \leq C_{\mathcal{F}_h}|\psi - \psi_h|_{2,h}|\mathbf{v}_h|_{1,h}.$$

Proof. Upon employing the definition (6.6.11), we obtain

$$\big|\mathcal{F}_h(\psi,\mathbf{f})(\mathbf{v}_h)-\mathcal{F}_h(\psi_h,\mathbf{f})(\mathbf{v}_h)\big| \le \nu \sum_{K\in\mathcal{T}_h}\big|a^K(\boldsymbol{\Pi}_K^{\boldsymbol{\nabla}}\mathbf{curl}\,(\psi-\psi_h),\boldsymbol{\Pi}_K^{\boldsymbol{\nabla}}\mathbf{v}_h)\big|$$
$$+\sum_{K\in\mathcal{T}_h}\big|((\boldsymbol{\nabla}\boldsymbol{\Pi}_K^1\mathbf{curl}\,\psi)\boldsymbol{\Pi}_K^1\mathbf{curl}\,\psi,\boldsymbol{\Pi}_K^0\mathbf{v}_h)_{0,K}-((\boldsymbol{\nabla}\boldsymbol{\Pi}_K^1\mathbf{curl}\,\psi_h)\boldsymbol{\Pi}_K^1\mathbf{curl}\,\psi_h,\boldsymbol{\Pi}_K^0\mathbf{v}_h)_{0,K}\big|.$$

Since $\boldsymbol{\Pi}_K^{\boldsymbol{\nabla}}$ is a continuous operator with respect to the H^1-inner product, we bound the first term as follows

$$\nu\sum_{K\in\mathcal{T}_h}\big|a^K(\boldsymbol{\Pi}_K^{\boldsymbol{\nabla}}\mathbf{curl}\,(\psi-\psi_h),\boldsymbol{\Pi}_K^{\boldsymbol{\nabla}}\mathbf{v}_h)\big|\le C\nu|\psi_h-\psi|_{2,h}|\mathbf{v}_h|_{1,h}.$$

By adding and subtracting the term $((\boldsymbol{\nabla}\boldsymbol{\Pi}_K^1\mathbf{curl}\,\psi_h)\boldsymbol{\Pi}_K^1\mathbf{curl}\,\psi,\boldsymbol{\Pi}_K^0\mathbf{v}_h)_{0,K}$, applying the Hölder inequality and Theorem 6.4.1, along with stability properties of projectors $\boldsymbol{\Pi}_K^{\boldsymbol{\nabla}}$, $\boldsymbol{\Pi}_K^1$ and $\boldsymbol{\Pi}_K^0$,, we obtain

$$\begin{aligned}
&\sum_{K\in\mathcal{T}_h}\big|((\boldsymbol{\nabla}\boldsymbol{\Pi}_K^1\mathbf{curl}\,\psi)\boldsymbol{\Pi}_K^1\mathbf{curl}\,\psi,\boldsymbol{\Pi}_K^0\mathbf{v}_h)_{0,K}-((\boldsymbol{\nabla}\boldsymbol{\Pi}_K^1\mathbf{curl}\,\psi_h)\boldsymbol{\Pi}_K^1\mathbf{curl}\,\psi_h,\boldsymbol{\Pi}_K^0\mathbf{v}_h)_{0,K}\big|\\
&=\sum_{K\in\mathcal{T}_h}\big|((\boldsymbol{\nabla}\boldsymbol{\Pi}_K^1\mathbf{curl}\,(\psi-\psi_h))\boldsymbol{\Pi}_K^1\mathbf{curl}\,\psi,\boldsymbol{\Pi}_K^0\mathbf{v}_h)_{0,K}\big|\\
&\quad+\big|((\boldsymbol{\Pi}_K^1\mathbf{curl}\,\psi_h)\boldsymbol{\Pi}_K^1\mathbf{curl}\,(\psi-\psi_h),\boldsymbol{\Pi}_K^0\mathbf{v}_h)_{0,K}\big|\\
&\le C|\psi-\psi_h|_{2,h}|\psi|_{2,\Omega}|\mathbf{v}_h|_{1,h}+C|\psi_h|_{2,h}|\psi-\psi_h|_{2,h}|\mathbf{v}_h|_{1,h}.
\end{aligned}$$

The desired result follows by combining the above estimates. □

In continuation, we define the consistency error $\Theta_h(\cdot,\cdot)$ as follows: given $\psi\in\Phi$ the solution of problem (6.2.3), we consider

$$\Theta_h(\psi,\mathbf{v}_h):=\mathcal{F}_h(\psi,\mathbf{f})(\mathbf{v}_h)-b_h(\mathbf{v}_h,p)\qquad\forall\mathbf{v}_h\in\boldsymbol{\mathcal{U}}_h. \tag{6.6.13}$$

We have the following abstract error estimate for the pressure recovery scheme.

Theorem 6.6.4. *Let $\psi\in\Phi\cap\mathrm{H}^{2+\gamma}(\Omega)$, with $\gamma\in(1/2,1]$ and $\psi_h\in\mathcal{M}_h$ be the solutions of problems (6.2.3) and (6.4.1), respectively. Moreover, let $(\mathbf{w},p)\in\mathrm{H}\times Q$ and $(\mathbf{w}_h,p_h)\in\boldsymbol{\mathcal{U}}_h\times Q_h$ be the solutions of problems (6.6.7) and (6.6.12). Then, there exists a positive constant C, independent of h, such that*

$$\|p-p_h\|_{0,\Omega}\le C\Big(\inf_{q_h\in Q_h}\|p-q_h\|_{0,\Omega}+\sup_{\substack{\mathbf{v}_h\in\boldsymbol{\mathcal{U}}_h\\ \mathbf{v}_h\neq\mathbf{0}}}\frac{|\Theta(\psi,\mathbf{v}_h)|}{|\mathbf{v}_h|_{1,h}}+|\psi-\psi_h|_{2,h}\Big), \tag{6.6.14}$$

where $\Theta(\psi,\cdot)$ is the consistency error defined in (6.6.13).

Proof. Adding and subtracting adequate terms in (6.6.12), for each $\mathbf{v}_h\in\boldsymbol{\mathcal{U}}_h$ we have

$$\begin{aligned}
a_h(\mathbf{w}_h,\mathbf{v}_h)&=\mathcal{F}_h(\psi_h,\mathbf{f})(\mathbf{v}_h)-b_h(\mathbf{v}_h,p_h)\\
&=\mathcal{F}_h(\psi_h,\mathbf{f})(\mathbf{v}_h)-\mathcal{F}_h(\psi,\mathbf{f})(\mathbf{v}_h)+\mathcal{F}_h(\psi,\mathbf{f})(\mathbf{v}_h)-b_h(\mathbf{v}_h,p)+b_h(\mathbf{v}_h,p-p_h)\\
&=(\mathcal{F}_h(\psi_h,\mathbf{f})(\mathbf{v}_h)-\mathcal{F}_h(\psi,\mathbf{f})(\mathbf{v}_h))+\Theta(\psi,\mathbf{v}_h)+b_h(\mathbf{v}_h,p-p_h).
\end{aligned} \tag{6.6.15}$$

Taking $\mathbf{v}_h = \mathbf{w}_h$ in (6.6.15), then by using the fact that $b_h(\mathbf{w}_h, q_h) = b_h(\mathbf{w}_h, p_h) = 0 \quad \forall q_h \in Q_h$, the continuity of $b_h(\cdot,\cdot)$ and Lemma 6.6.2, we get

$$|\mathbf{w}_h|_{1,h} \leq C\Big(|\psi - \psi_h|_{2,h} + \|p - q_h\|_{0,\Omega} + \sup_{\substack{\mathbf{v}_h \in \boldsymbol{\mathcal{U}}_h \\ \mathbf{v}_h \neq \mathbf{0}}} \frac{|\Theta(\psi, \mathbf{v}_h)|}{|\mathbf{v}_h|_{1,h}}\Big). \tag{6.6.16}$$

By using again (6.6.15) and the linearity of $b_h(\cdot,\cdot)$, for all $q_h \in Q_h$ we have

$$\begin{aligned} b_h(\mathbf{v}_h, q_h - p_h) &= b_h(\mathbf{v}_h, q_h - p) + b_h(\mathbf{v}_h, p - p_h) \\ &= b_h(\mathbf{v}_h, q_h - p) + a_h(\mathbf{w}_h, \mathbf{v}_h) - (\mathcal{F}_h(\psi_h, \mathbf{f})(\mathbf{v}_h) - \mathcal{F}_h(\psi, \mathbf{f})(\mathbf{v}_h)) - \Theta(\psi, \mathbf{v}_h). \end{aligned}$$

Thus, by using the two last estimate above, Lemma 6.6.2, the inf-sup condition in Lemma 6.6.3, we obtain

$$\beta\|q_h - p_h\|_{0,\Omega} \leq C\Big(\|p - q_h\|_{0,\Omega} + |\mathbf{w}_h|_{1,h} + \sup_{\substack{\mathbf{v}_h \in \boldsymbol{\mathcal{U}}_h \\ \mathbf{v}_h \neq \mathbf{0}}} \frac{|\Theta(\psi, \mathbf{v}_h)|}{|\mathbf{v}_h|_{1,h}}\Big).$$

The desired result follows from the triangle inequality, the above estimate and (6.6.16). □

Lemma 6.6.3. *Let $\psi \in \Phi \cap \mathrm{H}^{2+\gamma}(\Omega)$ be the solution of problem (6.2.3). Then, for $p \in Q \cap \mathrm{H}^{\gamma}(\Omega)$ there exists a positive constant C, independent of h, such that*

$$|\Theta_h(\psi, \mathbf{v}_h)| \leq Ch^{\gamma}(\|p\|_{\gamma,\Omega} + \|\psi\|_{2+\gamma,\Omega} + \|\mathbf{f}\|_{0,\Omega})|\mathbf{v}_h|_{1,h} \qquad \forall \mathbf{v}_h \in \boldsymbol{\mathcal{U}}_h.$$

Proof. By using the definition of the consistency term $\Theta_h(\psi,\cdot)$ (cf. (6.6.13)), the weak continuity of the discrete function of the Crouzeix-Raviart space on edges, and employing standard arguments as [164, Theorem 13], together with the real method of interpolation, we can obtain the required result. □

Finally, the next result provides the rate of convergence for our pressure VE scheme.

Theorem 6.6.5. *Under same assumptions of Theorem 6.6.4, for $p \in Q \cap \mathrm{H}^{\gamma}(\Omega)$, there exists $C > 0$, independent of h, such that*

$$\|p - p_h\|_{0,\Omega} \leq Ch^{\gamma}(\|p\|_{\gamma,\Omega} + \|\psi\|_{2+\gamma,\Omega} + \|\mathbf{f}\|_{0,\Omega}).$$

Proof. The proof follows from (6.6.14), taking $q_h = \Pi_K^0 p$ in Theorem 6.6.4, Lemma 6.6.3 and Theorem 6.5.2.

□

Remark 6.6.1. *We recall that if we are interesting to approximate only the main unknown of problem (6.2.3), we can consider the Morley-type VE introduced in [4, Subsection 3.2], avoiding the construction of the Stokes complex sequence. Moreover, we are able to recover the velocity and vorticity fields by using the postprocessing of subsections 6.6.1 and 6.6.2, and obtain the theoretical analysis presented here. However, the pressure recovery would not be available. Thus, we point out that the main advantage to use the Stokes complex sequence associated to $\mathcal{M}_h$ and $\boldsymbol{\mathcal{U}}_h$ is that we can additionally compute the pressure field from the discrete stream-function, with optimal rate of convergence, making the suitable setting.*

6.7 Numerical results

In this section, we present four numerical experiments to test the practical performance of the proposed VE discretization (6.4.1) and assess the theoretical predictions as estimated in Sections 6.5 and 6.6. We first approximate the discrete stream-function ψ by employing Morley-type VE space (6.3.4), and then we recover the velocity and vorticity fields by employing suitable projection operators. Further, we recover the pressure variable by solving a saddle point problem, where the velocity space is in Stokes complex relationship with the stream-function space (cf. Section 6.6.3). In each test, in order to solve the nonlinear system resulting from (6.4.1), we apply the Newton method, with a fixed tolerance of $\mathrm{Tol} = 10^{-8}$ and the initial guess is given by $\psi_h^{\mathrm{in}} = 0$. We have tested the method by using different families of meshes such as:

- $\mathcal{T}_h^1$: Square meshes;
- $\mathcal{T}_h^2$: Triangular meshes;
- $\mathcal{T}_h^3$: Sequence of CVT (Centroidal Voronoi Tessellation);
- $\mathcal{T}_h^4$: Trapezoidal meshes,

which are posted in Figure 6.1. We quantify the errors by employing the projection operators: Π_K^{D}, $\boldsymbol{\Pi}_K^1$, and Π_K^0. The following formulas are used for the computation of experimental errors, for all $i \in \{0,1,2\}$ and for each $j \in \{0,1\}$:

$$\begin{aligned} \mathcal{E}_i(\psi) &:= \Big(\sum_{K\in\mathcal{T}_h} |\psi - \Pi_K^{\mathrm{D}}\psi_h|_{i,K}^2 \Big)^{1/2}, \qquad \mathcal{E}_j(\mathbf{u}) := \Big(\sum_{K\in\mathcal{T}_h} |\mathbf{u} - \boldsymbol{\Pi}_K^1 \mathbf{curl}\,\psi_h|_{j,K}^2 \Big)^{1/2}; \\ \mathcal{E}_0(\omega) &:= \Big(\sum_{K\in\mathcal{T}_h} \|\omega - \Pi_K^0 \Delta\psi_h\|_{0,K}^2 \Big)^{1/2}, \quad \mathcal{E}_0(p) := \Big(\sum_{K\in\mathcal{T}_h} \|p - p_h\|_{0,K}^2 \Big)^{1/2}. \end{aligned} \tag{6.7.1}$$

Furthermore, we let $\mathcal{R}_i(\chi)$, where $\chi \in \{\mathbf{u}, \psi, \omega\}$ and $i \in \{0,1,2\}$, denotes the experimental rates of convergence of the approximate solutions in broken H^2-, H^1- and L^2-norms.

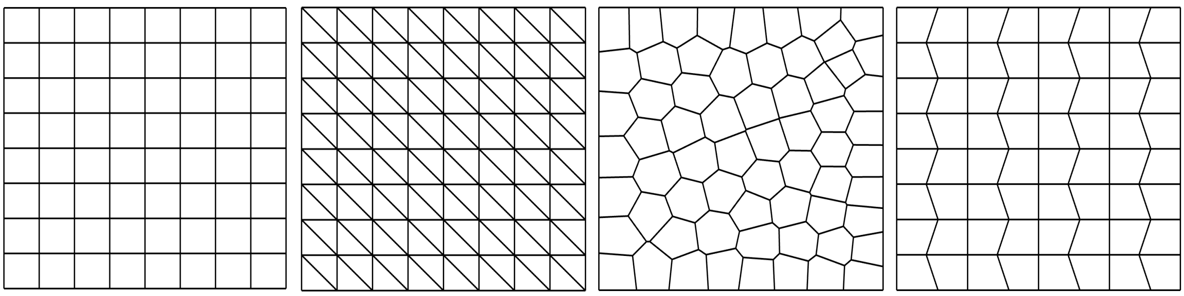

Figure 6.1: Sample meshes. $\mathcal{T}_h^1$, $\mathcal{T}_h^2$, $\mathcal{T}_h^3$ and $\mathcal{T}_h^4$ (from left to right).

6.7.1 Test 1. Kovasznay flow

In this numerical test, we solve the Navier-Stokes problem (6.1.1) on the domain $\Omega := (-0.5, 1.5) \times (0, 2)$. We take the load term $\mathbf{f}$ and boundary conditions in such a way that the analytical solution is given by the Kovasznay solution:

$$\mathbf{u}(x,y) := \begin{pmatrix} 1 - \exp(\lambda x)\cos(2\pi y) \\ \frac{\lambda}{2\pi}\exp(\lambda x)\sin(2\pi y) \end{pmatrix}, \quad \psi(x,y) := y - \frac{1}{2\pi}\exp(\lambda x)\sin(2\pi y),$$
$$p(x,y) := -(1/2)\exp(2\lambda x) + \bar{p}, \qquad \omega := \left(\frac{\lambda^2 - 4\pi^2}{2\pi}\right)\exp(\lambda x)\sin(2\pi y),$$

where $\lambda = \frac{Re}{2} - \left(\frac{Re^2}{4} + 4\pi^2\right)^{1/2}$ with $Re = \nu^{-1}$ and $\bar{p}$ is a constant that is set to satisfy zero mean condition. We have computed the discrete stream-function for different values of viscosity coefficient, e.g., $\nu = 1, 0.01$, and errors for the stream-function (cf. (6.7.1)) are posted in Figure 6.2, and Figure 6.4, respectively. Further, by employing the formulas (6.6.2) and (6.6.3), we have recovered discrete velocity and vorticity fields for $\nu = 1, 0.01$. The error curves of the velocity and vorticity are posted in Figure 6.3, and Figure 6.5, while the error curves for the pressure are posted in Figure 6.6 for both values of ν. Besides, for all the meshes the maximum number of iterations that are required to achieve the tolerance in the Newton method is 4 for $\nu = 1$ and 6 for $\nu = 0.01$.

In Figure 6.7, we have posted the discrete stream-function and pressure fields for $\nu = 1$, using the mesh $\mathcal{T}_h^1$, with $h = 1/32$.

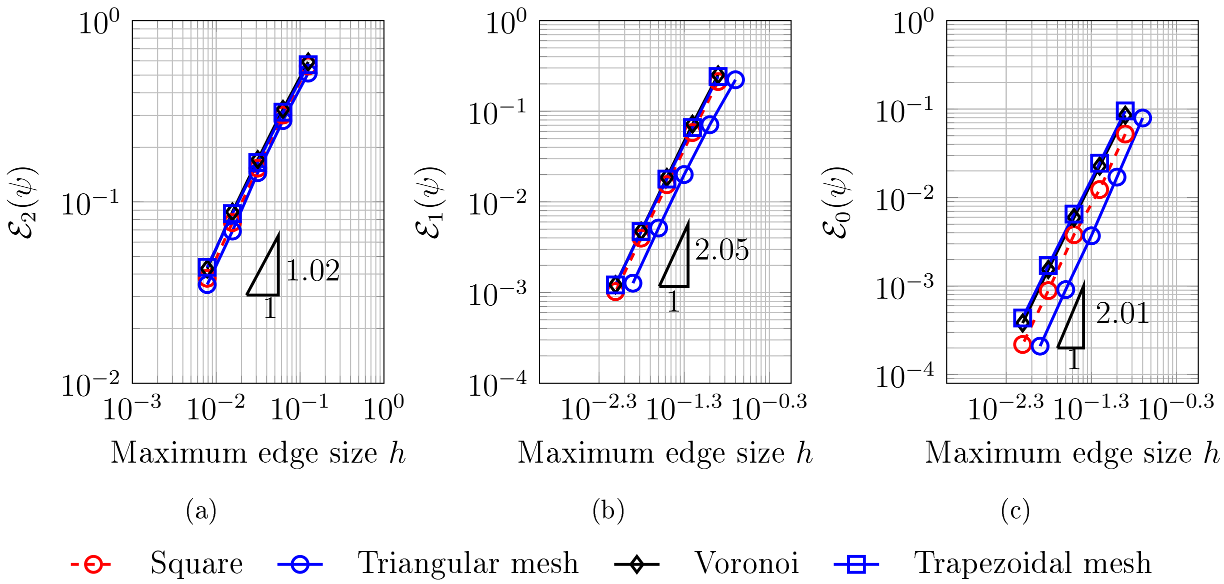

Figure 6.2: Test 1: Convergence of the stream-function ψ in broken H^2-, H^1- and L^2-norms with mesh refinement for different types of meshes, using $\nu = 1$.

6.7.2 Test 2. L-shaped domain

In this example, we would like to examine the rates of convergence of the discrete stream-function, velocity and vorticity fields on a nonconvex L-shaped domain, where the exact solution

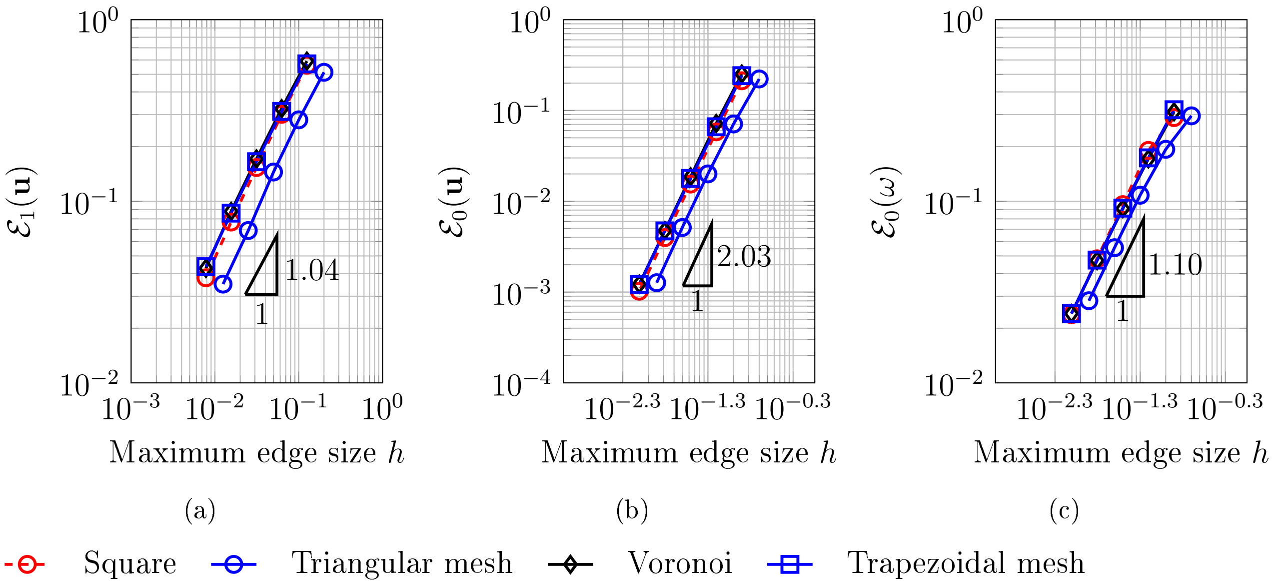

Figure 6.3: Test 1: Convergence of the velocity field $\mathbf{u}$ in broken H^1- and L^2-norms, and vorticity field ω in L^2-norm (from left to right) with mesh refinement for different types of meshes, using $\nu = 1$.

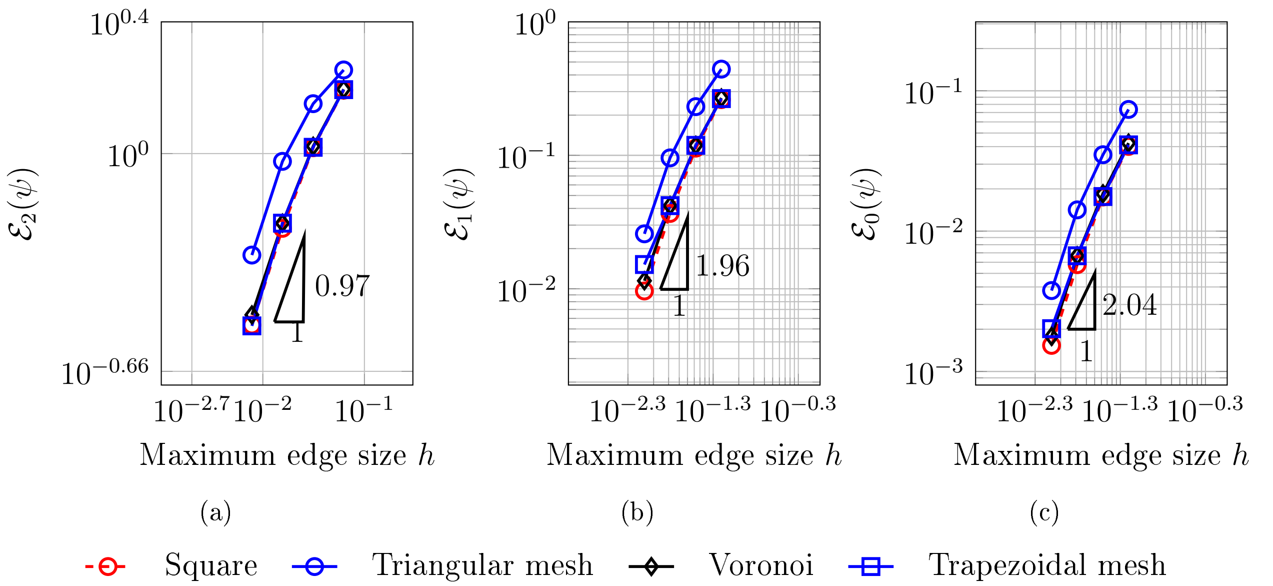

Figure 6.4: Test 1: Convergence of the stream-function in broken H^2, H^1- L^2-norms with mesh refinement for different types of meshes, using $\nu = 0.01$.

ψ has less regularity. For the computational domain, we considered $\Omega = (-1,1) \times (-1,1) \setminus \big([0,1) \times (-1,0]\big)$. The exact solution is given by $\psi(r,\theta) := r^{5/3} \sin(\frac{5\theta}{3})$, where $r := (x^2+y^2)^{1/2}$, and θ is the angle with the vertical axis. Since $\frac{\partial \psi}{\partial r}$ is unbounded near the origin, then the solution ψ has weak regularity near the origin. The rate of convergence of stream-function velocity and vorticity solutions are posted in Table 6.1 for viscosity $\nu = 1$, and using the mesh $\mathcal{T}_h^2$. From the posted results, we observed that the rates of convergence are in accordance

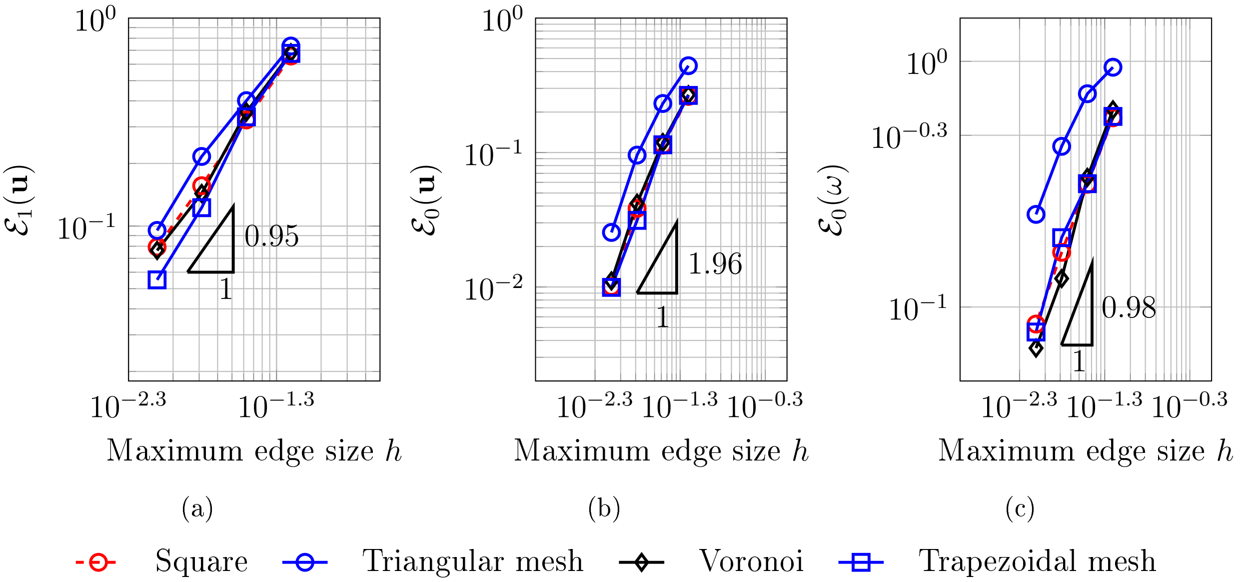

Figure 6.5: Test 1: Convergence of the velocity field $\mathbf{u}$ in broken H^1- and L^2-norms, and vorticity field ω in L^2-norm (from left to right) with mesh refinement for different types of meshes, using $\nu = 0.01$.

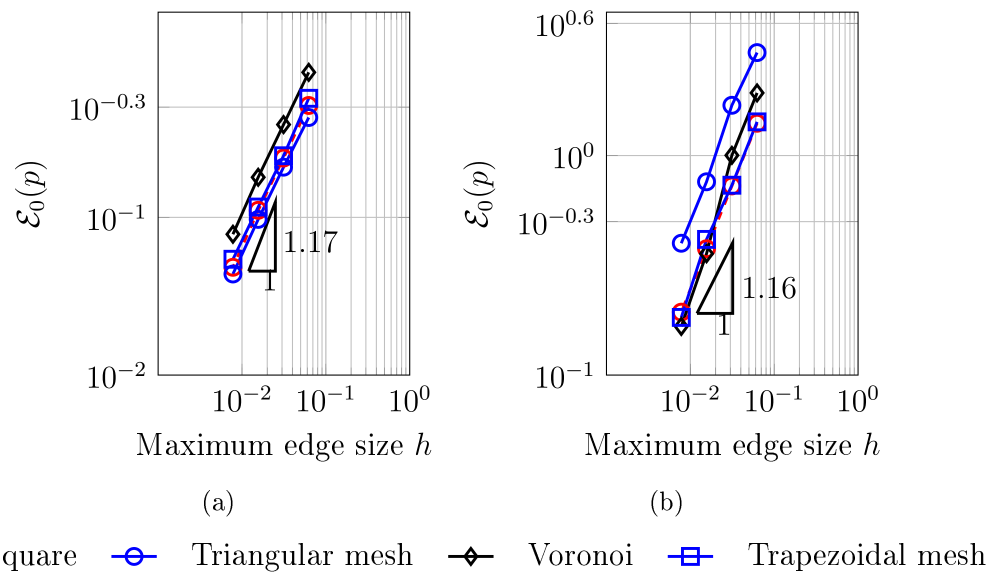

Figure 6.6: Test 1: Convergence of the pressure (p) in L^2-norm with mesh refinement for different types of meshes, using $\nu = 1$ and $\nu = 0.01$. Left panel shows the errors curve of p for $\nu = 1$, and right panel shows the errors curve of p for $\nu = 0.01$.

with the theoretical prediction for all the variables. Further, we have chosen exact pressure as $p := \sin(x) - \sin(y) - \overline{p}$, where $\overline{p}$ is a constant that is set to satisfy zero mean condition, i.e., $(p, 1)_{0,\Omega} = 0$. The convergence behavior of the pressure field is posted in Table 6.2. It is observed that initially the rate of convergence is slightly higher than the predicted order as in Theorem 6.6.3. However, for finer mesh we observe expected order of convergence, i.e., $\mathcal{O}(h^{2/3})$. Further, we report that the presence of singularity of the stream-function at re-entrant corner

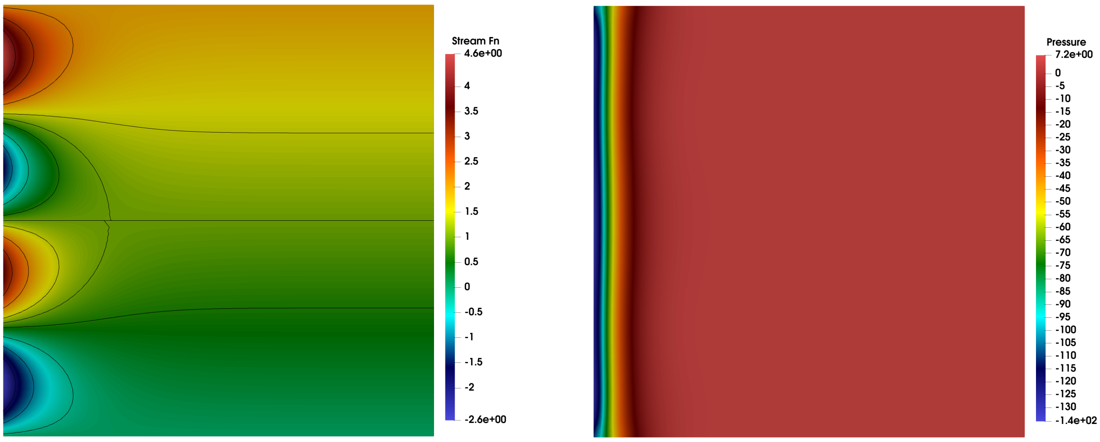

(*a*) Discrete stream-function (*b*) Discrete pressure

Figure 6.7: Test 1: "Snapshots" of the approximate stream-function and pressure, using $\nu = 1$ and the mesh $\mathcal{T}_h^1$, $h = 1/32$.

affects the convergence order of pressure field as proven in Theorem 6.6.3. In this example, the number of iterations that are required for the Newton method is 4.

h	$\mathcal{E}_2(\psi)$	$\mathcal{R}_2(\psi)$	$\mathcal{E}_1(\psi)$	$\mathcal{R}_1(\psi)$	$\mathcal{E}_0(\psi)$	$\mathcal{R}_0(\psi)$	$\mathcal{E}_1(\mathbf{u})$	$\mathcal{R}_1(\mathbf{u})$	$\mathcal{E}_0(\mathbf{u})$	$\mathcal{R}_0(\mathbf{u})$	$\mathcal{E}_0(\omega)$	$\mathcal{R}_0(\omega)$
1/4	5.7631e-2	—	7.6316e-3	—	3.3797e-3	—	1.0336e-1	—	7.5336e-3	—	6.1773e-2	—
1/8	3.8328e-2	0.59	2.9766e-3	1.34	1.2923e-3	1.38	6.7243e-2	0.62	2.8964e-3	1.37	4.2442e-2	0.54
1/16	2.4854e-2	0.62	1.1634e-3	1.35	5.5365e-4	1.22	4.3160e-2	0.64	1.1236e-3	1.36	2.7923e-2	0.60
1/32	1.5907e-2	0.64	4.6577e-4	1.32	2.3946e-4	1.20	2.7492e-2	0.65	4.5976e-4	1.29	1.7999e-2	0.63
1/64	1.0032e-2	0.66	1.9139e-4	1.28	1.0326e-4	1.21	1.7435e-2	0.66	1.8729e-4	1.29	1.1483e-2	0.65

Table 6.1: Test 2. Errors for the stream-function, and the post-processed velocity, vorticity fields in broken H^2-, H^1- and L^2-norms for $\nu = 1$, using the mesh $\mathcal{T}_h^2$.

h	$\mathcal{E}_0(p)$	$\mathcal{R}_0(p)$
1/4	3.3613e-1	—
1/8	1.7549e-1	0.93
1/16	9.3685e-2	0.90
1/32	5.2943e-2	0.82
1/64	3.1274e-2	0.75

Table 6.2: Test 2. Errors for the pressure variable in L^2-norm for $\nu = 1$, using the mesh $\mathcal{T}_h^2$.

6.7.3 Test 3. The lid-driven cavity problem

In the third example, we assess the nature of the fluid for the lid-driven cavity flow. This is a benchmark test to validate the numerical schemes for different values of viscosity ν. The computational domain is unit square with upper horizontal lid is moving with uniform velocity $\mathbf{u} := (1, 0)$, and fixed boundary condition, i.e., $\mathbf{u} := (0, 0)$ is applied to other static walls.

In stream-function formulation, we have imposed the following Dirichlet boundary conditions: $\psi = \psi_x = 0$, and $\psi_y = 1$ on moving lid, and $\psi = \frac{\partial \psi}{\partial \mathbf{n}} = 0$ on all other static walls. In Figure 6.8, we posted the discrete stream-function and pressure field for $\nu = 0.01$ and using the mesh $\mathcal{T}_h^3$, with $h = 1/64$. The small values of ν exhibits singularities near $x = 0$, and $x = 1$ [102, 143], which increases for smaller values of ν. Such behaviors are noticed in other methods [102], and persists also for finer grid. Further, we observed that the vortex center has moved towards the direction of velocity for small values of ν. For this numerical experiment, the number of iterations that are required for the Newton method is 5.

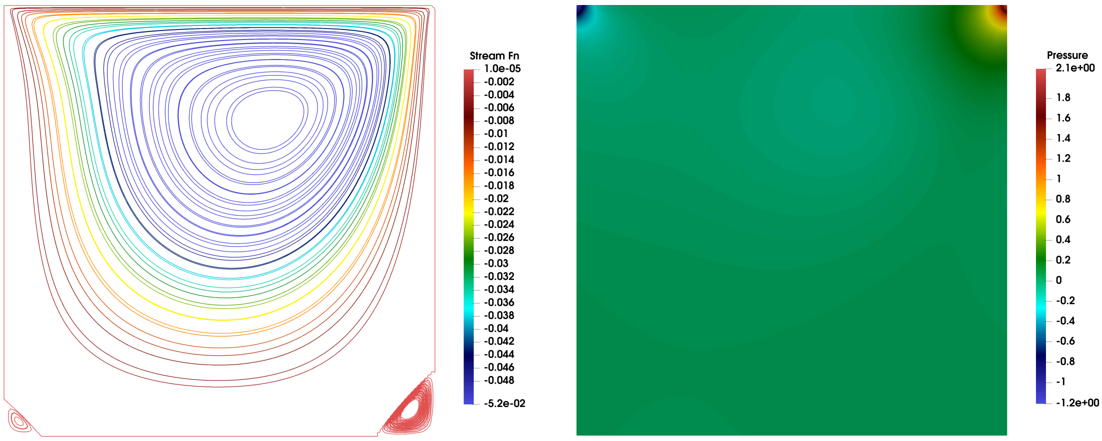

(a) Discrete stream-function

(b) Discrete pressure

Figure 6.8: Test 3: “Snapshots” of the approximate stream-function and pressure for $\nu = 0.01$, using the mesh $\mathcal{T}_h^3$, with $h = 1/64$.

6.7.4 Test 4. Performance of the scheme for small viscosity

In this example, we mainly focus to discuss the performance of the scheme for small values of viscosity coefficients. We consider the exact stream-function, velocity and pressure solutions as

$$\psi(x, y) := x^2 y^2 (1-x)^2 (1-y)^2, \ \mathbf{u}(x, y) := \begin{pmatrix} x^2(1-x)^2(2y - 6y^2 + 4y^3) \\ -y^2(1-y)^2(2x - 6x^2 + 4x^3) \end{pmatrix}, \ p(x, y) := x^3 y^3 - \frac{1}{6}.$$

The numerical approximations of the stream-function are computed by employing the scheme (6.4.1), with the alternative load term given by (6.5.25) (cf. Remark 6.5.2). The computational domain is considered as $\Omega := (0, 1)^2$. Further, we discretize the domain with square elements with different mesh sizes, and computed the errors for stream-function in broken H^2-norm for different values of ν, which are posted in Figure 6.9. We observed that the errors are accurate when the parameter ν within the range $\nu \in [10^{-3}, 10^0]$ and the errors increase for $\nu = 10^{-4}$. We claim that these results are in accordance with the general behaviour of the exactly divergence-free Galerkin schemes which are more robust with respect to small viscosity parameters, see for instance [35] in the VEM approach. However, we would like to point out that our scheme is not pressure robust. Finally, we report that the maximum number of iterations that are required to achieve the tolerance in the Newton method is 7.

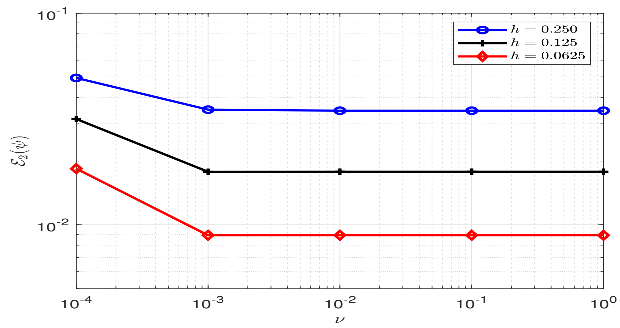

Figure 6.9: Test 4. Errors of the stream-function $\mathcal{E}_2(\psi)$, using the VE scheme (6.4.1) with the alternative load term (6.5.25), for different values of ν and the mesh $\mathcal{T}_h^1$.

Chapter 7

Conclusions and future work

7.1 Concluding remarks

In this thesis we have designed, analyzed and implemented several conforming and nonconforming virtual element methods for solving problems with application to the fluid mechanics and large scale wind-driven ocean circulation, reformulated in terms of the stream-function of the velocity field. More precisely, we have proposed C^1-virtual element schemes to approximate the quasi-geostrophic equations of the ocean, the Oseen problem, the nonlinear Navier-Stokes equations and the coupled Boussinesq system under the stream-function approach.

Furthermore, by using an alternative discretization, we have developed a nonconforming Morley-type virtual element scheme to solve the Navier-stream problem in stream-function form.

The study has included analysis for discrete schemes, novel and rigorous analysis of convergence in several norms of interest. Moreover, it includes numerical implementation to validate the theoretical results and illustrate the behaviour of the numerical schemes have been reported.

The main conclusions of this thesis are:

1. In **Chapter** 2, we have proposed a C^1-VEM of lowest order (i.e., $k = 2$) for the quasi-geostrophic equations of the ocean in stream-function form. The C^1 virtual space and the discrete scheme are built in a straightforward way due to the flexibility of the virtual approach. Besides, the computational cost in terms of the degrees of freedom is low; the scheme employ only 3 DoFs per vertex of the mesh. We have established the well-posedness of the discrete problem by using the Banach fixed-point Theorem and assuming smallness of the data. Besides, under standard assumptions on the computational domain, optimal error estimates in H^2-norm for the stream-function have been provided. Finally, several numerical experiments that illustrate the behavior of the virtual scheme and confirm our theoretical results on different families of polygonal meshes have been reported.

   The results of this chapter are in article [136].

2. In **Chapter** 3, we have written a stream-function weak formulation for the Oseen problem, which corresponds to a fourth-order PDEs. Thus, a conforming virtual element discretization requires globally C^1-continuity. In this chapter, we have exploited the possibility of VEM to implement global discrete spaces of H^2 in a straightforward way even on general polygonal meshes. Under a CLF-type condition we have established the well-posedness of

the discrete problem and an error estimate in H^2-norm is provided.Furthermore, strategies for recovering additional variables of interest, such as velocity, vorticity, and pressure fields, have been developed, along with the corresponding error analysis. Finally, we have reported a set of numerical experiments, which allows us to assess the performance of the proposed method.

The results contained in this work are in the book chapter [137].

3. In **Chapter** 4, we have designed VEMs of high-order for solving the steady Navier-Stokes equations in stream-function form on polygonal meshes. A novel and rigorous error analysis have been developed, allowing the derivation of optimal error bounds in several important norms, under minimal regularity condition of the weak solution. In addition, we have extend this scheme the Navier-Stokes system with boundary conditions on the pressure. Algorithms to obtain high order approximations of several variables of interest in fluid mechanics have also been provided. These procedures are based on adequate postprocessing of the discrete stream function and allow to derive optimal error estimates. Moreover, we have reported several benchmark numerical experiments illustrating the behaviour and highlighting salient features of the present stream virtual element schemes. We have included the approximation of the Kovasznay and lid-driven cavity solutions on general polygonal meshes and using small values of the viscosity ν. Additionally, in Test 4.7.3, we investigated the performance of our VEMs, considering a hydrostatic fluid problem. We noted that the outcomes achieved in this study are in agreement with Galerkin methods that maintain the divergence-free property, where the partial separation of velocity and pressure errors positively impacts the velocity calculations. In addition, we have reported a numerical example with less regularity, which validates our new theoretical findings in Theorem 4.4.3.

   The results of this chapter are in the following submitted article [138].

4. In **Chapter** 5, we have designed and analyzed a high order fully-discrete virtual element for the nonsteady Boussinesq system in terms of the stream-function and temperature variables. We combined the C^1- and C^0-conforming virtual element approaches with backward Euler schemes and proposed a fully-coupled formulation which is implicit in the nonlinear terms. By using fixed-point arguments we proved the existence of discrete solutions and, under a small time step condition, we have shown uniqueness of such solutions. The ensuing numerical method is unconditionally stable. Error estimates in $\mathrm{L}^2(\mathrm{H}^2) \cap \mathrm{L}^\infty(\mathrm{H}^1)$ and $\mathrm{L}^2(\mathrm{H}^1) \cap \mathrm{L}^\infty(\mathrm{L}^2)$ are provided for the stream-function and temperature, respectively. A set of benchmark numerical experiments have been reported, illustrating the good performance of the method and the theoretical rates of convergence. In particular, we have included the benchmark natural convection test, and it can be seen that the results show good agreement with the results presented in the existing literature.

   The results contained in this chapter gave rise to the article [40].

5. In **Chapter** 6, we have developed a Stokes complex sequence associate to the Morley- and Crouzeix-Raviart-type VE spaces enabling not only the approximation of the stream-function but also the pressure reconstruction of the stationary Navier-Stokes equation in stream-function formulation on simply connected polygonal domains (not necessarily convex). Based on the ideas presented in [107, 75], a new enriching operator has been constructed from the sum space $\Phi + \mathcal{M}_h$ to the conforming counterpart of the nonconforming

Morley space $\mathcal{M}_h$. Then, by using this operator and its approximation properties, we have provided novel discrete Sobolev embeddings for the sum space $\Phi + \mathcal{M}_h$. With the above tools and the classical Banach fixed-point Theorem, the well-posedness of the discrete problem has been established. In addition, by employing this enriching operator a rigorous error analysis to obtain optimal error bounds in broken H^2-, H^1- and L^2-seminorms, under *minimal regularity* conditions on the weak stream-function solution have been developed. Procedures to compute additional fields of physical interest, such as the velocity, vorticity and pressure have been proposed. More precisely, by employing suitable projection operators, we have computed the velocity and vorticity fields via postprocessing formulas of the discrete stream-function. However, we emphasize that we cannot recover the pressure variable directly from the discrete stream-function. So, we have developed a new pressure recovery algorithm by employing the Stokes complex relation of the Morley- and the Crouzeix-Raviart VE spaces, allowing the derivation of optimal error estimates in L^2-norm.

The results developed in this chapter mark a noteworthy step in furthering the progress of design and analysis of new schemes based on the fully nonconforming Morley-type VEM for solving fourth-order problems in more complicated scenarios, such as, nonlinear coupled and/or time dependent systems present in the fluid and solid mechanics, and in large scale wind-driven ocean circulation. In particular, we note that the discrete Sobolev embedding (cf. Theorem 6.4.1) can be used to provided a well-posedness analysis for thermal convection problems in stream-function–temperature form, the von Karmán plate system and the quasi-geostrophic equations of the ocean, among others.

The results contained in this chapter are in the article [5].

In general, it observed that the present stream-function approach provides an attractive and competitive alternative to solve two dimensional fluid flow problems; we eliminated the vector velocity field and fluid pressure from the weak formulation. Thus, there is only a scalar unknown and the approach leads to a smaller system compared with the classical velocity-pressure formulation. In addition, the incompressibility constraint is automatically satisfied, and the formulation avoids the difficulties related with the boundary values for the vorticity field (which is presented in the stream-function–vorticity form).

In addition, from the numerical experiments (see for instance, the tests reported in Subsections 4.7.2, 4.7.4, 5.6.2 and 6.7.4), it can observed numerically that our VE schemes presents certain robustness with respect to small diffusion parameters. Moreover from test 4.7.3 the C^1-VEM yields an hydrostatic velocity solution to the no flow problem for the Navier-Stokes equations; this good behaviour can be attributed to the fact that the incompressibility condition is satisfied automatically, a scenario in which the partial decoupling of the velocity and pressure errors leads a positive effect on the velocity computation. Furthermore, we observed that the resulting trilinear forms (continuous and discrete) in the momentum equation are naturally skew-symmetric, allowing more direct stability and convergence arguments. The advantages described above come at the price of a scheme without velocity and pressure fields, which need to be recovered. However for the stationary cases, if the primitive fields (velocity and pressure) are required, we have proposed algorithms to recover these variables. Additionally, we computed the intrinsic vorticity variable. Other potential drawbacks are a larger condition number due to the higher order derivatives involved, and a more complex extension to the three dimensional case.

Finally, it observed that the C^1-VEMs approach employed in this study provides an attractive and competitive alternative to solve fourth-order PDEs that involve the stream-function formulation in the context of fluid flow problems, by employing a low number of degrees of freedom. For instance, in the lowest order case $k = 2$, the total degrees of freedom used were $3N_{\mathbf{v}}$, where $N_{\mathbf{v}}$ denotes the number of vertices in the polygonal mesh and for the case $k = 3$, the total of degrees of freedom employed were $3N_{\mathbf{v}} + N_e$, where N_e denotes the number of edges in the polygonal mesh. Moreover, from the analysis provided in Section 4.4.2 (see also Theorem 4.4.3), we observed that the C^1-VE of lowest order needs the slightest regularity requirement for the weak stream-function to establish optimal error estimates, even for the nonlinear Navier-Stokes problem in stream-function form, compared with the classical C^1-FEMs (cf. Table 1.1).

7.2 Future work

In this section we propose different challenging topics which (are currently and) can be explored, building upon the theoretical and numerical paths developed in the thesis.

1. To extend the nonconforming VE scheme presented in **Chapter** 6 to the steady Boussinesq equations with temperature-dependent parameters, formulated in terms of the stream-function and temperature fields. This system is an extension of the classical Boussinesq model. In addition to the standard nonlinear coupling through the buoyancy term and the convective heat transfer, the system has an additional nonlinearity due to the introduction of temperature-dependent viscosity and thermal conductivity, which makes the problem even more challenging. In particular, we are interested in designing and analyzing new VEMs for solving this problem by coupling the Morley-type VE scheme developed in **Chapter** 6 and the nonconforming VEMs approach presented in [14, 65].

2. To develop a C^1-VEM on curved domains with applications to fluid mechanics problems in stream-function formulation. We observe that the special construction of the VEM avoids the explicit expression of the basis functions and allows the direct definition of the physical space (no reference element is employed), even on elements that are curved. In particular, we are interesting in:

   - to design a C^1-VEM of high order $k \geq 2$ for solving two dimensional fourth-order problems with curved edges;
   - to construct a suitable interpolant in the virtual element space;
   - to provide a rigorous analysis of stability and optimal error estimates;
   - to delivery numerical implementation and applications to fluid flow problems. For instance, to solve the Stokes and Navier-Stokes equations in stream-function form.

   These topics above are currently under investigation.

3. To derive a posteriori error estimators for the subjects studied in **Chapters** 4 and 6. We plan to extend the results presented in [75, 67] to develop reliable and efficient residual-based a posteriori error estimators for the C^1-conforming and Morley-type VEMs designed in these chapters to the nonlinear Navier-Stokes problem in stream-function form.

4. To study of the challenging three-dimensional case of the stream-function formulation by using conforming and/or nonconforming approaches. We are interested in carrying out the three-dimensional case by exploiting the VEM framework. It is important to note that in this case, the situation is more complicated. The stream-function is now a vector function (also referred to as a vector potential). Additionally, challenges arise due to factors such as the geometry, the "gauge condition" (it is required that the vector potential be also divergence-free), and the boundary conditions associated with the vector potential. We plan to study this topic by exploiting conforming and/or nonconforming approaches.

Bibliography

[1] D. Adak, V. Anaya, M. Bendahmane and D. Mora, *Conforming and nonconforming virtual element methods for fourth order nonlocal reaction diffusion equation*, Math. Models Methods Appl. Sci., **33**(10) (2023), pp. 2035–2083.

[2] D. Adak and G. Manzini, *The nonconforming virtual element method for Oseen's equation using a stream-function formulation*, ESAIM Math. Model. Numer. Anal., DOI: https://doi.org/10.1051/m2an/2023075, in press (2023).

[3] D. Adak, D. Mora, S. Natarajan and A. Silgado, *A virtual element discretization for the time dependent Navier-Stokes equations in stream-function formulation*, ESAIM Math. Model. Numer. Anal., **55**(5) (2021), pp. 2535–2566.

[4] D. Adak, D. Mora and A. Silgado, *A Morley-type virtual element approximation for a wind-driven ocean circulation model on polygonal meshes*, J. Comput. Appl. Math., **425** (2023), Article 115026.

[5] D. Adak, D. Mora and A. Silgado, *The Morley-type virtual element method for the Navier-Stokes equations in stream-function form*, Comput. Methods Appl. Mech. Engrg., **419** (2024), Paper No. 116573.

[6] R.A. Adams and J.J.F. Fournier, *Sobolev Spaces, 2nd ed.*, Academic Press, Amsterdam, 2003.

[7] B. Ahmad, A. Alsaedi, F. Brezzi, L.D. Marini and A. Russo, *Equivalent projectors for virtual element methods*, Comput. Math. Appl., **66** (2013), pp. 376–391.

[8] J. Aghili and D. Di Pietro, *An advection-robust hybrid high-order method for the Oseen problem*, J. Sci. Comput., **77** (2018), pp. 1310–1338.

[9] R. Agroum, C. Bernardi and J. Satouri, *Spectral discretization of the time-dependent Navier-Stokes problem coupled with the heat equation*, Appl. Math. Comput., **268** (2015), pp. 59–82.

[10] I. Al Balushi, W. Jiang, G. Tsogtgerel and T.Y. Kim, *A posteriori analysis of a B-spline based finite-element method for the stationary quasi-geostrophic equations of the ocean*, Comput. Methods Appl. Mech. Engrg., **371** (2020), 113317.

[11] R. Aldbaissy, F. Hecht, G. Mansour and T. Sayah, *A full discretisation of the time-dependent Boussinesq (buoyancy) model with nonlinear viscosity*, Calcolo, **55**(4) (2018), Paper No. 44, 49.

[12] V. Anaya, M. Bendahmane, D. Mora and R. Ruiz-Baier, *On a vorticity-based formulation for reaction-diffusion-Brinkman systems*, Netw. Heterog. Media, **13**(1) (2018), pp. 69–94.

[13] V. Anaya, A. Bouharguane, D. Mora, C. Reales, R. Ruiz-Baier, N. Seloula and H. Torres, *Analysis and approximation of a vorticity-velocity-pressure formulation for the Oseen equations*, J. Sci. Comput., **88**(3) (2019), pp. 1577–1606.

[14] V. Anaya, G. N. Gatica, D. Mora and R. Ruiz-Baier, *An augmented velocity–vorticity–pressure formulation for the Brinkman equations*, Int. J. Numer. Methods Fluids, **79** (2015) pp. 109–137.

[15] V. Anaya, D. Mora, C. Reales and R. Ruiz-Baier, *Vorticity-pressure formulations for the Brinkman-Darcy coupled problem*, Numer. Methods Partial Differential Equations, **35**(2) (2019), pp. 528–544.

[16] P.F. Antonietti, L. Beirão da Veiga and G. Manzini, The Virtual Element Method and its Applications, SEMA SIMAI Springer Series, Springer, Cham, Vol. 31, 2022.

[17] P.F. Antonietti, L. Beirão da Veiga, D. Mora and M. Verani, *A stream virtual element formulation of the Stokes problem on polygonal meshes*, SIAM J. Numer. Anal., **52** (2014), pp. 386–404.

[18] P.F. Antonietti, L. Beirão da Veiga, S. Scacchi and M. Verani, *A C^1 virtual element method for the Cahn–Hilliard equation with polygonal meshes*, SIAM J. Numer. Anal., **54** (2016), pp. 36–56.

[19] P.F. Antonietti, G. Manzini, S. Scacchi and M. Verani, *A review on arbitrarily regular conforming virtual element methods for second- and higher-order elliptic partial differential equations.* Math. Models Methods Appl. Sci. **31**(14) (2021), pp. 2825–2853.

[20] P. F. Antonietti, G. Manzini, and M. Verani, *The fully nonconforming virtual element method for biharmonic problems*, Math. Models Methods Appl. Sci., **28**(2) (2018), pp. 387–407.

[21] P.F. Antonietti, G. Vacca and M. Verani, *Virtual element method for the Navier–Stokes equation coupled with the heat equation*, IMA J. Numer. Anal., (2021), DOI: https://doi.org/10.1093/imanum/drac072.

[22] B. Ayuso de Dios, K. Lipnikov and G. Manzini, *The nonconforming virtual element method.* ESAIM Math. Model. Numer. Anal., **50**(3) (2016), pp. 879–904.

[23] T.P. Barrios, J.M. Cascón and M. González, *Augmented mixed finite element method for the Oseen problem: a priori and a posteriori error analyses*, Comput. Methods Appl. Mech. Engrg., **313** (2017), pp. 216–238.

[24] T.P. Barrios, J.M. Cascón and M. González, *On an adaptive stabilized mixed finite element method for the Oseen problem with mixed boundary conditions*, Comput. Methods Appl. Mech. Engrg., **365** (2020), 113007, 21 pp.

[25] G.R. Barrenechea and A. Wachtel, *Stabilised finite element methods for the Oseen problem on anisotropic quadrilateral meshes*, ESAIM Math. Model. Numer. Anal., **52** (2018), pp. 99–122.

[26] A. Behzadan and M. Holst, *Multiplication in Sobolev spaces, revisited*, Ark. Mat., **59**(2) (2021), pp. 275–306.

[27] L. Beirão da Veiga, F. Brezzi, A. Cangiani, G. Manzini, L.D. Marini and A. Russo, *Basic principles of virtual element methods*, Math. Models Methods Appl. Sci., **23** (2013), pp. 199–214.

[28] L. Beirão da Veiga, F. Brezzi, L.D. Marini and A. Russo, *Virtual element method for general second-order elliptic problems on polygonal meshes*, Math. Models Methods Appl. Sci., **26**(4) (2016), pp. 729–750.

[29] L. Beirão da Veiga, F. Brezzi, L.D. Marini and A. Russo, $H(\mathrm{div})$ *and* $H(\mathbf{curl})$*-conforming virtual element methods*, Numer. Math., **133**(2) (2016), pp. 303–332.

[30] L. Beirão da Veiga, F. Dassi and A. Russo, *A* C^1 *virtual element method on polyhedral meshes*, Comput. Math. Appl., **79**(7) (2020), pp. 1936-1955.

[31] L. Beirão da Veiga, F. Dassi and G. Vacca, *The Stokes complex for virtual elements in three dimensions*, Math. Models Methods Appl. Sci., **30**(3) (2020), pp. 477–512.

[32] L. Beirão da Veiga and A. Ern, *Preface Special issue – Polyhedral discretization for PDE*, ESAIM Math. Model. Numer. Anal., **50**(3) (2016), pp. 633–634.

[33] L. Beirão da Veiga, C. Lovadina and A. Russo, *Stability analysis for the virtual element method*, Math. Models Methods Appl. Sci., **27**(13) (2017), pp. 2557–2594.

[34] L. Beirão da Veiga, C. Lovadina and G. Vacca, *Divergence free virtual elements for the Stokes problem on polygonal meshes*, ESAIM Math. Model. Numer. Anal., **51** (2017), pp. 509–535.

[35] L. Beirão da Veiga, C. Lovadina and G. Vacca, *Virtual elements for the Navier-Stokes problem on polygonal meshes*, SIAM J. Numer. Anal., **56**(3) (2018), pp. 1210–1242.

[36] L. Beirão da Veiga and G. Manzini, *A virtual element method with arbitrary regularity*, IMA J. Numer. Anal., **34** (2014), pp. 759–781.

[37] L. Beirão da Veiga and G. Manzini, *Residual a posteriori error estimation for the virtual element methods for elliptic problems*, ESAIM Math. Model. Numer. Anal., **49**(2) (2015), pp. 577–599.

[38] L. Beirão da Veiga, D. Mora and G. Rivera, *Virtual elements for a shear-deflection formulation of Reissner-Mindlin plates*, Math. Comp., **88**, (2019), pp. 149–178.

[39] L. Beirão da Veiga, D. Mora, G. Rivera and R. Rodríguez, *A virtual element method for the acoustic vibration problem*, Numer. Math., **136**(3) (2017), pp. 725–763.

[40] L. Beirão da Veiga, D. Mora and A. Silgado, *A fully-discrete virtual element method for the nonstationary Boussinesq equations in stream-function form*, Comput. Methods Appl. Mech. Engrg., **408** (2023), Paper No. 115947.

[41] L. Beirão da Veiga, D. Mora and G. Vacca, *The Stokes complex for virtual elements with application to Navier-Stokes flows*, J. Sci. Comput., **81**(2) (2019), pp. 990–1018.

[42] L. Beirão da Veiga, A. Pichler and G. Vacca, *A virtual element method for the miscible displacement of incompressible fluids in porous media*, Comput. Methods Appl. Mech. Engrg., **375** (2021), Paper No. 113649, 35 pp.

[43] P.L. Betts and V. Haroutunian, *A stream function finite element solution for two-dimensional natural convection with accurate representation of Nusselt number variations near a corner*, Int. J. Numer. Methods Fluids., **3** (1983), pp. 605–622.

[44] C. Bernardi and M. Amara, *Convergence of a finite element discretization of the Navier–Stokes equations in vorticity and stream function formulation*, ESAIM Math. Model. Numer. Anal., **33**(5) (1999), pp. 1033–1056.

[45] C. Bernardi, T. Chacón Rebollo, D. Yakoubi, *Finite element discretization of the Stokes and Navier-Stokes equations with boundary conditions on the pressure*, SIAM J. Numer. Anal., 53 **3** (2015), pp. 1256–1279.

[46] C. Bernardi and N. Chorfi, *Spectral discretization of the vorticity, velocity, and pressure formulation of the Stokes problem*, SIAM J. Numer. Anal., **44** (2006), pp. 826–850.

[47] C. Bernardi, B. Métivet and B. Pernaud-Thomas, *Couplage des équations de Navier-Stokes et de la chaleur: le modèle et son approximation par éléments finis.* ESAIM Math. Model. Numer. Anal., **29**(7) (1995), pp. 871–921.

[48] S. Bertoluzza, V. Chabannes, C. Prud'homme and M. Szopos, *Boundary conditions involving pressure for the Stokes problem and applications in computational hemodynamics*, Comput. Methods Appl. Mech. Engrg. **322** (2017), pp. 55-80.

[49] H. Blum and R. Rannacher, *On the boundary value problem of the biharmonic operator on domains with angular corners*, Math. Methods Appl. Sci., **2**(4) (1980), pp. 556–581.

[50] J. Boland and W. Layton, *An analysis of the finite element method for natural convection problems*, Numer. Methods Partial Differential Equations, **2** (1990), pp. 115–126.

[51] O. Botella and R. Peyret, *Benchmark spectral results on the lid-driven cavity flow*, Comput. and Fluids, **27** (1998), pp. 421–433.

[52] M. Braack, E. Burman, V. John and G. Lube, *Stabilized finite element methods for the generalized Oseen problem*, Comput. Methods Appl. Mech. Engrg., **196** (2007), pp. 853–866.

[53] S.C. Brenner, S. Gu, T. Gudi and L.-Y. Sung, *A quadratic C^0 interior penalty method for linear fourth order boundary value problems with boundary conditions of the Cahn-Hilliard type*, SIAM J. Numer. Anal., **50**(4) (2012), pp. 2088–2110.

[54] S.C. Brenner and R.L. Scott, *The Mathematical Theory of Finite Element Methods*, Springer, New York, 2008.

[55] S.C. Brenner and L.Y. Sung, *Virtual element methods on meshes with small edges or faces*, Math. Models Methods Appl. Sci., **28**(7) (2018), pp. 1291–1336.

[56] S.C. Brenner, L.-Y. Sung and Z. Tan, *A C^1 virtual element method for an elliptic distributed optimal control problem with pointwise state constraints*, Math. Models Methods Appl. Sci., **31**(14) (2021), pp. 2887–2906.

[57] S.C. Brenner, P. Monk and J. Sun, *C^0 interior penalty Galerkin method for biharmonic eigenvalue problems*, in Spectral and High Order Methods for Partial Differential Equations. Lect. Notes Comput. Sci. Eng., **106** (2015), pp. 3–15.

[58] F. Brezzi and L.D. Marini, *Virtual elements for plate bending problems*, Comput. Methods Appl. Mech. Engrg., **253** (2013), pp. 455–462.

[59] E. Cáceres and G.N. Gatica, *A mixed virtual element method for the pseudostress-velocity formulation of the Stokes problem*, IMA J. Numer. Anal., **37** (2017), pp. 296–331.

[60] E. Cáceres, G.N. Gatica and F. Sequeira, *A mixed virtual element method for the Brinkman problem*, Math. Models Methods Appl. Sci., **27** (2017), pp. 707–743.

[61] Z. Cai and B. Chen, *Least-squares method for the Oseen equation*, Numer. Methods Partial Differential Equations, **32** (2016), pp. 1289–1303.

[62] A. Cangiani, E.H. Georgoulis and P. Houston, *hp-version discontinuous Galerkin methods on polygonal and polyhedral meshes*, Math. Models Methods Appl. Sci., **24**(10) (2014), pp. 2009–2041.

[63] A. Cangiani, E.H. Georgoulis, T. Pryer and O.J. Sutton, *A posteriori error estimates for the virtual element method*, Numer. Math., **137**(4) (2017), pp. 857-893.

[64] A. Cangiani, V. Gyrya and G. Manzini, *The nonconforming virtual element method for the Stokes equations*, SIAM J. Numer. Anal., **54**(6) (2016), pp. 3411–3435.

[65] A. Cangiani, G. Manzini and O.J. Sutton, *Conforming and nonconforming virtual element methods for elliptic problems*, IMA J. Numer. Anal., **37** (2017), pp. 1317–1354.

[66] C. Carstensen, R. Khot and A.K. Pani, *A priori and a posteriori error analysis of the lowest-order NCVEM for second-order linear indefinite elliptic problems*, Numer. Math., **151**(3) (2022), pp. 551–600.

[67] C. Carstensen, R. Khot and A.K. Pani, *Nonconforming virtual elements for the biharmonic equation with Morley degrees of freedom on polygonal meshes*, SIAM J. Numer. Anal., **61**(5) (2023), pp. 2460–2484.

[68] C. Carstensen, G. Mallik and N. Nataraj, *Nonconforming finite element discretization for semilinear problems with trilinear nonlinearity*, IMA J. Numer. Anal., **41** (2021), pp. 164–205.

[69] J.M. Cascón, G.C. Garcia and R. Rodríguez, *A priori and a posteriori error analysis for a large-scale ocean circulation finite element model*, Comput. Methods Appl. Mech. Engrg., **192** (2003), pp. 5305-5327.

[70] D. Castañón Quiroz and D.A. Di Pietro, *A hybrid high-order method for the incompressible Navier-Stokes problem robust for large irrotational body forces*, Comput. Math. Appl., **79**(9) (2020), pp. 2655–2677.

[71] M. Cayco and R.A. Nicolaides, *Finite element technique for optimal pressure recovery from stream function formulation of viscous flows*, Math. Comp., **46**(174) (1986), pp. 371–377.

[72] M. Cayco and R.A. Nicolaides, *Analysis of nonconforming stream function and pressure finite element spaces for the Navier-Stokes equations*, Comput. Math. Appl., **18**(8) (1989), pp. 745–760.

[73] C.L. Chang and S.-Y. Yang, *Analysis of the $[L^2, L^2, L^2]$ least-squares finite element method for incompressible Oseen-type problems.* Int. J. Numer. Anal. Model., 4(3-4) (2007), pp 402–424.

[74] L. Chen and J. Huang, *Some error analysis on virtual element methods*, Calcolo, **55**(1) (2018), pp. 5–23.

[75] M. Chen, J. Huang and S. Lin, *A posteriori error estimation for a C^1 virtual element method of Kirchhoff plates*, Comput. Math. Appl., **120** (2022), 132–150.

[76] A. Chernov, C. Marcati and L. Mascotto, *p- and hp- virtual elements for the Stokes problem*, Adv. Comput. Math., **47** (2021), Art. 24, 31 pp.

[77] C. Chinosi and L.D. Marini, *Virtual element method for fourth order problems: L^2-estimates*, Comput. Math. Appl., **72**(8) (2016), pp. 1959–1967.

[78] A. Cesmelioğlu, B. Cockburn, N.C. Nguyen, and J. Peraire, *Analysis of HDG methods for Oseen equations.* J. Sci. Comput., 55(2) (2013), pp. 392–431.

[79] P.G. Ciarlet, *The Finite Element Method for Elliptic Problems*, SIAM, 2002.

[80] B. Cockburn, G. Fu and W. Qiu, *A note on the devising of superconvergent HDG methods for Stokes flow by M-decompositions*, IMA J. Numer. Anal., **37**(2) (2017), pp. 730–749.

[81] A. Dedner and A. Hodson, *Robust nonconforming virtual element methods for general fourth–order problems with varying coefficients*, IMA J. Numer. Anal., **42**(2) (2022), pp. 1364–1399.

[82] H. Dallmann and D. Arndt, *Stabilized finite element methods for the Oberbeck-Boussinesq model*, J. Sci. Comput., **69**(1), (2016), pp. 244–273.

[83] M. Dehghan, Z. Gharibi and R. Ruiz-Baier, *Optimal error estimates of coupled and divergence-free virtual element methods for the Poisson–Nernst–Planck/Navier–Stokes equations*, J. Sci. Comput., **94**(3) (2023), Paper No. 72, 50 pp.

[84] F. Dassi and G. Vacca, *Bricks for the mixed high-order virtual element method: Projectors and differential operators*, Appl. Numer. Math., **155**, (2020), pp. 140–159.

[85] J. de Frutos, B. García-Archilla and Julia Novo, *Grad-div stabilization for the time-dependent Boussinesq equations with inf-sup stable finite elements*, Appl. Math. Comput., **349** (2019), pp. 281–291.

[86] D.A. Di Pietro and A. Ern, *A hybrid high-order locking-free method for linear elasticity on general meshes*, Comput. Methods Appl. Mech. Engrg., **283** (2015), pp. 1–21.

[87] D.A. Di Pietro and S. Krell, *A hybrid high-order method for the steady incompressible Navier-Stokes problem*, J. Sci. Comput., **74**(3) (2018), pp. 1677–1705.

[88] Z. Dong and A. Ern, *Hybrid high-order and weak Galerkin methods for the biharmonic problem*, SIAM J. Numer. Anal., **60**(5) (2022), pp. 2626–2656.

[89] A. Ern, *Vorticity-velocity formulation of the Stokes problem with variable density and viscosity*, Math. Models Methods Appl. Sci., **8**(2), (1998), pp. 203–218.

[90] F. Fairag, *A two-level finite-element discretization of the stream function form of the Navier-Stokes equations*, Comput. Math. Appl., **36** (1998), pp. 117–127.

[91] F. Fairag, *Numerical computations of viscous, incompressible flow problems using a two-level finite element method*, SIAM J. Sci. Comput., **24** (2003), pp. 1919–1929.

[92] D. Fishelov, M. Ben-Artzi and J.-P. Croisille, *Recent developments in the pure stream-function formulation of the Navier–Stokes system*, J. Sci. Comput., **45** (2010), pp. 238–258.

[93] G. Fix, *Finite element models for ocean circulation problems*, SIAM J. Appl. Math., **29** (1975), pp. 371–387.

[94] S. Franz, K. Höhne and M. Gunar, *Grad-div stabilized discretizations on S-type meshes for the Oseen problem*, IMA J. Numer. Anal., **38** (2018), pp. 299–329.

[95] E.L. Foster, T. Iliescu and Z. Wang, *A finite element discretization of the stream function formulation of the stationary quasi-geostrophic equations of the ocean*, Comput. Methods Appl. Mech. Engrg., **261**/**262**(2) (2013), pp. 105–117.

[96] E.L. Foster, T. Iliescu and D. Wells, *A conforming finite element discretization of the streamfunction form of the unsteady quasi-geostrophic equations*, Int. J. Numer. Anal. Model., **13**(6) (2016), pp. 951–968.

[97] D. Frerichs and C. Merdon, *Divergence-preserving reconstructions on polygons and a really pressure-robust virtual element method for the Stokes problem*, IMA J. Numer. Anal., **42**(1) (2022), pp. 597–619.

[98] G.N. Gatica, M. Munar and F. Sequeira, *A mixed virtual element method for the Navier-Stokes equations,* Math. Models Methods Appl. Sci., **28**(14) (2018), pp. 2719–2762.

[99] G.N. Gatica, M. Munar and F. Sequeira, *A mixed virtual element method for the Boussinesq problem on polygonal meshes,* J. Comput. Math., **39**(3) (2021), pp. 392–427.

[100] G.N. Gatica and F. Sequeira, *An L^p spaces-based mixed virtual element method for the two-dimensional Navier-Stokes equations*, Math. Models Methods Appl. Sci., **31**(14) (2021), pp. 2937–2977.

[101] E.H. Georgoulis and P. Houston, *Discontinuous Galerkin methods for the biharmonic problem*, IMA J. Numer. Anal., **29**(3) (2009), pp. 573–594.

[102] U. Ghia, K.N. Ghia and C.T. Shin, *High-Re solutions for incompressible flow using the Navier–Stokes equation and a multigrid method.* J. Comput. Phys., **48** (1982), pp. 387–411.

[103] V. Girault and P.A. Raviart, *Finite Element Methods for Navier-Stokes Equations*, Springer-Verlag, Berlin, 1986.

[104] R.J. Greatbatch and B.T. Nadiga, *Four-gyre circulation in a barotropic model with double-gyre wind forcing,* J. Phys. Oceanogr., **30** (2000), pp. 1461-1471.

[105] Q. Guan, *Some estimates of virtual element methods for fourth order problems*, Electronic Research Archive, **29**(6), (2021), pp. 4099–4118.

[106] D.B. Haidvogel, A.R. Robinson and E.E. Schulman, *The accuracy, efficiency, and stability of three numerical models with application to open ocean problems*, J. Comput. Phys., **34** (1980), pp. 1-53.

[107] J. Huang and Y. Yu, *A medius error analysis for nonconforming virtual element methods for Poisson and biharmonic equations*, J. Comput. Appl. Math., **386** (2021), Paper No. 113229, 20 pp.

[108] X. Hu, L. Mu, and X. Ye, *A weak Galerkin finite element method for the Navier–Stokes equations*, J. Comput. Appl. Math., **362** (2019), pp. 614–625.

[109] V. John, A. Linke, C. Merdon, M. Neilan and L.G. Rebholz, *On the divergence constraint in mixed finite element methods for incompressible flows*, SIAM Rev., **59**(3) (2017), pp. 492–544.

[110] D. Kim, T.Y. Kim, E.J. Park and D.W. Shin, *Error estimates of B-spline based finite-element methods for the stationary quasi-geostrophic equations of the ocean*, Comput. Methods Appl. Mech. Engrg., **353** (2018), pp. 255–272.

[111] D. Kim, A.K. Pani and E.J. Park, *Morley finite element methods for the stationary quasi-geostrophic equation*, Comput. Methods Appl. Mech. Engrg., **375** (2021), 113639, 21 pp.

[112] T.Y. Kim, E.J. Park and D.W. Shin, *A C^0-discontinuous Galerkin method for the stationary quasi-geostrophic equations of the ocean*, Comput. Methods Appl. Mech. Engrg., **300** (2015), pp. 225–244.

[113] T.Y. Kim, T. Iliescu and E. Fried, *B-spline based finite-element method for the stationary quasi-geostrophic equations of the ocean*, Comput. Methods Appl. Mech. Engrg., **286** (2015), pp. 168–191.

[114] K. Kirk and S. Rhebergen, *Analysis of a pressure-robust hybridized discontinuous Galerkin method for the stationary Navier-Stokes equations*, J. Sci. Comput., **81**(2) (2019), 881–897.

[115] M.J. Lai and P. Wenston, *Bivariate spline method for numerical solution of steady state Navier-Stokes equations over polygons in stream function formulation*, Numer. Methods Partial Differential Equations, **16**(2), (2000), pp. 147–183.

[116] M. Li, J. Zhao, C Huang and S. Chen, *Conforming and nonconforming VEMs for the fourth–order reaction–subdiffusion equation: a unified framework*, IMA J. Numer. Anal., **42**(3) (2022), pp. 2238–2300.

[117] X. Liu, R. Li and Z. Chen, *A virtual element method for the coupled Stokes-Darcy problem with the Beaver-Joseph-Saffman interface condition*, Calcolo, **56**(4), (2019), Art. 48, 28 pp.

[118] X. Liu and Z. Chen, *The nonconforming virtual element method for the Navier-Stokes equations*, Adv. Comput. Math., **45**(1) (2019), pp. 51–74.

[119] X. Liu, R. Li and Y. Nie, *A divergence-free reconstruction of the nonconforming virtual element method for the Stokes problem*, Comput. Methods Appl. Mech. Engrg., **372** (2020), Paper No. 113351, 21 pp.

[120] J.G. Liu, C. Wang and H. Johnston, *A fourth order scheme for incompressible Boussinesq equations*, J. Sci. Comput., **18**(2) (2003), pp. 253–285.

[121] S. A. Lorca and J.L Boldrini, *The initial value problem for a generalized Boussinesq model.* Nonlinear Anal., **36**(4) (1999) Ser. A: Theory Methods, pp. 457–480.

[122] C. Lovadina, D. Mora and I. Velásquez, *A virtual element method for the von Kármán equations*, ESAIM Math. Model. Numer. Anal., **55**(2) (2021), pp. 533–560

[123] A. Majda, *Introduction to PDEs and Waves for the Atmosphere and Ocean*, American Mathematical Society, New York, 2003.

[124] A. Majda and X. Wang, *Nonlinear Dynamics and Statistical Theories for Basic Geophysical Flows*, Cambridge University Press, 2006.

[125] M.T. Manzari, *An explicit finite element algorithm for convective heat transfer problems*, Internat. J. Numer. Methods Heat Fluid Flow, **9** (1999), pp. 860–877.

[126] L. Mascotto, I. Perugia and A. Pichler, *Non-conforming harmonic virtual element method: h- and p-versions*, J. Sci. Comput., **77**(3) (2018), pp. 1874–1908.

[127] L. Mascotto, I. Perugia and A. Pichler, *A nonconforming Trefftz virtual element method for the Helmholtz problem.* Math. Models Methods Appl. Sci. **29**(9) (2019), pp. 1619–1656.

[128] N. Massarotti, P. Nithiarasu and O.C. Zienkiewicz, *Characteristic-Based-Split (CBS) algorithm for incompressible flow problems with heat transfer*, Internat. J. Numer. Methods Heat Fluid Flow, **8** (1998), pp. 969–990.

[129] J. McWilliams, *Fundamentals of Geophysical Fluid Dynamics*, Cambridge University Press, 2006.

[130] T.T. Medjo, *Numerical simulations of a two-layer quasi-geostrophic equation of the ocean*, SIAM J. Numer. Anal., **37** (2000), pp. 2005–2022.

[131] J. Meng, L. Mascotto and L. Beirão da Veiga, *Stability and interpolation properties for Stokes-like virtual element spaces*, J. Sci. Comput., **94**(3) (2023), Paper No. 56, 23 pp.

[132] P.G. Myers and A.J. Weaver, *A diagnostic barotropic finite-element ocean circulation model*, J. Atmos. Ocean Technol. **12** (1995), pp. 511–526.

[133] D. Mora, C. Reales and A. Silgado, *A C^1-virtual element method of high order for the Brinkman equations in stream function formulation with pressure recovery*, IMA J. Numer. Anal., **42**(4) (2022), pp. 3632–3674.

[134] D. Mora, G. Rivera and R. Rodríguez, *A virtual element method for the Steklov eigenvalue problem*, Math. Models Methods Appl. Sci., **25** (2015), pp. 1421–1445.

[135] D. Mora, G. Rivera and I. Velásquez, *A virtual element method for the vibration problem of Kirchhoff plates*, ESAIM Math. Model. Numer. Anal., **52** (2018), pp. 1437–1456.

[136] D. Mora and A. Silgado, *A C^1 virtual element method for the stationary quasi-geostrophic equations of the ocean*, Comput. Math. Appl., **116** (2022), pp. 212–228.

[137] D. Mora and A. Silgado, *Virtual element methods for a stream-function formulation of the Oseen equations*, In: Antonietti, P.F., Beirão da Veiga, L., Manzini, G. (eds), The Virtual Element Method and its Applications. SEMA SIMAI Springer Series, vol 31, pp. 321-361, (2022). Springer, Cham.

[138] D. Mora and A. Silgado, *Virtual elements for the Navier-Stokes system: stream-function form and primitive variables recovery algorithms*, submitted for publication (2023).

[139] D. Mora and I. Velásquez, *Virtual elements for the transmission eigenvalue problem on polytopal meshes*, SIAM J. Sci. Comput., **43**(4) (2021), A2425–A2447.

[140] H. Morimoto, *Nonstationary Boussinesq equations*, J. Fac. Sci. Univ. Tokyo Sect. IA Math., **39**(1), (1992), pp. 61–75.

[141] L.S.D. Morley, *The triangular equilibrium element in the solution of plate bending problems*, Aero. Quart., **19** (1968), pp. 149–169.

[142] I. Mozolevski and E. Süli, *A priori error analysis for the hp-version of the discontinuous Galerkin finite element method for the biharmonic equation*, Comput. Methods Appl. Math., **3**(4) (2003), pp. 596–607.

[143] I. Mozolevski, E. Süli and P.R. Bösing, *Discontinuous Galerkin finite element approximation of the two-dimensional Navier-Stokes equations in stream-function formulation*, Comm. Numer. Methods Engrg., **23**(6) (2007), pp. 447–459.

[144] R. Oyarzúa, T. Qin and D. Schötzau, *An exactly divergence-free finite element method for a generalized Boussinesq problem*, IMA J. Numer. Anal., **34**(3) (2014), pp. 1104–1135.

[145] J. Pedlosky, *Geophysical Fluid Dynamics*, Springer, 1987.

[146] A. Quarteroni and A. Valli, *Numerical Aproximation of the Partial Differential Equation*, Springer-Verlag Berlin Heidelberg, 1994.

[147] P. W. Schroeder and G. Lube *Pressure-robust analysis of divergence-free and conforming FEM for evolutionary incompressible Navier–Stokes flows*, J. Numer. Math., **25**(4) (2017), pp. 249–276.

[148] W.N.R. Stevens, *Finite element, stream function–vorticity solution of steady laminar natural convection*, Int. J. Numer. Methods Fluids, **2** (1982), pp. 349–366.

[149] A. Tabarraei and N. Sukumar, *Conforming polygonal finite elements*, Int. J. Numer. Methods Engrg., **61** (2004), pp. 2045–2066.

[150] M. Tabata and D. Tagami, *Error estimates of finite element methods for nonstationary thermal convection problems with temperature-dependent coefficients*, Numer. Math., **100**(2) (2005), pp. 351–372.

[151] A. Tagliabue, L Dedé and A. Quarteroni, *Isogeometric analysis and error estimates for high order partial differential equations in fluid dynamics*, Comput. & Fluids, **102** (2014), pp. 277–303.

[152] Z. Tian and Y. Ge, *A fourth-order compact finite difference scheme for the steady stream function-vorticity formulation of the Navier-Stokes/Boussinesq equations*, Internat. J. Numer. Methods Fluids, **41**(5) (2003), pp. 495–518.

[153] G. Vacca and L. Beirão da Veiga, *Virtual element methods for parabolic problems on polygonal meshes*, Numer. Methods Partial Differential Equations, **31**(6) (2015), pp. 2110–2134.

[154] G. Vacca, *An H^1-conforming virtual element for Darcy and Brinkman equations*, Math. Models Methods Appl. Sci., **28** (2018), pp. 159–194.

[155] D. de Vahl Davis, *Natural convection of air in a square cavity: A benchmark solution*, Internat. J. Numer. Methods Fluids, **3** (1983), pp. 249–264.

[156] G.K. Vallis, *Atmosphere and Ocean Fluid Dynamics: Fundamentals and Large-Scale Circulation*, Cambridge University Press, 2006.

[157] N. Verma and S. Kumar, *Lowest order virtual element approximations for transient Stokes problem on polygonal meshes*, Calcolo, **58**(4) (2021), Paper No. 48, 35 pp.

[158] D.C. Wan, B.S.V. Patnaik and G.W. Wei, *A new benchmark quality solution for the buoyancy-driven cavity by discrete singular convolution*, Numer. Heat Transfer, **40** (2001), pp. 199–228.

[159] F. Wang and J. Zhao, *Conforming and nonconforming virtual element methods for a Kirchhoff plate contact problem*, IMA J. Numer. Anal., **41**(2) (2021), pp. 1496–1521.

[160] C. Wang, J.G. Liu and H. Johnston, *Analysis of a fourth order finite difference method for the incompressible Boussinesq equations*, Numer. Math., **97**(3) (2004), pp. 555–594.

[161] Y. Zhang, Y. Hou and J. Zhao, *Error analysis of a fully discrete finite element variational multiscale method for the natural convection problem*, Comput. Math. Appl., **68**(4) (2014), pp. 543–567.

[162] B. Zhang, J. Zhao and M. Li, *The divergence-free nonconforming virtual element for the Navier-Stokes problem*, Numer. Methods Partial Differential Equations, **39**(3) (2023), pp. 1977–1995.

[163] J. Zhao, B. Zhang, S. Chen and S. Mao, *The Morley–type virtual element for plate bending problems*, J. Sci. Comput., **76**(1) (2018), pp. 610–629.

[164] J. Zhao, B. Zhang, S. Mao and S. Chen, *The divergence-free nonconforming virtual element for the Stokes problem*, SIAM J. Numer. Anal., **57**(6) (2019), pp. 2730–2759.